AN ABSTRACT OF THE THESIS OF

Dale George Nagle for the degree of Doctor of Philosophy in Pharmacy

presented on December 7, 1994.

Title: Novel Oxylipins and Other Bioactive Metabolites From Marine Algae

Abstract approved:_ Redacted for Privacy

William H. Gerwick

I have participated in a drug discovery program designed to screen marine algae for inhibitors of cancer-related enzymes, antitumor compounds, antiinflammatory substances, and other agents of potential pharmaceutical utility. Over 1,500 lipid and aqueous extracts of marine plants and animals were surveyed for biomedical potential. Assays designed to screen extracts for new types of marine toxins have served to guide the isolation and identification of biologically active compounds.

Extracts of the Oregon marine alga *Constantinea simplex* were found to contain a mixture of constanolactones, and lactonized cyclopropyl-containing oxylipin metabolites that logically derive from arachidonic and eicosapentaenoic acids. Spectroscopic analysis and chiroptical measurements of the natural products and various synthetically produced derivatives afforded the structures of seven structurally related compounds.

Nakienones A-C and nakitriol, a series of reactive cytotoxic metabolites, were isolated from dead and necrotic branches of stony coral (*Acropora* sp.) which were completely covered with a gray-black mat of cyanobacteria (*Synechocystis* sp.). Their structures were determined spectroscopically by interpretation of 2D-NMR experiments, including heteronuclear multiple-bond coherence spectroscopy (HMBC) and 2-D nuclear Overhauser exchange spectroscopy (NOESY), and by comparison with model compounds.

Bioassay-guided fractionation of the organic extract of a Curaçao *Lyngbya majuscula* organic extract led to the isolation of an extremely potent brine shrimp toxin with antiproliferative activity. The structure of this new thiazoline ring-containing lipid, curacin A, was deduced from spectroscopic information and comparison of products obtained from chemical degradation of the natural product with the same substances prepared by synthesis. Curacin A is an antimitotic agent that inhibits microtubule assembly and the binding of colchicine to tubulin. In addition to curacin A, a potent new ichthyotoxic depsipeptide (antillatoxin), a new malyngamide derivative, and an unusual molluscicidal compound have been isolated from this alga.

Novel Oxylipins and Other Bioactive Metabolites From Marine Algae

by

Dale George Nagle

A THESIS

submitted to

Oregon State University

in partial fulfillment of

the requirements for the

degree of

Doctor of Philosophy

Completed December 7, 1994

Commencement June 1995

Doctor of Philosophy thesis of Dale George Nagle presented on December 7, 1994.

APPROVED:

Redacted for Privacy

Professor of Pharmacy in charge of major

Redacted for Privacy

Dean of College of Pharmacy

Redacted for Privacy

Dean of Graduate School

I understand that my thesis will become part of the permanent collection of Oregon State University libraries. My signature below authorizes release of my thesis to any reader upon request.

Redacted for Privacy

Dale George Nagle

ACKNOWLEDGEMENTS

My profound gratitude goes to my parents, Dorothy H. and George C. Nagle. Without their support, I would not have been able to pursue my research career. I am deeply grateful to my adviser Dr. William H. Gerwick for his guidance, inspiration and support throughout my graduate study at Oregon State University. He not only taught me what it means to be a good scientist, he also shared his friendship with me, which made working with him a deaply rewarding experience. I should like to thank the members of my graduate committee, Drs. Gary E. DeLander, T. Mark Zabriskie, Thomas F. Savage, and George H. Constantine for their valuable suggestions to my graduate program. I especially thank Dr. Constantine for his encouragement, friendship, and fraternal spirit.

I am indebted to the following people for their technical assistance in my graduate research: Dr. Gayle I. Hansen for her excellent phycological instruction; Rodger L. Kohnert at the Department of Chemistry for his assistance in NMR experiments; Brian Arbogast and Don Griffin for their commitment to extreme professionalism in providing the highest quality mass spectra; Dr. Paul H. Franklin for his patient help with computers; and Ms. Jeannine Lawrence for her generous instuction and assistence in obtaining CD data.

I should also like to acknowledge my good friends and colleagues for their support: Dr. Philip J. Proteau, a great travel partner and friend, his commitment family, friends and to rigorous scientific detail were inspirational; Dr. Matthew W. Bernart for his patient help and guidance in my early years of research; Dr. Jimmy Orjala for his friendship and his good cheer even during the stressful times of our lives; and to rest of our lab for their help, friendship and patience. I would also like to thank my fraternal Phi Delta Chi brothers—you have been a second family to me.

During the years of my graduate study at OSU, I was supported by research assistantships from American Society of Pharmacognosy, Oregon Sea Grant, National Institute of Health, and a N.L. Tarter Fellowship.

CONTRIBUTION OF AUTHORS

Chapters II and V of my thesis describe results from collaborative research projects. Chapter II details a survey of marine algae for biomedical potential. Algal extracts and purified compounds were evaluated for antiinflammatory, antiviral, and mechanism-based anticancer activities at Syntex Research (Palo Alto). Results presented in this chapter are a compilation of test results and chemical leads and represent the efforts of myself and other members of our research group, presented in order to establish the foundation of my research.

The curacin A project in Chapter V also represents a group effort. The cyanobacterial source of curacin A, *Lyngbya majuscula*, was discovered and collected by myself, Dr. Philip J. Proteau, and Prof. William H. Gerwick. Following extraction of this organism and subsequent pharmacological evaluation, Prof. Gerwick isolated the original sample of curacin A. Brine shrimp lethality assays used to guide the fractionation and purification of curacin A were performed, in this case, by Patrick Varga (Pharmacy Student, OSU College of Pharmacy). The planer structure of curacin A was deduced by Drs. Proteau and Gerwick. Robin S. Geralds prepared of the methoxy-methyl ketone derivative of curacin A. Hye-Dong Yoo prepared sufficient purified curacin A for pharmacological evaluations and the chemical degradation experiments. The methylsulfonic acid and methoxy-methyl ketone derivatives were synthesized by Dr. Mitch Nambu, Tae-Seong Kim, and Prof. James D. White (OSU Chemistry Dept.). Experiments to examine the mechanism of antimitotic activity of curacin A were run in the laboratories of Drs. Ernest Hamel and Andrei Blokin (Nation Cancer Institute, Bethesda). Structure elucidation of antillatoxin, barbarmide, and malyngamide H form *L. majuscula* discussed in Chapter V were performed by Dr. Jimmy Orjala (OSU, College of Pharmacy).

CONTRIBUTION OF AUTHORS (APPENDIX)

William C. McClatchey assisted in the chromatographic separation and HPLC purification of the sphingolipids described in the Appendix.

TABLE OF CONTENTS

List of Figures Page

List of Tables Page

List of Tables Continued

Page

LIST OF ABBREVIATIONS

AA	Arachidonic Acid
AP	Acetone Powder
CC	Column Chromatography
CD	Circular Dichroism
CIMS	Chemical Ionization Mass Spectrometry
COSY	^{1}H-^{1}H Chemical Shift Correlation Spectroscopy
CPM	Counts Per Minute
DEPT	Distortionless Enhancement by Polarization Transfer
DMSO	Dimethylsulfoxide
EC	Effective Concentration
EI	Electron Impact
EtOAc	Ethyl Acetate
FAB	Fast Atom Bombardment
FT	Fourier Transform
FTIR	Fourier Transformed Infrared Spectroscopy
GI	Growth Inhibition
GC	Gas Chromatography
HETCOR	Heteronuclear Correlation Spectroscopy
HEPE	Hydroxyeicosapentaenoic Acid
HETE	Hydroxyeicosatetraenoic Acid
HIV	Human Immunodeficiency Virus
HMBC	Heteronuclear Multiple-Bond Coherence Spectroscopy
HPETE	Hydroperoxyeicosapentaenoic Acid
HPLC	High-Performance Liquid Chromatography

HPODE	Hydroperoxyoctadecadienoic Acid
HRCIMS	High Resolution Chemical Ionization Mass Spectrometry
HRMS	High Resolution Mass Spectrometry
HSV	Herpes Simplex Virus
HT	Hydroxytryptamine
IC	Inhibitory Concentration
IMP	Inosine Monophosphate
IMPDH	Inosine Monophosphate Dehydrogenase
IPA	Isopropyl Alcohol
IR	Infrared or Infrared Spectroscopy
KETE	Ketoeicosatetraenoic Acid
LD	Lethal Dose
LT	Leukotriene
LX	Lipoxin
LPO or LO	Lipoxygense
MC	Menthoxycarbonate
MS	Mass Spectrometry
NAD	Nicotinamide Adenine Dinucleotide (oxidized form)
NADH	Nicotinamide Adenine Dinucleotide (reduced form)
NCI	National Cancer Institute
NCNPDDG	National Cooperative Natural Products Drug Discovery Group
NMR	Nuclear Magnetic Resonance
NOE	Nuclear Overhauser Effect
NOEDS	Nuclear Overhauser Effect Difference Spectrometry
NOESY	Nuclear Overhauser Exchange Spectrometry
PTK	Protein Tyrosine Kinase

PG	Prostaglandin
TGI	Total Growth Inhibition
TLC	Thin Layer Chromatography
TMS	Tetramethylsilane
TMSi	Trimethylsilyl
TXA	Thromboxane
UV	Ultraviolet or Ultraviolet Spectrometry
WHO	World Health Organization
XMP	Xanthosine Monophosphate
XHCORR	Heteronuclear Chemical Shift Correlation Spectroscopy

NOVEL OXYLIPINS AND OTHER BIOACTIVE METABOLITES FROM MARINE ALGAE

CHAPTER I.

GENERAL INTRODUCTION

Historically, terrestrial plants and, to a lesser degree, animals have provided many of the drugs and other products used to treat human disease. In 1815 C.A. Seydler, a medical student in Germany, coined the term "pharmacognosy" from the Greek words *pharmakon* (drug) and *gnosis* (knowledge) to describe the comprehensive study of natural drugs.[1] In the United States the term "natural products" is perhaps more commonly used to describe the study of naturally derived chemical substances and includes the study of natural drugs as well as non-medicinal agents. Pharmacognosy has traditionally focused upon the study of terrestrial plants and has evolved, with the discovery of antibiotic producing bacteria and fungi, to include the study of microbial metabolites.[1] Within the last thirty years the search for new natural products from the marine environment has experienced an explosive growth. Two series of reviews have provided comprehensive coverage of the advancement of marine natural products.[2-14] Marine natural products may now be considered a scientific discipline, independent of, yet inherently based upon the traditional practice of pharmacognosy.

Both marine and terrestrial natural products research have undergone an evolution over the past three decades. Recent advances in spectroscopic technologies have spurred a revolution in natural products research. The structures of trace metabolites with exquisitely potent activities may now be deduced, efforts inconceivable only a few years ago. In the 1980's high-field Fourier-transformed (FT) pulsed instrumentation first allowed researchers to determine the structures of new compounds available only in multimilligram

quantities. The introduction of proton-detected 2- and 3-D NMR techniques, especially HMQC and HMBC, has facilitated complete structural assignment of submilligram to milligram quantities of complex natural products.[15,16] These inverse-detected NMR techniques also dramatically reduce the instrument time required to determine long-range heteronuclear-coupling information which is routinely required to establish molecular connectivity. Currently, extremely high-field (500 to 800 MHz) and microprobe NMR technologies provide a means to investigate the structure of trace quantities of natural products.[17]

During the 1980s several marine natural product research groups began extensive microorganism culture efforts. Several recent reviews illustrate how marine bacteria,[18] dinoflaggelates,[19] diatoms,[19] and blue-green algae[19-21] which were impossible to evaluate from individual field collections are now producing exciting new leads in culture.

Marine Ethnomedicine and Natural Products

One approach to the study of the marine natural products is that of a classical ethnomedicinal investigation.[1] Traditional medical practices and folkloric toxicological information are utilized as a guide for the chemical investigation of marine organisms. Whereas the ethnobotanical method of terrestrial natural products research has directed the discovery of many effective therapeutic agents, the inaccessibility of the oceanic environment may have acted as a limiting influence on the folkloric utilization of marine organisms. The organisms which seem to have provided the greatest utility have been those limited to intertidal and shallow water environments, those species most accessible to indigenous peoples. Although the number of ethnomedical leads in marine science have been relatively small, several notable exceptions have provided exciting natural products research projects.

For centuries the people of China and Japan have prepared an extract from the

boiled fresh blades of the red alga *Digenea simplex* to use as a remedy for intestinal parasite infections of small children.[22] Following isolation, the structure of the anthelmintic constituent of *D. simplex* was determined to be that of an unusual amino acid, α-kainic acid **1** (Figure I.1).[23] Since its discovery, **1** has proven to be an extremely important neuropharmacological probe.[24] As a structural analog of proline and the excitatory amino acids aspartic and glutamic acid (**2**), **1** has defined the kainate receptor, a specific subtype of excitatory amino acid receptors, and is now an essential tool in neuroscience.

Two distinctly different types of Japanese marine organisms, which have long been observed to rapidly kill flies that land upon them, have provided valuable folkloric leads to important natural product discoveries. Aside from its beach fly insecticidal activity, the tropical red alga *Chondria armata* has, like *D. simplex*, represented a traditional anthelmintic remedy.[25] Subsequent research has shown *C. armata* to contain palytoxin analogs, domoic acid (**3**), and seven domoic acid derivatives.[26] The marine annelid *Lumbriconereis heteropoda* has long been used as fish bait in Tokyo Bay. Flies die when they contact these worms and fishermen which handle them have complained of respiratory problems, headaches, and vomiting.[27] An unusual toxic sulfur containing amine, nereistoxin (**4**), was later isolated from extracts of the annelid and served as a lead compound for the synthesis of a new insecticide, PADEN (**5**).

Aqueous extracts of the brown alga *Laminaria japonica* have been used in traditional oriental medicine for the treatment of hypertension.[28] The hypotensive effects of the alga have been attributed to an unusual ganglionic-blocking amino acid, laminine (**6**), present in numerous members of the Laminariaceae.[28]

Marine Toxins

Terrestrial plant pharmacognosy has as a primary focus the search for new medicinal agents, a theme which has traditionally predominated as the most important

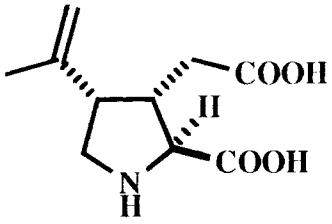

1
kainic acid

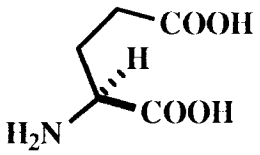

2
glutamic acid

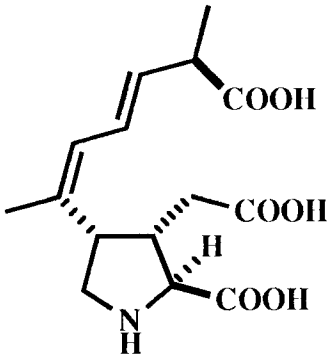

3
domoic acid

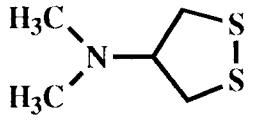

4
nereistoxin

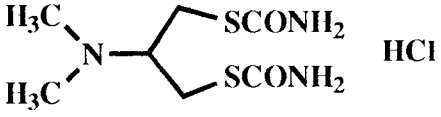

5
PADEN

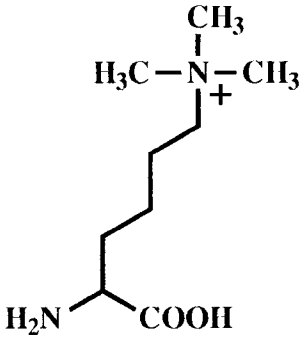

6
laminine

Figure I.1 Structures of Compounds Discovered From Marine Ethnopharmacological Leads and Related Structures.

direction of study. In contrast, a crucial force in marine natural products has been the exploration of marine toxins.[29,30] Some of the first scientists involved in the study of marine chemistry searched for the agents responsible for seafood intoxications.[27] Marine toxin research has since become an integral component of the field. Animal poisonings and human intoxications have been reported, or recounted in folkloric tales, to be caused by species representing members from a majority of all known phyla (or divisions) of marine organisms.[27,29-30] Marine toxins, because of their unique structures and pharmacological properties, have proved invaluable as research tools for biochemical, medical, and ecological studies.[29,30]

The potent water-soluble sodium channel blocker tetrodotoxin (**7**, Figure I.2) was first isolated from pufferfishes,[31] which are eaten in Japan, despite the fact they have been known for centuries to have toxic entrails.[27] Together with saxitoxin (**8**) and other paralytic shellfish toxins produced by dinoflagellates associated with red tides (*Gonyaulax* spp.), these toxins have allowed pharmacologists to study the location, shape, and function of sodium channels.[32] Brevitoxins A (**9**) and B (**10**), lipid-soluble toxins first isolated from Caribbean *Gonyaulax* spp., have also proved to be valuable tools as activators of sodium channels.[33]

The study of toxins still remains a major theme in marine chemistry. The introduction of modern high-field multi-dimensional NMR methods have recently facilitated the structure elucidation of maitotoxin (**11**, Figure I.3), a causative agent of ciguatera fish poisoning.[16] Ciguatera seafood poisoning is a form of neurological intoxication which is associated with the ingestion of carnivorous fishes which have concentrated levels of dinoflagellate (*Gambierdiscus toxicus*) toxins in their tissues.[34] Maitotoxin (**11**) acts as an extremely potent calcium channel activating toxin (LD_{50} in mice is ca. 50 ng/kg, ip) and is the largest natural product, other than a biopolymer, known.[34,35] With a molecular weight of 3422 (as the disodium salt), **11** is the only non-protein to rival

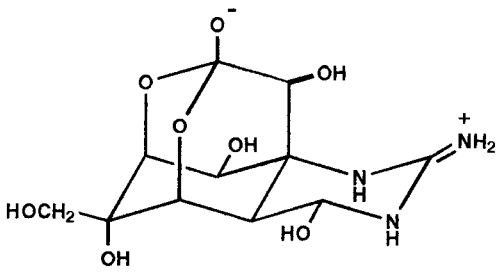

7
tetrodotoxin

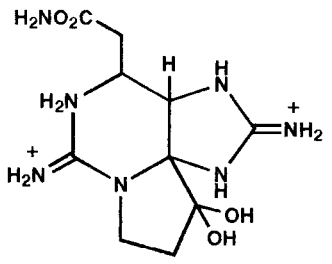

8
saxitoxin

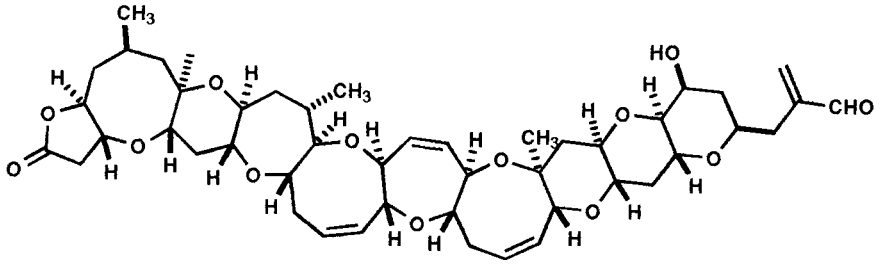

9
brevitoxin A

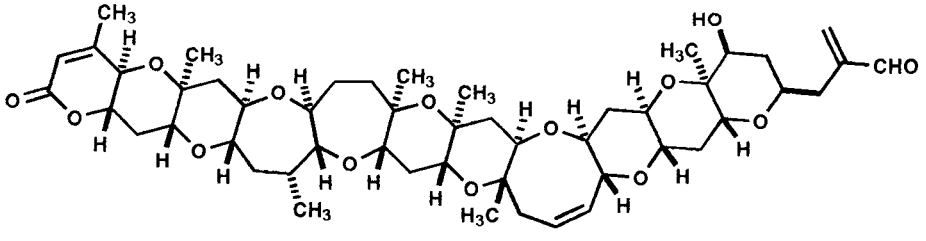

10
brevitoxin B

Figure I.2 Structures of Marine Toxins.

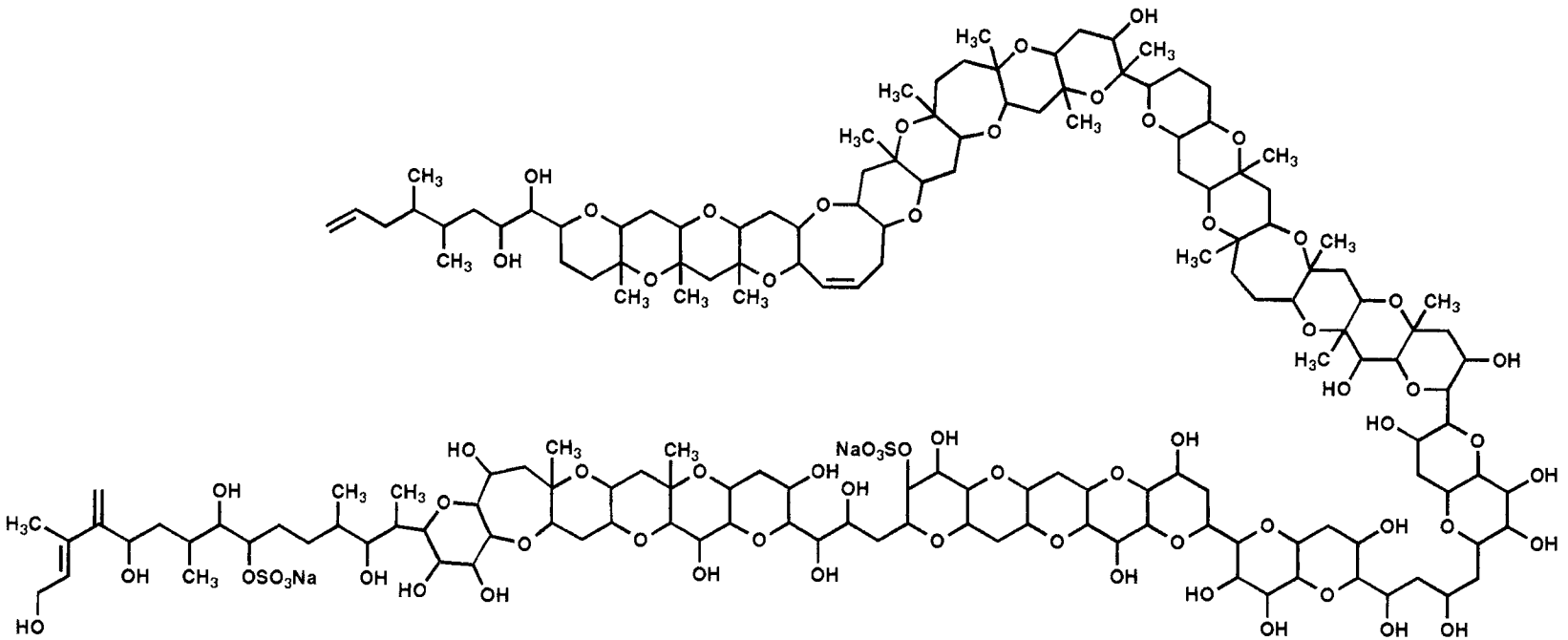

11

Figure I.3 Structure of Maitotoxin (**11**).

the soft coral metabolite palytoxin (**12**, Figure I.4) in toxicological potency and to exceed its molecular size. More recently, the toxin polycavernoside A (**13**) has been isolated from the red alga *Polycavernosa tsudai* (formerly *Gracilaria edulis*), following an intoxication of thirteen people, and the subsequent death of three in Guam.[36]

The search for ecologically significant chemistry represents another approach to marine natural products discovery. While still in its relative infancy, this field has contributed much to our understanding of the complex biochemical interactions which exemplify the marine environment. Marine chemical ecology involves, but is in no way limited to, chemical defence from herbivory or predation, chemical communication between organisms, and pheromonal chemical signals needed for reproduction. The ecological significance of only a fraction of the toxic or biologically active metabolites isolated have been described.[37,38]

Pharmacology and Natural Products Discovery

Perhaps the major approach to marine natural products research has remained, like its terrestrial equivalent, the pursuit of new pharmaceutical leads. Spurred by discovery of the antimetabolites spongothymidine (**14**) and spongouridine (**15**) (from the marine sponge *Cryptotethia crypta*) which led to the synthesis of the anticancer drug Ara-C (**16**) and the antiviral agent Ara-A (**17**), the marine environment rapidly became a viable alternative source of new leads for medical research (Figure I.5).[23,39] However, few truly promising leads emerged over the next twenty years. Only within the last few years have marine-derived natural products again come to the forefront of medical research. Potential drug candidates from marine animals, algae, and bacteria have begun to reach either clinical or preclinical evaluation. Just a few recent examples of marine-derived antineoplastic leads would include the bryostatins (bryostatin 1: **18**), dolastatin 10 (**19**), cephalostatin 1 (**20**),

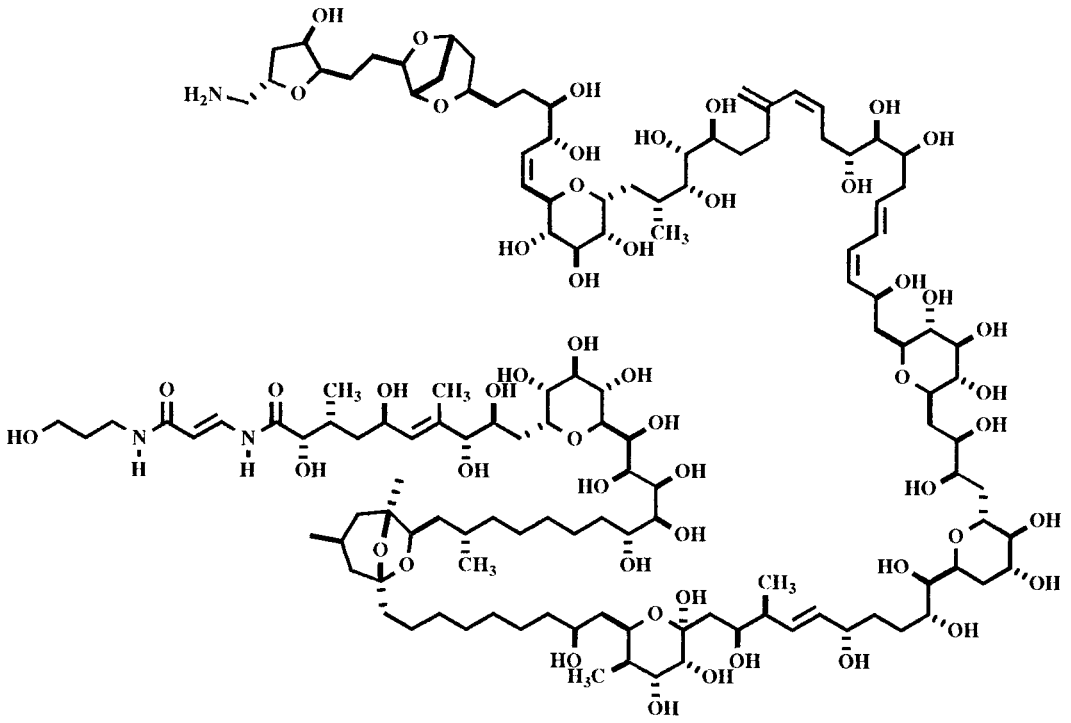

12

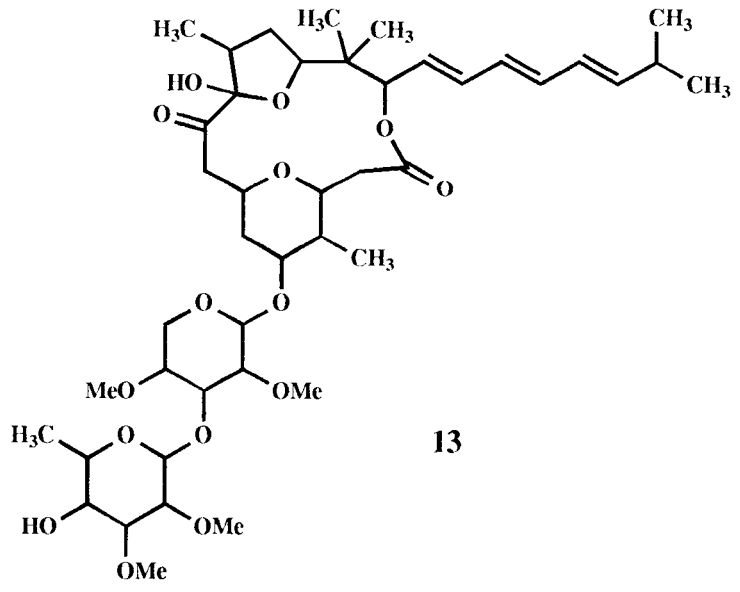

13

Figure I.4 Structure of Palytoxin (**12**) and Polycavernoside A (**13**).

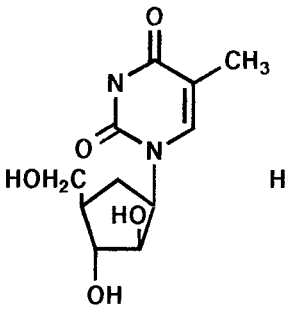

14

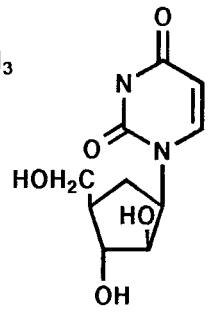

15

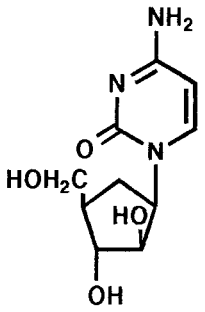

16

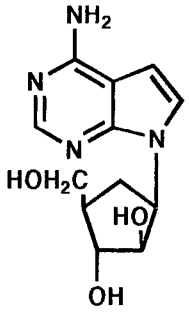

17

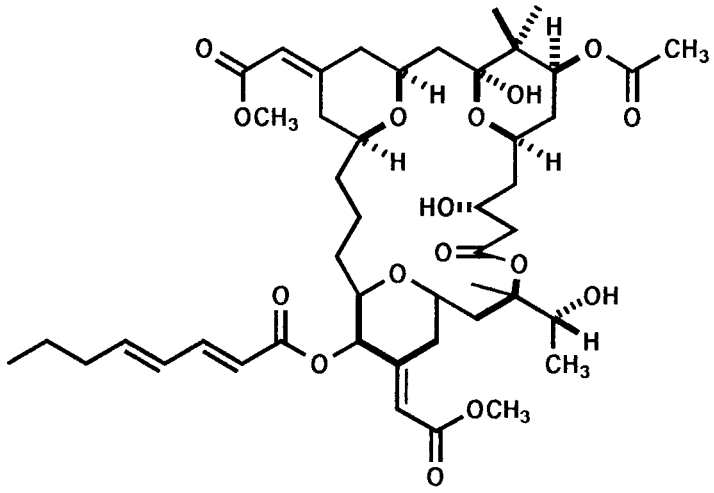

18

bryostatin 1

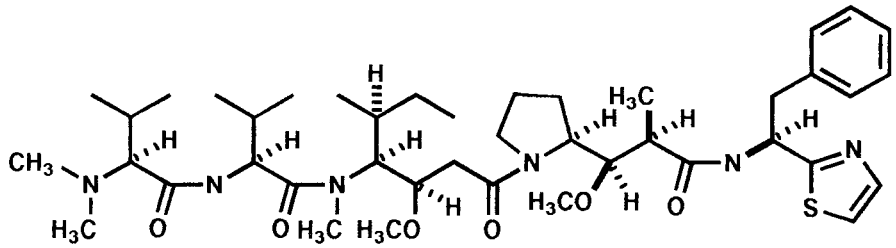

19

dolastatin 10

Figure I.5 Structures of Compounds From Marine Pharmacological Leads.

didemnin B (**2 1**), and halomone (**2 2**) a polyhalogenated monoterpene from the red alga *Portieria hornemannii* (Figure I.6).[40-43]

Oxylipins

It has been a relatively recent development in the study of natural products to recognize that marine organisms are a rich source of eicosanoids and related fatty acid derivatives, collectively known as oxylipins.[44,45] "Oxylipin" is defined as an encompassing term for oxidized compounds which are formed from fatty acids by reaction(s) involving at least one step of mono- or dioxygenase-dependent oxidation.[45] Thus, this term includes eicosanoids, C-20 metabolites of arachidonic acid (AA, **2 3**) and eicosapentaenoic acid (EPA, **2 4**), as well as biosynthetically related compounds of longer and shorter chain length (Figure I.7). In mammalian systems, prostaglandins (PGs) and thromboxanes (TXAs) are formed from AA via fatty acid cyclooxygenase; hydroperoxyeicosanoids (HPETEs), leukotrienes (LTs), and lipoxins (LXs) are produced by the action of lipoxygenase enzymes; and some hydroxyeicosanoids (HETEs) are produced by the action of several different cytochrome P450 monooxygenases (Figure I.8).[46] PGs, LTs, HETEs, and other metabolites of this class have been recognized to play a crucial role in both mammalian physiology and disease. Eicosanoids have been shown to participate in the regulation of a wide range of biological and physiological processes, including ion flux, vascular constriction, and the chemotactic movement of white blood cells.[46] These functions have been demonstrated to result from the intracellular second messenger activity of eicosanoids in signal transduction pathways.[46] Because of these findings, the interest in the structural chemistry, biosynthesis, and pharmacological activities of these marine products has recently become intense.

Marine oxylipin research traces its origins to the pioneering discovery of prostaglandin A_2 esters from the Caribbean gorgonian, *Plexaura homomalla.*[47] It is now

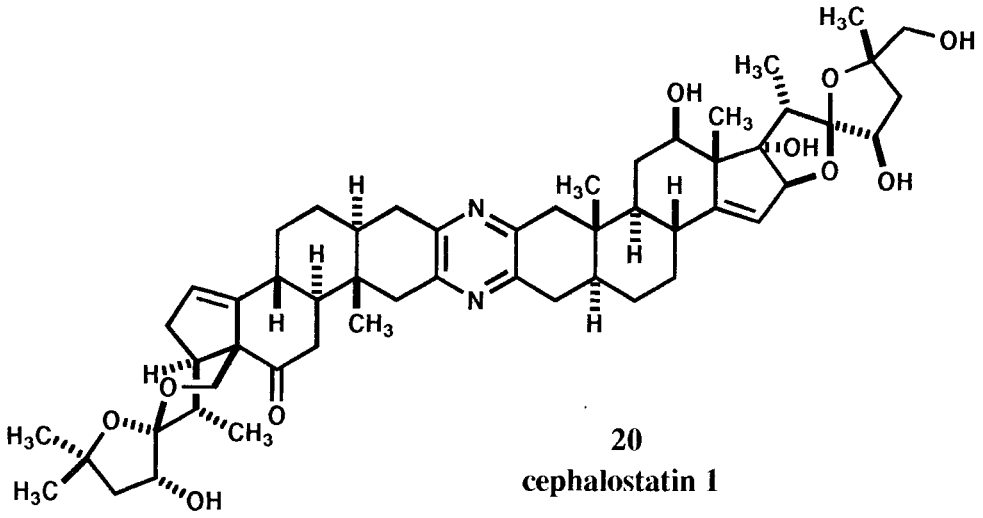

20
cephalostatin 1

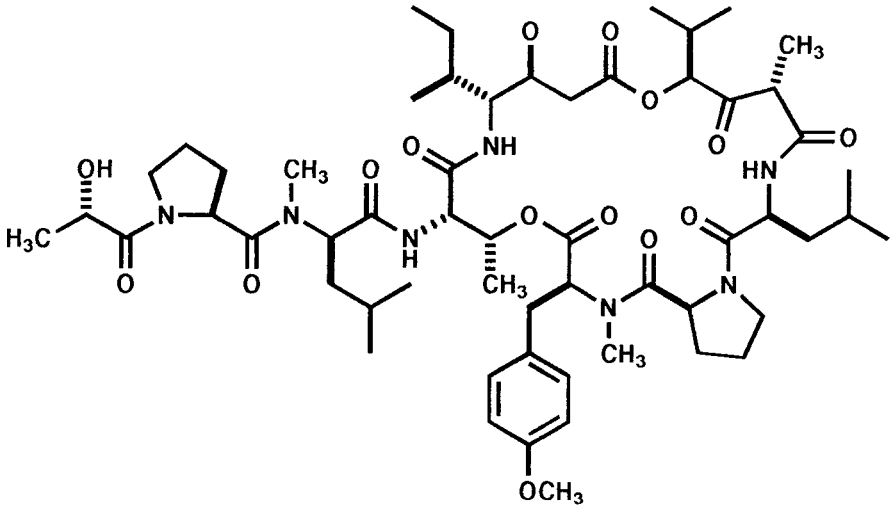

21
didemnin B

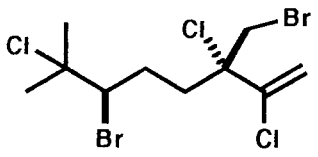

22
halomone

Figure I.6 Pharmacologically Active Lead Compounds.

23

24

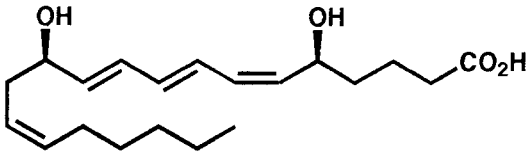

25

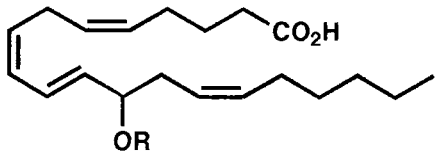

26 R=OH
29 R=H

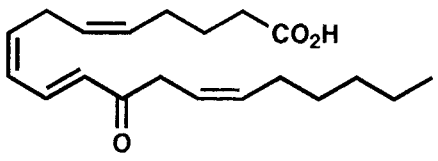

27

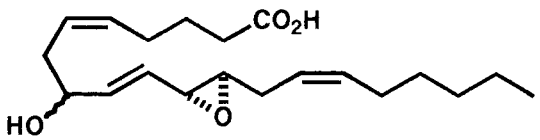

28

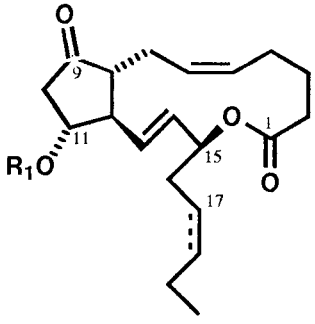

30

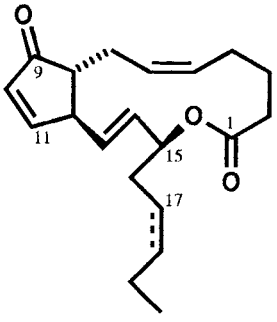

31

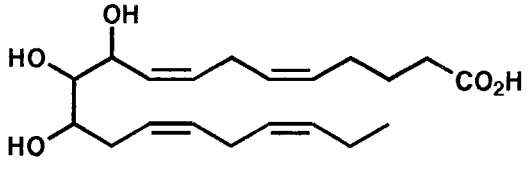

32

Figure I.7 Structures of Marine Fatty Acids and Oxylipins.

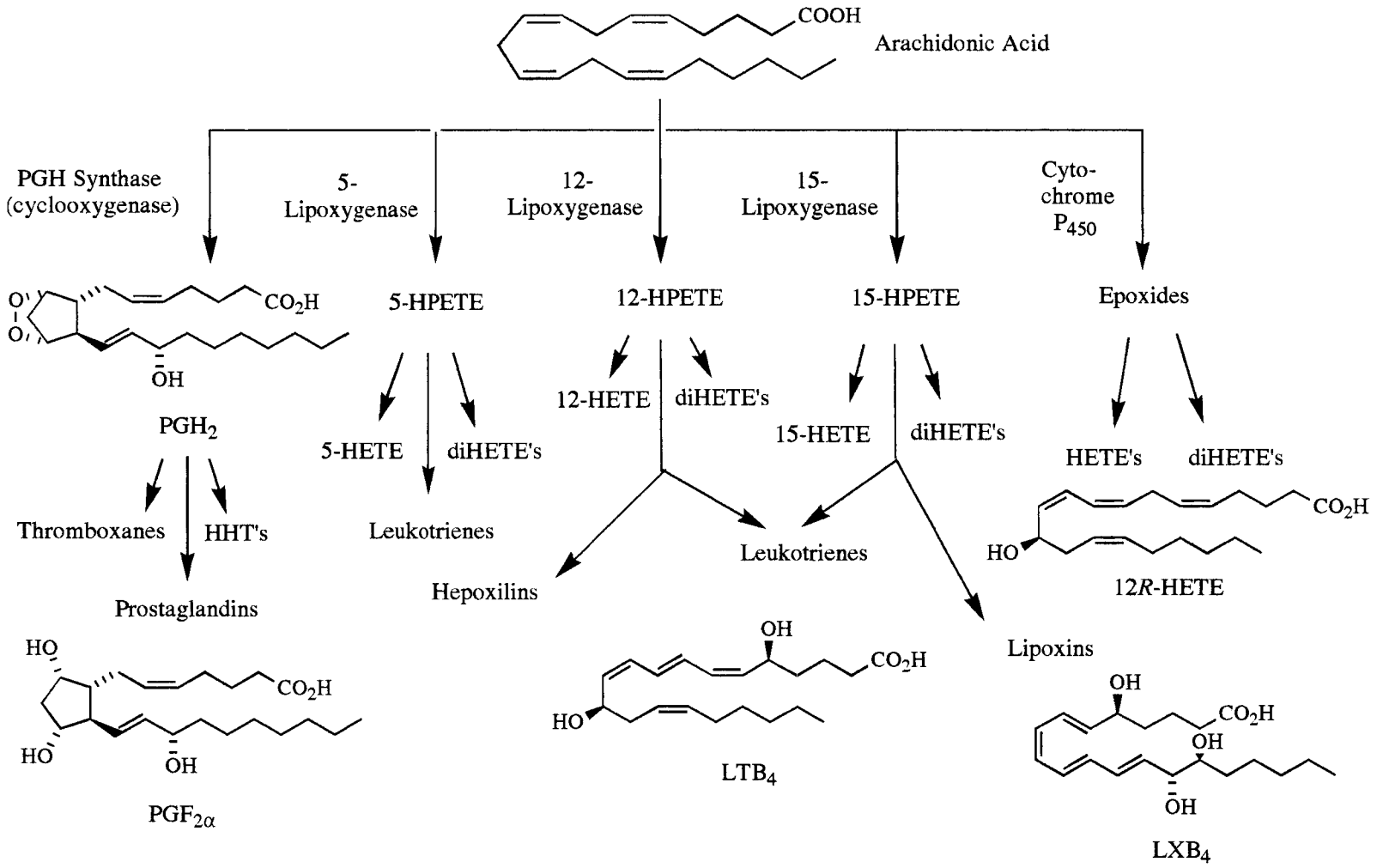

Figure I.8 Arachidonic Acid Metabolism in Mammalian Systems.

established that oxylipins are produced in a broad spectrum of life forms that inhabit the sea, including algae, bacteria,[48] invertebrates,[45] and fishes.[49,50] It is the marine algae which have predominated in the scientific efforts of our group for the past five years and has been the subject of several reviews.[51-55] Our research has evolved from an early discovery of the occurrence of mammalian immunoregulatory eicosanoids in red algae to the development of a vastly more complex appreciation of the structural diversity and novelty of marine carbocyclic oxylipin chemistry. Due to the wealth of new oxylipin structures encountered in marine organisms, the uniqueness of the biosynthetic pathways which lead to their formation, and the potency of their biological effects,[56] much is to be learned from study of this metabolism in the marine environment.[57]

Little is known concerning the biochemical, ecological, or physiological significance of oxylipin metabolism in marine organisms. However, several interesting correlations have emerged. Over 80 years ago Wilson demonstrated that when a living sponge was strained through a gauze cloth the dissociated sponge cells would move with amoeboid motion and form new sponge colonies.[58-60] When two distinct sponge species were similarly dissociated and mixed they reformed as homogeneous single sponges.[61,62] Inclusion of rabbit antiserum specific to only one sponge inhibited the aggregation of only that sponge species, similar to an antigen-antibody type reaction.[63] It was reported that the aggregation of dissociated marine sponge cells is a calcium-dependent process resembling the immunological response of human neutrophils and platelets.[64,65] The 5-LPO product leukotriene B_4 (LTB_4) (**2 5**), a known calcium ionophore,[66] was shown to cause sponge cell aggregation in *Microciona prolifera*.[67] Hence, it has been suggested that an endogenous LTB_4 analog may be involved in sponge cell aggregation phenomena.[67]

The relatively simple nervous system of the marine mollusc *Aplysia californica* has proven to be an invaluable model for neurochemical investigation. The large and readily isolated neurons of *Aplysia* have provided a wealth of biochemical information concerning

the function of oxylipins, especially AA metabolites, in neurochemical signal transduction. The role of AA metabolism in molluscan signal transduction has been the subject of several reviews.[68-70] Both active lipoxygenase and cyclooxygenase systems appear to be present in *Aplysia* neurons as evidenced by the conversion of AA to 5- and 12-HETE and PGE_2 and PGF_2 in nerve cell bodies and synaptosomes.[71] Synaptic stimulation with histamine was shown to induce the conversion of labeled ^{3}H-AA to ^{3}H-12-HETE in cerebral ganglia. It has been suggested that lipoxygenase metabolites may act as second messengers for presynaptic inhibition of sensory neurons of the abdominal and pleural ganglia.[72] It appears that LPO products may impart a second messenger-type regulation of the responses produced by the molluscan inhibitory tetrapeptide FMRF amide (Phe-Met-Arg-Phe amide) which opens S-channels (specialized 5-hydroxytryptamine (5-HT) sensitive K^+ channels). Aracidonic acid mimics the effect of FMRF amide and is converted to the hydroperoxide 12-HPETE (**2 6**) following FMRF amide stimulation.[72,73] In addition, the lipoxygenase inhibitor NDGA (nordihydroquariaretic acid) blocks the effect of both FMRF amide and AA, while the cyclooxygenase inhibitor indomethacin has no effect. Additionally, 12-HPETE mimics the actions produced by both AA and FMRF amide, although it remains unclear whether 12-HPETE or one of its many metabolites actually act as second messengers.[74] Several 12-HPETE derived compounds, including 12-KETE (12-ketoeicosatetraenoic acid) (**2 7**) and hepoxilin A_3 (8-hydroxy-11,12-epoxyeicosa-5,9,14-trienoic acid, **2 8**), appear to modulate the K^+ S-channels in *Aplysia* neurons, while another 12-HPETE metabolite, 12-HETE (**2 9**), produces no response.[75-78] It was suggested that unlike other second messengers, eicosanoids may also function as first messengers, facilitating direct communication between adjacent cells.[69] Further, it is hypothesized that this first messenger-type activity may relate to "long-term potentiation" phenomena as observed in mammalian hippocampus derived NMDA-type glutamate receptors where prolonged postsynaptic responses are observed following presynaptic stimulation.[74] It

appears that the study of *Aplysia* neurochemistry may eventually lead to a better understanding of neuropharmacological processes in higher animals.

Soft coral PGs have been shown to induce vomiting in reef fishes and have been suggested to act as feeding deterents.[79] Soft coral oxylipin chemistry has been extensively reviewed.[45] The PGs produced by soft corals are believed to derive from allene oxide containing precursors, rather than from cyclooxygenase and the endoperoxide intermediate PGH_2.[45]

Research into the chemical ecology of Mediterranean opisthobranchs has yielded a great deal of information concerning the sophisticated, often chemically mediated, defensive strategies that these shell-less molluscs use to avoid predation.[80-84] When handled, the dorsal cerata of *T. fimbria* are autotomized. These appendages continue to contract for up to 8 hours by way of epithelial smooth muscle fibers.[85] PG-1,15-lactones in the cerata are converted to their free acid form. PG free acids are well-characterized inducers of smooth muscle contraction and relaxation in vertebrates. Simultaneously, a mucous-slime containing high levels of PG-lactones is secreted from epithelial glands in the cerata. Experiments have shown PG-1,15-lactones of the E (**30**) and A (**31**) series are toxic to mosquito fish at concentrations of 1 and 10 $\mu g\ ml^{-1}$, respectively.[85] A dual role for PGE-lactones in *T. fimbria* has been suggested: (1) as direct acting ichthyotoxic defense allomones; (2) as a source of PG free acids which contract the cerata and may facilitate mucous release. PGs have also been demonstrated to participate in the osmotic regulation, reproductive biology, and spawning of marine gastropod molluscs.[45]

Early studies in the search for the "barnacle hatching factor", a substance released into the mantle cavity that stimulates hatching, suggested that a prostaglandin-like compound might be responsible.[86] Subsequent research elucidated the structure of the hatching factor from *Balanus balanoides* as 10,11,12-trihydroxyeicosa-5,8,14,17-tetraenoic acid (**32**).[87]

With the exception of PGs and jasmonic acid derivatives, few examples of carbocyclic oxylipins have been characterized from terrestrial sources.[88] However, an emergent theme in the marine environment appears to be that of complex carbocyclic and heterocyclic oxylipin production.[54] Many of these metabolites seem to be formed as a result of uniquely marine biochemical processes acting upon hydroxy-fatty acid precursors similar to those found in mammalian systems. Representatives of these highly functionalized oxylipins have recently been isolated from many completely unrelated marine organisms. The formation of these unusual metabolites and the co-isolation of lipoxygenase-type metabolites has provided evidence which suggests that, in the algae, prostaglandins and other carbocyclic oxylipins may result from further modifications of hydroperoxide intermediates produced by lipoxygenase-type enzyme systems, rather than from cyclooxygenases as in mammalian systems or from allene oxide intermediates as demonstrated in most soft corals.[53-55]

General Thesis Contents

This thesis consists of five chapters and an appendix. Following this general introduction, chapter two describes our efforts to discover new lead compounds from a survey of the biomedical potential of marine algae and represents an update of an ongoing investigation designed to assess the medicinal potential of marine algae. To date, a total of over 300 species of macrophytic marine algae and over 250 strains of microalgae have been cultured, extracted, analyzed by thin layer chromatography (TLC), and screened for bio-activity. Evaluations were performed in-house for antimicrobial, molluscicidal, ichthyotoxic, and brine shrimp lethality activities. Extensive pharmacological testing, with the assistence of several key external collabors were done. Methods of evaluating samples and significant findings will be discussed. Chapter two also outlines a series of bioassays used in the isolation of novel biologically active natural products.

The third chapter consists of an extensive investigation of carbocyclic-oxylipin metabolism in *Constantinea simplex*, a temperate red alga evaluated as part of the Pacific algal survey. Chapter three represents the most detailed study of marine cyclopropyl-containing oxylipin chemistry to date. The results of my isolation and chemical structure determination of these unique metabolites, trivially called constanolactones, the biosynthetic implications, and biochemical significance of *C. simplex* fatty acid chemistry are considered.

The occurrence of nakienones, new cytotoxic C-11 metabolites found in extracts of blue-green algal (*Synechocystis* sp.) material which was overgrowing living colonies of an *Acropora* sp. of Okinawan staghorn coral, is described in chapter four. This chapter details the isolation, spectroscopic chemical characterization, and biomedicinal evaluation of these compounds.

Chapter five describes our recent discovery of potent new toxins, inhibitors of cancer-associated enzymes, and exciting lead compounds for anticancer research. Experimental methods and the investigation of recently characterized active metabolites are described.

The structure elucidation of new sphingolipids and a heterocycle from the Oregon marine sponge *Halichondria panicea* follow the general thesis as part of an appendix. This work appears in appendix form as some of the findings are the result of work initiated as an undergraduate research project and the subject material may be considered outside the scope of the general thesis.

CHAPTER II.

A SURVEY OF MARINE ALGAE FOR BIOMEDICAL POTENTIAL

Abstract

I have participated in a drug discovery program designed to screen both macrophytic and microscopic marine algae for inhibitors of cancer-related enzymes, antitumor compounds, antiinflammatory substances, and other agents of potential pharmaceutical utility. Over 1,500 lipid and aqueous extracts of marine plants and animals were surveyed for biomedical potential. Assays designed to screen extracts for new types of marine toxins have served to guide the isolation and identification of unique biologically active compounds from marine algae.

Introduction

Influenza, smallpox, and some sanitation-related bacterial diseases that once killed millions of people no longer represent major causes of morbidity or mortality in modern society. Heart disease, cancer, diabetes, AIDS, and an assortment of parasitic infections (ie. drug resistant malaria, schistosomiasis) are now major causes of illness worldwide. Only through increased efforts to develop new drugs and other effective means of treatment for these conditions can we hope to relieve some of this burden. Additionally, competition with insects and other organisms for crops has created a tremendous demand for new environmentally and ecologically compatible insecticides, molluscicides, and nematocidal agents.

The approach I have adopted is to envision natural products chemistry not necessarily as an exploration for new sources of medicinal agents, but as a search for chemical "ideas" or leads. For instance, the insecticide PADEN was developed from the fly-toxic marine annelid compound nereistoxin and the antimetabolites Ara-C and Ara-A were derived from chemical ideas generated by the discovery of sponge nucleosides (Chapter 1). These chemical ideas, biologically or pharmacologically active metabolites with novel structural features, serve as templates for the rational design of new drugs, insecticides, and other biological products. Natural products are examined for structure-activity relationships and used to guide synthetic efforts to produce products with enhanced biochemical properties. This approach is, by design, ecologically and environmentally preferable to the evaluation of plants and animals as new sources of crude materials or commercial products. The cultivation of many terrestrial plants may be commercially profitable, yet it is unlikely that many marine organisms, especially slow-growing marine invertebrates, could be economically farmed and may therefore require ecologically disastrous field harvest to provide the enormous quantity of materials that are necessary for the product development and marketing of medicinal agents.

Over half a million deaths are expected to occur in the U.S. each year as a result of various forms of cancer.[89] Cancer is currently second only to coronary disease as a cause of death in the U.S. These statistics cannot even begin to demonstrate the immense pain and suffering associated with this level of morbidity. A recent report entitled "A War Not Won" points out that even when adjusted for changes in the population size and age, National Cancer Institute (NCI) data suggests that despite the millions of dollars spent on cancer research over the past few decades a 7 percent increase in cancer mortality rates occurred between 1975 and 1990.[89]

Boyd, in a recent perspective on NCI new drug development, reported that although chemotherapy may be the treatment of choice for many forms of cancer and has a high cure rate for some rare forms of leukemia and lymphoma (50-75%), few agents are effective for the treatment of most common tumors.[90] Further, most of the approximately 40 cytostatic and cytotoxic agents target rapidly proliferating cells, often by similar mechanisms, and are not useful for "solid mass" tumors such as those of the lung, colon, breast, and prostate. These diseases currently account for most U.S. cancer deaths. Characteristically narrow therapeutic margins and rapidly developing multidrug resistance often seriously impair even the most effective forms of treatment. These limitations have spurred considerable effort to discover new chemically diverse agents with novel mechanisms of action.[90] Thus, our research group initiated a drug discovery program designed to assess the anticancer drug potential of marine algae.

Objectives

Two major themes, a biochemical evaluation of Pacific Northwest marine algae and an investigation of cyanobacteria for new anticancer leads, comprise the bulk of our research efforts. Since the summer of 1985 our group has conducted a survey of temperate

marine macroalgae for their biomedical potential. What began initially as an investigation of Oregon seaweed species developed over time into an extensive chemical exploration of Pacific coast algae species collected over a far greater range. Specimens have since been collected from central California, Oregon, Washington, British Columbia, and Alaska.

Four years ago our laboratory also became part of a NCI sponsored joint drug discovery group.[90] This NCNPDDG (National Cooperative Natural Products Drug Discovery Group) program design brings academic, industrial, and government drug research groups together to facilitate the investigation of innovative "high-risk" techniques for the discovery of new anticancer agents. My role as a "primary" investigator in this program was to collect, extract, isolate, and identify new chemotherapeutic leads from marine cyanobacteria.

Materials and Methods

Small collections (ca. 2-8 L) of temperate marine algae were obtained from intertidal and subtidal locations in northern California, Oregon, Washington, British Columbia, and Alaska (Figures II.1 and II.2). Specimens were frozen on site with dry ice for transport back to our storage facility (-20 °C). Each sample was coded to indicate the date and site of collection: two letter code indicating an Oregon site or three letter code indicating other sites; date of collection; numerical designation. Voucher specimens from each collection were taken and stored frozen (-20 °C) for future identification. Taxonomic classification of uncertain species were performed by Dr. Gayle Hansen (Dept. of Botany and Plant Pathology, Oregon State University).

Tropical algae collected from sites shown in Figure II.2 were placed in 1 or 2 L plastic bottles and preserved on site by immersion with isopropyl alcohol. Several collections were preserved in either methanol or ethanol due to problems with local solvent availability. Preserved specimens were kept frozen whenever possible throughout the

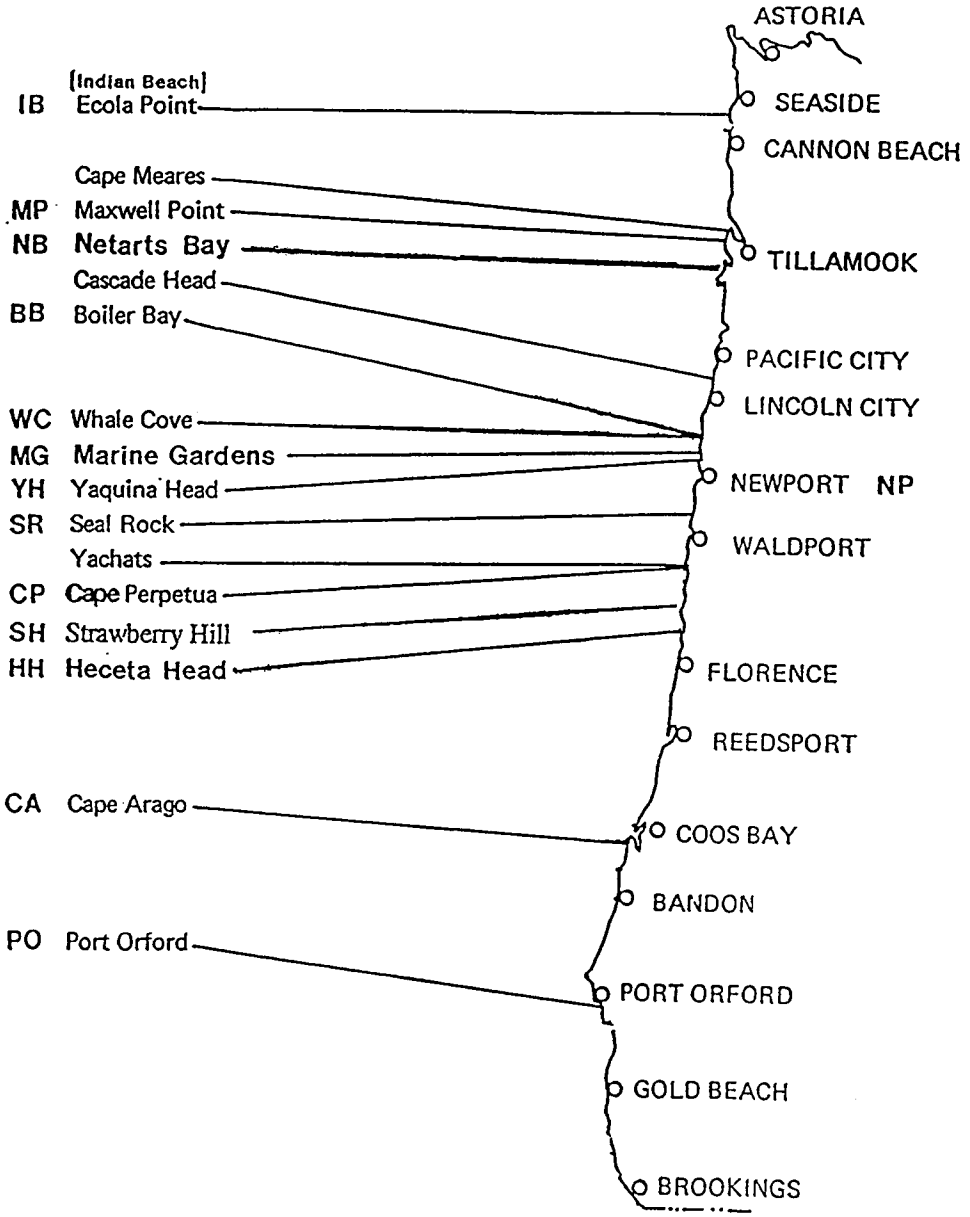

Figure II.1 Major Algae Collecting Sites on the Oregon Coast.

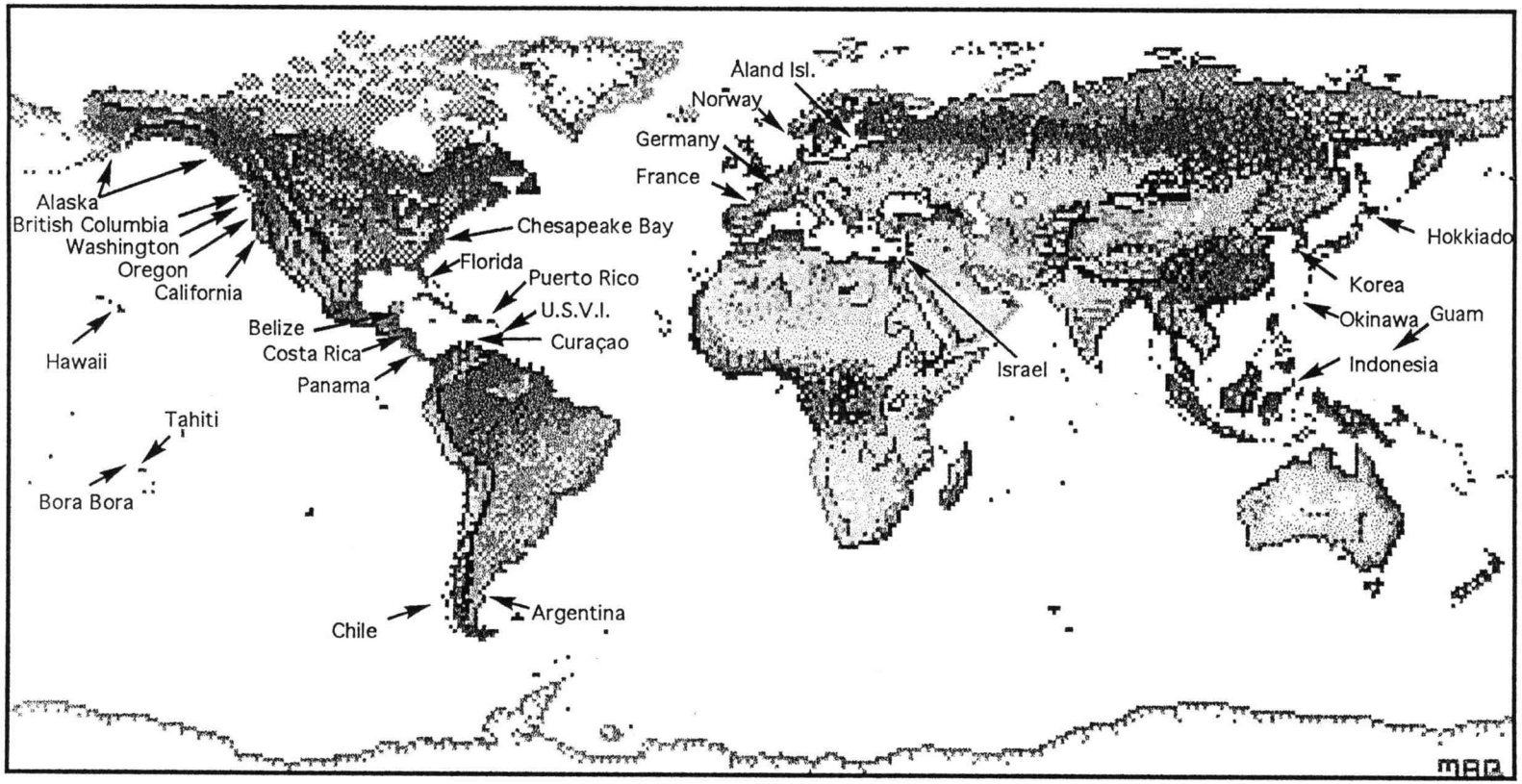

Figure II.2 Sources of Temperate and Tropical Algae for Chemical and Pharmacological Evaluation.

duration of collecting trips and stored at -20 °C until extracted following return to our laboratory. Voucher specimens of preserved algae were removed prior to extraction. Classification of taxonomically difficult macroalgae species were accomplished by Dr. David L. Ballantine (Dept. of Marine Sciences, University of Puerto Rico). Mary A. Roberts (College of Pharmacy, Oregon State University) classified cyanobacteria and other microalgae.

Several selection criteria were employed to guide algal collection efforts. These criteria varied somewhat for the evaluation of macroalgae and cyanobacteria. However several key factors remained consistent. Organisms which were not previously investigated for natural products were given high priority. Algae from genera known to be rich in secondary metabolite production were also evaluated. Biodiversity was considered in sample selection in order to take advantage of variation in biosynthetic potential. Chemical-ecological interactions were also taken into consideration in the field. Algae with little or no physical defense and which were growing in herbivore rich environments were given high priority. Attempts were made to sample algae from a wide variety of habitats. Therefore, specimens were collected from exposed high-surf conditions, intertidal splash zones, sheltered coves, and low-intertidal locations. Subtidal habitats were harvested by snorkeling or SCUBA. Estuaries, bays, and other brackish water environments were also selected for sampling.

Extraction Method

Lipid extracts were produced in a standardized fashion as depicted in Figure II.3. Frozen algae collections (2-8 L) were macerated in $CHCl_3$/MeOH (2:1, v/v), allowed to soak at least one hour, and filtered through cheese cloth. The algal material was placed in fresh solvent ($CHCl_3$/MeOH (2:1, v/v)), heated to a gentle boil for up to 20 minutes, and

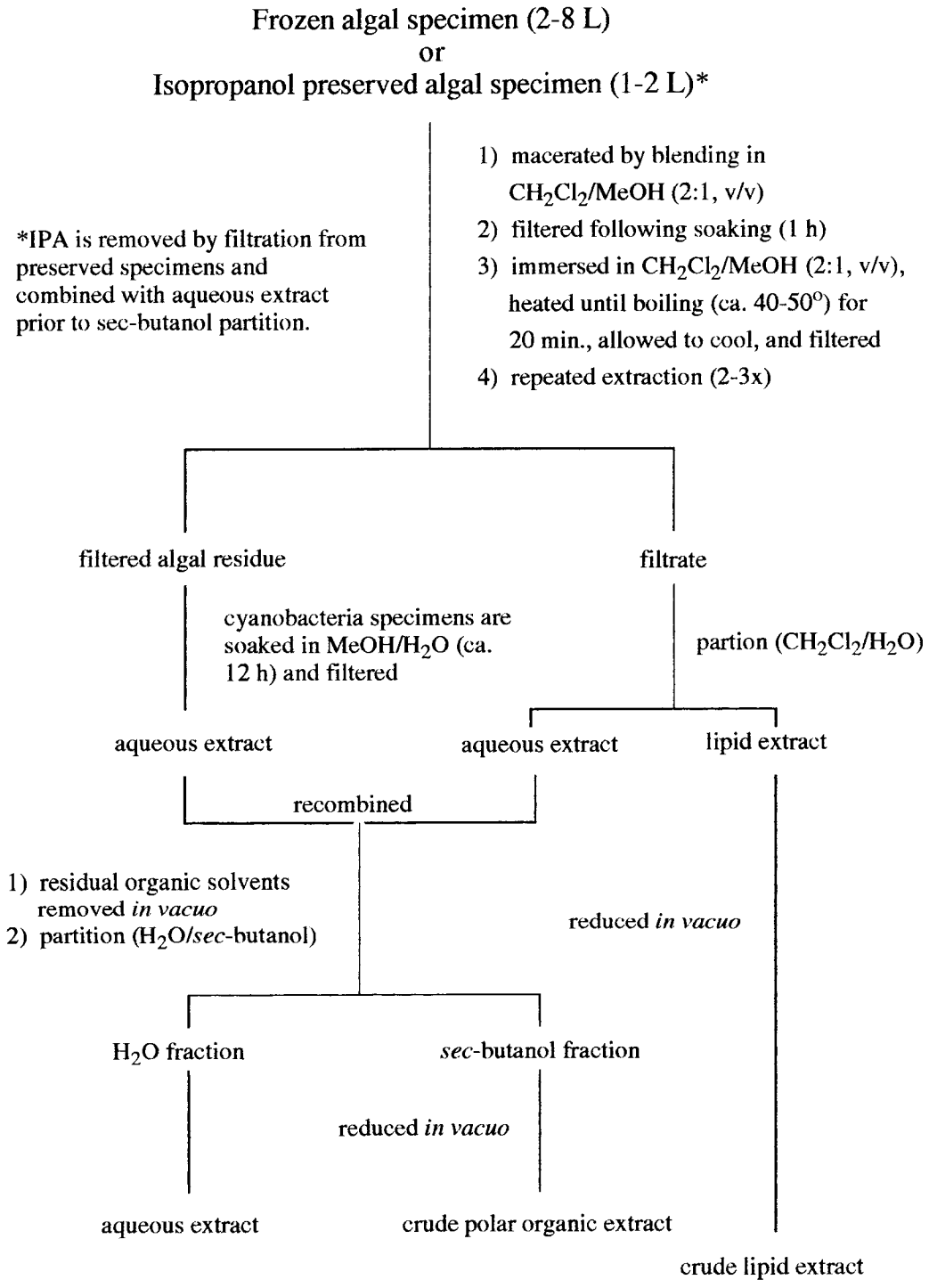

Figure II.3 Generalized Extraction Scheme.

filtered. This process was repeated two to three times. The filtrate was partitioned with water and the lipid fraction was reduced *in vacuo* and stored in Et_2O.

Alcohol preserved samples (1 to 2 L) were drained or filtered prior to extraction. This alcohol was removed from the filtrate by evaporation *in vacuo* and added to the aqueous extract.

Cyanobacteria collections were extracted as above. However, extracted algal solids were soaked in MeOH/H_2O (3:1, v/v) overnight, filtered, and the alcohol removed *in vacuo*. These aqueous extracts were partitioned between *sec*-butanol and water. The *sec*-butanol fractions were reduced *in vacuo* and stored in MeOH or EtOH.

In Vitro Antimicrobial Assays

Antimicrobial disc assay were performed according to standard protocols.[91,92] Crude lipid extracts were dissolved in Et_2O (polar and aqueous extracts were placed in either MeOH or water) and applied to sterilized paper discs (Difco Lab., Detroit, MI) and allowed to air dry. Extracts of algae collected after 1986 were quantitatively assayed at 2 mg/disc. These were applied to Mueller Hinton Agar which were inoculated with one of the following pathogenic microorganisms: *Bacillus subtilis* (Bs); *Candida albicans* (Ca); *Escherichia coli* (Ec); *Pseudomonas aeruginosa* (Pa); *Salmonella typhimurium* (St); or *Staphylococcus aureus* (Sa). Assays were run with negative (air dried solvent) and positive controls (streptomycin for bacteria and nystatin for *C. albicans*). The petri dishes were incubated at 37 °C. After 12 to 15 hours zones of growth inhibition were measured as total zone diameter and include the paper disc.

Ichthyotoxicity Assays

Observations of fish toxicity have lead to the discovery of important biologically active compounds[93] and may suggest possible ecological interactions deserving further

investigation. Insect antifeedants, antitumor agents, plant growth inhibitors, and insecticides have been isolated from ichthyotoxic plants.[93]

Fish toxicity assays were performed using a modification of the method described by Bakus and Green.[94] The test organisms were small (ca. 3.5 cm) goldfish (*Carassius auratus*). Stock solutions were prepared by dissolving crude lipid extracts in EtOH or MeOH. Aqueous extracts were dissolved in distilled water. Stock solutions (20 or 50 μL) were dissolved in 20 mL distilled water (30 mL beaker). Fish were added to each beaker and monitored for 1 hour. Tests were performed in duplicate and run against alcohol (20 or 50 μL)-distilled water controls. End points were established as death (lack of breathing) and inability to swim against a manually induced current for LD and EC measurement, respectively.

Molluscicidal Assays

The freshwater mollusc *Biomphalaria glambrata* is an intermediate host for three species of parasitic trematode blood flukes (schistosomes). Over 200 million people in over 75 countries are infected with schistosomiasis (bilharzia).[95] Chronic infection may result in disturbances of the central nervous system, liver fibrosis, portal hypertension, and possibly liver cancer.[96] The difficulty and costs involved in treating these large groups of people in remote impoverished areas has prompted a concerted effort by the World Health Organization (W.H.O.) to look for new means of preventing infection by controlling the snail vector.[97]

The molluscicidal potential of algae extracts were evaluated by a method similar to the procedure described by Hostettmann et al., and recommended by the W.H.O.[93,97] Crude extracts were dissolved in EtOH and diluted to 20 or 40 ml with distilled water in a beaker to make a 100 μg/mL (100 ppm) solution. Two *Biomphalaria glambrata* (strain 13-16-K89, courtesy Dr. Christopher J. Bayne, Prof. of Zoology, Oregon State University)

were placed in each beaker and the beakers covered for the duration of the assay. The condition of the molluscs were evaluated after 24 hours. Snails were considered dead when no heart beat could be observed on microscopic investigation. Minimum lethal dose requirements to kill the snails (LD_{100}) were recorded. Snails were disposed of by placing them in isopropanol.

Brine Shrimp Lethality Bioassays

Brine shrimp lethality assays were routinely used as a rapid in-house screen for selection and fractionation of toxic crude algal extracts. Brine shrimp (*Artemia salina* Leach) assays were run according to general methods developed by McLaughlin et al.[98] Further description of this assay, its use in the discovery of physiologically active compounds, and a discussion of its relevancy as a screen for cytotoxic agents is provided in a recent review.[99] Brine shrimp eggs were incubated in artificial sea water 24-36 hours prior to assay. Crude algal extracts were dissolved in EtOH and diluted in test vials with sea water to concentrations of 1000 (optional), 200, and 50 ppm for initial screening. Assays were conducted in duplicate and with EtOH/sea water controls. Live brine shrimp (n = 10-15) were added and the vials were stored at 37 °C for 24 hours at which time the number of living and dead shrimp were recorded. Brine shrimp toxicity was then used to guide extract fractionation and purification methods. Finally, purified active compounds were serially diluted to concentrations where LD_{50} measurements could be obtained.

Thin Layer Chromatography Analysis

One-dimension thin layer chromatograms (TLC) on silica gel 60 F_{254} (E. Merck) were developed in MeOH/$CHCl_3$ (1:1, v/v) and either Et_2O/benzene (1:1, v/v) or EtOAc/hexanes (1:1, v/v). Two-dimensional TLC was performed on 10 cm x 10 cm silica gel sheets and developed first in MeOH/$CHCl_3$ (1:1, v/v), air dried, then developed in

EtOAc/hexanes (1:1, v/v). Pigmented compounds were bracketed by pencil and color coded. Ultraviolet absorptions were observed at 254 nm and recorded by circling with pencil. The plates were sprayed with H_2SO_4 (50%) and gently heated on a hot plate. Colorless compounds that charred following heating were assigned pencil check marks (√) and coded by the color reaction observed. The following color codes were used: pk = pink, pu = pr =purple, o = or =orange, y = yl = yellow, gr = gy = gray, g = green, br = √ = brown, bl = bk = black, b = blue.

Following visual inspection, thin layer chromatograms were coded to indicate the presence of potentially interesting new compounds. The chromatograms were coded as follows: (+) lowest priority, primary metabolites; (++) minor secondary compounds present, marginal interest factor; (+++) several minor secondary natural products present, worthy of pursuit; (++++) major new compounds present, highest priority.

15-Lipoxygenase Enzyme Inhibition Assay

Lipoxygenases (LOs) convert arachidonic acid released from membrane phospholipids into leukotrienes, hepoxilins, hydroxyeicosanoids, and other modulators of the inflammation process which play a crucial role in both mammalian physiology and disease.[46] Therefore, inhibitors of lipoxygenase enzymes represent targets for the development of new antiinflammatory agents. In collaboration with Syntex Research (Palo Alto), we screened marine algae extracts for the ability to inhibit recombinant human 15-LO. The ability of algal substances to inhibit the conversion of linoleic acid to 13(*S*)-9Z,11Z-hydroperoxyoctadecadienoic acid (13-HPODE) was determined by colorimetric assay. Extracts were considered active if they decrease the production of 13-HPODE to less than 20% at 40 μg/mL.

Anti-HIV Activity Assay

Human Immunodeficiency Virus (HIV-1) infected continuous human T-lymphocytic cells were incubated (ca. 7 days) with dilutions of algal extracts (Syntex Research). Differential toxicity between infected and mock infected cells was recorded. Anti-HIV activity was confirmed by subsequent reverse transcriptase (RT) assay. EC_{50} levels were defined as the concentration of extract or compound which reduces RT counts ($[^3H]$-thymidine incorporation, scintillation spectrophotometer) by 50%, without extract/compound-associated toxicity. Zidovudine (AZT) was used as a positive control. Extracts which reached EC_{50} concentrations at greater than one dilution level below minimal toxic concentration were considered active.

Anti-Herpes Simplex Assays

Monkey Vero cells infected with either Herpes Simplex I or II Viruses (HSV-I or HSV-II) were incubated with algal extracts and observed for virus-associated morphological changes and differential cellular toxicity (Syntex Research). Acyclovir was used as a positive reference compound. Extracts were considered active if they reached the effective concentration of extract required to inhibit virus-associated morphological cellular changes to 50% (ED_{50}), without causing cellular toxicity.

Inosine Monophosphate Dehydrogenase Inhibition Assay

Potential anticancer-type activity of marine algal extracts was evaluated (Syntex Research) by a mechanism-based inosine 5′-monophosphate dehydrogenase (IMPDH) enzyme inhibition assay . IMPDH converts inosine monophosphate (IMP) to xanthosine 5′-monophosphate (XMP), a rate-limiting enzyme in purine biosynthesis. The inhibition of IMPDH has been shown to have anticancer and immunosuppressive effects.[100,101] Crude extracts, chromatographic fractions, and pure compounds were evaluated for

enzyme inhibitory activity using purified recombinant human IMPDH.[102] NADH production was used to spectrophotometrically (UV 340 nm) monitor enzyme activity (Figure II.4). Extracts with EC_{50}s ≤ 8 µg/mL were considered active.

$$IMP + NAD^+ + H_2O \xrightarrow{IMPDH} XMP + NADH + H^+$$

Figure II.4 Enzymatic Formation of Xanthosine Monophosphate and NADH From Inosine Monophosphate and NAD in the Presence of IMP Dehydrogenase.

Protein Kinase Inhibition Assays

Protein Tyrosine Kinase Inhibition Assays—Signaling pathways which mediate the effects of growth factors and oncogenes on cellular proliferation have recently become targets for the development of unique mechanism-based anticancer drugs. Protein tyrosine kinases (PTKs) have been implicated as oncogene products, phosphorylating tyrosine residues of substrate proteins, in tumorigenic processes.[103] Protein tyrosine kinase ($pp60^{v\text{-}src}$) was isolated from Rous sarcoma virus-transformed rat cells and its activity measured at Syntex by a modification of the method used by Goldberg.[104] The IC_{50} is defined as the concentration of extract or compound which causes a 50% decrease in enzyme activity compared to solvent vehicle control. Extracts which inhibited kinase activity by ≥ 45% at 50 µg/mL in initial ELISA assays were subsequently measured for PTK inhibitory activity by the method described by Lee et al.[105]

Protein Kinase C Inhibition Assay—Protein kinase C (PKC, rat brain isoenzyme) activity was quantified by measuring ^{32}P incorporation from γ-^{32}P ATP into synthetic peptide substrates. Staurosporine was used as a positive inhibition control. Enzymatic inhibition activities were expressed in % inhibition (1.0 - [(sample CPM - basal CPM)/(total CPM - basal CPM)] x 100) as defined from radiolabel counts.

Topoisomerase Inhibition Assay

In collaboration with Dr. Louis Barrows (University of Utah, Department of Pharmacology & Toxicology) we examined lipid and aqueous extracts and purified compounds from marine organisms for cytotoxicity in a series of tumor cell lines designed to screen for agents interacting with DNA replication enzymes (topoisomerase I and II). Two tumor cell lines were screened to evaluate the general cytotoxicity of an extract or compound. KB (human epidermoid carcinoma) and HCT 116 (colonic carcinoma) cell lines were among those selected to estimate general extract cytotoxicity. EM9 (topoisomerase I sensitive Chinese hamster ovary line), XRS-6 (topoisomerase II sensitive), UV20 (DNA cross-linking agent sensitive), and BR1 (DNA repair competent) cell lines were used to screen for compounds which have the ability to interact with DNA repair mechanisms.

National Cancer Institute Assays

Throughout a ten year period from 1975 to 1985, *in vivo* P388 mouse leukemia assays were used by the National Cancer Institute (NCI) for the preliminary screening of crude extracts, chromatographic fractions, and pure compounds.[90] Only a handful of new anticancer drugs were discovered as a direct result of these tests and the methodology was later revised. As discussed in chapter I, one limitation inherent in leukemia-based assays is that the majority of neoplastic disorders are solid tumor cancers. Therefore, while P388 models may perhaps serve as screens for compounds which are cytotoxic to these rapidly dividing leukemic tissues, they provide little or no selectivity for other forms of metastatic disease.

Since 1985, the NCI has implemented a primary screening program using a battery of *in vitro* disease-oriented human tumor cell lines organized into disease-specific subpanels.[90] Extracts are tested over a wide range of concentrations for cytotoxicity or

antiproliferative activity. This *in vitro* 60-cell line panel is made up of tumors of the lung, colon, kidney, ovary, breast, prostate, and brain, and includes several leukemias and melanomas. The primary advantage of this disease-specific form of assay is that it is designed to screen for relatively selective antitumor agents with specificity to individual forms of neoplastic disease rather than testing for general cytotoxins.

Tumor cells are typically incubated for two days with plant or animal extracts at five serially diluted concentrations (10^{-2} to 10^{2} μg/mL). Pure compounds are initially evaluated at a concentration range of from 10^{-8} to 10^{-4} M. Results are presented in the form of disease-specific dose response curves or as mean bar graphs relative to the average antiproliferative or cytotoxic effect in each assay (see Chapter V). Agents showing selective cytotoxicity in specific tumor cell lines or disease-specific panels are subsequently screened using *in vivo* human tumor xenograft models.

The NCI has developed a computerized pattern-recognition algorithm program called COMPARE which compares the mean graph fingerprints of active extracts or pure compounds with all other compounds in the NCI screening database.[106] By matching test substances with known compounds and anticancer agents COMPARE has provided valuable correlations between compounds with similar mechanisms of action and provides an indication as to whether the action of a test compound may be the result of a new mechanism.

Criteria for Selection of Natural Product Projects

Natural product projects may be selected on the basis of any number of different criteria. Often bioassay-guided fractionation of extracts considered active in any of the previously mentioned biological or pharmacological assays may result in the discovery of interesting new lead compounds. The isolation of curacin A (Chapter V) is an example of the use of this technique. Alternatively, chromatographic separation and purification of

compounds with unusual TLC characteristics, suggestive of a secondary metabolic origin, have provided an equally rich diversity of projects. The discovery of the unique oxylipins constanolactones A-G (Chapter III) are the result of TLC-guided isolation efforts. Additionally, projects may be selected because of interesting observations provided by ecological or toxicological leads from outside the laboratory or by a combination of these criteria. The nakienones (Chapter IV) were discovered as a result of ecological observations in the field, followed throughout the fractionation process by their unusual TLC characteristics, and evaluated in pharmacological and toxicological assays.

Results and Discussion

Over 1,500 extracts (Table II.1), representing nearly 300 species of macrophytic marine algae (Chlorophyta: > 50; Chrysophyta: > 58; Rhodophyta: > 163 spp.), numerous microalgae (Table II.2), and over 30 species of marine invertebrates were investigated for new natural products and evaluated for biomedical potential. This effort represents a continuation of the Oregon Seaweed Survey previously discussed in the M.S. Thesis of Albert Lopez (1987)[107] and other updates in print.[20,51-55] The scope of previously discussed research efforts has been expanded to include results obtained from the evaluation of marine organisms collected in seven states and obtained from over 12 countries. These screening efforts have provided several dozen natural product projects and are currently guiding the direction of new research.

Many of the marine algae species screened show some level of antimicrobial activity (Table II.3). This trend is consistent with previously reported marine algae survey results.[107] A total of 450 extracts (223 lipid, 175 aqueous) representing 196 species of macrophytic algae were screened for antimicrobial activity. The majority of algae tested possessed some degree of antimicrobial activity (Table II.3). Typically, Gram (+) bacteria were the most sensitive to the constituents of algal extracts (60% active against *S. aureus*,

74% active against *B. subtilis*). However, only 3% of algae species were designated "highly active" (disc assay zone of inhibition >18 mm in diameter) against these organisms. Gram (-) organisms were the least effected, overall. Only 9% of the algae species tested inhibited *S. typhimurium* growth *in vitro*. In general, extracts of red algae (Rhodophyta) showed greater antimicrobial activity than those of the other groups tested (i.e. > 90% inhibitory to *B. subtilis*).

Table II.1 Partial List of Worldwide Field Collection Sites for Tropical and Temperate Marine Algae and Numbers of Representative Algal Groups Collected.

Site	Number of Rhodophyta collections	Number of Chrysophyta collections	Number of Chlorophyta collections	Number of Cyanophyta collections (large scale)	Total number of collections per site
Caribbean					
Anguilla (1993)	–	–	–	3	3
Costa Rica (1992)	–	–	–	6	6
Curaçao (1992-1994)	21	10	24	241 (29)	327
Florida (1991)	3	2	2	17 (1)	25
Puerto Rico (1987-1994)	10	1	3	61 (17)	92
San Martin (1993)	2	–	–	10	12
St. Croix, USVI (1989)	11	3	1	(1)	16
St. Thomas, USVI (1993)	1	–	1	10 (2)	14
Tropical Pacific					
Guam (1992-1994)	–	–	–	8	8
Tahitian Islands (1992)	15	4	6	61 (15)	101
Okinawa (1993)	7	2	6	50 (4)	69
Temperate Pacific					
Hokkaido, Japan (1993)	11	9	2	1	23
Yellow Sea, Korea (1993)	–	–	–	14	14
Pacific Northwest					
Alaska (1987-1989)	29	3	2	–	34
British Columbia (1991)	12	3	–	–	15
California (1988-1993)	49	3	–	15	67
Oregon (1985-1993)	371	96	78	26	571
Washington (1988-1993)	51	21	6	20	98
Ship Bilge (1991)	–	–	–	6	6
Total	593	157	133	549 (69)	1501

Table II.2 Genera of Microalgae in Survey.

Cyanophyceae		
Chroococcales	*Aphanocapsa*	*Mersmopedia*
	Chroococcus	*Microcystis*
	Gloeocapsa	*Synechocystis*
	Gloeothece	*Synechoccus*
Chamaesiphonales	*Pleurocapsa*	
Hormogonales	*Anabaena*	*Rivularia*
	Hormothamnion	*Scytonema*
	Lyngbya	*Schizothrix*
	Nostoc	*Spirulina*
	Oscillatoria	*Stigonema*
	Phormidium	*Symploca*
	Plectonema	
Bacillariophyceae		
	Isthmia	*Naviula*
Crytophyceae		
	Hemiselmis	*Ochromonas*
	Poterioochromonas	
Prymnesiophyceae		
	Coccolithus	*Ochrosphaera*
	Cricospheria	*Pavlova*
	Isochrysis	
Xanthophyceae		
	Mischococcus	
Chlorophyta		
	Chlorococcum	*Pseudendoclonium*
	Percursaria	
Eugleophyta		
	Euglena	

Table II.3 Summary of Antimicrobial Activity for Marine Macrophytic Algae Screened.

Test Organism	Number of Rhodophyta high/mod/low [a] (%)	Number of Chrysophyta high/mod/low [a] (%)	Number of Chlorophyta high/mod/low [a] (%)	Total for algae tested high/mod/low [a] (%)
Gram (+)				
Bacillus subtilis	4/29/69 (3/21/69)	2/7/23 (5/18/59)	0/3/12 (0/14/57)	6/36/104 (3/18/53)
Staphylococcus aureus	4/17/56 (3/12/41)	0/6/23 (0/15/59)	2/1/9 (10/5/43)	6/24/88 (3/12/45)
Gram (-)				
Escherichia coli	2/5/18 (2/4/13)	0/1/5 (0/3/13)	0/0/2 (0/0/10)	2/6/25 (1/3/13)
Pseudomonas aeruginosa	0/4/9 (0/3/7)	0/2/7 (0/5/18)	0/0/3 (0/0/14)	0/6/19 (0/3/10)
Salmonella typhimurium	1/2/6 (1/2/8)	0/0/1 (0/0/5)	0/0/0 (0/0/0)	1/2/7 (1/2/6)
Fungi (yeast)				
Candida albicans	3/8/26 (2/6/19)	0/2/6 (0/5/15)	0/1/4 (0/5/19)	3/11/36 (2/6/18)
Tested Species	139	39	21	196

a) Activity rated by zone of inhibition diameter observed in antimicrobial disc assay. High: > 18 mm; Moderate: 12 to 18 mm; Low: 8 to 11.5 mm. Extracts were considered completely inactive if zone of inhibition was less then 8 mm with a 6 mm test disc.

A handful of algal species were highly inhibitory to a multitude of pathogenic organisms. Three red algae (*Erythrophyllum delesserioides*; *Odonthalia flocossa*; *O. washingtoniensis*) were highly antimicrobial to the majority of organisms tested.

We have tested extracts from nearly 100 marine organisms in brine shrimp lethality assays and found that more than 38% of those tested showed toxicity at a concentration of 50 ppm. Greater than 36% of the algae and a remarkable 50% of the invertebrate species tested were toxic to brine shrimp. Some of the most potent brine shrimp toxic algae species are shown in Table II.4. The toxins responsible for this activity remain unknown for the majority of these species.

Table II.4 Brine Shrimp Toxic Marine Algae.[a]

Rhodophyta
- Rhodophyceae
  - Bangiales
    - Bangiaceae
      - *Porphyra nereocystis* (lipid extract)
      - *Porphyrella gardneri* (lipid and aqueous extracts)
  - Ceramiales
    - Ceramiaceae
      - *Microcladia* sp. (lipid and aqueous extracts)
    - Delesseriaceae
      - *Delesseria decipiens* (lipid and aqueous extracts)
    - Rhodomelaceae
      - *Laurencia spectabilis* (aqueous extract)
      - *Odonthalia washingtoniensis* (lipid extract)
  - Gigartinales
    - Dumontiaceae
      - *Dilsea californica* (lipid extract)
      - *Farlowia mollis* (lipid and aqueous extracts)
    - Endocladiaceae
      - *Endocladia muricata* (aqueous extract)
    - Gigartinaceae
      - *Mazzaella splendens*, formerly *Iridea spendens* (aqueous extract)
      - *Mazzaella* sp. (lipid extract)
    - Gloiosiphoniaceae
      - *Gigartina* sp. (aqueous extract)
      - *Gloiosiphonia capillaris* (lipid and aqueous extracts)
      - *Gloiosiphonia verticillaris* (lipid and aqueous extracts)
    - Halymeniaceae
      - *Prionitis lyallii* (lipid and aqueous extracts)
    - Phyllophoraceae
      - *Ahnfeltia plicata* (lipid and aqueous extracts)
    - Plocamiaceae
      - *Plocamium violaceum* (lipid extract)
    - Solieriaceae
      - *Opuntiella californica* (lipid extract)
  - Gracilariales
    - Gracilariaceae
      - *Gracilariopsis lemaneiformis* (lipid extract)
  - Unknown
      - Calif. collection (aqueous extract)
      - Oregon collection, *Callophyllis*-type (lipid extract)

Table II.4 Continued. Brine Shrimp Toxic Marine Algae.[a]

Chrysophyta
- Phaeophyceae
  - Desmarestiales
    - Desmarestiaceae
      - *Desmarestia ligulata* (lipid extract)
  - Fucales
    - Fucaceae
      - Pelvetiopsis limitata (lipid extract)
  - Laminariales
    - Laminariaceae
      - *Laminaria sinclairii* (aqueous extract)
    - Lessoniaceae
      - *Nereocystis luetkeana* (lipid and aqueous extracts)

Chlorophyta
- Bryopsidophyceae
  - Cladophorales
    - Cladophoraceae
      - *Chaetomorpha linum* (lipid extract)
- Codiolophyceae
  - Acrosiphoniales
    - Acrosiphoniaceae
      - *Acrosiphonia coalita* (aqueous extract)

Cyanophyta
- Cyanophyceae
  - Hormogonales
    - Oscillatoriaceae
      - *Lyngbya majuscula*, OUK 1 Jul 93 (lipid and aqueous extracts)
      - *Lyngbya majuscula*, NAC 15 Dec 93 (lipid and aqueous extracts)
      - *Lyngbya majuscula*, NSB 10/15 Dec 93 (lipid and aqueous extracts)

a) crude extracts toxic to brine shrimp (*Artemia salina* Leach) at 50 ppm.

However, brine shrimp lethality assays have provided exciting leads as summarized in several publications.[108,109] The investigation of curacin A (Chapter V) is an example of a project in which brine shrimp lethality was used to guide the chromatographic fractionation and isolation of exciting new lead compounds.

Molluscicidal and ichthyotoxicity testing have proven an invaluable tools for the detection and isolation of biologically active natural products. The isolation of two new ichthyotoxic compounds and a novel snail toxin are described in chapter V.

Evaluation by thin layer chromatography (TLC) has proven an invaluable technique for surveying algal extracts for new natural products. Once trained to recognize the often subtle differences between the TLC characteristics of various algal primary metabolic products (pigments, triglycerides, steroids, phospholipids, etc.) from those of secondary metabolites (terpene, alkaloids, etc), TLC analysis provides a means to rapidly screen large numbers of extracts for the presence of unusual chemical constituents.

Examination of over 200 species of marine algae by TLC suggests that these organisms are a rich source of secondary natural products (Table II.5). Remarkably, 25% of the species chromatographed show the presence of major new compounds as indicated by a (++++) rating. TLC analysis indicates that this trend is consistent throughout all three groups tested (Chlorophyta, 26%; Rhodophyta 26%; Chrysophyta 21%). These findings stress the exciting potential for further study in this area.

Table II.5 Results from TLC Analysis of Macrophytic Marine Algae.

	TLC Rating[a] ++++	TLC Rating[b] +++	TLC Rating[c] ++ or less	Total Species Tested
Chlorophyta	10	8	21	39
Rhodophyta	33	24	69	126
Chrysophyta	10	6	32	48
Totals	53	38	122	213

TLCs were coded to indicate the presence of potentially interesting new compounds. The chromatograms were coded as follows: **a)** (++++) major new compounds present, highest priority; **b)** (+++) several minor secondary natural products present, worthy of pursuit; **c)** (++) minor secondary compounds present, marginal interest factor; and (+) lowest priority, primary metabolites only.

Our discovery of the widespread occurrence of oxylipin chemistry in temperate marine algae (Table II.6) was made possible by recognition skills developed through years of experience analyzing hundreds of organic extracts. Subsequently, unique bullet shaped spots which often charred blue or other unusual colors with gentle heating, typically observed by TLC analysis of algal extracts, soon became the signature of oxylipin production. As previously described in the first chapter, what began as an early discovery of the occurrence of mammalian immunoregulatory eicosanoids in red algae developed into a vastly more complex appreciation of the structural diversity and novelty of marine carbocyclic oxylipin chemistry. The study of new oxylipin structures encountered in marine algae (Figure II.5), chemotaxonomic differences in their oxidation (Figure II.6), their unique biosynthesis, and their potent biological functions has predominated the scientific efforts of our group for the past five years and has been the subject of several reviews.[51-55] Chapter III details an extensive investigation of carbocyclic-oxylipin metabolism in *Constantinea simplex*, a temperate red alga evaluated as part of the our Pacific algal survey. The *C. simplex* project is an example of a chemical study resulting from a TLC analysis of algae extracts. The biological and ecological significance of this class of oxidized fatty acid chemistry (Chapter I) remains an impetus for continued research.

Extracts of over 125 species of marine organisms were screened for inosine 5′-monophosphate dehydrogenase (IMPDH) inhibition activity. All 13 of the active extracts (EC_{50} values less than 8 μg/mL) were from marine algae. Two chlorophytes, two chrysophytes, four rhodophytes, four cryptophytes, and a cyanobacterium potently inhibited IMPDH. Eight other algae (2 chrysophytes, 6 rhodophytes) and two marine invertebrates inhibited IMPDH at slightly higher concentrations.

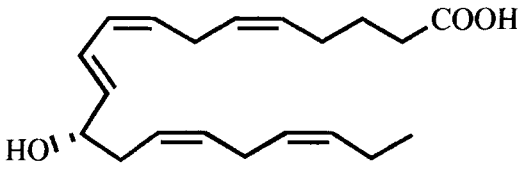

12-HEPE from
Murrayella periclados

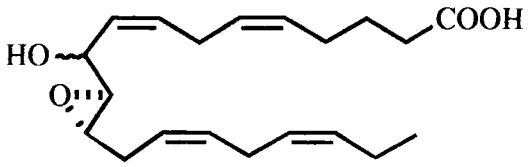

Hepoxilin B_3 from
Platysiphonia miniata

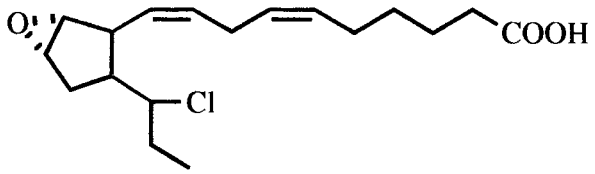

Egregiachloride from
Egregia menziesii

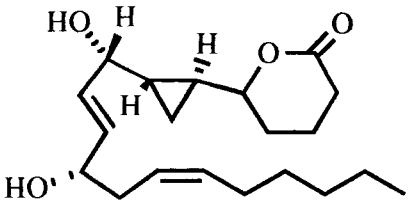

Constanolactone from
Constantinea simplex

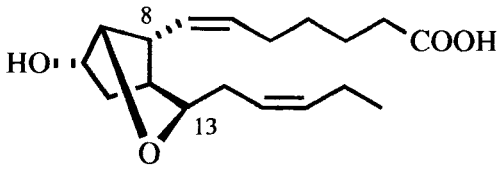

Cymathere ether A from
Cymathere triplicata

Figure II. 5 Unusual Structures of Oxylipins From Marine Algae.

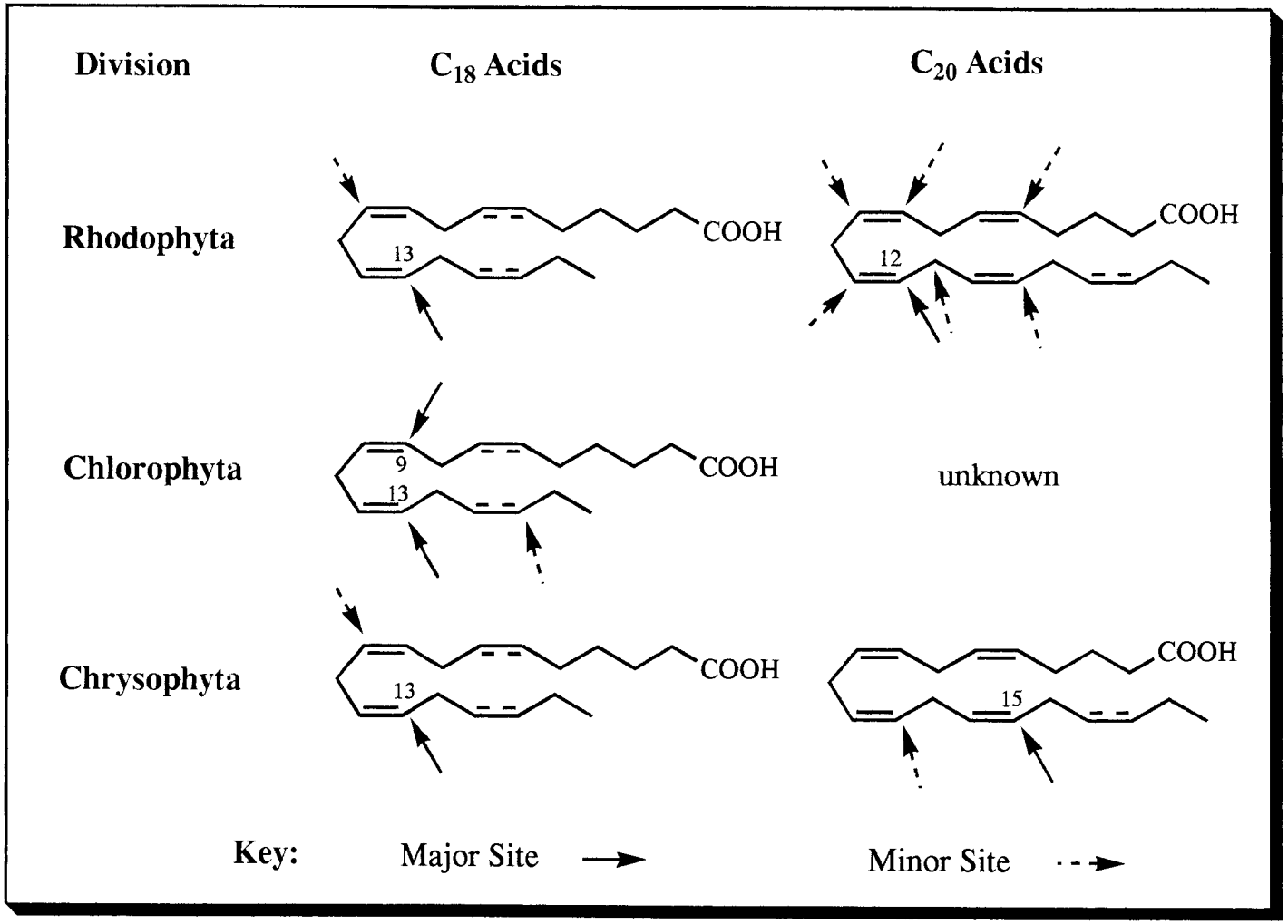

Figure II.6 Positional Patterns of Oxidation Observed in Marine Algal Oxylipins.

Table II.6 Algal Species Found to Contain Oxylipin Chemistry.

Rhodophyta
- Rhodophyceae
  - Gelidiales
    - Gelidiaceae
      - *Gelidium latifolium* Bornet & Thuret
  - Corallinales
    - Corallinaceae
      - *Bossiella orbigniana* Silva
      - *Lithothamnion corallioides* Crouan
      - *Lithothamnion calcareum* (Pallas) Areschough
  - Gigartinales
    - Dumontiaceae
      - *Constantinea simplex* Setchell
      - *Farlowia mollis* (Harvey & Bailey) Farlow & Setchell
    - Solieriaceae
      - *Sarcodiotheca gaudichaudii* (Montagne) Gabrielson
  - Gracilariales
    - Gracilariaceae
      - *Gracilaria edulis* (Gmelin) Silva (as *G. lichenoides*)
      - *Gracilaria verrucosa* = *G. pacifica* (Abbott)
      - *Gracilariopsis lemaneiformis* (Bory) Dawson, Acleto & Foldvik
  - Rhodymeniales
    - Rhodymeniaceae
      - *Rhodymenia pertusa* (Postels & Ruprecht) J.G. Agardh
    - Champiaceae
      - *Gastroclonium subarticulatum* (Turner) Kutzing
  - Ceramiales
    - Ceramiaceae
      - *Neoptilota asplenioides* (Esper) Kylin *ex* Scagel, Garbary, Golden & Hawkes
      - *Ptilota filicina* J.G. Agardh
    - Rhodomelaceae
      - *Laurencia hybrida* (DeCandolle) Lenormand
      - *Laurencia spectabilis* Postels and Ruprecht
      - *Murrayella periclados* (C. Agardh) Schmitz
    - Delesseriaceae
      - *Cottoniella filamentosa* Borgesen
      - *Platysiphonia miniata* (C. Agardh) Borgesen
      - *Polyneura latissima* (Harvey) Kylin

Table II.6 (continued) Algal Species Found to Contain Oxylipin Chemistry.

Chrysophyta
- Phaeophyceae
  - Cordariales
    - Notheiaceae
      - *Notheia anomala* (Bailey & Harvey)
  - Laminariales
    - Laminariaceae
      - *Ecklonia stolonifera* Okamura
      - *Laminaria setchellii* Silva
      - *Laminaria saccharina* (Linnaeus) Lamouroux
      - *Laminaria sinclairii* (Harvey *ex* Hooker f. & Harvey) Farlow, Anderson & Eaton
      - *Cymathere triplicata* (Postels & Ruprecht) J.G. Agardh
    - Alariaceae
      - *Alaria marginata* Postels et. Ruprecht
      - *Egregia menziesii* (Turner) Areschoug

Chlorophyta
- Bryopsidophyceae
  - Cladophorales
    - Cladophoraceae
      - *Cladophora columbiana* Collins
- Codiolophyceae
  - Acrosiphoniales
    - Acrosiphoniaceae
      - *Acrosiphonia coalita* (Ruprecht) Scagel, Garbary, Golden & Hawkes

Cyanophyta
- Cyanophyceae
  - Oscillatoriales
    - Oscillatoriaceae
      - *Lyngbya majuscula* Harvey
      - *Oscillatoria nigro-viridis* Thwaites
      - *Schizothrix calcicola* (C. Agardh) Gomont

Protein tyrosine kinase (PTK) inhibition assays have also effectively guided the selection of natural product research projects. A total of 363 extracts, representing more than two hundred species of marine organisms, were screened for PTK inhibition activity (Table II.7). Extracts which inhibited the enzyme PTK by at least 45% at the test concentration of 50 µg/mL were considered active and worthy of further pursuit. The only active macroalga, from nearly 170 screened, was a cold water kelp (chrysophyte). However, extracts from five species of microalgae were potently PTK inhibitory (4, chrysophytes; 1 cyanobacterium). Extracts of the cultured cryptophyte *Poterioochromonas malhamensis* were the most active. Assay with *P. malhamensis* polar extracts showed essentially 100% inhibition of PTK. Dr. Jian Lu Chen isolated unusual chlorinated sulpholipids from this organism which were reponsible for this activity and are futher discussed in chapter V.

Table II.7 Results From Protein Tyrosine Kinase (PTK) Inhibition Assays.

Type of marine organism	Number of species (or culture strains) tested	Number of PTK active[a] species
Chlorophyta	29	–
Rhodophyta	107	–
Chrysophyta	33	1
Bacillariophyceae	2	–
Cyanophyceae	(60)	1
Crytophyceae	(64)	4
Invertebrates	13	–
Angiosperms	2	–

a) Actives are defined as extracts which inhibit PTK ≥ 45% at 50 µg/mL.

Conclusions

This survey of marine organisms for biomedical utility has resulted in the discovery of widespread oxylipin production in marine algae, novel inhibitors of cancer-related

enzymes, a new antimitotic agent, and potent marine toxins. Moreover, this work continues to inspire innovative forms of research and suggests the exciting potential of marine organisms, and algae in particular, as rich sources of exciting new natural products.

CHAPTER III.

THE CHEMISTRY AND BIOSYNTHESIS OF CONSTANOLACTONES A-G, NEW OXYLIPINS FROM THE OREGON RED ALGA *CONSTANTINEA SIMPLEX*

Abstract

Extracts of the Oregon marine alga *Constantinea simplex* were found to contain a mixture of ω6 and ω3 unsaturated constanolactones, lactonized cyclopropyl-containing oxylipin metabolites, that logically derive from arachidonic and eicosapentaenoic acids, respectively. Detailed spectroscopic analysis of the isolated compounds, as natural products and various ester derivatives, afforded the planar structures of seven structurally related constanolactones. Constanolactones A-D possess 1,4-diol functionalities while constanolactones E-G contain a vicinal diol functionality. The absolute stereochemistry at all stereocenters in constanolactones A-D and at two stereocenters in constanolactones E and F were determined by chiroptical measurements of various mono- and di-benzoate derivatives and by comparable rotations within the two series (A-D and E-G). Isolation of these various diastereomeric diols, as well as of two methanol adducts from $CHCl_3$/MeOH extracts of *C. simplex*, leads us to speculate on the occurrence of highly unstable allylic epoxides in this red alga.

Introduction

Marine invertebrates[45,110] and algae[51-53] are a rich source of oxidized, often carbocyclic[54], fatty acid metabolites which have recently become known as "oxylipins".[111]

Perhaps the most unusual oxylipins found to date in the Porifera have been isolated from *Halichondria okadai* collected off the coast of Japan.[112] Both spectroscopic and degradative chemical evidence were used to elucidate the structures of two cyclopropyl and lactone containing eicosanoids: halicholactone (**1**) and neohalicholactone (**2**) (Figure III.1). Halicholactone (**1**) was reported to exhibit weak inhibitory activity against the 5-lipoxygenase from guinea pig polymorphonuclear leukocytes (IC_{50} = 630 μM).[112] However, a subsequent report detailing the three-dimensional structure of the ω3 unsaturated neohalicholactone (**2**) describes it as a "potent lipoxygenase inhibitor", but no additional experimental data was provided.[113]

The cyclopropane and lactone containing eicosanoid **3** has been isolated from the soft coral *Plexaura homomalla*[114] and an unsymmetrical eicosanoid dimer aplydilactone (**4**) has been isolated from lipid extracts of the Japanese sea hare *Aplysia kurodai*.[115,116] The structure of **4** was established by spectroscopic analysis of the natural product, a diacetate derivative, and several degradative fragments. By this methodology, the relative stereochemistry of the *trans*-cyclopropyl group and double bond geometries were determined. This unusual oxylipin dimer has been shown to produce a two-fold activation of phospholipase A_2 *in vitro*, however, only at very high concentrations (50 mM).

The isolation of the cyclopropyl lactone eicosanoid hybridalactone (**5**) from the Rhodophyte *Laurencia hybrida* represented the first example of a carbocyclic oxylipin from a marine alga.[117] Brown algae and other red algae have since been demonstrated, chiefly by the efforts of our group, to produce unusual carbocyclic and heterocyclic oxylipins.[53,54] Prostaglandins of the A, E, and F series have been isolated from Japanese collections of the

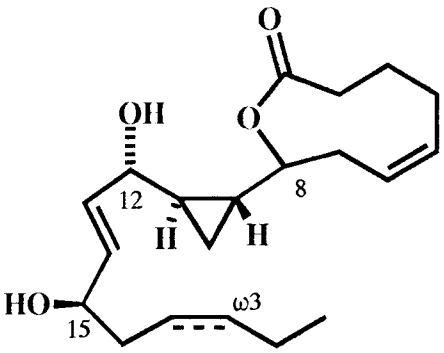

1
2 ω3 unsaturated

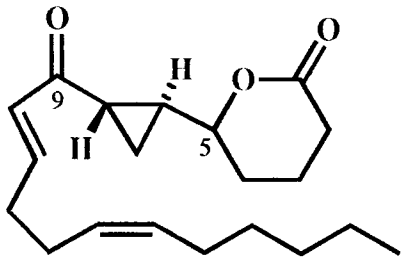

3

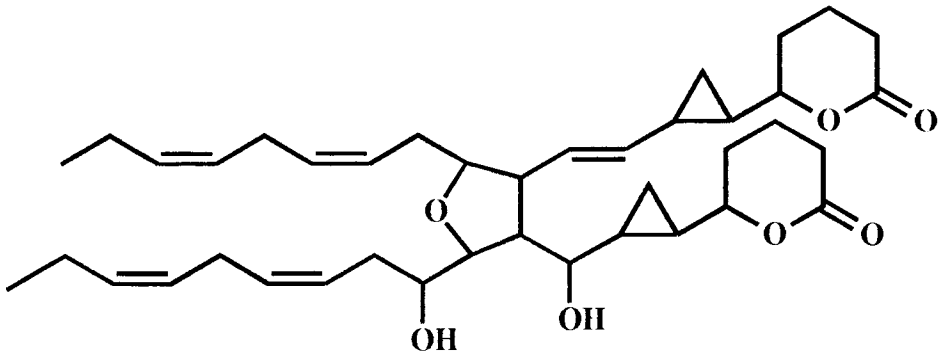

4

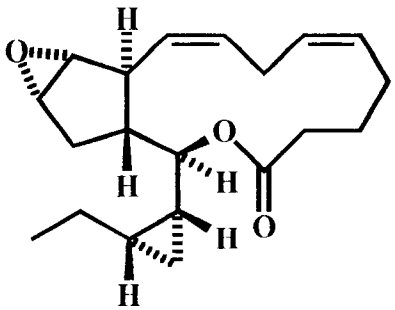

5

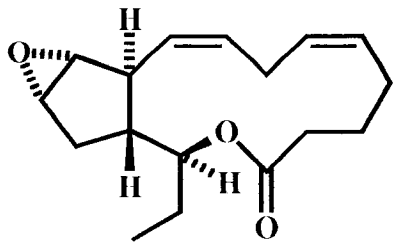

6

Figure III.1 Unusual Carbocyclic Oxylipins from Marine Organisms.

red alga *Gracilaria verrucosa* and Australian samples of *G. lichenoides.*[118-120] The Japanese brown alga *Ecklonia stolonifera* (order, Laminariales) and, more recently, the Oregon brown alga *Egregia menziessi*, also of the Laminariales, have been shown to produce lactonized epoxyprostanoids, termed ecklonialactones A-E (A: **6**, Figure III.1).[121-123] The formation of these unique metabolites and the co-isolation of lipoxygenase-type metabolites has provided evidence which suggests that, in the algae, prostaglandins and other carbocyclic oxylipins may result from further modifications of hydroperoxide intermediates produced by lipoxygenase-type enzyme systems, rather than from cyclooxygenases as in mammalian systems or from possible allene oxide intermediates as is believed for most soft corals.[53-55]

As part of our survey of marine algae for biomedical potential I initiated what would soon become an extensive exploration of oxylipin metabolism in the Oregon red alga *Constantinea simplex* Setchell.

Spring and early Summer collections of small (blade diameter typically 2-5 cm.) *C. simplex* plants were obtained from exposed low-intertidal locations along the central Oregon coast and were found to be the source of new lactonized cyclopropyl oxylipins which I have named the constanolactones A-G.[124,125] Extracts of large "older" individuals (diameter > 6 cm.) collected from relatively non-exposed sites contained insignificant oxylipin concentrations. The isolation of the constanolactones, in combination with stereochemical analysis and examination of key biosynthetic processes,[126] provides important clues to the unique mechanism of cyclopropyl-lactone formation in this alga. The seasonal variation in *C. simplex* oxylipin chemistry is rather intriguing in regard to the life cycle of this unusual red alga.

Constantinea simplex is a small (typically 2 to 10 cm dia.) "mushroom-shaped" red alga which grows attached to low intertidal and subtidal rocks from California to Alaska. Observation by Powell suggest that *C. simplex* produces only one blade per year.[127] As

the new blade grows from the apex of the stipe the old blade completes reproduction and begins to erode. Old blade scars indicate that *C. simplex* live from seven to over fourteen years.

Induction of new blade formation in C. simplex results from response to a short day (SD) photoperiod of 11 to 12 hours for three to four weeks.[128] Blade formation begins from the tips of the stipes in September or October. Powell observed that the young blade expands during the winter, matures to fertility the following summer, and is subsequently shed as another new blade forms. He also was able to show that *C. simplex* blades would continue to grow during a continuous period of darkness of four and one-half months.[128] Evidence suggests that the new blade growth is supported by carbohydrate reserves resorbed from old blades. *C. simplex* blades complete the lag phase of their growth during the winter, allowing them to out-compete other perennials which depend on the increased light of spring and summer. These seasonal changes in the biochemical status of *C. simplex* tissues are also reflected in the chemical composition of specimens collected at different stages of development (see general methods in experimental).

Polyhedral crystalline particles 5 to 7 mm in diameter have been observed in the medullary chloroplasts of *C. subulifera* and *simplex.*[129] X-ray microanalysis identified these crystals as the first phytoferritin particles found in marine algae.[130] In *C. simplex*, these particles are only found in the medullary and cortical cells of the old blade which is also associated with numerous plastoglobuli and an abundance of floridian starch. Phytoferritin was absent from young blades and were also low in floridian starch and possessed few plastiglobuli. Phytopherritin is associated with impaired photosynthesis, viral infection, and senescent conditions in higher plants.[131] The formation of phytoferritin in connection with the young blade's ability to utilize carbohydrate stores from old blades was put forth as demonstrating that blade senescence in *Constantinea* is in some ways similar to the senescence process of higher plant leaves.

In the late 1970's, crude aqueous extracts of *C. simplex, Cryptosiphonia woodii, Farlowia mollis,* as well as other members of the family Dumontiaceae (Rhodophyta) were shown to possess antiviral activity against herpes simplex viruses I and II in cell culture.[132] Highly sulphated polysaccharides which may have contained some protein molecules were demonstrated to be responsible for this antiviral activity.[132]

Results and Discussion

As part of an extensive survey of the biomedical potential of seaweeds (Chapter II), the crude lipid extract of *C. simplex* (Seal Rock, Oregon) was found by TLC to contain a diversity of likely eicosanoid-type natural products giving colorful H_2SO_4 charring reactions. Vacuum chromatography of the extract from a June collection yielded fractions that were mixtures of related substances. Following acetylation, methylation, and HPLC of one chromatographic fraction, two closely related new compounds (**7** and **8**) were isolated as synthetic diacetate derivatives (**9** and **10**). Another vacuum chromatography fraction was methylated prior to HPLC to yield minor amounts of three known oxylipins, 12-*S*-HETE (**11**, 0.1%), 12-*S*-HEPE (**12**, 0.015%) and 12-oxo-5*Z*, 8*E*, 10*E*-dodecatrienoic acid (**13**, 0.044%), all isolated as their corresponding methyl ester derivatives (**14-16**). Additionally, a third new oxylipin-peracetate derivative (**17**) was isolated as a presumed isolation artifact (Figure III.2).

Constanolactone A diacetate (**9**), $[\alpha]_D^{23} = -5.4^\circ$ (c = 3.05, $CHCl_3$), was a colorless oil which gave a prominent $(M + H - 2HOAc)^+$ by HR CIMS (CH_4) at 301.2165 (0.3 mamu dev.) analyzing for $C_{20}H_{29}O_2$. The diacetate character of this derivative was readily apparent from NMR and LR CIMS (obs. m/z 421 [$(M+H)^+$, 6%], 361 [$(M+H-AcOH)^+$, 50%], 301 [$(M+H-2HOAc)^+$, 100%]). Five of the seven degrees of unsaturation were accounted for by four olefinic carbons and 3 ester carbonyls (Table III.1), and thus, **9** was bicyclic. As derivative **9** was unreactive to CH_2N_2 and showed the C-2 protons as a

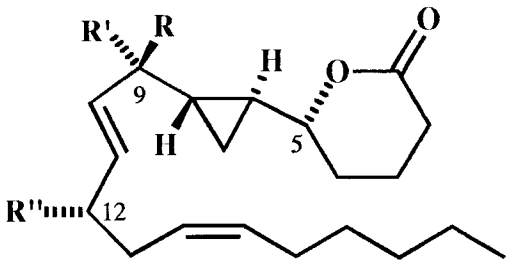

7 R=H, R'=R''=OH
8 R=R''=OH, R'=H
9 R=H, R'=R''=OAc
10 R=R''=OAc, R'=H

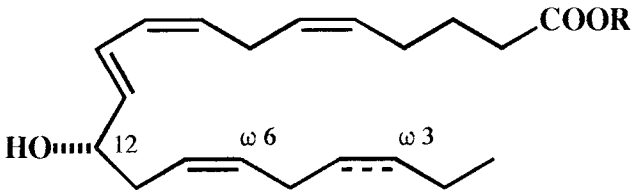

11 12*S*-HETE: ω 6, R=H
12 12*S*-HEPE: ω 3, R=H
14 ω 6, R=CH_3
15 ω 3, R=CH_3

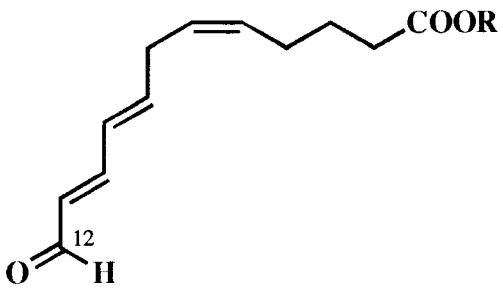

13 R=H
16 R=CH_3

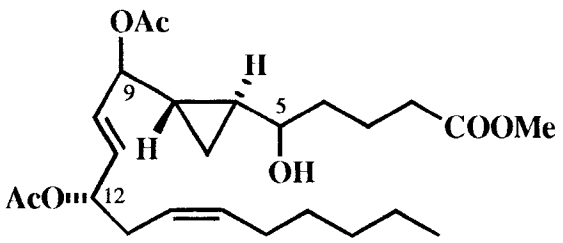

17

Figure III.2 Oxylipin Chemistry Found in *C. simplex*.

Table III.1 ^{1}H and ^{13}C NMR Data for Constanolactone Diacetates A (**9**), B (**10**) and hydrolysis product **17**.[a]

	Derivative **9**		Derivative **10**		Derivative **17**
#C	^{13}C (C_6D_6)[c]	^{1}H ($CDCl_3$)[b]	^{13}C (C_6D_6)[c]	^{1}H ($CDCl_3$)[b]	^{1}H (C_6D_6)[b]
1	169.78[f]		169.97[f]		
2	29.65	a)2.56 dt (11.6,5.6) b)2.4-2.5 m	29.47	a)2.54 m b)2.49 m	2.15 t (7)
3	18.38	a)1.80 m b)1.9-2.05 m	18.27	a)1.80 m b)1.97 m	a)1.75 m b)1.68 m
4	27.68[h]	a)1.98 m b)1.6-1.7 m	27.56	a)1.98 m b)1.65 m	1.45 m
5	82.07	3.80 ddd (10.7, 7.4, 3.0)	81.53	3.82 ddd (10.0, 6.6, 3.1)	2.68 dt (7, 7)
6	22.90[d]	1.03 m	22.01[d]	1.2 m	0.55-0.68 m
7	8.1	a)0.625 ddd (8.8, 5.2, 5.2) b)0.726 ddd (8.4, 5.2, 5.2)	6.65	a)0.68 ddd (8.5, 5.2, 5.2) b)0.60 ddd (8.5, 5.2, 5.2)	a)0.3 ddd (8, 5, 5) b)0.55-0.68 m
8	21.2[d]	1.2-1.3 m	21.04[d]	1.2 m	1.0 m
9	75.91	4.90 ddd (6.9, 6.2, 1.1)	75.47	4.85 bdd (7.9, 2.7)	4.84 dd (7, 5, 7)
10	131.45[e]	5.68 dd (15.5, 6.2)	130.78[e]	5.72 m	5.9 dd (15, 7)
11	129.73[e]	5.81 ddd (15.5, 6.2, 1.1)	130.28[e]	5.70 m	5.75 dd (15, 7)
12	73.41	5.2-5.33 m	73.34	5.2 m	5.39 ddd (7, 7, 7)
13	32.72	a)2.35 m b)2.45 m	32.76	a)2.35 m b)2.4 m	a)2.35 ddd (14, 7, 7) b)2.45 ddd (14, 7, 7)
14	124.0	5.2-5.33 m	124.01	5.2 m	5.45 m
15	133.23	5.5 bdt (10.9, 7, 3)	133.33	5.5 bdt (10.8, 7.1)	5.5 bdt (10, 7)
16	27.69[h]	1.95-2.05 m	27.69	2.02 m	2.0 bdt (7, 7)
17	29.48	1.21-1.36 m	29.58	1.35 m	1.3 m
18	31.78	1.21-1.36 m	31.76	1.35 m	1.3 m
19	22.93[d]	1.21-1.36 m	22.90	1.30 m	1.25 m
20	14.26	0.886 t (6.7)	14.24	0.885 t (6.7)	0.90 t (7)
OAc	169.50[f]		169.49[f]		
	20.82[g]	2.08[i]	20.89[g]	2.06s[h]	1.76 s
	169.00[f]		169.45[f]		
	20.71[g]	2.07[i]	20.76[g]	2.1s[h]	1.70 s
OMe					3.35

complex second order pattern, one of the cycles involved lactonization of the carboxylic acid. The final degree of unsaturation was present as a cyclopropyl ring as revealed by characteristic ^{1}H NMR resonances at 0.625, 0.726, 1.03 and 1.2 ppm (Figure III.3). Hence, **9** was a 20-carbon eicosanoid with 1 lactone, 2 secondary acetates, 2 olefins, and a cyclopropyl ring.

The location of these functional groups followed from analysis of the ^{1}H-^{1}H COSY in $CDCl_3$ (Figure III.4) in which it was possible to define the spin system throughout the entire carbon skeleton (Table III.1). Coupling constants for the C10-C11 (15.5 Hz) and C14-C15 (10.9 Hz) olefins defined them as E and Z, respectively. Further, couplings between the C6-7-8 cyclopropyl protons defined a *trans* (*S**, *S**) geometry ($J_{6\text{-}7a}$ = 5.2 Hz, $J_{6\text{-}7b}$ = 8.4 Hz, $J_{7a\text{-}7b}$ = 5.2 Hz, $J_{7a\text{-}8}$ = 8.8 Hz, $J_{7b\text{-}8}$ = 5.2 Hz). Relative stereochemistry at C5, C9 and C12 remained uncertain, however, I speculated that C12 was probably *S* based on the co-occurrence of other 12-*S* eicosanoids in this alga.

Derivative **10** of constanolactone B (**8**), $[\alpha]_D^{23}$ = -4.8° (c = 2.08, $CHCl_3$) gave a small $(M+H)^+$ at 421.2590 and a large $(M + H - 2 \times AcOH)^+$ fragment ion at 301.2168 (pos. CI, CH_4) which analyzed for $C_{24}H_{37}O_6$ (0.0 mamu dev.) and $C_{20}H_{29}O_2$ (0.0 mamu dev.) by HR mass measurement, respectively. Again, the diacetate character of this derivative was readily confirmed by NMR (Table III.1). In fact, the spectral data for **10** were nearly identical to that obtained for derivative **9**, and extensive ^{1}H-^{1}H COSY defined the location of all functional groups in **10** just as in **9** (Figure III.5). Differences between the two compounds in their a) coupling constants to H9 (**9**, $J_{8\text{-}9}$ = 6.9 Hz, $J_{9\text{-}10}$ = 6.2 Hz; **10**, $J_{8\text{-}9}$ = 7.9 Hz, $J_{9\text{-}10}$ = 2.7 Hz), b) ^{13}C NMR chemical shifts at C5, C7, and C9, and c) ^{1}H NMR shifts at H6 through H11 (Table III.1) indicated that constanolactone B diacetate (**10**) was the C9 epimer of constanolactone A diacetate (**9**).

Further insight as to the position of lactonization in constanolactone A, and hence of B as well, was afforded by isolation of the ring opened hydrolysis product (**17**) as an

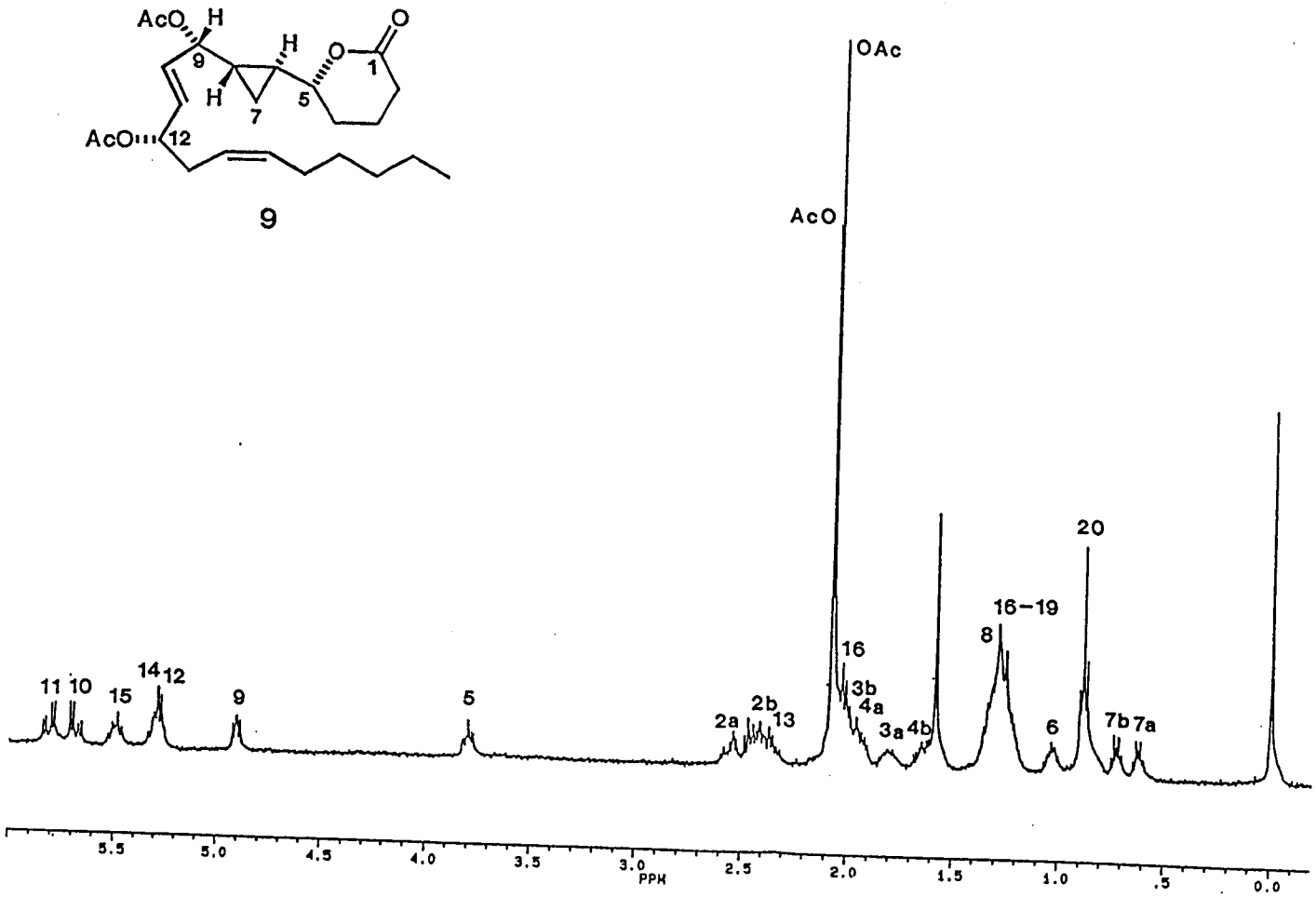

Figure III.3 ^{1}H NMR Spectrum of Constanolactone A Diacetate (**9**) in $CDCl_3$.

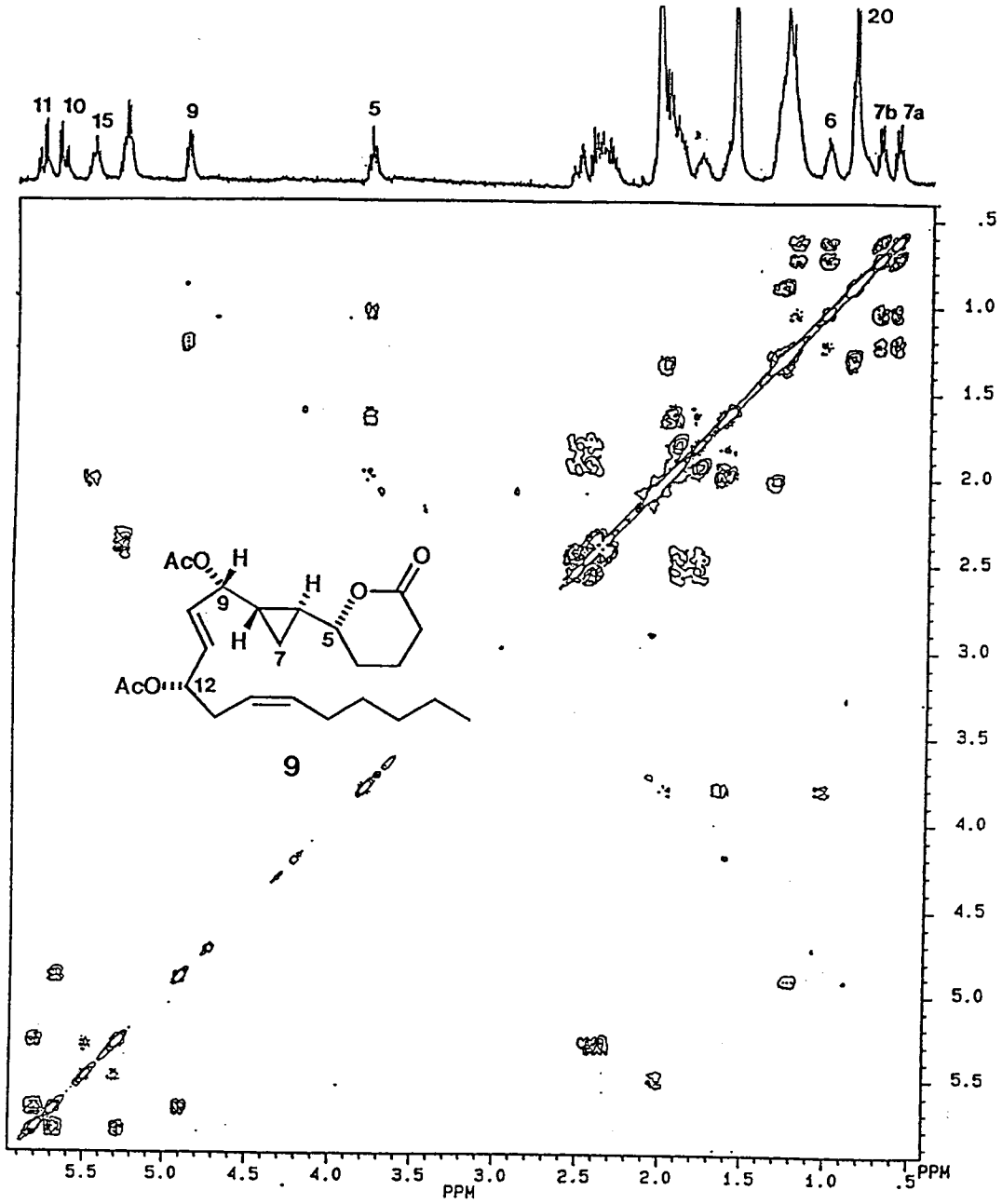

Figure III.4 COSY Spectrum of Constanolactone A Diacetate (**9**) in $CDCl_3$.

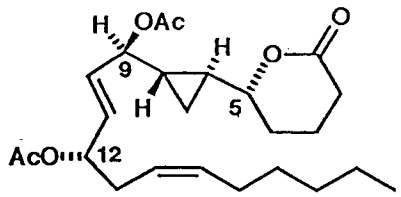

10

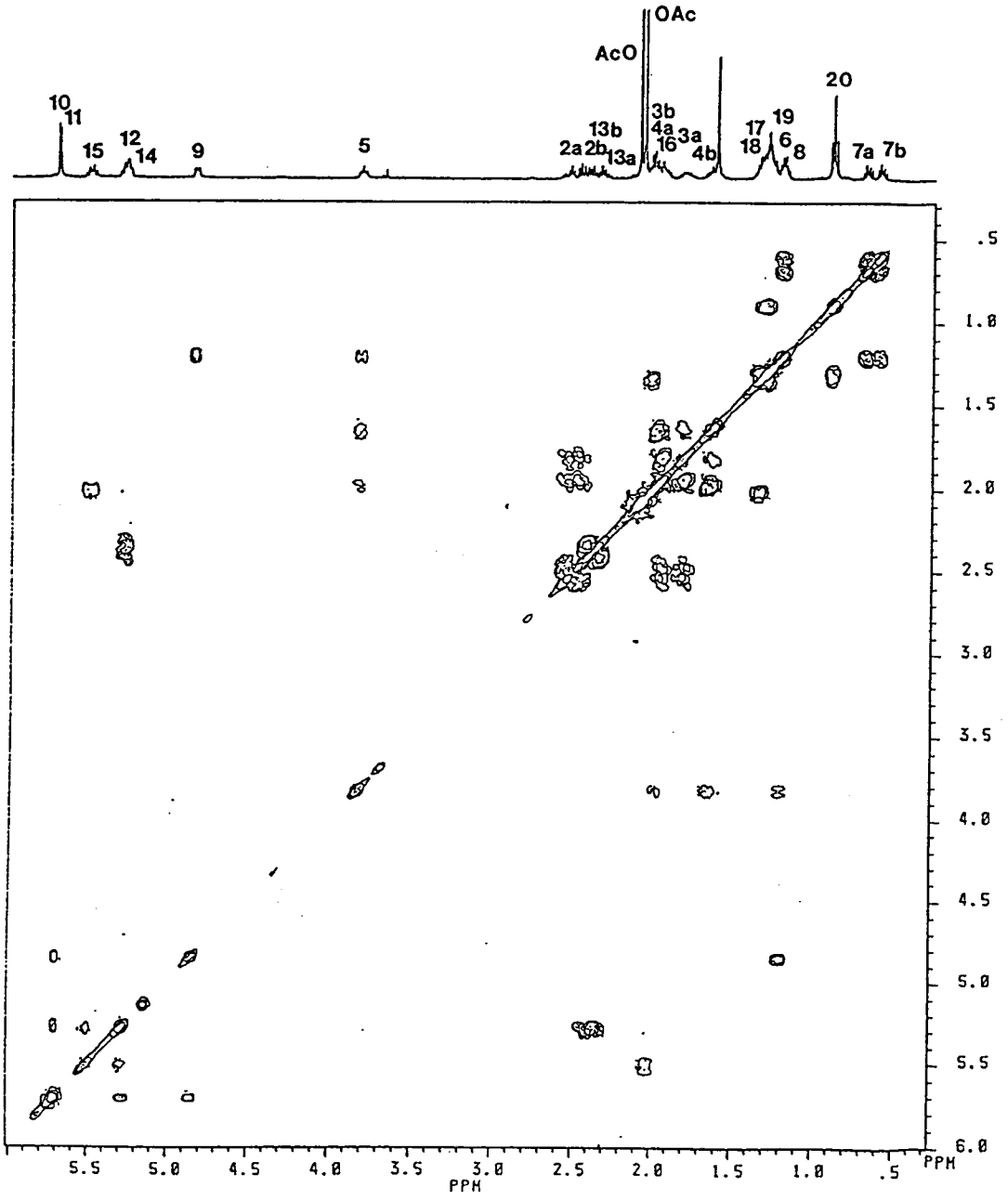

Figure III.5 COSY Spectrum of Constanolactone B Diacetate (**10**) in $CDCl_3$.

artifact (Table III.1). This was apparently formed during workup of the acetylation reaction since acetates were present at C9 and C12 but not at C5. Further, because **17** contained a methyl ester, opening of the lactone must have occurred prior to treatment with CH_2N_2. Proof that it was the C5 alcohol which was free in **17** followed from ^{1}H NMR analysis of acetylation product **18** in which the C5 methine shifted from 2.65 to 4.35 ppm (Figures III.6 and III.7).

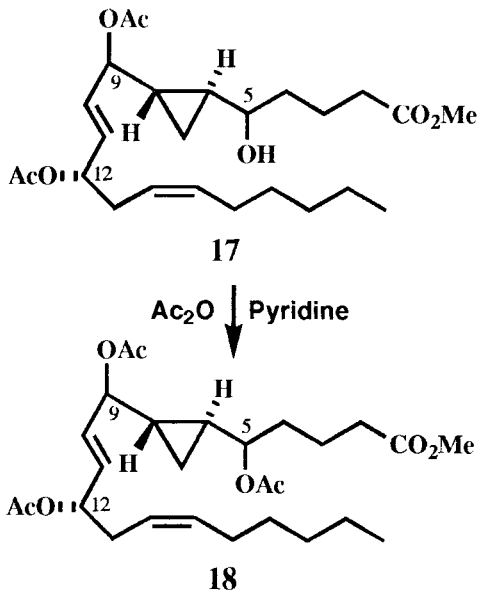

Figure III.6 Formation of **18**

Since the initial isolation of constanolactones A (**9**) and B (**10**), additional intertidal collections of *C. simplex* collected between 1989 and 1993 from the Oregon coast have been similarly extracted and analyzed for oxylipins. Constanolactones A (**7**) and B (**8**) were re-isolated during this effort as natural products by a combination of normal and reversed phase HPLC and their stereochemistries deduced by various spectrochemical techniques. The identities of **7** and **8** were assigned spectroscopically and confirmed by acetylation and comparison by ^{1}H-NMR with authentic samples of **9** and **10**.

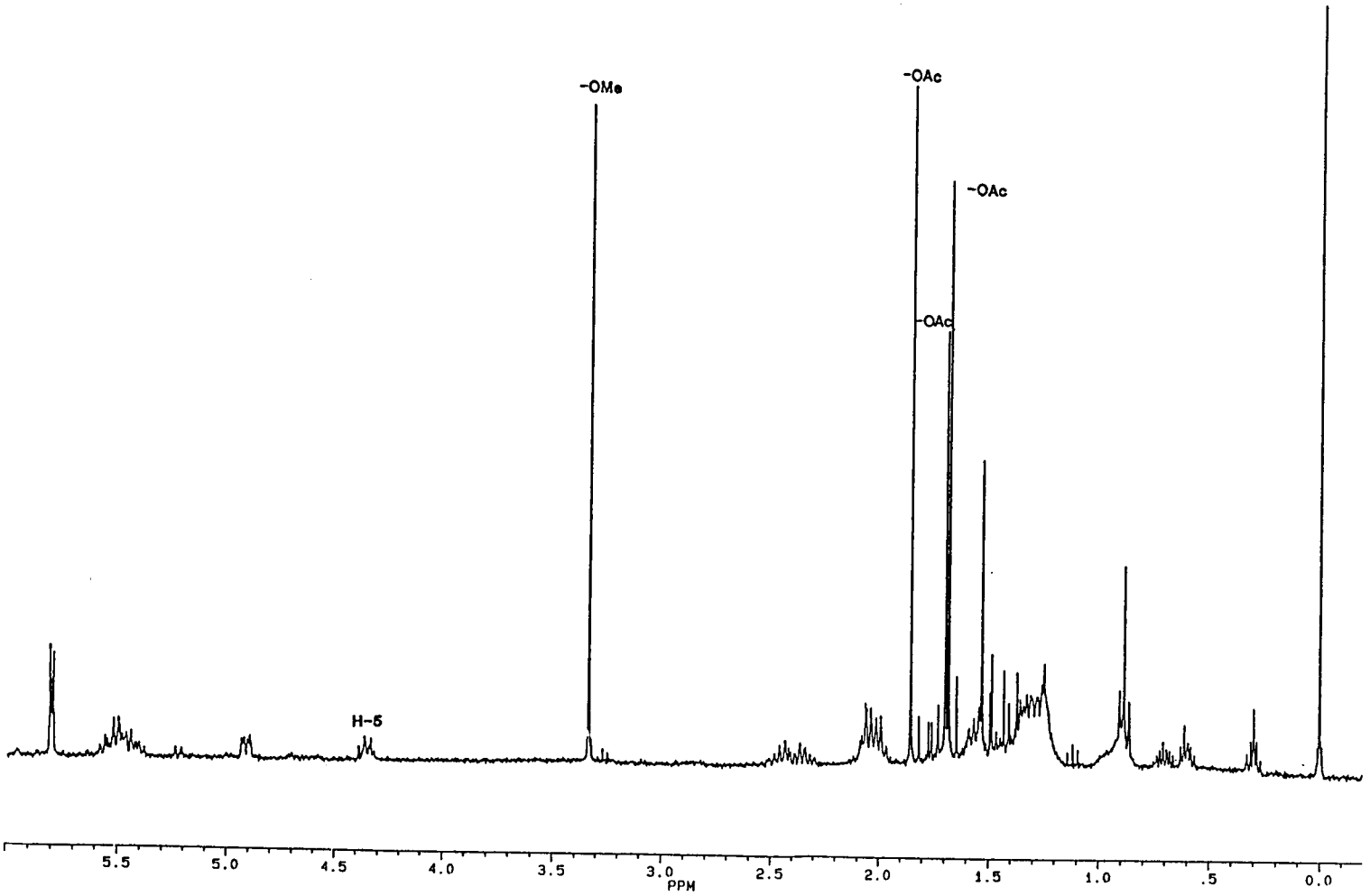

Figure III.7 ^{1}H NMR Spectrum of Acetylation Product **18** in C_6D_6.

The relative stereochemistry of C-5 to C-9 in constanolactone A and B was spectroscopically deduced using the diacetate derivatives **9** and **10**. Coupling constants between the C-6-7-8 protons defined the *trans* (*S**, *S**) geometry of the cyclopropyl group in **9** ($J_{6\text{-}7a}$ = 5.2 Hz, $J_{6\text{-}7b}$ = 8.4 Hz, $J_{7a\text{-}7b}$ = 5.2 Hz, $J_{7a\text{-}8}$ = 8.8 Hz, $J_{7b\text{-}8}$ = 5.2 Hz) and **10** ($J_{6\text{-}7a}$ = 5.2 Hz, $J_{6\text{-}7b}$ = 8.5 Hz, $J_{7a\text{-}7b}$ = 5.2 Hz, $J_{7a\text{-}8}$ = 8.5 Hz, $J_{7b\text{-}8}$ = 5.2 Hz). Further, in both **9** and **10**, significant nOe interactions were observed from H-5 to H-7a and H-8, as well as from H-5 to H-3b and H-4a. However, the nOe profile of **9** and **10** were significantly different in the region proximate to C-9. NOe interactions in **9** were observed from H-8 to H-7a and H-10, and from H-9 to H-6 and H-7b (Table III.2, Figure III.8). Compound **10**, the C-9 epimer of **9**, exhibited nOe interactions between H-5, H-6 and H-7b and the overlapping resonance observed for the olefinic protons H-10 and H-11 (Table III.3, Figure III.9). The structurally related metabolite **3** has recently been synthesized and its relative configuration assigned.[134] A 5*R**, 6*S**, 8*S** configuration in **9** and **10** was shown by direct spectroscopic comparison of the C-5 proton resonance of **9** (δ 3.80 ddd, 10.7, 7.4, 3.0 Hz) and **10** (δ 3.82 ddd, 10.0, 6.6, 3.1 Hz) with synthetic **3** (δ 3.88 ddd, 10.2, 7.5, 3.3 Hz) as well as with the 5*R**, 6*S**, 8*S** (δ 3.90 ddd, 10.6, 7.7, 3.2 Hz) and 5*S**, 6*S**, 8*S** (δ 4.06 ddd, 10.2, 6.8, 3.2 Hz) 2,4-dinitrophenylhydrazine derivatives of **3**, prepared as intermediates in the synthesis of **3**.[134] I therefore deduce a relative configuration of 5*R**, 6*S**, 8*S**, 9*S** in **9** and 5*R**, 6*S**, 8*S**, 9*R** in **10**.

The stereochemistry at C-12 in both **7** and **8** was determined by forming semi-synthetic (-)-menthoxycarbonyl (MC) derivatives followed by ozonolysis and comparison with standards using ^{1}H NMR and GC-MS. The bis-MC derivative (**20**) was prepared by treatment of **7** with an excess of (-)-menthoxycarbonyl chloride (**19**) and isolated by elution over silica gel. The presence of two MC-esters in **20** was confirmed by ^{1}H NMR shifts for H-9 and H-12 at δ4.83 and 5.10, respectively, a downfield shift of 1 ppm compared with those of **7**, clearly indicating esterification of both free hydroxyl groups

Table III.2 Key ^{1}H-^{1}H NOESY Correlations for Constanolactone A Per-acetate (**9**).

Proton #	NOESY Correlations
H-3b	H-4, H-5, H-8
H-5	H-7a, H-8, H-12 or H-14
H-6	H-7b, H-9
H-7a	H-8
b	H-9
H-8	H-9, H-11
H-9	H-10, H-11
H-10	H-12 or H-14
H-11	H-12 or H-14
H-12	H-13a, H-15, H-16, H_6-(17-19), -OAc
H-13a	H-16
b	H-16, -OAc
H-14	H-15, H-16, H_6-(17-19), -OAc
H-15	H-16
H-16	H_6-(17-19), -OAc
H_6-(17-19)	H-20

Table III.3 Key ^{1}H-^{1}H NOESY Correlations for Constanolactone B Per-acetate (**10**).

Proton #	NOESY Correlations
H-3	H-4a
H-4a	H-5
H-5	H-6* or H-8, H-7a*, H-10 or H-11, H-12
H-6 or H-8	H-7a, H-7b*, H-9, H-10 or H-11
H-7b	H-9, H-10 or H-11
H-9	H-10 or H-11
H-10 or H-11	H-12, H-13a, H-13b, H-15, H-16
H-12 or H-14	H-13a, H-13b, H-15, H-16
H-13a	H-14, H-16
b	H-14
H-15	H-16
H-16	H-17 or H-18, -OAc
H_6-(17-19)	H-20, -OAc

* Confirmed by nOe Difference Spectroscopy (NOEDS).

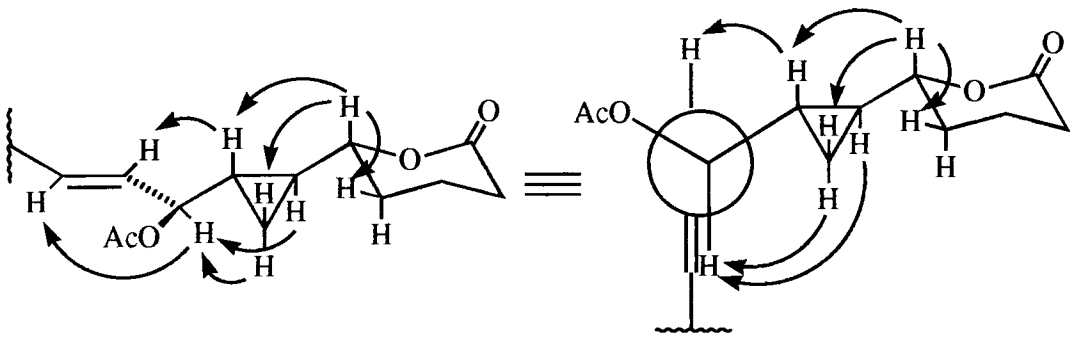

Figure III.8 Depiction of Selected NOESY Correlations for Per-acetate Derivative of Constanolactone A (**9**).

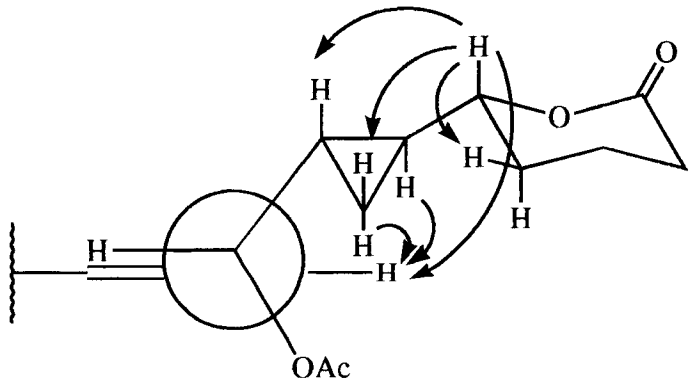

Figure III.9 Depiction of Selected NOESY Correlations for Per-acetate Derivative of Constanolactone B (**10**).

(Figure III.10). Ozonolysis of the bis-MC derivative **20**, followed by an oxidative work-up with peracetic acid, methylation, and preparative TLC purification resulted in a 30% yield of dimethyl-MC-malate derivative **21** (Figure III.11). The ^{1}H NMR spectra of the synthetic standards, 2*S* (**21**) and 2*R* (**22**) dimethyl-MC-malate, showed them to be differentiated by the chemical shift dispersion of the ester methyl groups [δ 3.778 and 3.722 (Δδ = 0.056) in **21**; δ 3.792 and 3.720 (Δδ = 0.072) in **22**]. As obtaining baseline separation of these malate derivatives by GC is sometimes problematic, this ^{1}H NMR method is a useful alternative when sample size permits (I estimate a reliable ^{1}H NMR determination can be made on as little as 50 μg of malate derivative). Comparison of the ^{1}H-NMR spectra of the two standard dimethyl-MC-malates with that produced from constanolactone A (**7**) showed the latter to be identical to that prepared from L-malate, thereby establishing the C-12 stereochemistry in **7** as *S* (Figure III.12-14). These results were confirmed by GC retention times as synthetic *S*- and constanolactone A-derived dimethyl-MC-malates (**21**) coeluted (t_R = 26.34 min) while the *R* derivative **22** had a longer retention time (t_R = 26.46 min).

Constanolactone B diacetate (**10**) was saponified and then converted to the MC derivative, ozonized and methylated to yield the C-11 to C-14 fragment as a dimethyl-MC-malate derivative. This derivative was analyzed by GC using conditions giving baseline separation of the two malate enantiomers and showed a peak only at the retention time corresponding to the *S*-malate (**21**).

The absolute stereochemistry at C-9 in constanolactone A (**7**) was determined by circular dichroic (CD) analysis of mono- and bis-*p*-bromobenzoate derivatives of **7**. Treatment of **7** with 4-bromobenzoyl chloride and a catalytic quantity of 4-dimethylaminopyridine yielded the bis-(*p*-bromobenzoate) **23** and the mono-*p*-bromobenzoate mono-acetate derivative **24**, presumably a trans-esterification product of mono-(*p*-bromobenzoate) **25** and EtOAc during work-up (Figure III.15). The C-12

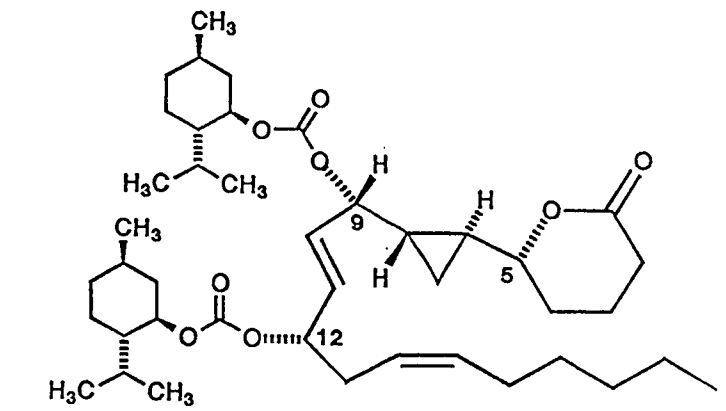

20

Figure III.10 ^{1}H NMR Spectrum of Bis-(Menthoxycarboonyl)-Constanolactone A (20) in $CDCl_3$.

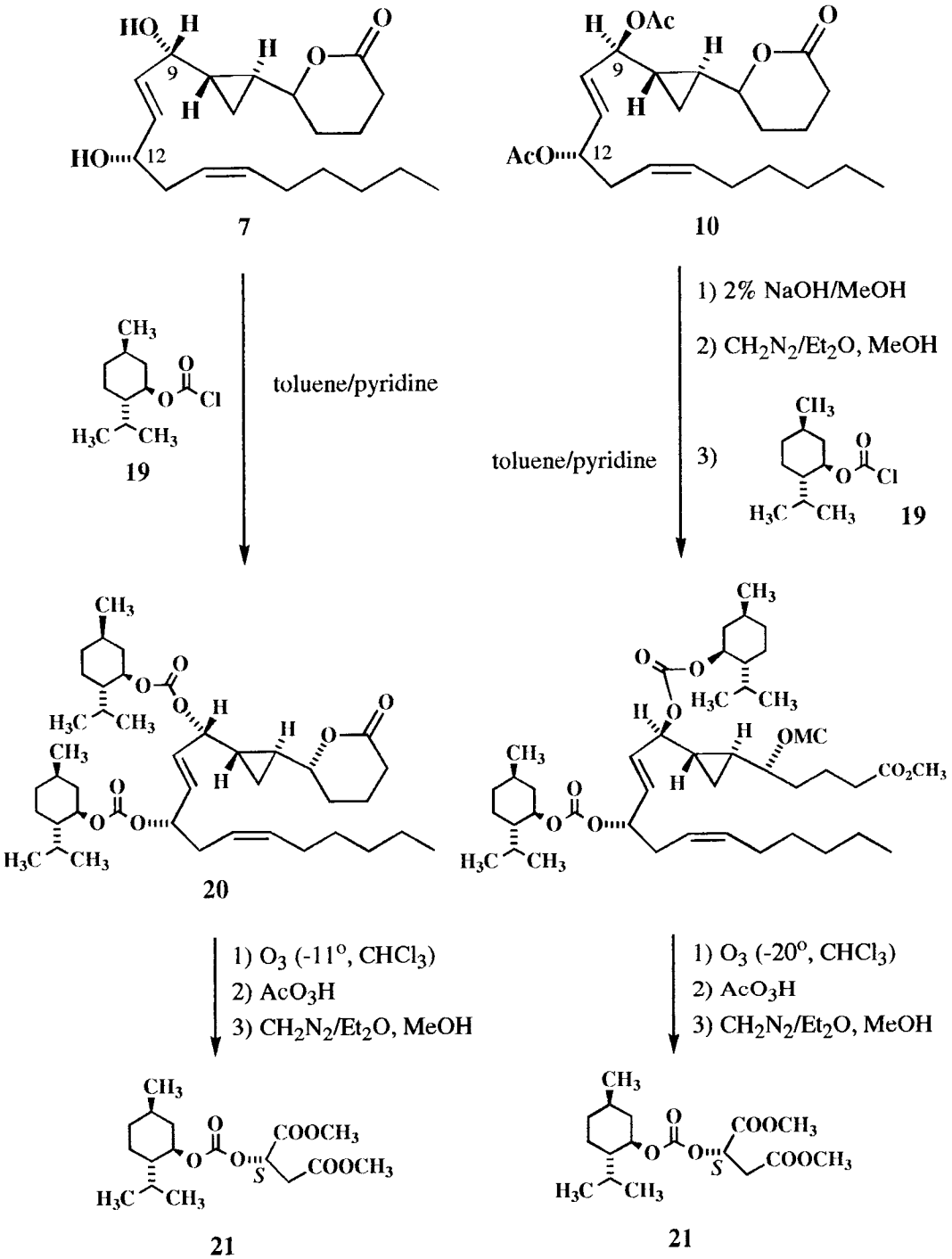

Figure III.11 Formation of Methyl-(-)-Menthoxycarbonyl Malate Derivative (**21**) from **7** and **10**.

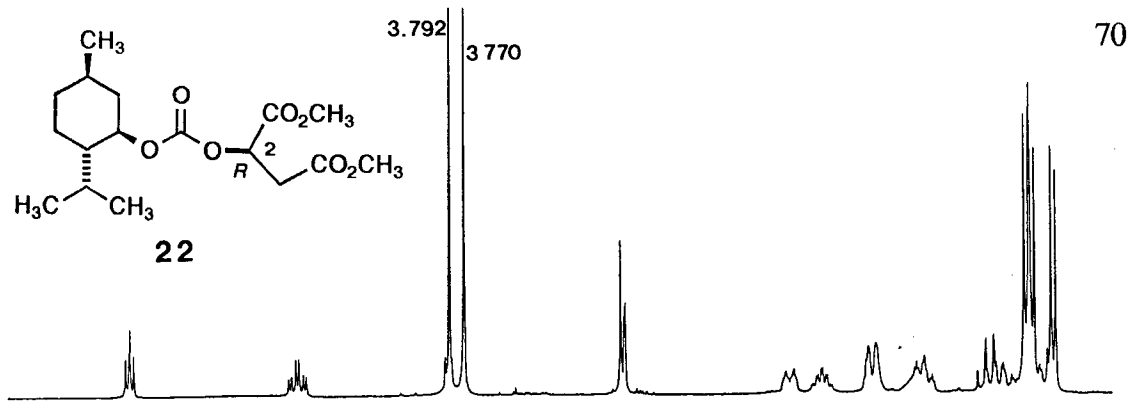

Figure III.12 ^{1}H NMR Spectra of Authentic *R*-Standard Dimethyl-Menthoxycarbonyl-Malate (**22**) in $CDCl_3$.

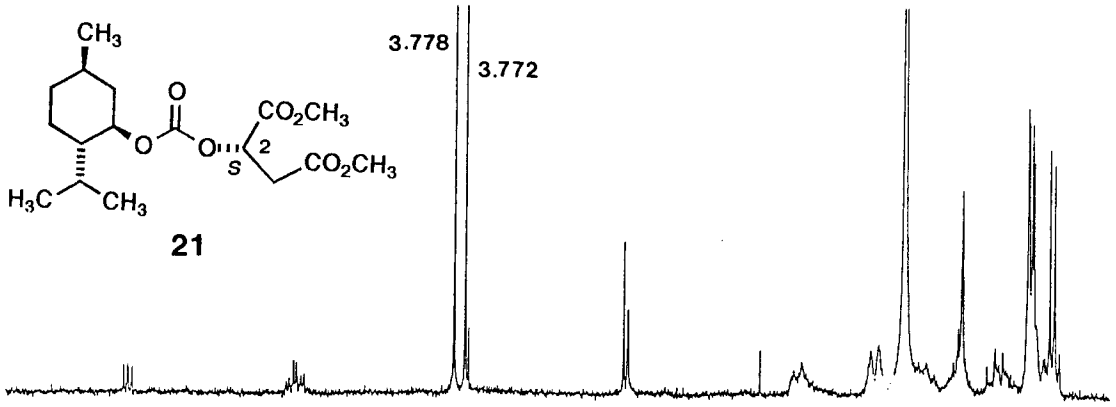

Figure III.13 ^{1}H NMR Spectra of Dimethyl-Menthoxycarbonyl-Malate (**21**) from Ozonolysis of (**20**), in $CDCl_3$.

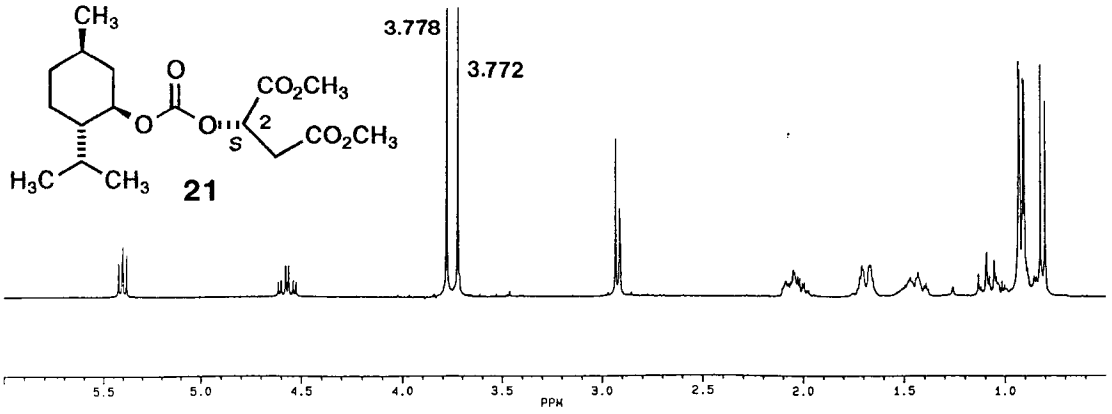

Figure III.14 ^{1}H NMR Spectra of Authentic *S*-Standard Dimethyl-Menthoxycarbonyl-Malate (**21**) in $CDCl_3$.

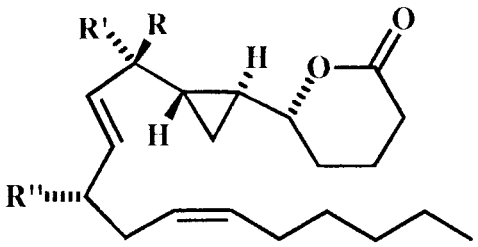

23 R=H, R'=R''=$OCOC_6H_5Br$
24 R=H, R'=$OCOC_6H_5Br$, R''=OAc
25 R=H, R'=$OCOC_6H_5Br$, R''=OH

Figure III.15 Structures of Constanolactone A *p*-Bromobenzoate Derivatives.

acetate and C-9 *p*-bromobenzoate substitutions were assigned based upon a comparison of the α-ester ^{1}H NMR resonances in **2 4** with those of the diacetate derivative **9**. In both H-12 resonated at δ5.3 while in mixed ester **2 4** H-9 was downfield (δ5.17) compared to diacetate **9** (δ4.90). While the CD spectrum of bis-(*p*-bromobenzoate) **2 3** was not reliably interpretable because of free rotation in centers separating the various chromophores, the C-9 allylic *p*-bromobenzoate chromophore in mixed ester **2 4** was ideally suited for determination of the C-9 stereochemistry by exciton chirality.[135] The combination of a negative nondegenerate *p*-bromobenzoate Cotton effect (Δε -7.3) at 244.5 nm in **2 4**, and a preferred rotomer conformation for C-9-C-10 in which the C-H and C=C bonds eclipse as indicated by a $^3J_{H9\text{-}H10}$ = 5.3 Hz (typically 5.2-9.2 Hz),[136,137] indicated a left-handed helicity between these groups and defined the stereochemistry at C-9 as *S* (Figures III.16 and III.17).

The uncertain origin of the mixed ester **2 4** prompted us to repeat the bromobenzoylation of **7** in the absence of 4-dimethylaminopyridine catalyst in the hopes of producing the C-9 mono-*p*-bromobenzoate **2 5**. Following workup, derivative **2 5** was isolated by silica gel flash chromatography and HPLC. Its identity as the C-9 mono-*p*-bromobenzoate was effectively revealed by the chemical shifts of the C-9 (δ5.07) and C-

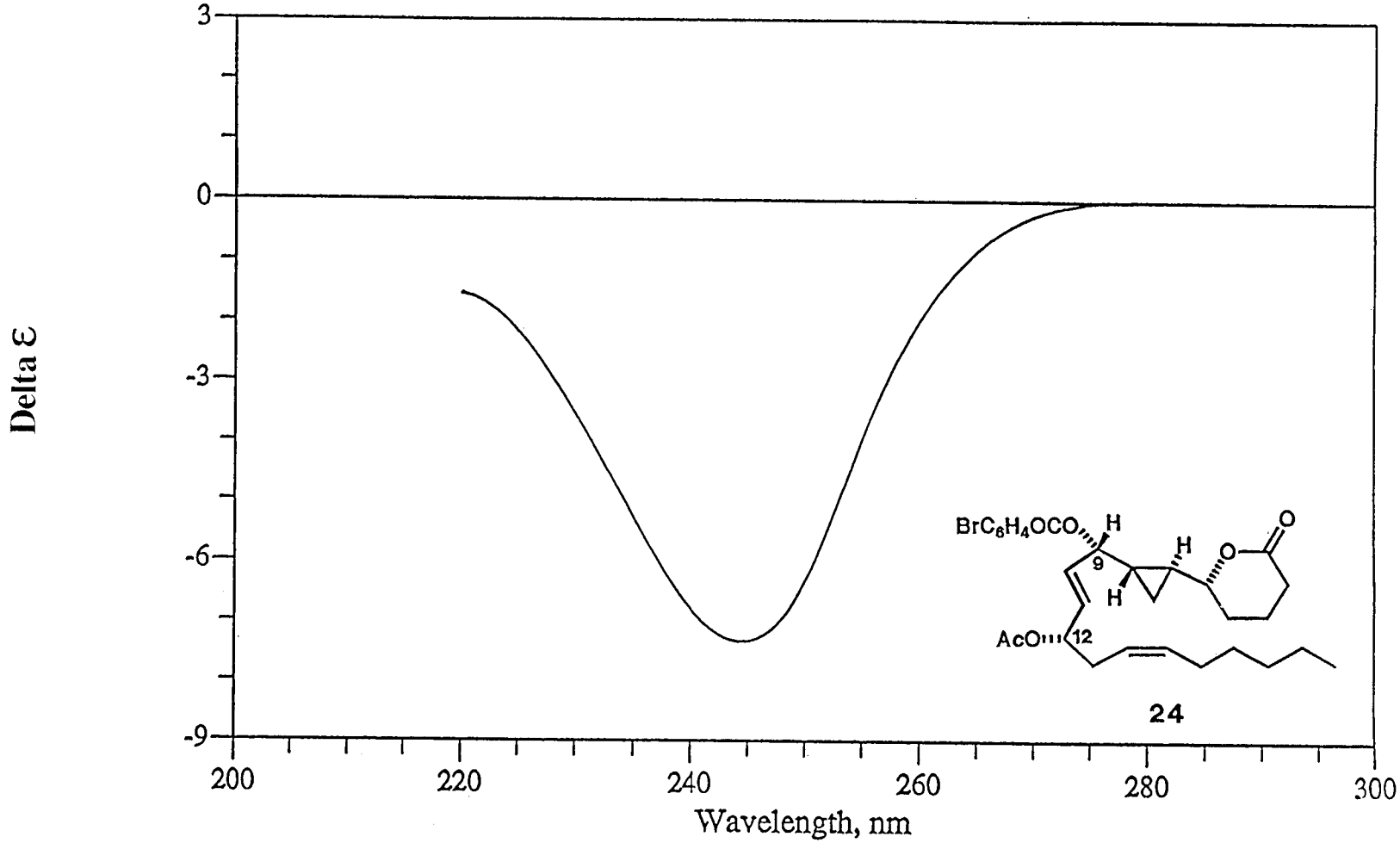

Figure III.16 CD Spectrum of 12-Acetoxy-9-(*p*-Bromobenzoyl)-Constanolactone A (**24**) in EtOH.

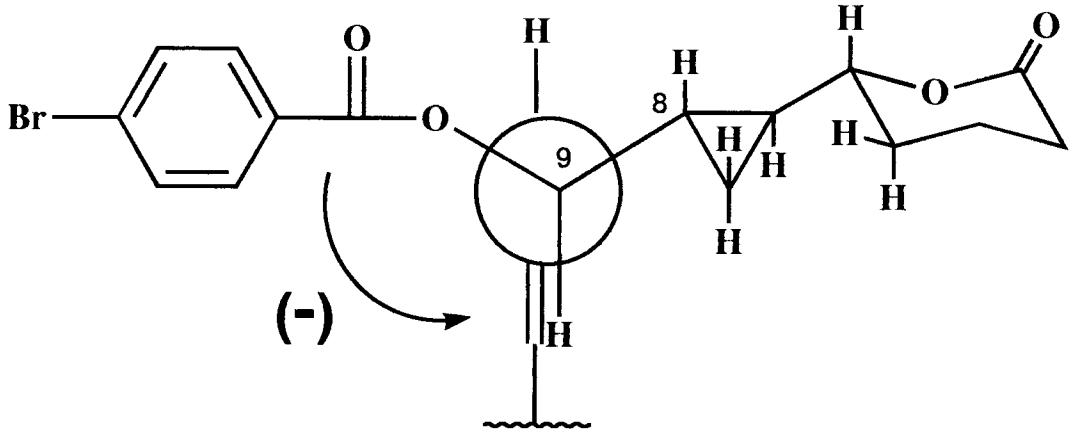

Figure III.17 Newman Projection of Predicted Favored Rotamer of 9-(*p*-Bromobenzoate) Derivatives **2 4** and **2 5** Used in CD Analysis for Determination of Absolute Stereochemistry.

12 (δ4.20) proton resonances in comparison with the natural product **7** (C-12 = δ4.17) and bis-(*p*-bromobenzoate) **2 3** (C-9 = δ5.17). A relatively large C-9 to C-10 $^3J_{HH}$ = 6.2 Hz and similar CD spectrum to that of **2 4** (Δε -4.6 at 242 nm) confirmed the 9*S* stereochemistry of **2 5**, as above. Therefore, taking into consideration the relative configuration as assigned by NOESY and coupling constants, the C-12 stereochemistry from analysis of the chiral MC-derivative **2 1**, and the above CD analysis, the absolute configuration of **7** is 5*R*, 6*S*, 8*S*, 9*S*, 12*S*. Since constanolactone B (**7**) is the C-9 epimer of **7** and yields the same chiral MC-derivative (**2 1**) upon reaction with (-)-menthoxycarbonyl chloride (**1 9**) followed by ozonolysis, the absolute configuration of **8** may be assigned as 5*R*, 6*S*, 8*S*, 9*R*, 12*S*.

Further investigation of minor compounds obtained from acetylation of a crude mixture of constanolactone natural products resulted in the isolation and identification of two new constanolactone analogs (**2 6** and **2 7**) as synthetic diacetate derivatives (**2 8** and

29) (Figure III.18). The new derivatives **28** and **29** possess nearly identical ^{1}H and ^{13}C NMR features to the diacetates of constanolactone A (**9**) and constanolactone B (**10**). Further, by MS, these diacetate derivatives were 2 mass units smaller than constanolactone A diacetate (**9**) and constanolactone B diacetate (**10**), and hence, each possessed one additional olefinic bond. The location of the new olefin was revealed through signals for an additional two proton bis-allylic triplet at 2.78 ppm and a downfield and sharp C-20 methyl triplet (Figures III.19 and III.20, Table III.4), thus defining **28** and **29** as ω-3 unsaturated analogs of **9** and **10**, respectively. Relative stereochemistry in diacetate **28** and **29** was assigned the same as in **9** and **10** based on the near superimposability of ^{1}H and ^{13}C NMR shifts and coupling constants for all pertinent regions of the spectra (Table III.1 and Table III.4). Additionally, the CD spectrum for **30**, the synthetic bis-(*p*-bromobenzoate) derivative of **27**, was nearly identical to that of **31**, the bis-(*p*-bromobenzoate) derivative of constanolactone B (**8**), indicating that they possess the same overall absolute stereochemistry.

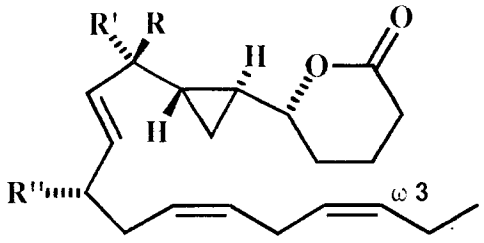

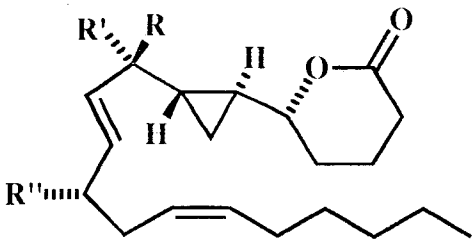

26 R=H, R'=R''=OH
27 R=R''=OH, R'=H
28 R=H, R'=R''=OAc
29 R=R''=OAc, R'=H
30 R=R''=$OCOC_6H_5Br$, R'=H

31 R=R''=$OCOC_6H_5Br$, R'=H

Figure III.18 Structures of Constanolactone C, D, and B Derivatives (**26-30** and **31**).

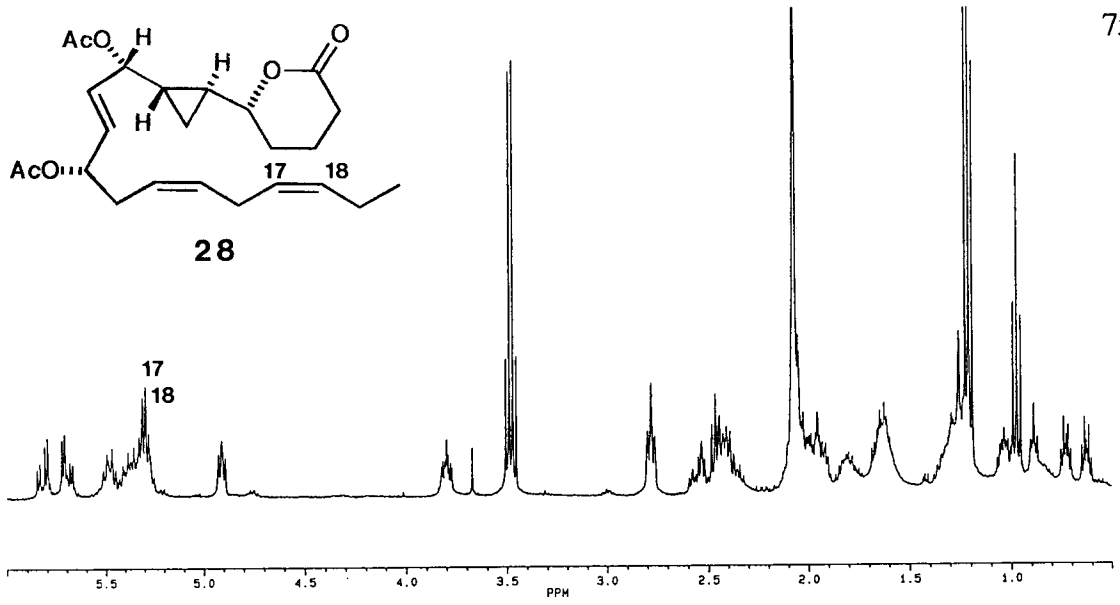

Figure III.19 ^1H NMR Spectrum of Constanolactone C Diacetate (**28**) in $CDCl_3$.

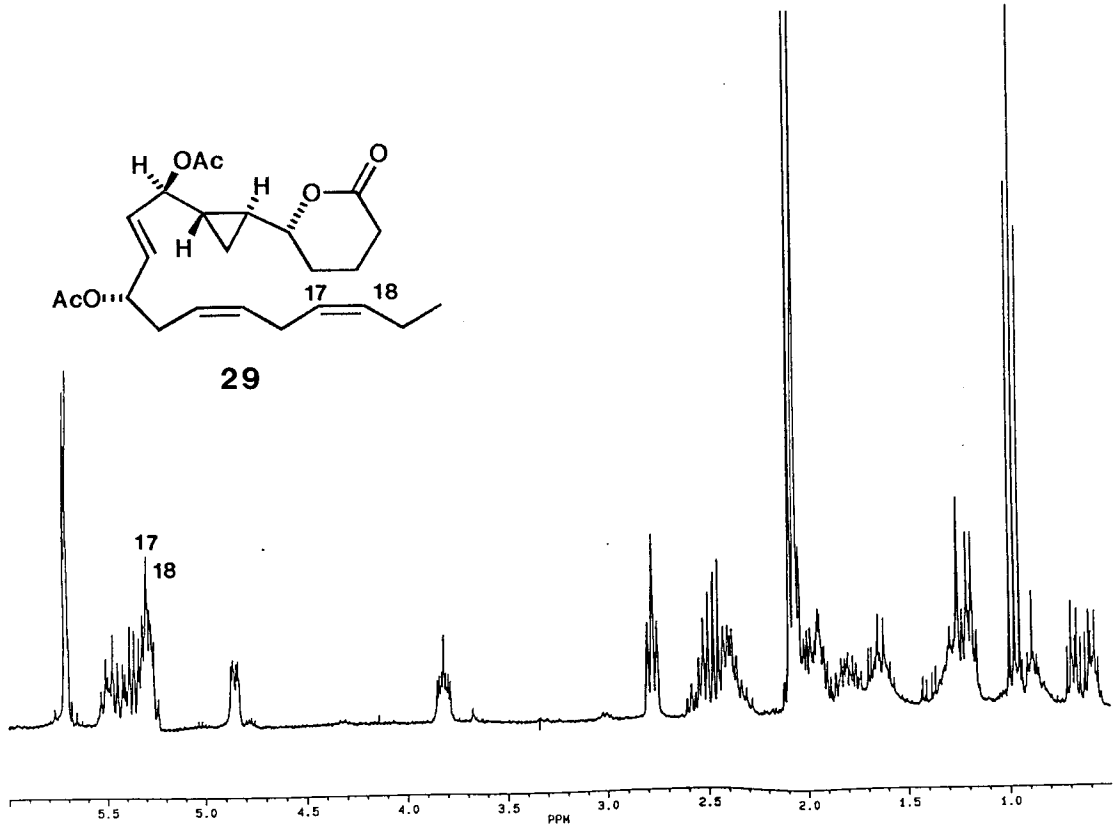

Figure III.20 ^1H NMR Spectrum of Constanolactone D Diacetate (**29**) in $CDCl_3$.

Table III.4 ^{1}H and ^{13}C NMR Data for Per-acetates of Constanolactones C (**28**) and D (**29**).

Position	Constanolactone C per-acetate (**28**) ^{1}H ($CDCl_3$)	^{13}C[a]	Constanolactone D per-acetate (**29**) ^{1}H ($CDCl_3$)	^{13}C[a]
1		NA		NA
2a	2.40 ddd (17.7, 8.5, 6.8)	29.52	2.44 ddd (17.5, 8.4, 6.8)	29.52
b	2.56 bdt (17.7, 6.6)		2.55 bdt (17.5, 7.4)	
3a	1.80 m	18.42	1.80 m	18.28
b	1.96 m		1.94 m	
4a	1.60 m	27.87	1.65 m	27.79
b	2.0 m		2.0 m	
5	3.80 ddd (10.5, 7.4, 3.1)	82.30	3.82 ddd (10.0, 7.2, 3.1)	81.91
6	1.2-1.3 m	20.75[b]	1.20 m	21.71[c]
7a	0.62 dt (8.6, 5.3)	7.62	0.59 dt (8.6, 5.5)	6.73
b	0.73 dt (8.8, 5.3)		0.68 dt (8.5, 5.5)	
8	1.04 m	20.75[b]	1.2 m	21.22[c]
9	4.91 dd (7.2, 5.6)	75.30	4.85 bdd (7.9, 2.6)	75.49
10	5.69 ddd (15.7, 5.6, 0.9)	130.89	5.71 m	130.42
11	5.82 ddd (15.7, 6.0, 1.0)	129.16	5.71 m	129.45
12	5.29 m	73.06	5.3 m	73.01
13	2.4 m	32.22	2.4 m	32.31
14	5.26-5.4 m	123.78	5.2-5.4 m	123.63
15	5.47 dtt (10.8, 7.3, 1.5)	131.29	5.49 dtt (10.7, 7.2, 1.5)	131.38
16	2.78 t (7.1)	25.64	2.78 t (7.2)	25.64
17	5.26-5.4 m	126.79	5.2-5.4 m	126.79
18	5.26-5.4 m	132.17	5.2-5.4 m	132.16
19	2.0 m	20.54	2.0 m	20.10
20	0.98 t (7.5)	15.24	0.98 t (7.5)	14.23
	Acetate Esters		Acetate Esters	
	2.07 s	20.09[d]	2.06 s	20.30[e]
	2.08 s	20.09[d]	2.09 s	21.22[e]

a) ^{13}C NMR data from ^{13}C DEPT (135°); (b-e) Assignments may be interchanged.

A subsequent collection of *C. simplex* yielded, following extraction with warm $CHCl_3$/MeOH, silica gel chromatography and HPLC, two additional constanolactone-related products, **32** (0.02%) and **33** (0.049%) (Figure III.21). Their structures were elucidated principally by comparison of NMR data with that of constanolactone A (**7**) and B (**8**). The only significant differences between the NMR spectra of these new compounds and the natural products **7** and **8** were a new three proton methyl singlet resonance at 3.32 ppm in **32** and at 3.27 ppm in **33**, and an upfield shifted C-9 proton ($\Delta\delta$ = 0.3 ppm in **32** and $\Delta\delta$ = 0.53 in **33**, Figure III.22, Table III.5). Hence, these new compounds were the C-9 methyl ether analogs of **7** and **8**, respectively, and presumably arise as solvolysis artifacts produced during extraction with MeOH. The significance of this finding is discussed in more detail below.

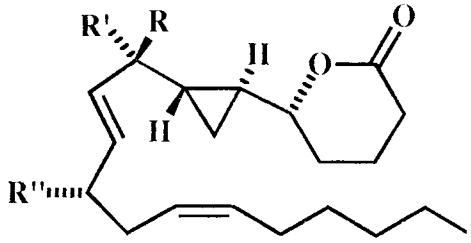

32 R=H, R'=OCH_3, R''=OH
33 R=OCH_3, R'=H, R''=OH

Figure III.21 Structures of 9-OMe Analogs of Constanolactone A and B (**32** and **33**).

Three additional metabolites were isolated from the same collection of *C. simplex* which yielded the original per-acetate derivatives constanolactone A (**9**) and B (**10**). A silica gel vacuum chromatographic fraction eluting with 45% EtOAc in hexanes was acetylated to give, following additional purification by normal-phase HPLC, three new constanolactones, E-G (**34-36**), as diacetate derivatives (**37-39**) (Figure III.23). Since both the proton and carbon count and mass spectrum for **37** and **38** were identical with

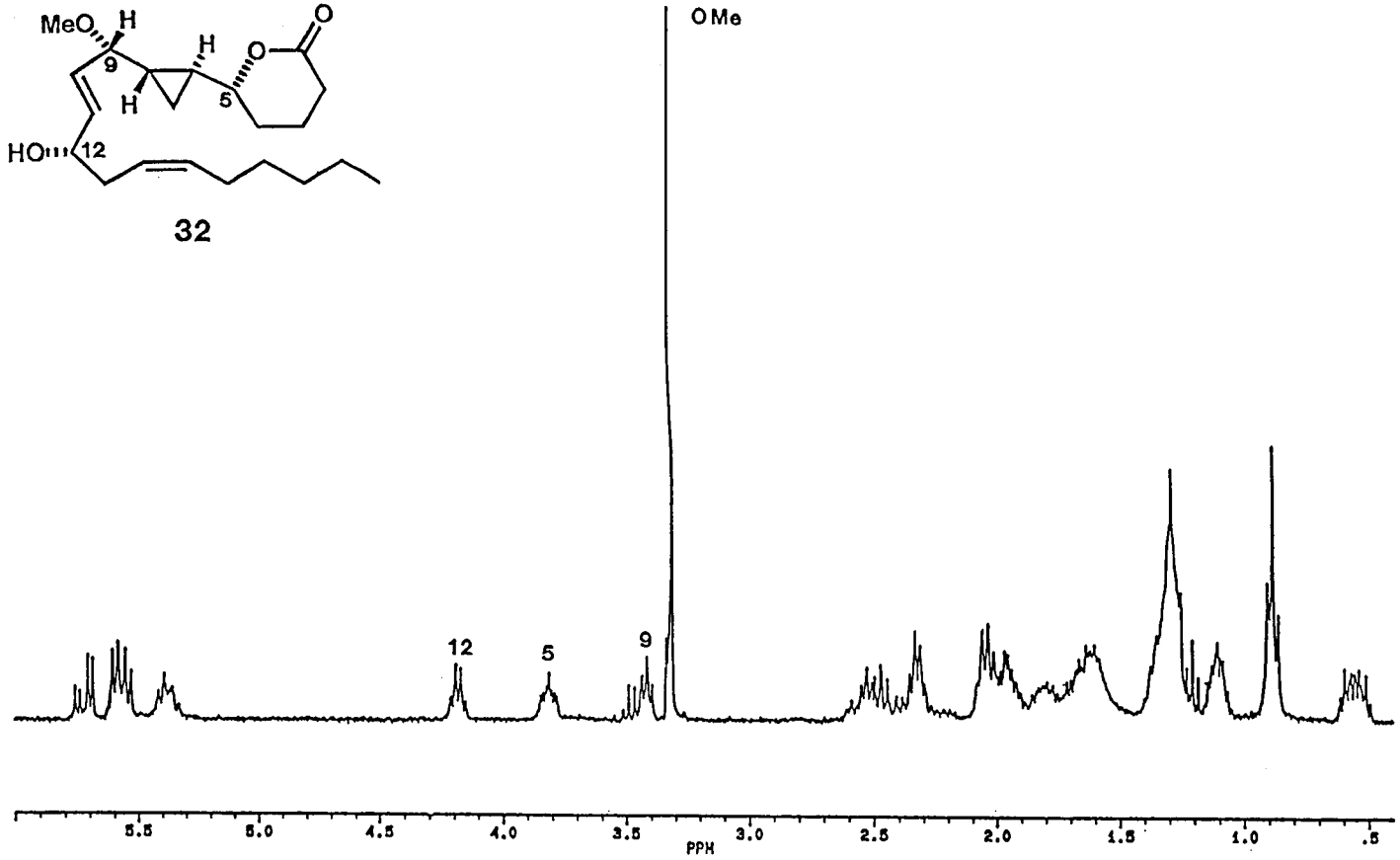

Figure III.22 ^1H NMR Spectrum of 9-O-Methyl Constanolactone A (32) in $CDCl_3$.

Table III.5 ^{1}H and ^{13}C NMR Data for C-9 Methyl Ethers of Constanolactones A (**32**) and B (**33**) in $CDCl_3$.

Position	Derivative **32** ^{1}H	$^{13}C^{a}$	Derivative **33** ^{1}H
1		NA	
2a	2.44 ddd (17.6, 8.5, 6.8)	29.01	2.44 ddd (17.7, 8.3, 6.8)
b	2.55 dddd (17.6, 7.0, 5.3, 1.3)		2.55 ddd (17.7, 6.9, 6.7)
3a	1.80 m	18.16	1.80 m
b	1.96 m		1.98 m
4a	1.67 m	27.46	1.68 m
b	2.0 m		2.04 m
5	3.82 ddd (10.2, 7.2, 3.1)	82.96	3.70 td (9.5, 3.3)
6	1.11 m	20.68	1.09 m
7a	0.52 dt (8.4, 5.4)	5.24	0.65 dt (8.5, 5.2)
b	0.58 dt (8.6, 5.4)		0.79 dt (8.7, 5.3)
8	1.6 m	20.69	1.65 m
9	3.42 bt (6.9, 5.7)	81.69	3.12 bt (7.0)
10	5.57 ddd (16.2, 6.9, 1.1)	135.19	5.66 m
11	5.72 ddd (16.2, 5.7, 0.6)	124.01	5.66 m
12	4.18 bq (6)	71.39	4.19 bq (6.1)
13	2.32 bq (6.2)	35.10	2.34 m (9 lines)
14	5.37 dtt (10.9, 6-7.5, 1.6)	129.05	5.39 bdt (10.9, 7.1)
15	5.55 m	133.50	5.54 bdt (10.9, 7.3)
16	2.0 m	27.24	2.0 m
17	1.35 m	29.35	1.35 m
18	1.3 m	31.31	1.3 m
19	1.3 m	22.34	1.3 m
20	0.89 t (6.8)	13.83	0.89 t (6.8)
OMe	3.32 s (3H)	56.09	3.27 s (3H)

a) ^{13}C NMR data from ^{13}C DEPT (135°)

those of the per-acetate constanolactone derivatives **9** and **10** ($C_{24}H_{36}O_6$), it was apparent that **37** and **38** were either regio- or stereochemical isomers of **9** and **10**. By ^1H and ^{13}C NMR, the C-1 to C-8 portion of both **37** and **38** were the same as in **9** and **10** (Table III.1 and Table III.6). However, from COSY analysis, the new compounds differed from **9** and **10** in the C-9 to C-12 region. This was reflected by a downfield shift of the C-8 methine proton (δ1.6 and 1.54 in **37** and **38**, respectively, versus δ1.2-1.3 in **9** and **10**), C-9 and C-10 protons occurring at shifts typical for an olefin, and the C-11 and C-12 protons occurring at shifts consistent with these positions bearing acetoxy groups (Table III.6). The C-9-C-10 olefin in both **37** and **38** was of a *trans* geometry as revealed by a $J_{H9\text{-}H10}$ = 15 Hz coupling constant. The ^1H NMR spectrum of derivative **39**, constanolactone G diacetate, was highly analogous to that of **38**, differing only in the absence of the methylene band at δ1.30-1.35 and the presence of additional olefinic and bis-allylic resonances, thus defining derivative **39** as the ω-3 analog of constanolactone F diacetate (**38**).

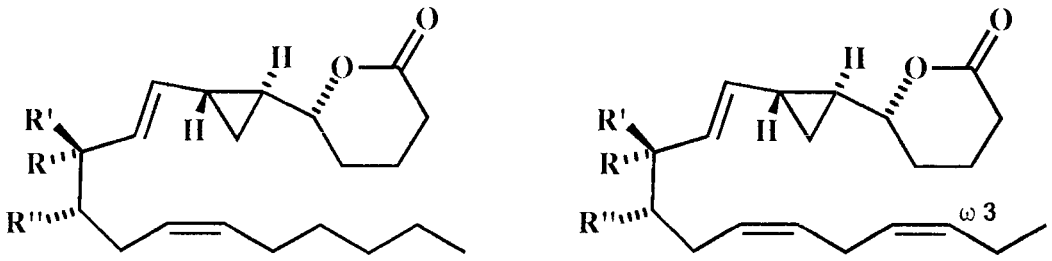

34 R=R''=OH, R'=H
35 R=H, R'=R''=OH
37 R=R''=OAc, R'=H
38 R=H, R'=R''=OAc

36 R=H, R'=R''=OH
39 R=H, R'=R''=OAc

Figure III.23 Structures of Constanolactones E, F, G (**34-36**) and Derivatives (**37-39**).

Constanolactones E (**34**) and F (**35**) were subsequently isolated as natural products from another extract of frozen *C. simplex* (May 1992). The diols **34** and **35** were

Table III.6 ^{1}H and ^{13}C NMR Data for Constanolactones E (3 4) and F (3 5) and Diacetate Derivatives (3 7) and (3 8) in $CDCl_3$.[a]

Position	Constanolactone E (3 4) ^{1}H	Constanolactone E (3 4) ^{13}C	Constanolactone E diacetate (3 7) ^{1}H	Constanolactone E diacetate (3 7) ^{13}C	Constanolactone F (3 5) ^{1}H	Constanolactone F (3 5) ^{13}C	Constanolactone F diacetate (3 8) ^{1}H	Constanolactone F diacetate (3 8) ^{13}C
1		171.50		171.32		171.50		171.40
2a	2.46 ddd (17.6, 8.5, 7.0)	29.26	2.46 ddd (17.7, 8.7, 7.0)	29.16	2.46 ddd (17.8, 8.6, 6.9)	29.29	2.5-2.6 m	29.16
b	2.57 bdt (17.6, 6.3)		2.57 dt (17.7, 6.6)		2.57 ddd (17.8, 7.9, 6.5)			
3a	1.8 m	18.40	1.8 m	18.45	1.8-2.0 m	18.45	1.8-2.0 m	18.43
b	1.94 m		1.94 m					
4a	1.7 m	27.74	1.66 td	27.81	1.66 m	27.79	1.66 m	27.78
b	2.0 m		2.0 m		1.99 m		1.99 m	
5	3.79 ddd (10.2, 7.8, 3.1)	83.25	3.78 ddd (9.6, 7.7, 3.1)	82.99	3.78 ddd (10.2, 7.8, 3.1)	83.29	3.74 ddd (10.8, 7.4, 3.1)	83.15
6	1.12 m (7 lines)		1.12 m	24.87	1.11 m (7 lines)	24.95	1.12 m (7 lines)	24.94
7a	0.72 dt (8.8, 5.3)	10.64	0.71 dt (8.7, 5.2)	10.75	0.71 dt (8.7, 5.2)	10.50	0.68 dt (8.6, 5.2)	10.59
b	0.77 dt (8.4, 5.3)		0.79 dt (8.6, 5.2)		0.76 dt (8.5, 5.3)		0.75 dt (8.6, 5.2)	
8	1.59 m (7 lines)	19.32	1.6 m	19.25	1.57 m	19.35	1.54 m	19.37
9	5.4 bdd (15.7, 8.1)	135.64	5.39 dd (15.4, 8.2)	138.65	5.39 dd (15.5, 8.2)	135.51	5.4 m	138.16
10	5.63 dd (15.7, 6.8)	124.74	5.55 dd (15.4, 7.6)	122.16	5.57 dd (15.5, 6.8)	127.96	5.3-5.5 m	123.01
11	4.10 dd (6.8, 3.8)	74.84	5.29 m	74.81	3.91 t (6.3)	75.13	5.31 m	74.19
12	3.66 m (5 lines)	73.90	5.03 td (6.0, 3.7)	73.70	3.48 dd (6.3, 5.7)	74.20	4.99 q (6.2)	73.71
13	2.25 m	29.93	2.28 m	28.05	2.25 m	31.05	2.30 bt (6.5)	28.54
14	5.37 m	126.37	5.27 m	123.37	5.4 m	124.54	5.3 m	123.01
15	5.5 m	133.54	5.49 bdt (10.8, 6.8, 1.5)	133.26	5.55 m	133.53	5.48 m	133.46
16	2.0 m	27.39	2.0 m	27.37	1.98 m	27.39	1.98 m	27.29
17	1.35 m	29.50	1.35 m	29.51	1.35 m	29.53	1.35 m	29.51
18	1.3 m	31.47	1.3 m	31.47	1.3 m	31.52	1.3 m	31.49
19	1.3 m	22.53	1.3 m	22.55	1.3 m	22.55	1.3 m	22.54
20	0.89 t (6.8)	14.03	0.89 t (6.8)	14.04	0.89 t (6.7)	14.06	0.89 t (6.7)	14.04
$CO\underline{C}H_3$			2.04 s	21.04			2.06 s	21.14
			2.05 s	21.17			2.07 s	20.95
$\underline{C}OCH_3$				170.45				170.38
				169.93				169.94

slightly less polar than constanolactone A (**7**) and B (**8**), eluting with 50% EtOAc in hexanes from silica gel and were readily purified by normal-phase HPLC. Overlapping olefinic/α-acetoxyl regions in derivatives **37** and **38** were resolved in the ^{1}H NMR spectra of natural products **34** and **35** (Table III.6), allowing for straight forward deduction of the C-8 to C-12 region of these molecules (Figures III.24 and III.25). The difference in ^{1}H-^{1}H coupling constants between H-11 and H-12 in the vicinal-diols **34** ($^3J_{11\text{-}12}$ = 3.8 Hz) and **35** ($^3J_{11\text{-}12}$ = 6.3 Hz) suggested an *erythrolthreo* relationship for these two compounds. The relative configurations at C-5, C-6, and C-8 in vicinal-diols **34-36** were deduced to be identical to that in constanolactones A-D (5*R**, 6*S**, 8*S**) by comparison of the ^{1}H and ^{13}C NMR of authentic **7-10** with the C-5 to C-8 region in **34** and **35** and the per-acetate derivatives **37-39**.

A series of derivatives of **34** and **35** were produced in order to further investigate the stereochemistry at C-11 and C-12. Treatment of **34** or **35** with 2,2-dimethoxypropane gave the methyl ester acetonide derivatives of constanolactone E (**40**) and F (**41**) (Figure III.26). A relatively small $^3J_{\text{H11-H12}}$ value (6.2 Hz) and dissimilar magnetic environment of acetonide methyl groups (Δδ = 0.14 ppm) were indicative of an *erythro* configuration in derivative **40**, while a relatively large H-11 to H-12 $^3J_{\text{HH}}$ value (8.1 Hz) and similar magnetic environment of acetonide methyl groups (Δδ = 0.007 ppm) established the diol configuration in derivative **41** as *threo* (Figures III.27 and III.28).[138]

The absolute stereochemistry of C-11 and C-12 in constanolactones E (**34**) and F (**35**) were determined by CD analysis of the corresponding bis-(*p*-bromobenzoate) derivatives, **42** and **43** (Figure III.29). The structures of the bis-(*p*-bromobenzoate) derivatives **42** and **43** were confirmed by UV, ^{1}H-NMR, and CIMS. However, for both derivatives, the CD spectra showed a weak positive homochromophoric exciton coupling (Figure III.30). Apparently, the two bis-(*p*-bromobenzoate) derivatives adopt different conformations so as to both give weakly positive split Cotton effects. However, in

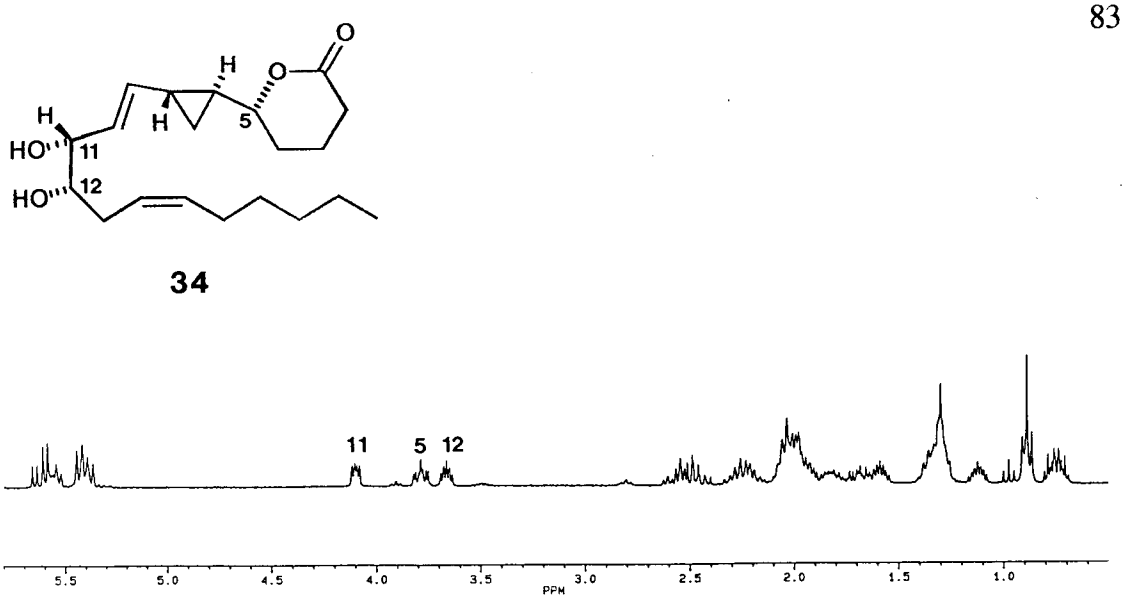

34

Figure III.24 ^{1}H NMR Spectrum of Constanolactone E (**3 4**) in $CDCl_3$.

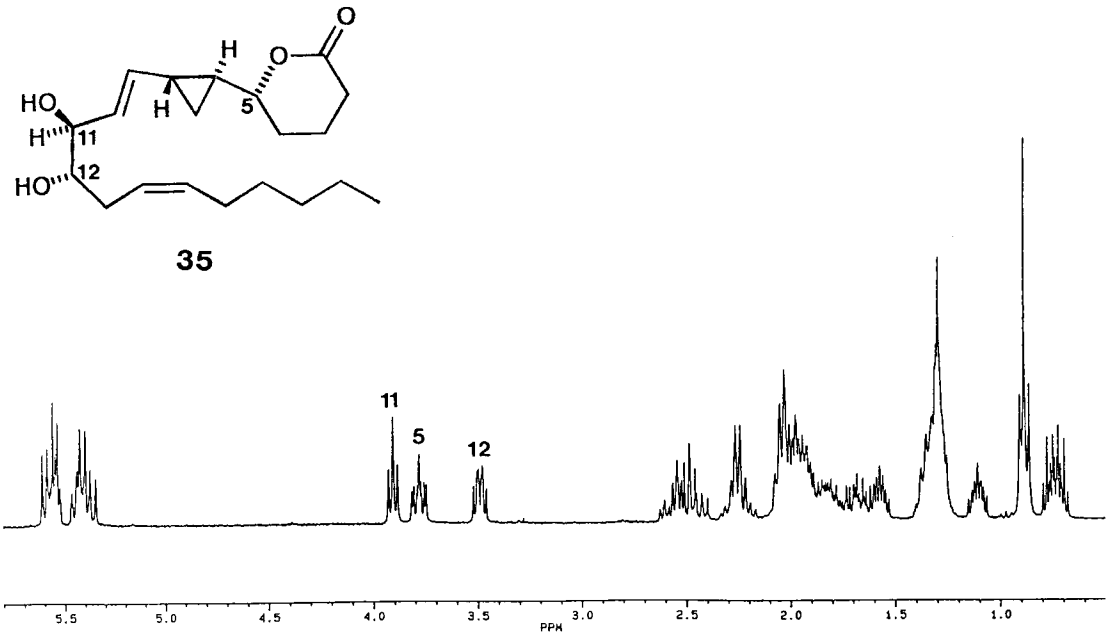

35

Figure III.25 ^{1}H NMR Spectrum of Constanolactone F (**3 5**) in $CDCl_3$.

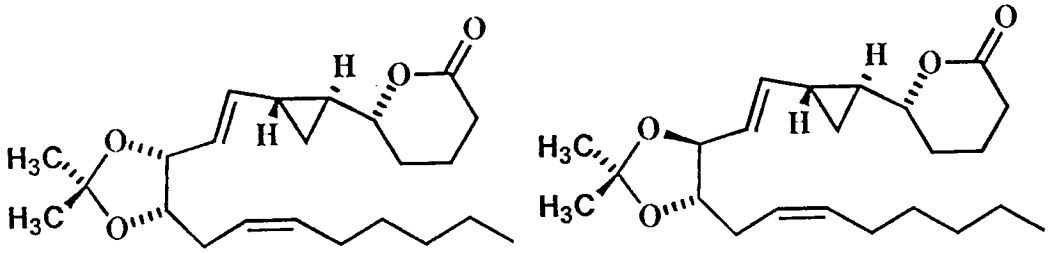

40 41

Figure III.26 Structures of Methylated Acetonide Derivatives **40** and **41**.

derivative **43**, a pronounced bathochromic shift in the CD maxima (λ_{max} = 255, 240 nm) was observed. I interpret this to signify that the C-11 benzoate shows exciton coupling both to the C-12 benzoate (positive) and C-9-C-10 olefin (negative, $\Delta\varepsilon$ + 5.4, −11.8; λ_{max} = 255, 240 nm).[135] A computerized simulation in which the negative C-9 benzoate to C-10-C-11 olefin coupling observed for compound **25** was mathematically subtracted from the curve obtained for **43** produced a symmetrical CD curve with maxima more typical of benzoate to benzoate couplings (λ_{max} = 238, 253 nm, Figures III.30 and III.31). Similarly, bis-(*p*-bromobenzoate) derivative **42** gave anomalous intensities in its CD spectrum ($\Delta\varepsilon$ +9.1; λ_{max} = 252.5 nm) which I interpret to be due to a positive C-11 benzoate to olefin coupling which overlaps a positive benzoate-benzoate coupling. In both derivatives **32** and **33** relatively large C-9 to C-10 proton coupling constants of 8 Hz and 7 Hz, respectively (typically 5.2-9.2 Hz),[136-137] established the preferred rotomer conformations, in each case, with eclipsed C-H and C=C bonds. Thus, in derivative **42** the positive C-11 *p*-bromobenzoate to olefin coupling indicates a right-handed helicity

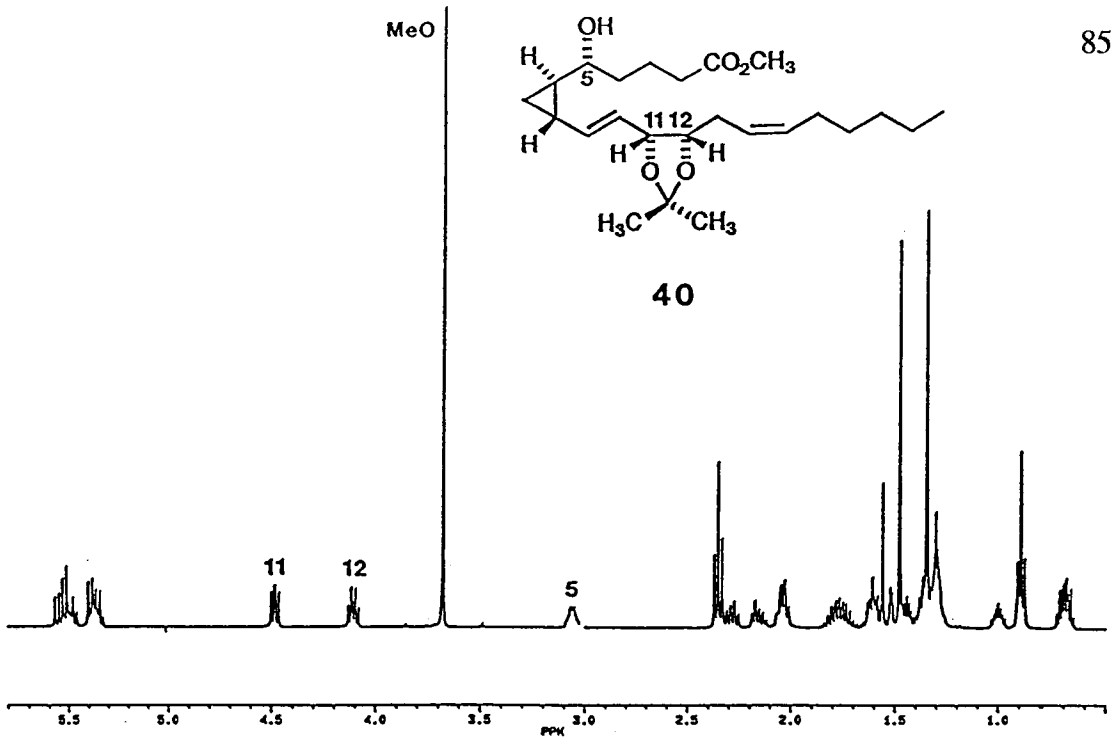

Figure III.27 ^1H NMR Spectrum of Acetonide of Methyl Constanolactone E (40) in $CDCl_3$.

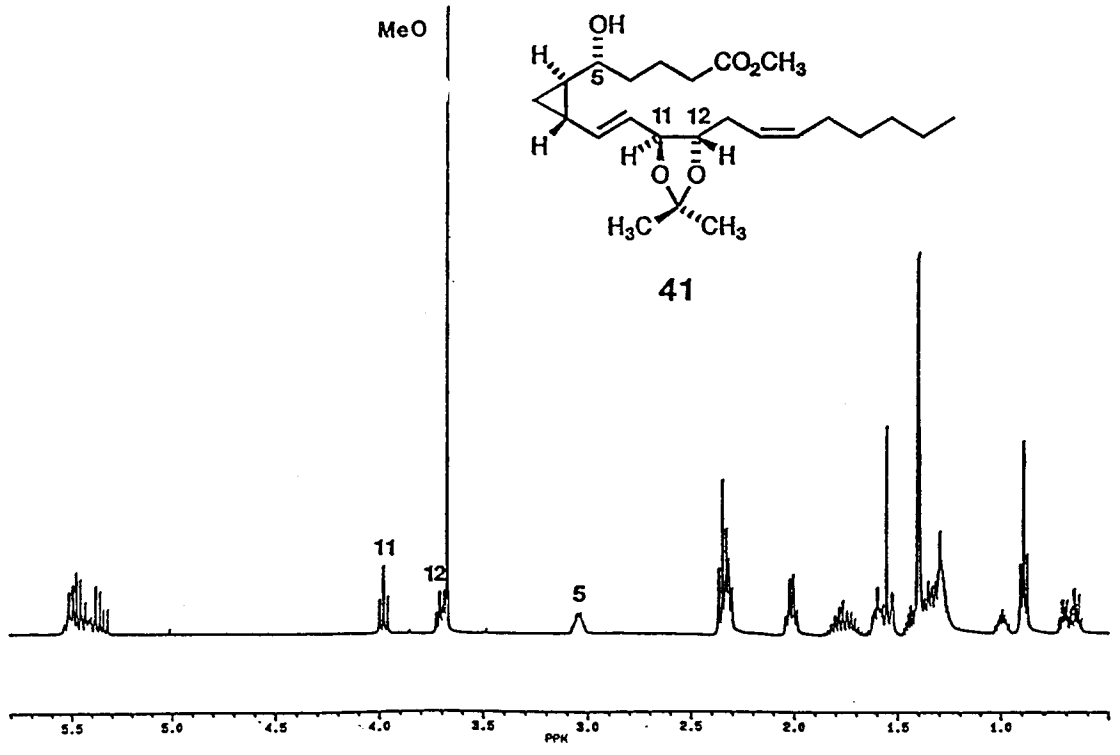

Figure III.28 ^1H NMR Spectrum of Acetonide of Methyl Constanolactone F (41) in $CDCl_3$.

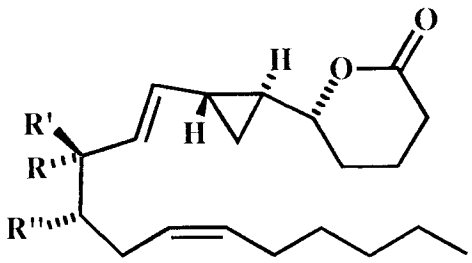

42 R=R''=$OCOC_6H_5Br$, R'=H
43 R=H, R'=R''=$OCOC_6H_5Br$

Figure III.29 Structures of Constanolactone E and F Bis-(*p*-Bromobenzoate)

Derivatives.between these groups and defines the stereochemistry at C-11 as *R* while the negative C-11 *p*-bromobenzoate to olefin coupling in **43** indicates a left handed helicity or 11*S* stereochemistry (Figure III.32). As the relationship between alcohols in **34** and **35** was shown to be *erythro* and *threo*, respectively, from analysis of the acetonide derivatives **40** and **41**, the absolute stereochemistry at C-11 and C-12 is given as 11*R*, 12*S* for constanolactone E (**34**) and 11*S*, 12*S* for constanolactone F (**35**). Thus, the overall stereochemistry in constanolactone E (**34**) is defined as $5R^*$, $6S^*$, $8S^*$, 11*R*, 12*S*, and constanolactone F (**35**) as $5R^*$, $6S^*$, $8S^*$, 11*S*, 12*S*.

It has been suggested that these carbocyclized 20 carbon compounds may be the ultimate result of an involved form of arachidonic acid metabolism, but no conclusive evidence was available.[112,115,124,139] Therefore, I initiated an investigation of *in vitro* arachidonic acid (**44**) metabolism in *Constantinea simplex*. Crude *C. simplex* enzyme preparations were produced by macerating and "defatting" algal tissues at low temperatures in non-denaturing solvents (≈ -70 °C, CO_2(s)/acetone). This process was repeated until

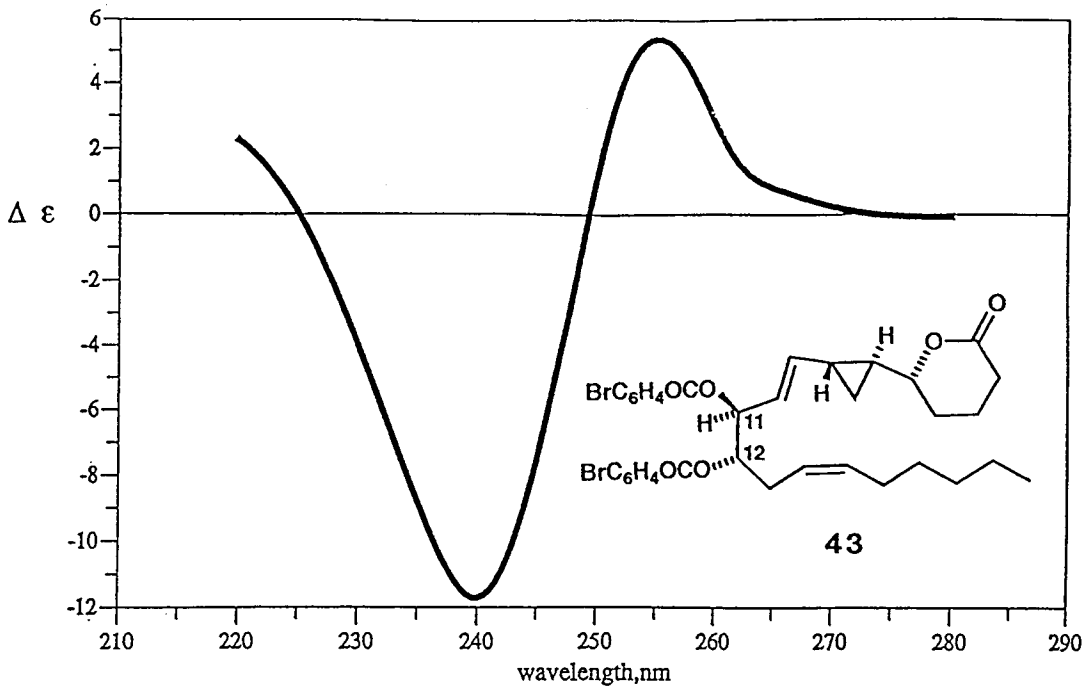

Figure III.30 CD Spectrum of Bis-(*p*-Bromobenzoyl)-Constanolactone F (43) in EtOH.

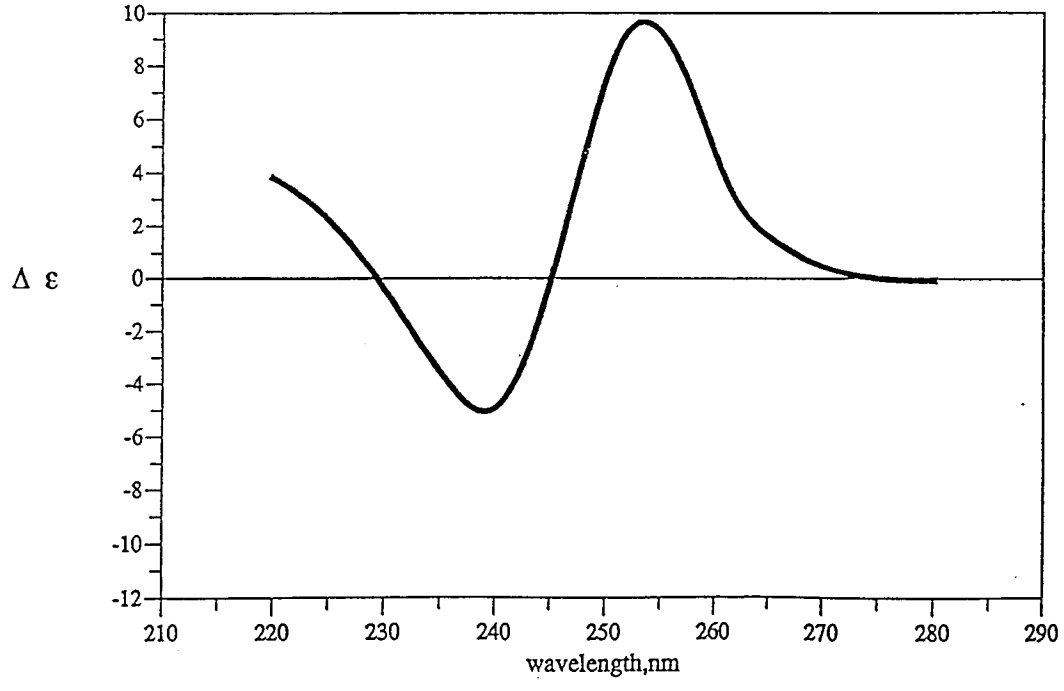

Figure III.31 CD Spectral Simulation of Bis-(*p*-Bromobenzoyl)-Constanolactone F (43) in EtOH, with Olefin-p-Bromobenzoyl Exiton Coupling Mathematically Subtracted.

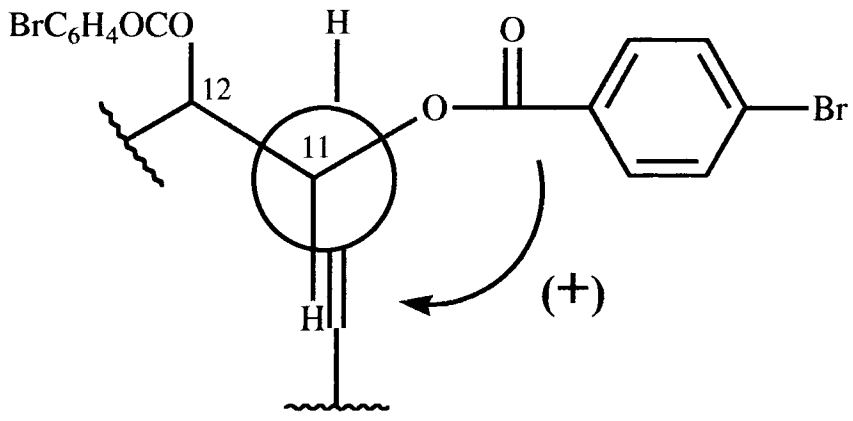

42

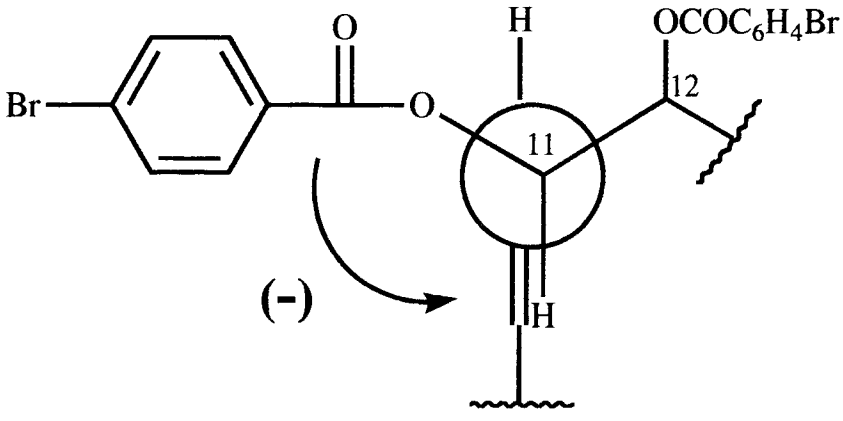

43

Figure III.32 Newman Projections of Predicted Favored Rotamers of Bis-(*p*-Bromobenzoate) Derivatives **42** and **43** Used in CD Analysis for Determination of Absolute Stereochemistry.

nearly all pigments, lipids, and other acetone soluble compounds were removed. The pulverized-extracted algal material was then dried under a nitrogen stream to form an acetone-extracted powder or "acetone powder" (AP). The AP was placed in pH 7.4 buffer and incubated with exogenous arachidonic acid (AA, **44**) and used in a series of experiments to examine the mechanism of constanolactone biosynthesis.

Chloroform extracts of dry "AP alone" were shown to produce no detectable hydroxyeicosanoids by TLC analysis (no UV-active and/or blue charring spots with 50% H_2SO_4, Figure III.33). However, extracts from buffer incubated "AP alone" (without added AA) contained traces of oxylipin products (TLC, blue charring spots, R_f=0.55, 0.47). These findings suggest that low levels of substrate may either be only sparingly acetone soluble or tightly bound to the enzyme powder. Incubation of the "AP alone" in buffer allows for the enzymatic conversion of endogenous substrate to eicosanoid-type products.

Incubation experiments were performed and the products (constanolactones A and B) were acetylated (Ac_2O/Pyridine, ca. 12h) and analyzed by normal phase HPLC with differential refractometer detection at a constant flow rate. Enzyme products were quantified by HPLC area under the curve measurements coupled with actual recovered product masses.

HPLC analysis of "AA + AP" incubations indicate that, at a given temperature, constanolactone product formation is directly proportional to the quantity of AA substrate added to each treatment. Incubations were conducted at 1 °C, 9 °C, and 25 °C using a range of AA substrate levels (0.0 mg, 0.1 mg, 1.0 mg, and 10.0 mg per incubation). Greater than five fold increases in the formation of eicosanoid products were observed at 25 °C when AA substrate levels were incrementally increased from a control level of 0.0 mg up to 10.0 mg (Figure III.34). "AA + boiled AP" treatments yielded significant quantities of AA and none of the metabolites associated with active AP incubations, suggesting that the formation of the constanolactones is the result of a heat labile, substrate and temperature dependent, enzyme mediated process (Figure III.33).

Additionally, it has been suggested that carbocyclic algal oxylipins may result from a lipoxygenase-initiated peroxidation of AA (**4 4**, Figure III.35).[45, 51-54] Incorporation of molecular oxygen from a dioxygenase into key hydroperoxide intermediates (i.e. 12-

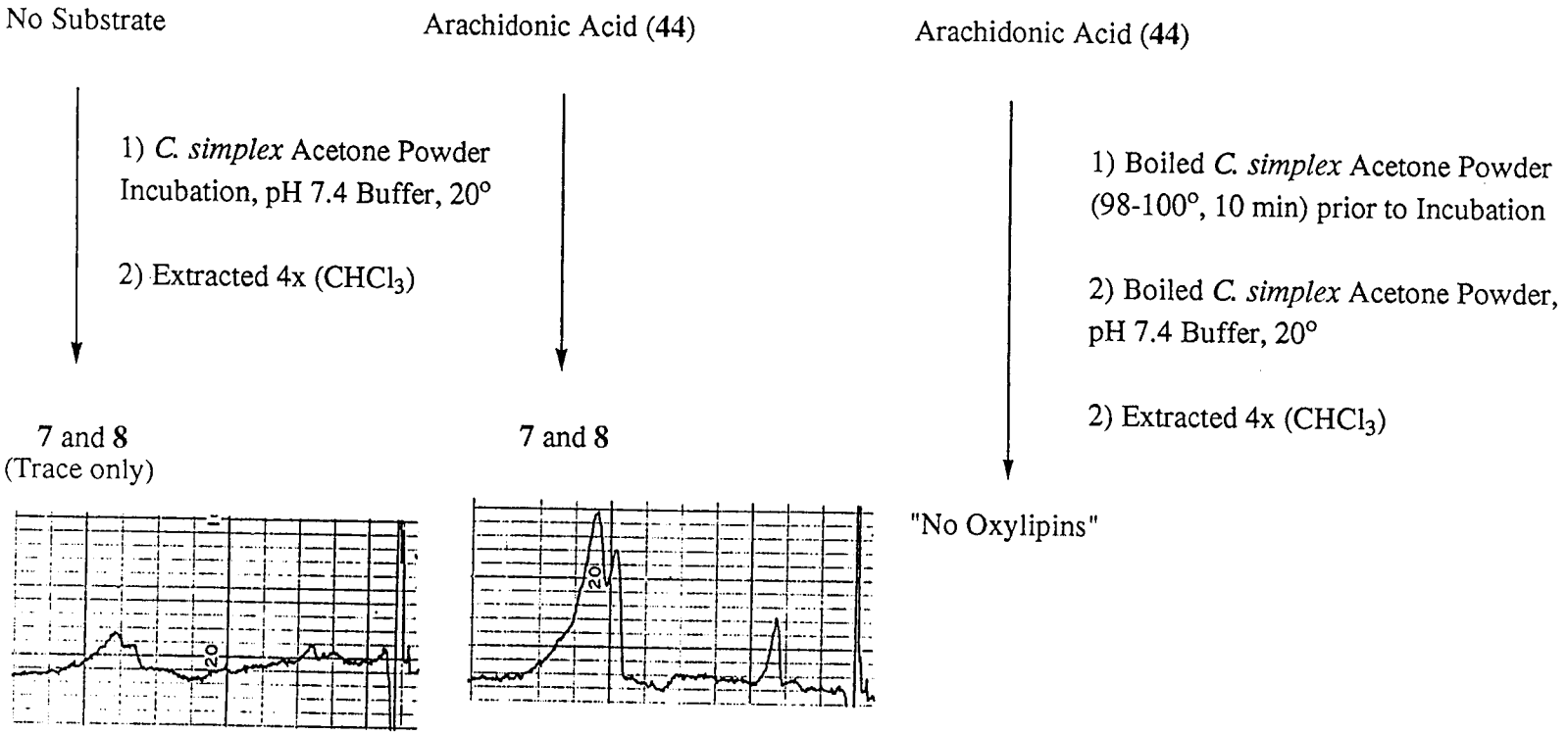

Figure III.33 *C. simplex* Acetone Powder Incubations and HPLC Analysis.

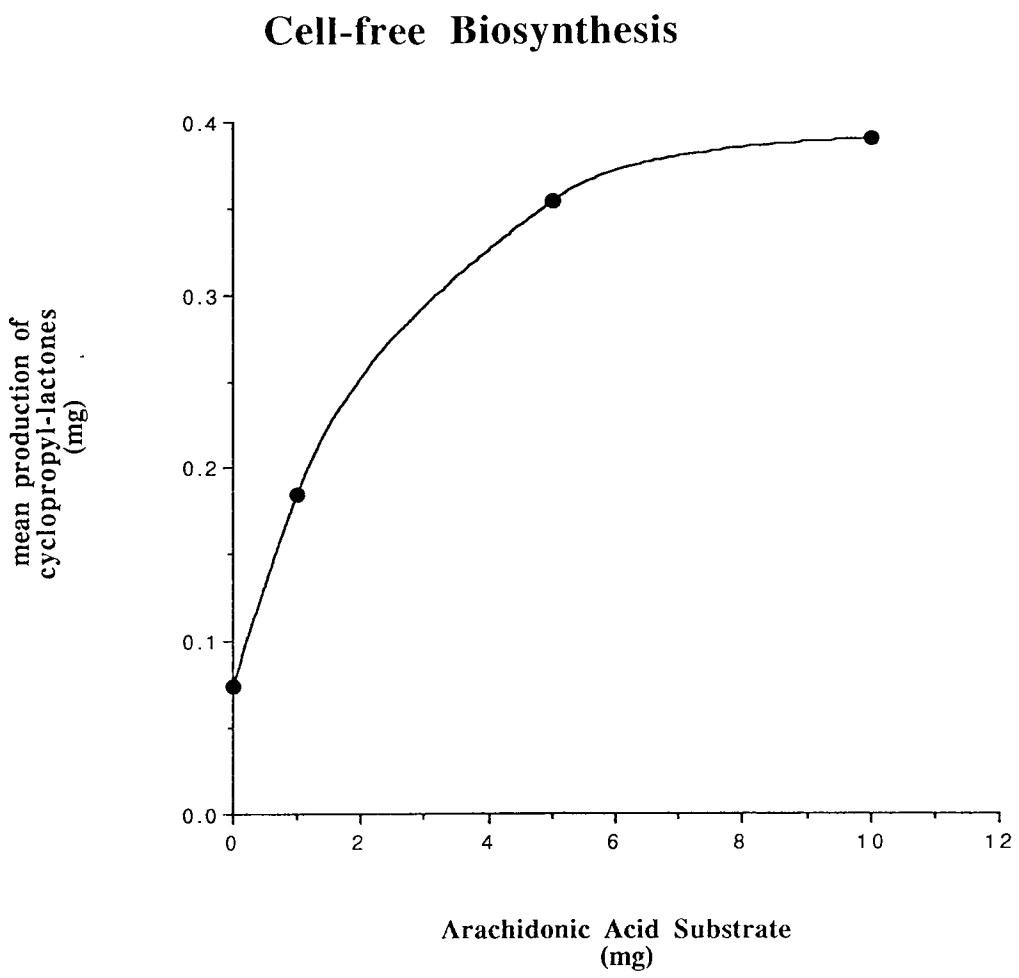

Figure III.34 Mean Production of Constanolactones A and B in Cell-Free Acetone Powder Incubation at 25 °C (n = 2).

hydroperoxyeicosatetraenoic acid (**4 5**), 12-HpETE) may therefore be evaluated by $^{18}O_2$-labeling during carbocyclic-oxylipin formation. Biosynthetic experiments with marine macroalgae have traditionally encountered difficulties with poor cell wall penetration of exogenously supplied substrates and competition with endogenous substrate pools.[140] Fortunately, I have been able to avoid these obstacles through the use of these cell-free systems. The successful incorporation of exogenously supplied **4 4** suggested the possibility of further probing the intermediacy of a lipoxygenase-type enzyme in the formation of **7** and **8**.

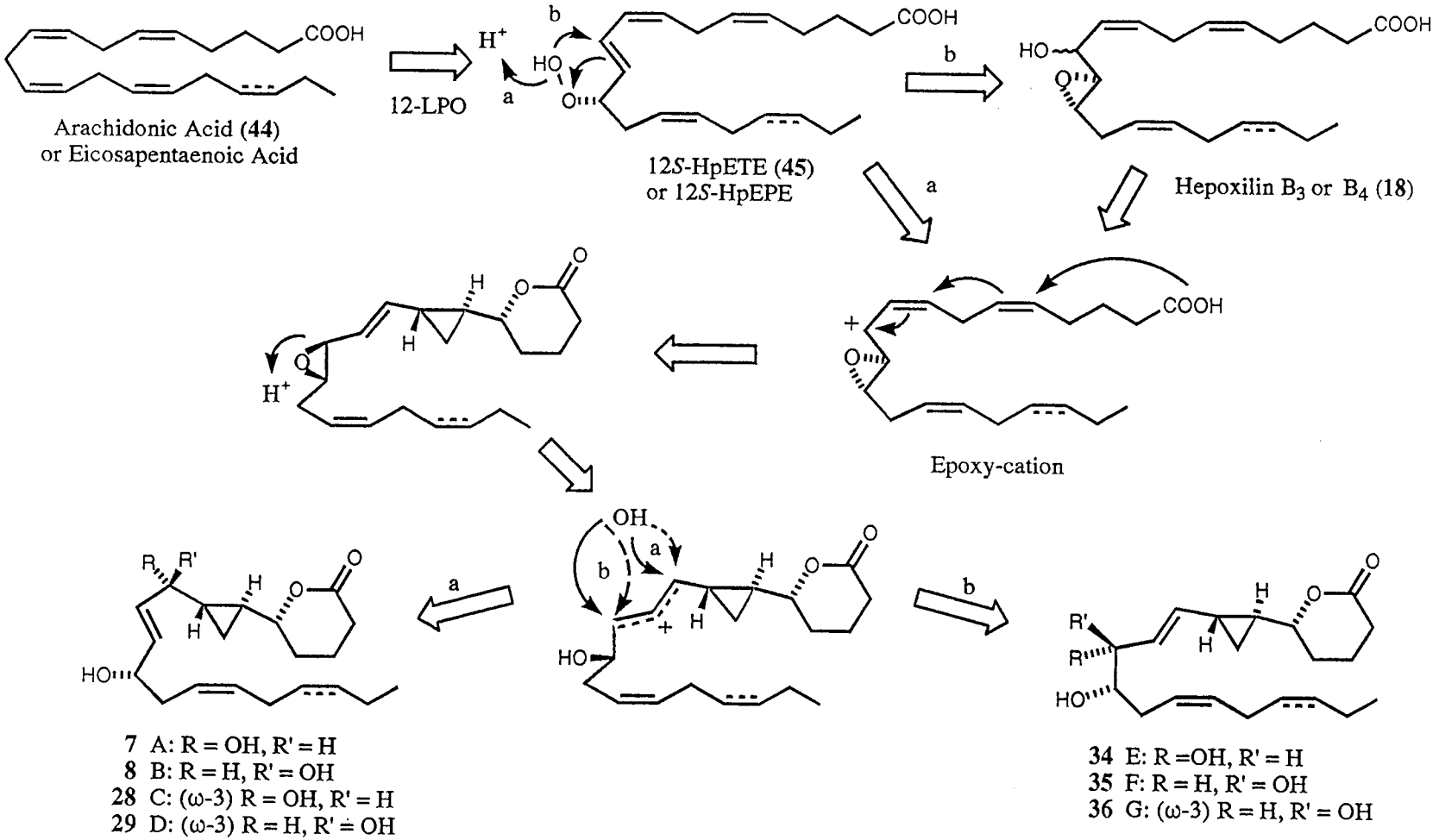

Figure III.35 Biosynthetic Proposal for Origin of *C. Simplex* Cyclopropyl-Lactones.

Arachidonic acid (**44**) was incubated with the *C. simplex* acetone powder in a closed vessel enriched with $^{18}O_2$ (^{18}O, 50%). Following extraction and methylation of the products (as above) the oxylipins were analyzed by GC-EIMS of their corresponding bis-trimethylsilyl (TMSi) ethers (**46** and **47**). Incorporation of labeled O_2 was observed by analysis of isotopic abundance patterns in key MS fragments in labeled and non-labeled products. Significant incorporation of one ^{18}O was achieved as evidenced by an enhancement of the ion at *m/z* 371 $[M - CH_3(CH_2)_4CH{=}CHCH_2 + 2]^+$ (28±1% incorp.), corresponding to cleavage α to the C-12 TMSi ether (Figure III.36). Unfortunately the position of ^{18}O-label substitution was not clearly identifiable by the fragmentation pattern. Catalytic hydrogenation (H_2, $PtCl_2$) of ^{18}O-labeled and unlabeled control incubation products afforded constanolactone derivatives which were re-silated to form a mixture of 10,11,14,15-tetrahydro-TMSi ethers (**48** and **49**). These compounds exhibited highly definable EIMS fragmentation patterns useful for locating the position of isotopic substitution (Figures III.36 - III.38). Again, enhancement of the C-12 α-cleavage ion now at *m/z* 373 $[M - CH_3(CH_2)_7 + 2]^+$ (35±6% incorp.) was observed. Additionally, two other major fragments showed critical isotopic abundance patterns from which the substitution of the label was clearly definable. First, a C-12 α-cleavage ion at *m/z* 215 $[M - CH_3(CH_2)_7COSi(CH)_3]^+$ which showed a high level of ^{18}O incorporation by the increased abundance of a peak at *m/z* 217 $[M - CH_3(CH_2)_7COSi(CH)_3 + 2]^+$ (30±8% incorp.) (Figures III.37 and III.38), placing the ^{18}O label at C-12. Further support was provided by the presence of a major fragment at *m/z* 241 $[C_{12}H_{21}O_3Si]^+$ resulting from a breaking of the C-9 to C-10 bond by an α- cleavage mechanism which is intensified by the TMSi ether substituent at C-9. This C-1 to C-9 containing fragment showed no enhancement of the peak at *m/z* 243 $[C_{12}H_{21}O_3Si + 2]^+$ over that of natural abundance.

Thus, the C-12 hydroxyl group derives from the incorporation of molecular oxygen and is consistent with a mechanism which involves the intermediacy of a lipoxygenase-type

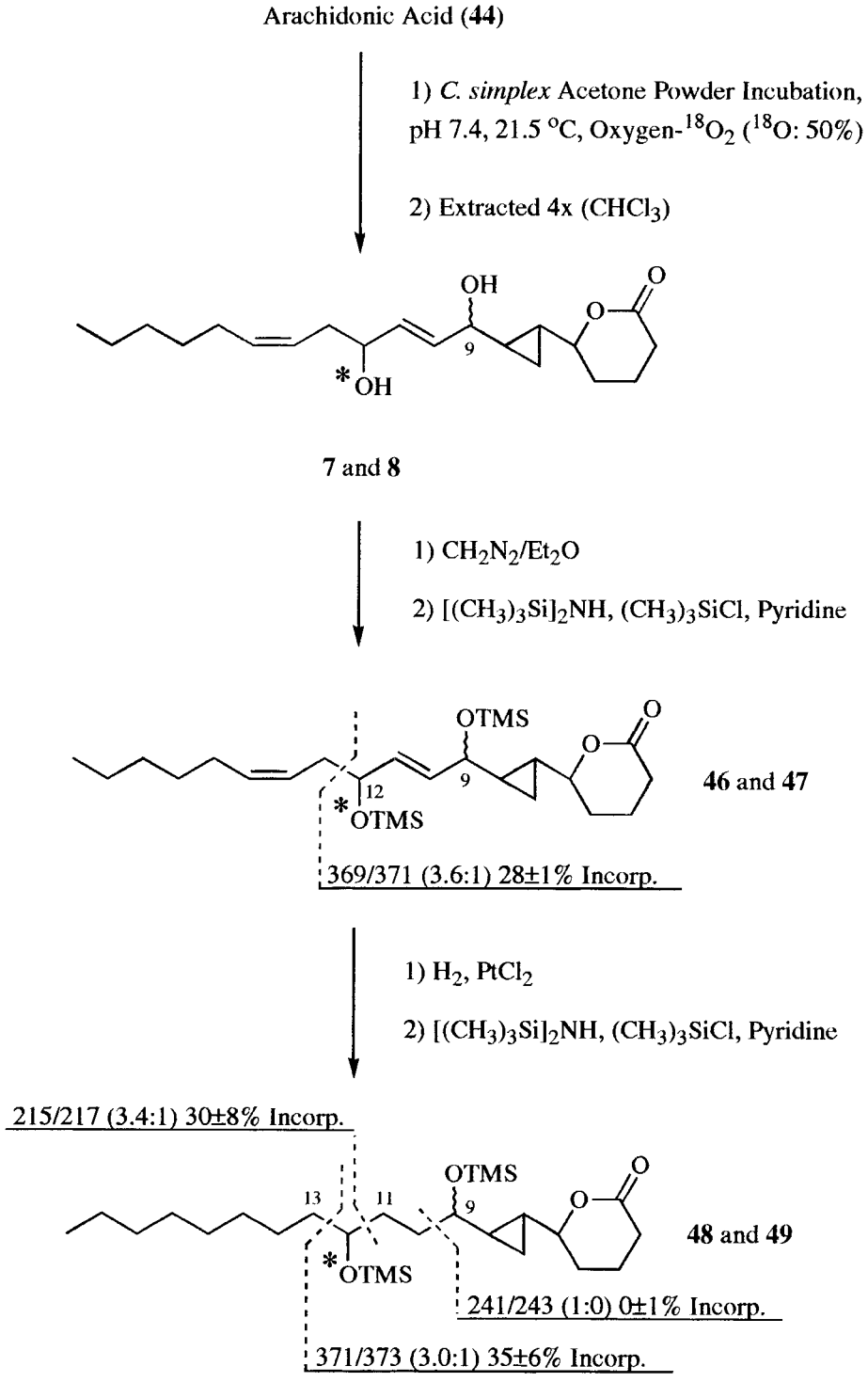

Figure III.36 Formation of ^{18}O-Labeled Derivatives **48** and **49** which Afforded Definitive EI Mass Spectral Fragmentation Patterns.

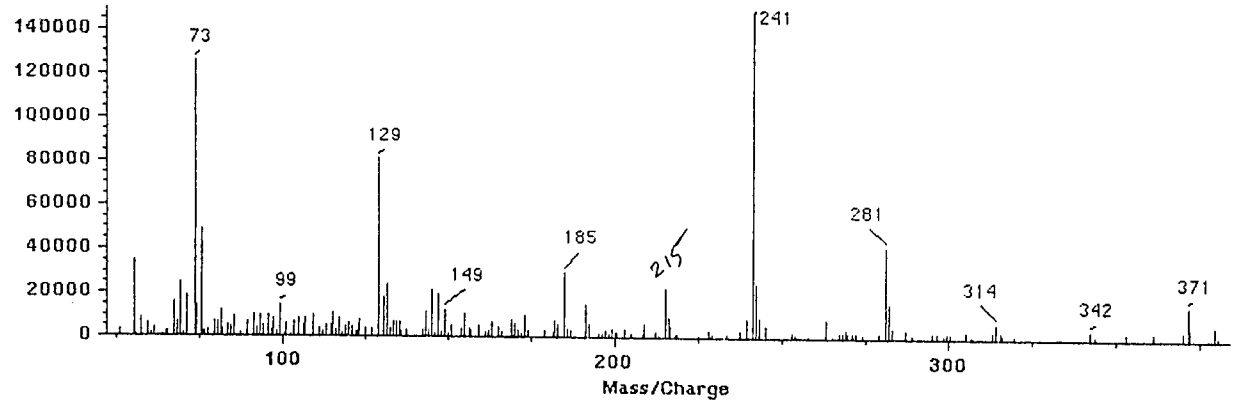

Figure III.37 EI Mass Spectrum of Unlabeled Hydrogenated Methyl TMSi-Ether Derivative **48**.

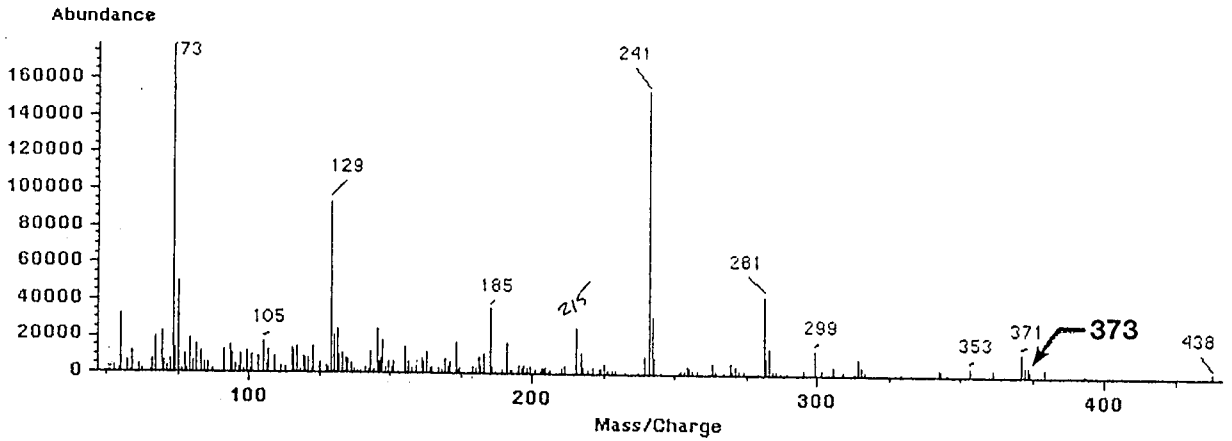

Figure III.38 EI Mass Spectrum of ^{18}O-labeled Hydrogenated Methyl TMSi-Ether Derivative **48**.

peroxidation of fatty acid precursors. Additionally, the absence of any label of the oxygen at C-9 is consistent with the formation of, and subsequent non-stereospecific 1,4-addition of water to, a reactive allylic epoxide intermediate (Figure III.35).

The red marine alga *Constantinea simplex* utilizes arachidonic and eicosapentaenoic acids to produce both simple (i.e. 12*S*-hydroxyeicosatetraenoic acid (**1 1**), 12*S*-hydroxyeicosapentaenoic acid (**1 2**))[124] as well as highly functionalized oxylipins (e.g. constanolactones A-G). I have demonstrated that these metabolites could biogenetically derive from a mechanism consistent with a lipoxygenase-initiated oxidation of polyunsaturated fatty acid precursors.[52,53] Key to my hypothesis (Figure III.35), and in common with additional suspected routes of oxylipin metabolism in other algae,[123] is the formation of an epoxy-cation intermediate in which the cation induces cyclopropyl and lactone ring formation. This leads in turn to the formation of an allylic epoxide, a potential end product of the enzymatic pathway. As both epimers at C-9 in the 1,4-diols (constanolactones A-D) and C-11 in the 1,2-diols (constanolactone E, F) were isolated, it is possible that these diol products result from non-enzymatic hydrolysis (1,2 or 1,4) of the α,β-unsaturated epoxide intermediate. This hypothesis is substantiated by my isolation of the two epimeric C-9 methyl ether derivatives (**3 2** and **3 3**), presumed MeOH solvolysis products of an allylic epoxide, and are formed in the extraction process (Figure III.39).

An analogous biogenetic hypothesis has been proposed (Figure III.40)[45,139] for the formation of the sponge metabolites halicholactone (**1**) and neohalicholactone (**2**).[112,113] However, the sponge metabolites are proposed to derive from the 15-lipoxygenase metabolites 15-hydroperoxyeicosatetraenoic acid (15-HpETE) and 15-hydroperoxyeicosapentaenoic acid (15-HpEPE) rather than from 12-HpETE **4 5** and 12-hydroperoxyeicosapentaenoic acid (12-HpEPE) as in *C. simplex*. Further, isolation of the ω-3 unsaturated constanolactones C (**2 6**) and D (**2 7**) from this red alga is informative as these were proposed as biogenetic precursors to aplydilactone (**4**, Figure III.41),[45] a non-

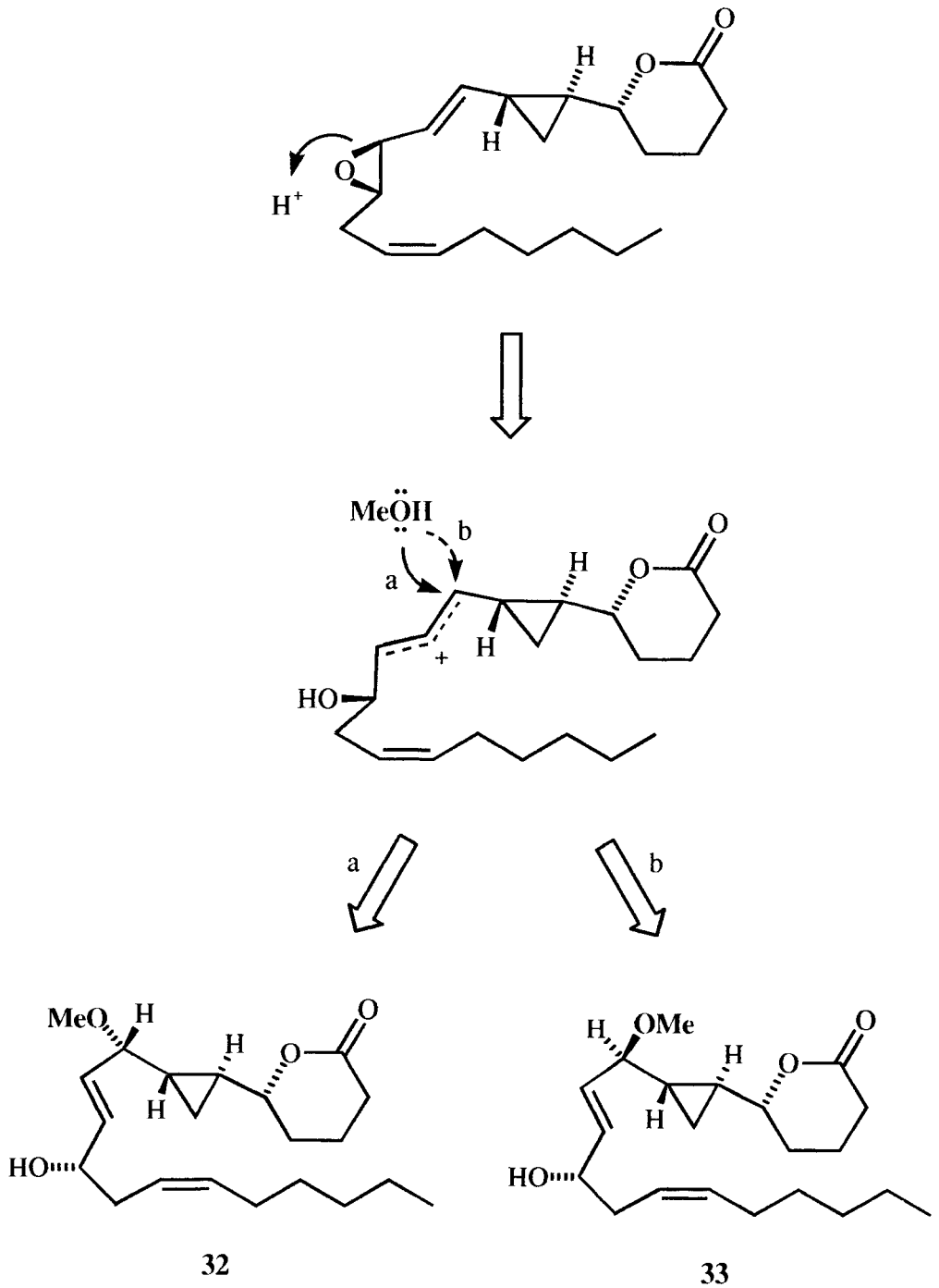

32 33

Figure III.39 Proposal for Origin of *C. simplex* 9-OMe Constanolactone Derivatives (**32** and **33**).

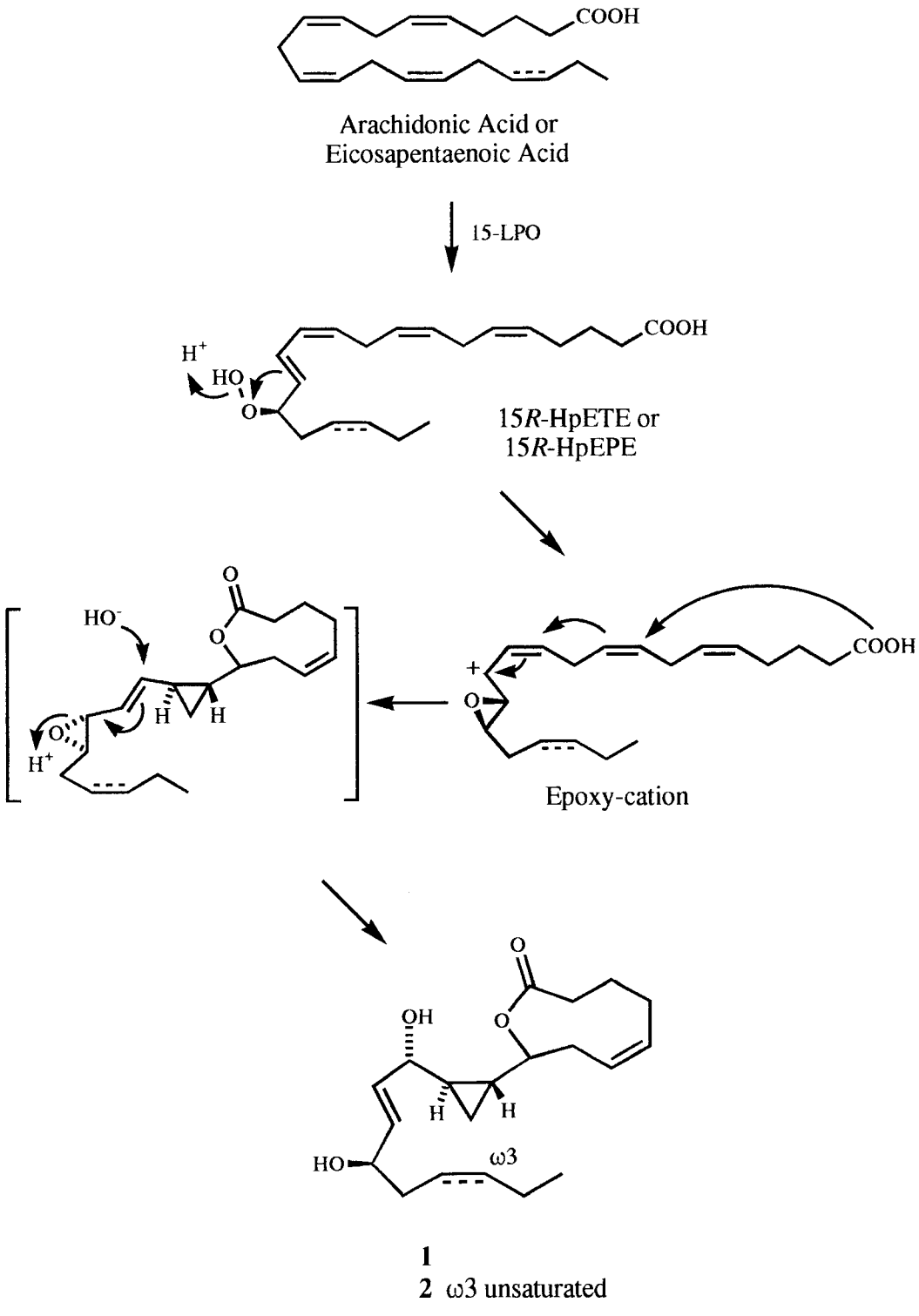

Figure III.40 Proposed Biogenesis of Halicholactones.

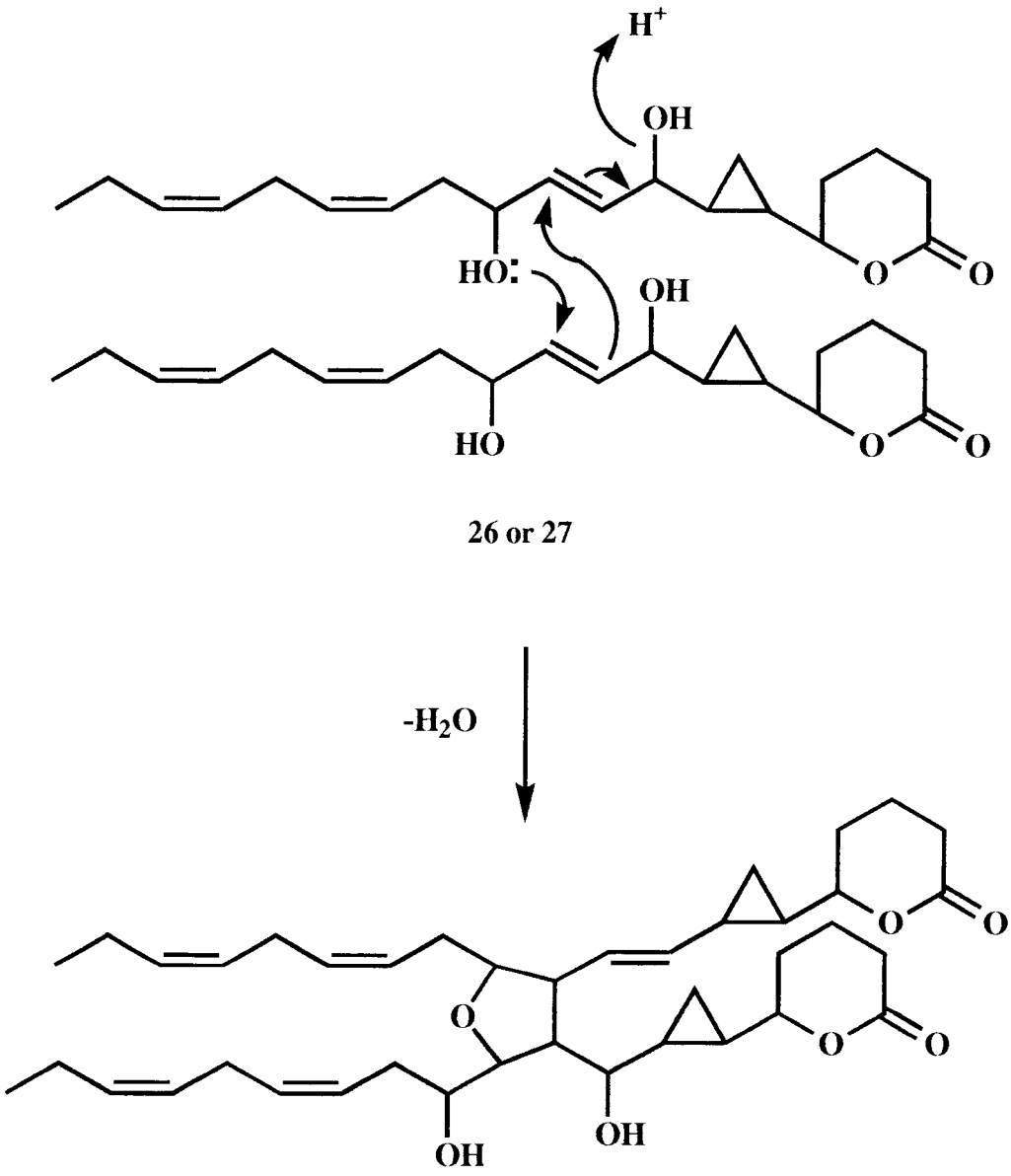

Figure III.41 Proposed Formation of Aplydilactone (**4**) from ω3 Unsaturated Constanolactone Precursors.

symmetrical oxylipin dimer isolated from the herbivorous mollusc *Aplysia kurodai.*[115,116] As *Aplysia* are well known assimilators of algal natural products, these metabolites may be formed from dietary precursors.[82]

It is interesting to note that oxylipins containing cyclopropyl and lactone rings are a growing class of marine-derived natural product, having now been isolated from red[54] and brown algae,[139] sponges,[112,113] opisthobranch molluscs,[115,116] and corals.[114] It has been suggested that if these findings parallel other cases of novel oxylipin discovery, first in primitive creatures and latter in mammalian systems,[141,142] then I may perhaps anticipate isolation of this structure class from yet more complex life forms in the future.[45]

Experimental

General Methods. Spring and early Summer collections of small (blade diameter typically 2-5 cm.) *C. simplex* plants were obtained from exposed low-intertidal locations (-0.3 to -0.8 M) at Seal Rock and Boiler Bay, Oregon. These were frozen on site with CO_2(s) and stored frozen prior to extraction ($CHCl_3$/MeOH 2:1 or CH_2Cl_2/MeOH 2:1). Extracts of large "older" individuals (diameter > 6 cm.) collected from relatively non-exposed sites contained an insignificant oxylipin content. UV spectra were recorded on a Hewlett Packard 8452A diode array spectrophotometer and IR spectra were recorded on a Nicolet 510 FT-IR spectrometer. CD measurements were obtained on a Jasco 41A spectropolarimeter. Low resolution mass spectra were obtained on either a Varian MAT CH7 spectrometer or by GC-MS using a Hewlett Packard 5890 Series II gas chromatograph and a 5971 mass selective detector. HRMS were obtained on a Kratos MS 50 TC. HPLC was performed using a M-6000 pump, U6K injector, and either a R401 differential refractometer or a lambda-Max 480 lc spectrophotometer. NMR data were obtained on either Bruker AC 300 or Bruker AM 400 spectrometers. ^{1}H NMR spectra were acquired with tetramethylsilane (TMS) as an internal chemical shift reference. ^{13}C

spectra were referenced to the center line of $CDCl_3$ at 77.0 ppm. ^{13}C assignments are based on ^{1}H-^{13}C HETCOR, DEPT multiplicity data, and comparison with previously identified constanolactone derivatives. TLC-grade (10-40 μm) silica gel was used for vacuum chromatography and Kieselgel 60 silica (40-63 μm) was used for flash chromatography . Aluminum-backed thin-layer chromatography sheets were used for TLC, and all solvents were distilled prior to use.

Isolation of Constanolactones A (7) and B (8). Approximately 8 L of frozen *C. simplex* (400 g extracted dry weight) was repetitively extracted (3X, as above), to yield 12.49 g of a dark green oil. The extract was subjected to silica gel vacuum chromatography, using a stepwise gradient from 0 to 100% (v/v) EtOAc in hexanes. Fractions eluting with EtOAc concentrations greater than 50% were determined by TLC to be of similar composition, and were pooled. This combined fraction was further purified by silica gel flash chromatography, using a stepwise gradient from 10 to 100% (v/v) MeOH in $CHCl_3$. Reversed-phase chromatographic separation (Sep-Pak® C_{18} cartridge, 85% (v/v) MeOH in H_2O) proved necessary in order to remove significant amounts of co-eluting glycolipid impurities. The natural products were then isolated by NP-HPLC (10-μm Phenomenex Maxsil Si column; 500 x 10 mm; 20% (v/v) isopropanol in hexanes; differential refractometer detection; flow rate at 6.0 mL/min) to yield constanolactone A (7 12.4 mg, 0.10%) and B (**8** 15.8 mg, 0.13%).

Constanolactone A (7). Oil: $[\alpha]_D$ +1.4° (c 1.00, MeOH); $[\alpha]_D$ -3.8° (c 1.31, $CHCl_3$); IR (neat) 3320, 2958, 2924, 1712, 1258, 1248, 1099, 1045, 1031 cm^{-1}; ^{1}H NMR: (300 MHz, $CDCl_3$) δ 5.78 (m, 2H, H-10 and H-11), 5.54 (dt, 1H, J = 10.8, 7.3, H-15), 5.39 (dt, 1H, J = 10.8, 7.2, H-14), 4.17 (dt, 1H, J = 4.6, 6.1, H-12), 3.72 (m, 2H, H-5 and H-9), 2.56 (dt, 1H, J = 17.8, 6.4, H2b), 2.44 (ddd, 1H, J = 17.8, 8.5, 6.9, H2a), 2.32 (bq, 2H, J = 6.7, H-13), 2.05 (m, 2H, H-16), 1.99 (m, 1H, H4b), 1.96 (m, 1H, H3b), 1.80 (m, 1H, H-3a), 1.68 (ddd, 1H, J = 13.2, 9.9, 4.5, H-4a), 1.35 (m, 2H,

H-17), 1.3 (m, 4H, H-18 and H-19), 1.20 (m, 1H, H-8), 1.02 (m, 1H, H-6), 0.88 (t, 3H, J = 6.7, H-20), 0.75 (dt, 1H, J = 8.7, 5.3, H-7b), 0.61 (dt, 1H, J = 8.5, 5.3, H-7a); (300 MHz, C_6D_6) δ 5.97 (m, 2H, H-10 and H-11), 5.67 (dt, 1H, J = 10.9, 6.8, H-15), 5.56 (dt, 1H, J = 10.9, 7.0, H-14), 4.30 (dt, 1H, J = 4.3, 6.4, H-12), 3.75 (dd, 1H, J = 6.9, 4.3, H-9), 3.12 (td, 1H, J = 8.9, 3.4, H-5), 2.5 (m, 2H, H-13), 1.98-2.13 (m, 8H, H-2 to H-4, and H-16), 1.32 (m, 2H, H-17), 1.25 (m, 4H, H-18 and H-19), 1.1 (m, 1H, H-6), 0.88 (t, 3H, J = 6.9, H-20), 0.81 (m, 1H, H-8), 0.62 (dt, 1H, J = 8.7, 5.2, H-7b), 0.32 (dt, 1H, J = 8.5, 5.2, H-7a); ^{13}C NMR: (75 MHz, $CDCl_3$) δ 171.70 (C-1), 133.65 (C-15), 133.17, 131.74, 124.48 (C-14), 83.77 (C-5), 74.07 (C-9), 71.59 (C-12), 34.95 (C-13), 31.46 (C-18), 29.48 (C-2), 29.25 (C-17), 27.71, 27.38, 23.36 (CH, C-6 or C-8), 22.52 (C-19), 20.31 (CH, C-6 or C-8), 18.29 (C-3), 14.03 (C-20), 7.50 (C-7); (75 MHz, C_6D_6) δ 171.06 (C-1), 134.03 (C-15), 132.38, 132.13, 126.00 (C-14), 83.52 (C-5), 74.00 (C-9), 71.91 (C-12), 35.86 (C-13), 31.86 (C-18), 29.78 (C-2), 29.49 (C-17), 27.84, 27.68, 23.70 (CH, C-6 or C-8), 22.98 (C-19), 20.43 (CH, C-6 or C-8), 18.32 (C-3), 14.32 (C-20), 7.61 (C-7); CIMS (CH_4, positive ion) *m/z* $[M+H - H_2O]^+$ 319 ((73), $[M+H - 2(H_2O)]^+$ 301 (100), 283 (11), $[M+H - C_8H_{15}]^+$ 225 (11), 217 (10), 207 (12), 163 (23), 111 (10); FABMS (glycerol, negative ion) *m/z* $[2(M)-H]^-$ 671.4 (8), 519.3 (12), [M-H + glycerol]$^-$ 427.3 (100), $[M-H + H_2O]^-$ 353.3 (18),$[M-H]^-$ 335.2 (78), [M-H - $C_8H_{15}]^-$ 223.1 (21); HR-FABMS (glycerol, negative ion), obs. 335.2221 calc for $C_{20}H_{31}O_4$ 335.2220 $[M-H]^-$.

Constanolactone B (**8**). Oil: $[\alpha]_D$ +10.2° (c 1.00, MeOH); IR (neat) 3390, 2955, 2925, 1727, 1725, 1716, 1243, 1035, 972 cm^{-1}; ^{1}H NMR (300 MHz, $CDCl_3$) δ 5.76 (m, 2H, H-10 and H-11), 5.54 (dt, 1H, J = 10.9, 7.2, H-15), 5.38 (dt, 1H, J = 10.9, 7.2, H-14), 4.15 (m, 1H, H-12), 3.73 (ddd, 1H, J = 10.0, 7.8, 2.9, H-5), 3.65 (m, 1H, H-9), 2.56 (dt, 1H, J = 17.7, 6.6, H2b), 2.45 (ddd, 1H, J = 17.7, 8.5, 6.9, H2a), 2.3 (m, 2H, H-13), 2.04 (m, 2H, H-16), 2.0 (m, 1H, H4b), 1.93 (m, 1H, H3b), 1.82 (m, 1H, H-3a),

1.7 (ddd, 1H, H-4a), 1.35 (m, 2H, H-17), 1.3 (m, 4H, H-18 and H-19), 1.13 (m, 2H, H-8 and H-6), 0.89 (t, 3H, J = 6.7, H-20), 0.61 (dt, 1H, J = 8.7, 5.3, H-7b), 0.56 (dt, 1H, J = 8.7, 5.3, H-7a); (300 MHz, C_6D_6) δ 5.96 (m, 2H, H-10 and H-11), 5.65 (dt, 1H, J = 11.0, 7.0, H-15), 5.56 (dt, 1H, J = 11.0, 7.0, H-14), 4.30 (dt, 1H, J = 5.6, 6.3, H-12), 3.70 (dd, 1H, J = 6.9, 5.3, H-9), 3.21 (td, 1H, J = 9, 3.3, H-5), 2.56 (dt, 1H, J = 14.4, 6.7, H-13b), 2.45 (dt, 1H, J = 14.4, 6.5, H-13a), 2.1 (m, 4H, H-2 and H-16), 1.34 (m, 2H, H-17), 1.1-1.4 (m, 4H, H-3 and H-4), 1.26 (m, 4H, H-18 and H-19), 1.1 (m, 2H, H-6 and H-8), 0.88 (t, 3H, J = 6.9, H-20), 0.47 (dt, 1H, J = 8.7, 5.1, H-7b), 0.27 (dt, 1H, J = 8.7, 5.1, H-7a); ^{13}C NMR (75 MHz, $CDCl_3$) δ 171.78 (C-1), 133.23 (C-15), 133.23, 131.68, 124.43 (C-14), 83.63 (C-5), 74.01 (C-9), 71.66 (C-12), 35.10 (C-13), 31.44 (C-18), 29.45, 29.23, 27.73, 27.37, 23.34 (CH, C-6 or C-8), 22.50 (C-19), 21.23 (CH, C-6 or C-8), 18.31 (C-3), 14.02 (C-20), 6.62 (C-7); (75 MHz, C_6D_6) δ 171.38 (C-1), 133.90 (C-15), 132.74, 132.29, 126.00 (C-14), 83.56 (C-5), 74.20 (C-9), 72.26 (C-12), 35.83 (C-13), 31.87 (C-18), 29.78, 29.54, 27.85, 27.66, 23.83 (CH, C-6 or C-8), 22.99 (C-19), 21.32 (CH, C-6 or C-8), 18.33 (C-3), 14.34 (C-20), 6.77 (C-7); CIMS (CH_4, positive ion) $[M+H - H_20]^+$ *m/z* 319 (56), $[M+H - 2(H_20)]^+$ 301 (100), 283 (10), $[M+H - C_8H_{15}]^+$ 225 (9), 217 (8), 207 (14), 163 (18), 111 (10).

Isolation of Constanolactones A-B Per-acetate Derivatives (**9-10**), Hydroxy- or Oxo-Oxylipin Methyl Ester Derivatives (**14-16**), Diacetate Derivative (**17**), and C-D Per-acetate Derivatives (**28-29**). Frozen *C. simplex* (collected at Seal Rock, Oregon, 620 g extracted dry weight alga) was extracted with CH_2Cl_2/MeOH (2:1), to yield 2.0 g of a dark green oil. The extract was subjected to silica gel vacuum chromatography, using a stepwise gradient from 0 to 100% (v/v) EtOAc in hexanes. TLC analysis of the fractions suggested the presence of likely eicosanoid-type natural products giving colorful (blue, yellow, red) $Cu(OAc)_2$ or H_2SO_4 staining reactions. The fractions eluting with 20 to 50% (v/v) EtOAc in hexanes were combined and further purified by a second silica gel vacuum

chromatography, also using a stepwise gradient from 0 to 100% (v/v) EtOAc in hexanes. The fraction which now slowly eluted with 10% (v/v) EtOAc in hexanes was reduced *in vacuo*. Following derivatization (CH_2N_2/Et_2O) and NP-HPLC (dual 10-μm Waters μ-Porasil silica columns; (2x) 300 x 3.9 mm; refractive index detection; 5% (v/v) EtOAc in hexanes; flow rate 1.5 mL/min) minor amounts of three known oxylipins were isolated: Methyl 12-*S*-HETE (**14**, 2.0 mg, 0.1%), Methyl 12-*S*-HEPE (**15**, 0.3 mg, 0.015%) and Methyl 12-oxo-5*Z*, 8*E*, 10*E*-dodecatrienoate (**16**, 0.9 mg, 0.044%). Another vacuum chromatography fraction (146 mg, 80% EtOAc/hex) was treated with Ac_2O/pyr followed by CH_2N_2/Et_2O and NP-HPLC (10-μm Alltech RSIL silica column; 500 x 10 mm; refractive index detection; 35% (v/v) EtOAc in hexanes; flow rate 9.0 mL/min) to yield three closely related new compounds (**7**, 32.7 mg, 1.6%; **8**, 39.9 mg, 2.0%; **9**, 2.3 mg, 0.11%) and the diacetate derivative **17** (2.3 mg, 0.12%). Further investigation of less abundant acetylated derivatives isolated from the same HPLC fractionation yielded two additional constanolactone per-acetate derivatives, **28** (4.2 mg, 0.17%) and **29** (5.7 mg, 0.23%).

Constanolactone A Per-acetate (**9**). Additionally, the following correlations were observed by ^1H-^1H NOESY (400 MHz, degassed $CDCl_3$) H-2a (H-2b), H-3a (H-3b), H-3b (H-4, 5, 8), H-5 (H-7a, 8, 12 or 14), H-6 (H-7b, 9), H-7a (H-8), H-7b (H-9), H-8 (H-9, 11), H-9 (H-10, 11), H-10 (H-12 or 14), H-11 (H-12 or 14), H-12 (H-13a, 15, 16, H_6-17-19, -OAc), 13a (H-16), 13b (H-16, -OAc), H-14 (H-15, 16, 17-19, -OAc), H-15 (H-16), H-16 (H_6-17-19, -OAc), H_6-17-19 (H-20).

Constanolactone B Per-acetate (**10**). Correlations observed by ^1H-^1H NOESY (400 MHz, degassed $CDCl_3$) H-2a (H-2b), H-3 (H-4a), H-4a (H-4b, 5), H-5 (H-6* or 8, 7a*, 10 or 11, 12), H-6 or 8 (H-7a, 7b*, 9, 10 or 11), H-7a (H-7b*), H-7b (H-9*, 10 or 11), H-9 (H-10 or 11), H-10 or 11 (H-12, 13a, 13b, 15, 16), H-12 or 14 (H-13a, 13b,

15, 16), 13a (H-14, 16), 13b (H-14), H-15 (H-16), H-16 (H-17 or 18, -OAc), H_6-17-19 (H-20, -OAc); *confirmed by nOe Difference Spectroscopy.

Methyl 12*S*-Hydroxyeicosa-5*Z*, 8*Z*, 10*E*, 14*Z*-tetraenoate (**14**). Oil: $[\alpha]_D^{21} = +8.0°$ (c 0.22, Acetone); ^1H (400 MHz, C_6D_6) δ 6.72 (dd, 1H, *J* = 15, 11, H-10), 6.04 (t, 1H, *J* = 11, H-9), 5.69 (dd, 1H, *J* = 15, 6.5, H-11), 5.51 (m, 2H, H-14 and H-15), 5.39 (m, 2H, H-6 and H-8), 5.27 (bdt, 1H, *J* = 10, 7.3, H-5), 4.15 (m, 1H, H-12), 3.34 (s, 3H, $-OCH_3$), 2.89 (dd, 2H, *J* = 6, 5, H-7), 2.36 (m, 1H, H-13b), 2.30 (m, 1H, H-13a), 2.07 (t, 2H, *J* = 7.3, H-2), 2.01 (bq, 2H, H-19), 1.94 (bq, 2H, H-3), 1.69 (bd, 1H, *J* = 6, -OH), 1.56 (5-lines, 2H, H-3), 1.2-1.35 (m, 4H, H-18 and H-19), 0.90 (t, 3H, *J* = 7.4, H-20); EIMS (70 eV) *m/z* $[M - H_2O]^+$ 316 (4), $[M - OMe]^+$ 303 (4), $[M - C_8H_{13}]^+$ 223 (100), 205 (51), 191 (45), 179 (15), 173 (41), 163 (73), 145 (36), 131 (45), 119 (17), 107 (40), 91 (27), 79 (40), 67 (34), 55 (38), 41 (32).

Methyl 12*S*-Hydroxyeicosa-5*Z*, 8*Z*, 10*E*, 14*Z*, 17*Z*-pentaenoate (**15**). Oil: $[\alpha]_D^{19} = +10.5°$ (c 0.33, Acetone); ^1H (400 MHz, C_6D_6) δ 6.72 (dd, 1H, *J* = 15, 11, H-10), 6.04 (t, 1H, *J* = 11, H-9), 5.67 (dd, 1H, *J* = 15, 6.5, H-11), 5.51 (m, 2H, H-14 and H-15), 5.39 (m, 4H, H-6, H-8, H-17, and H-18), 5.27 (bdt, 1H, *J* = 10, 7.3, H-5), 4.13 (m, 1H, H-12), 3.34 (s, 3H, $-OCH_3$), 2.89 (dd, 2H, *J* = 6, 5, H-7), 2.80 (t, 2H, *J* = 6, H-16), 2.36 (m, 1H, H-13b), 2.30 (m, 1H, H-13a), 2.07 (t, 2H, *J* = 7.3, H-2), 1.99 (bq, 2H, H-19), 1.94 (bq, 2H, H-3), 1.67 (bd, 1H, *J* = 6, -OH), 1.56 (5-lines, 2H, H-3), 0.90 (t, 3H, *J* = 7.4, H-20).

Methyl 12-Oxo-5*Z*, 8*E*, 10*E*-Dodecatrienoate (**16**). Oil: UV (EtOH) λ_{max}^{MeOH}273 nm (log ε 4.36); ^1H (400 MHz, C_6D_6) δ 9.4 (d, 1H, *J* = 8, H-12), 6.4 (dd, 1H, *J* = 13, 10, H-10), 5.92 (dd, 1H, *J* = 13, 8, H-11), 5.82 (bdd, 1H, *J* = 13, 10, H-9), 5.62 (dt, 1H, *J* = 13, 6, H-8), 5.31 (dt, 1H, *J* = 10, 6, H-6), 5.22 (dt, 1H, *J* = 10, 6, H-5), 3.35 (s, 3H, $-OCH_3$), 2.55 (t, 2H, *J* = 6, H-7), 2.06 (t, 2H, *J* = 6, H-2), 1.86 (q, 2H, *J* = 7, H-4), 1.55 (5-lines, 2H, H-3).

Bis-(Menthoxycarbonyl)-Constanolactone A (**20**). Constanolactone A (**7**, 2.6 mg, 7.7 μmol) was dissolved in a toluene/pyridine mixture (5:1, 120 μL), 100 μL of $CHCl_3$ was added to prevent precipitation of solids in flask, an excess of (-)-menthoxycarbonyl chloride (**19**, 50 μL of a 1.0 mM solution in toluene) was added, the flask was purged with N_2, sealed (flask occasionally opened to monitor reaction by TLC), and stirred (1.5 h, 23 °C). The reaction was stopped with the addition of 3.0 mL MeOH and evaporated under vacuum. The product was dissolved in 100% hexanes and applied to a small silica column. Components eluting in both 100% hexanes and 3% (v/v) EtOAc in hexanes were removed. The following fraction eluting with 10% (v/v) EtOAc in hexanes was evaporated to yield **20** (4.9 mg, 7.0 μmol, 90.4% yield). Oil: IR (neat) 2956, 2929, 2871, 1737, 1458, 1369, 1285, 1254, 1037, 956 cm^{-1}; ^1H NMR: (300 MHz, $CDCl_3$) δ 5.87 (m, 1H, *J* = 15.8, 6.2, H-11), 5.75 (dd, 1H, *J* = 15.8, 5.8, H-10), 5.51 (bdt, 1H, *J* = 10.9, 7.2, H-15), 5.32 (bdt, 1H, *J* = 10.9, 7.2, H-14), 5.10 (q, 1H, *J* = 6.2, H-12), 4.83 (bt, 1H, *J* = 6.6, H-9), 4.50 (m, 2H, 7 lines), 3.93 (ddd, 1H, *J* = 10.5, 6.4, 3.0, H-5), 2.55 (dt, 1H, *J* = 17.8, 6.2, H2b), 2.42 (ddd, 1H, *J* = 17.8, 8.3, 6.9, H2a), 1.9-2.1 (m, 6H), 1.96 (m, 1H, H-3b), 1.8 (m, 1H, H-3a), 1.68 (m, 4H), 1.35 (m, 2H, H-17), 1.2-1.5 (m, 8H), 0.99-1.1 (m, 2H), 0.90 (m, 15H, 7 lines), 0.84-0.9 (m, 1H), 0.79 (m, 6H, 3 lines), 0.77 (m, 1H, H-7b), 0.68 (dt, 1H, *J* = 8.6, 5.4, H-7a).

Formation of *Bis*-(Menthoxycarbonyl)-Constanolactone B from Constanolactone B Per-acetate (**10**) and Ozonolysis to form Dimethyl-menthoxycarbonyl-malate (**21**). Treatment of constanolactone B diacetate (**10**, 5 mg) with 0.4 ml of 10% NaOH and 1.6 ml MeOH for 18.5 hr at rt was followed by acidification to pH 3 (pH paper) and extraction with EtOAc. The reduced EtOAc-soluble product was redissolved in MeOH (0.5 ml) and treated with excess ethereal CH_2N_2 for 1 min. Excess reagent was removed under a stream of N_2 and applied as a band in Et_2O to a TLC plate and developed in 100% EtOAc. The major product, R_f = 0.07-0.17, was removed and extracted with EtOAc. A portion of the

product (1% by volume) was treated with equal volumes (3 drops) of pyridine, 1,1,1,3,3,3-hexamethyldisilazane and chlorotrimethylsilane for 20 min. Excess solvent and reagents were removed *in vacuo* , the products dissolved in hexane, and analyzed by GC-MS (120 °C to 220 °C, 10 min, 18.05 min retention) obs. *m/z* 405 (1), 384 (8), 383 (27), 293 (9), 257 (57), 243 (10), 203 (6), 167 (47), 129 (25), 103 (13), 73 (100). Hydrogenation of this TMS ether derivative with H_2/Pd on $CaCO_3$ in MeOH for 30 min followed by re-trimethylsilyation as detailed above, gave a derivative with clearer MS cleavage patterns: (120 °C-220 °C, 10 min, 19.80 min retention) obs. *m/z* 446 (2), 408 (1), 397 (19), 385 (8), 345 (28), 307 (8), 295 (14), 289 (14), 255 (50), 229 (17), 215 (19), 191 (14), 129 (96), 73 (100). One third of the remainder of the triol methyl ester was treated with 50 µl toluene, 10 µl pyridine and 50 µl of (-) menthoxycarbonylchloride for 30 min at rt. Tlc purification of the resulting derivative (10% EtOAc/hex) was followed by ozonolysis for 2 min at -20 °C followed by 10 min at rt. Excess O_3 was removed under a stream of N_2 and the product treated overnight with 0.3 ml of peracetic acid at 50 °C. Again, reagents were removed under a stream of N_2, methylated with CH_2N_2 as above for 1 min, solvents removed under N_2, dissolved in hexane and analyzed by GC versus standards: (170 °C) obs. 14.869 min retention (standard *S*-malate = 14.893 min, *R*-malate = 15.011 min). The constanolactone B-derived malate derivative did not show a detectable peak at the *R*-malate retention time, and is therefore, essentially "100%"*S*.

Ozonolysis of *Bis*-(Menthoxycarbonyl)-Constanolactone A (**20**) to form Dimethyl-menthoxycarbonyl-malate (**21**). The *bis*-(menthoxycarbonyl) derivative of constanolactone A (**20**, 3.4 mg, 4.9 µmol) was added to 1.0 mL $CHCl_3$, the solution cooled to -11 °C (ethylene glycol and solid CO_2), and O_3 was bubbled through the solution (2 min.). The reaction flask was removed from the bath and allowed to reach rt (10 min.) and then evaporated under vacuum. Conc. acetic acid (1.0 mL) and 30% H_2O_2 (250 µL) were added and the flask sealed in a 48 °C water bath overnight (17.5 h). The products were

dried under N_2, dissolved in MeOH (1.0 mL), and treated with CH_2N_2/EtOH (1.0 mL, 2 min., 23 °C). The product was evaporated under vacuum, dissolved in Et_2O, and isolated by prep-TLC (10% (v/v) EtOAc in hexanes) to yield **21** (0.5 mg, 1.5 μmol, 30% recovery). Oil: ^{1}H NMR: (300 MHz, $CDCl_3$) δ 5.40 (dd, 1H, J = 6.7, 5.7), 4.57 (td, 1H, J = 11.0, 4.4), 3.778* (s, 3H), 3.722* (s, 3H), 2.92 (m, 3 lines, 2H), 1.98-2.1 (m, 2H), 1.68 (bd, 2H, J = 12), 1.39-1.53 (m, 2H), 1.0-1.13 (m, 2H), 0.92 (m, 4 lines, 6H), 0.83-0.9 (m, 1H), 0.81 (d, 3H, J = 6.9); GC-EIMS (70 eV) *m/z* 206 (18), 138 (78), 123 (42), 113 (33), 95 (68), 81 (100), 71 (28), 56 (42), 44 (60), 41 (22). * data is reported to three decimal points in order to clearly differentiate **20** and **21**.

Formation of Authentic Dimethyl-menthoxycarbonyl-*S*-malate (**21**). L-malate (39.8 mg, 0.294 mmol, 99%) in 400 μL of MeOH was treated with an excess of CH_2N_2/Et_2O (3 min) in a 10 mL recovery flask and dried under N_2. The methylated L-malate (48.4 mg, 0.29 mmol) was dissolved in a toluene/pyridine mixture (4:1, 250 μL), an excess of (-)-menthoxycarbonyl chloride (**19**, 600 μL of a 1.0 mM solution in toluene) was added, the flask was purged with N_2, sealed, and stirred overnight (24 h, 23 °C). The product was dissolved in 1% (v/v) EtOAc in hexanes and fractionated over a small silica flash column. The fraction eluting in 3% (v/v) EtOAc in hexanes was evaporated to yield **21** (61.5 mg, 0.179 mmol, 60.9% yield): IR (neat) 2956, 2933, 1747, 1292, 1264, 1218, 1197, 1173, 1038, 956 cm^{-1}; ^{1}H NMR (300 MHz, $CDCl_3$) δ 5.40 (dd, 1H, J = 6.7, 5.7), 4.57 (td, 1H, J = 11.0, 4.4), 3.778* (s, 3H), 3.722* (s, 3H), 2.92 (m, 3 lines, 2H), 1.98-2.1 (m, 2H), 1.68 (bd, 2H, J = 12), 1.39-1.53 (m, 2H), 1.0-1.13 (m, 2H), 0.92 (m, 4 lines, 6H), 0.83-0.9 (m, 1H), 0.81 (d, 3H, J = 6.9); GC-EIMS (70 eV) *m/z* 207 (4), 138 (100), 123 (40), 113 (29), 95 (78), 81 (74), 55 (31). * data is reported to three decimal points in order to clearly differentiate **20** and **21**.

Formation of Authentic Dimethyl-menthoxycarbonyl-*R*-malate (**21**). D-malate (40.3 mg, 0.30 mmol, 99%) in 1.0 mL of MeOH was treated with an excess of

CH_2N_2/Et_2O (3 min) in a 10 mL recovery flask and dried under N_2. The methylated L-malate was dissolved in a toluene/pyridine mixture (4:1, 250 µL), an excess of (-)-menthoxycarbonyl chloride (**19**, 600 µL of a 1.0 mM solution in toluene) was added, the flask was purged with N_2, sealed, and stirred overnight (24 h, 23 °C). The product was dissolved in 1% (v/v) EtOAc in hexanes and fractionated over a small silica flash column. Components eluting in both 1% and 3% (v/v) EtOAc in hexanes were discarded. The following fraction eluting with 100% EtOAc was evaporated to yield **21** (106.2 mg, 0.30 mmol, 100% yield): IR (neat) 2957, 2933, 1747, 1439, 1371, 1292, 1265, 1219, 1198, 1174, 1039, 956 cm^{-1}; ^1H NMR (300 MHz, $CDCl_3$) δ 5.39 (dd, 1H, J = 6.6, 5.6), 4.54 (td, 1H, J = 10.9, 4.4), 3.792* (s, 3H), 3.720* (s, 3H), 2.93 (m, 3 lines, 2H), 2.1 (bd, 1H, J = 11.8), 1.94 (pd, 1H, J = 7.0, 2.6), 1.69 (bd, 2H, J = 11.4), 1.38-1.5 (m, 2H), 1.10 (q, 1H, J = 11.7), 0.97-1.11 (m, 1H), 0.91 (m, 3 lines, 6H), 0.83-0.9 (m, 1H), 0.79 (d, 3H, J = 6.8); ^{13}C NMR (75 MHz, $CDCl_3$) δ 169.17, 169.06, 153.75, 79.296, 70.88, 52.55, 51.99, 46.76, 40.39, 35.80, 33.90, 31.26, 25.93, 23.22, 21.78, 20.49, 16.13; GC-EIMS (70 eV) *m/z* 207 (3), 138 (100), 123 (44), 113 (29), 95 (74), 81 (68), 55 (27). * data is reported to three decimal points in order to clearly differentiate **20** and **21**.

Formation of *Bis*-(*p*-Bromobenzoyl)-Constanolactone A (**23**) and 12-Acetoxy-9-(*p*-Bromobenzoyl)-Constanolactone A (**24**). To 7.7 mg of **7** (0.023 mmol), 102 mg of 4-bromobenzoyl chloride (98%, 0.466 mmol) and a catalytic amount of 4-dimethylaminopyridine were added in dry CH_2Cl_2/triethylamine (3:1, 10 mL). The solution was purged with N_2 and stirred at rt (23 °C) for 22 h. The solvents were evaporated under vacuum and the products dissolved in hexanes and applied to a small silica flash column. The fractions eluting with 20 and 50% (v/v) EtOAc in hexanes were evaporated under vacuum and further purified by NP-HPLC (dual 10-µm Alltech Versapak Si columns; 300 x 4.1 mm; 30% (v/v) EtOAc in hexanes; UV detection at 254 nm; flow

rate 2.0 mL/min)to give 1.2 mg pure bis-(*p*-bromobenzoate) constanolactone A (**2 3**, 0.002 mmol) and 0.7 mg 12-acetoxy-9-(*p*-bromobenzoyl)-constanolactone A (**2 4**) (0.0013 mmol, 5.4% yield).

Bis-(*p*-Bromobenzoyl)-Constanolactone A (**2 3**). Oil: IR (neat) 2955, 2928, 1719, 1590, 1398, 1267, 1237 cm^{-1}; UV (MeOH) λ_{max} 246 nm (log ε 4.54); CD (MeOH) Δε +1.4, -1.7 (λ_{max} 252, 238 nm); ^1H NMR: (300 MHz, $CDCl_3$) δ 7.91 (2 broad lines, 4H, -OCOBzBr), 7.59 (4 broad lines, 4H, -OCOBzBr), 5.99 (ddd, 1H, *J* = 15.7, 6.1, 0.9, H-11), 5.86 (ddd, 1H, *J* = 15.7, 5.6, 0.7, H-10), 5.54 (q, 1H, *J* = 6.1-6.3, H-12), 5.49 (dtt, 1H, 10.8. 7.2, 3.3, H-15), 5.36 (dtt, 1H, 10.8, 7.1, 3.3, H-14), 5.17 (dd, 1H, *J* = 7.7, 5.8, H-9), 3.87 (ddd, 1H, 10.4, 7.0, 3.1, H-5), 2.50 (dt, 1H, *J* = 17.7, 6.1, H-2b), 2.43 (ddd, 1H, *J* = 17.7, 8.7, 7.0, H-2a), 2.02 (bt, 2H, 7.4, H-13), 2.0 (m, 2H, H-16), 1.6-1.9 (m, 4H, H-3 and H-4), 1.2-1.3 (m, 8H, H-8 and H-17 to H-19), 1.11 (m, 1H, H-6), 0.86 (t, 3H, *J* = 6.7, H-20), 0.80 (dt, 1H, *J* = 8.8, 5.3, H-7b), 0.70 (dt, 1H, *J* = 8.6, 5.4, H-7a).

12-Acetoxy-9-(*p*-Bromobenzoyl)-Constanolactone A (**2 4**). Oil: IR (neat) 2955, 2926, 1736, 1725, 1519, 1268, 1237 cm^{-1}; UV (MeOH) λ_{max} 246 nm (log e 4.47); CD (EtOH) Δe -7.3 (λ_{max} 244.5 nm); ^1H NMR: (300 MHz, $CDCl_3$) δ 7.92 (dt, 2H, *J* = 8.6, 2.1, -OCOBzBr), 7.59 (dt, 2H, *J* = 8.6, 2.1, -OCOBzBr), 5.88 (bdd, 1H, *J* = 16.0, 5.8, H-11), 5.78 (bdd, 1H, *J* = 16.0, 5.3, H-10), 5.48 (bdt, 1H, *J* = 10.9, 7, H-15), 5.30 (m, 1H, H-14), 5.30 (m, 1H, H-12), 5.17 (dd, 1H, *J* = 7.7, 5.3, H-9), 3.85 (m, 1H, H-5), 2.57 (bdt, 1H, *J* = 18, 6.8, H-2b), 2.45 (ddd, 1H, *J* = 18, 8.6, 6.8, H-2a), 2.39 (m, 2H, H-13), 2.07 (s, 3H, -OAc), 1.99 (m, 2H, H-16), 1.95 (m, 1H, H-3b), 1.95 (m, 1H, H-4b), 1.84 (m, 1H, H-3a), 1.65 (m, 1H, H-4a), 1.25-1.35 (m, 8H, H-8 and H-17 to H-19), 1.12 (ddd, 1H, *J* = 11.4, 9.6, 5.1, H-6), 0.87 (t, 3H, *J* = 6.9, H-20), 0.81 (dt, 1H, *J* = 8.8, 5.3, H-7b), 0.68 (dt, 1H, *J* = 8.5, 5.4, H-7a); CIMS (CH_4, positive ion) *m/z*

$[M+H]^+$ 561 (8), $[M+H - AcOH]^+$ 501 (17), $[M+H - (BrC_6H_4CO_2H)]^+$ 361 (35), $[M+H - (BrC_6H_4CO_2H) - AcOH]^+$ 301 (100), $[BrC_6H_4CO_2H + H]^+$ 201 (11).

Formation of 9-(*p*-Bromobenzoyl)-Constanolactone A (**25**). Constanolactone A (**7**) (2.5 mg, 7.9 μmol) was dissolved in dry CH_2Cl_2/triethylamine (5:1, 12 mL) and small portions of 4-bromobenzoyl chloride (98%) (typically 3 to 10 mg) were added regularly over a period of 5 days while the reaction was stirred at rt (23 °C). The solvents were evaporated under vacuum and the products were dissolved in hexanes and applied to a small silica flash column. The fraction eluting with 100% Et_2O was evaporated *in vacuo* and further purified by NP-HPLC (10-μm Phenomenex Maxsil Si column; 500 x 10.0 mm; 50% (v/v) EtOAc in hexanes; UV detection at 254 nm; flow rate at 8.0 mL/min) to give *ca.* 0.5 mg pure 9-*p*-bromobenzoyl-constanolactone A (**25**, 1.0 μmol, *ca.* 13% yield). Oil: IR (neat) 3400, 2956, 2926, 1716, 1589, 1268, 1241 cm^{-1}; UV (MeOH) λ_{max} 245 nm (log e 4.34); CD (EtOH) Δe -4.6 (λ_{max} 242.0 nm); ^1H NMR: (300 MHz, $CDCl_3$) δ 7.92 (bd, 2H, *J* = 8.6, -OCOBzBr), 7.59 (bd, 2H, *J* = 8.6, -OCOBzBr), 5.95 (bdd, 1H, *J* = 15.7, 5.7, H-11), 5.83 (bdd, 1H, *J* = 15.7, 6.4, H-10), 5.55 (bdt, 1H, *J* = 10.9, 7.4, H-15), 5.38 (bdt, 1H, *J* = 10.9, 7.2, H-14), 5.07 (dd, 1H, *J* = 8.3, 6.2, H-9), 4.20 (bq, 1H, *J* = 6.1, H-12), 3.78 (m, 1H, H-5), 2.57 (m, 1H, H-2b), 2.45 (m, 1H, H-2a), 2.33 (m, 2H, *J* = 6, H-13), 1.99 (m, 2H, H-16), 1.95 (m, 1H, H-3b), 1.95 (m, 1H, H-4b), 1.84 (m, 1H, H-3a), 1.65 (m, 1H, H-4a), 1.25-1.35 (m, 8H, H-8 and H-17 to H-19), 1.09 (m, 1H, H-6), 0.87 (t, 3H, *J* = 6.9, H-20), 0.9 (m, 1H, H-7b), 0.69 (dt, 1H, *J* = 8.5, 5.3, H-7a); CIMS (CH_4, positive ion) *m/z* $[M+H]^+$ 519 (5), $[M+H - H_2O]^+$ 501 (11), 347 (27), $[M+H - (BrC_6H_4CO_2H)]^+$ 319 (92), $[M+H - (BrC_6H_4CO_2H) - H_2O]^+$ 301 (100), 282 (11), $[BrC_6H_4CO_2H + H]^+$ 201 (97), 163 (43).

Constanolactone C Per-acetate (**28**). Oil: $[\alpha]_D$ 0 (c 0.62, MeOH); IR (neat) 3446, 2960, 2931, 2859, 1737, 1733, 1662, 1646, 1372, 1235, 1037, 1023 cm^{-1}; ^1H (400 MHz, $CDCl_3$) and ^{13}C NMR (100 MHz, $CDCl_3$) data in Table III.4; ^1H NMR (400 MHz,

C_6D_6) δ 6.13 (ddd, 1H, *J* = 15.3, 5.9, 1.3, H-11), 5.92 (ddd, 1H, *J* = 15.3, 5.0, 1.0, H-10), 5.58 (m, 2H), 5.5 (m, 1H), 5.43 (m, 2H), 4.99 (dd, 1H, *J* = 8.7, 5.0, H-9), 2.86 (m, 3H, H-5 and H-16), 2.62 (dt, 1H, *J* = 14.6, 6.5, H-13b), 2.52 (dt, 1H, *J* = 14.6, 6.4, H-13a), 2.04 (m, 2H, H-2), 1.96 (m, 1H), 1.80 (s, 3H, OAc), 1.76 (s, 3H, OAc), 1.32 (m, 1H), 1.27 (m, 1H), 1.17 (m, 1H), 1.01 (m, 1H), 0.92 (t, 3H, *J* = 7.5, H-20), 0.89 (m, 1H), 0.61 (m, 2H), 0.20 (dd, 1H, *J* = 8.3, 1.4, H-7a); GC-EIMS (70 eV) *m/z* $[M + H_2O]^+$ 436 (1), $[M+H - AcOH]^+$ 359 (1), 309 (10), $[M - 2(AcOH)]^+$ 298 (12), 267 (11), 231 (28), 207 (63), $[M - 2(AcOH) - C_8H_{13}]^+$ 189 (100), 171 (40), 129 (44), 99 (55), 91 (61); CIMS (CH_4, positive ion)$[M+H]^+$ *m/z* 419 (10), $[M+H - AcOH]^+$ 359 (35), $[M+H - 2(AcOH)]^+$ 299 (100); HR CIMS (CH_4, positive ion), obs $[M+H]^+$ 419.2433, calc for $C_{24}H_{35}O_6$ 419.2433.

Constanolactone D Per-acetate (29). Oil: $[\alpha]_D$ -4.7° (c 0.26, $CHCl_3$), $[\alpha]_D$ +0.2° (c 0.88, MeOH); IR (neat) 2960, 2931, 1737, 1372, 1237, 1037, 1021, 969 cm^{-1}; ^1H (400 MHz, $CDCl_3$) and ^{13}C NMR (100 MHz, $CDCl_3$) data in Table III.4; ^1H NMR (400 MHz, C_6D_6) δ 5.85 (m, 2H, H-10 and H-11), 5.5 (m, 2H), 5.4 (m, 2H), 4.99 (dd, 1H, *J* = 7, 5, H-9), 2.93 (m, 1H, H-5), 2.80 (t, 2H, *J* = 7, H-16), 2.50 (dt, 1H, *J* = 15, 7, H-13b), 2.35 (dt, 1H, *J* = 15, 7, H-13a), 2.0 (m, 4H), 1.87 (s, 3H, OAc), 1.72 (s, 3H, OAc), 1.3 (m, 1H), 1.25 (m, 1H), 1.05 (m, 4H), 0.92 (t, 3H, *J* = 7.5, H-20), 0.9 (m, 1H), 0.28 (dt, 1H, *J* = 8.5, 5.0, H-7b), 0.20 (dt, 1H, *J* = 8.5, 5.0, H-7a); GC-EIMS (70 eV)$[M + H_2O]^+$ *m/z* 436 (1), $[M+H - AcOH]^+$ 359 (1), 341 (3), 309 (8), $[M - 2(AcOH)]^+$ 298 (15), 281 (9), 267 (9), 231 (24), 207 (93), $[M - 2(AcOH) - C_8H_{13}]^+$ 189 (90), 171 (41), 129 (43), 117 (47), 109 (52), 107 (53), 99 (69), 91 (68), 81 (100); FAB-MS (glycerol, positive ion) *m/z* 461 (2), $[M+H]^+$ 419 (2), $[M+H - AcOH]^+$ 359 (1), $[M - 2(AcOH)]^+$ 299 (2), 185 (40), 93 (90), 79 (76), 67 (100), 55 (75); FABMS (glycerol, positive ion), obs 419.2434, calc for $C_{24}H_{35}O_6$ 419.2434 $[M+H]^+$.

Formation of *Bis*-(*p*-Bromobenzoyl)-Constanolactone B (31) and *Bis*-(*p*-

Bromobenzoyl)-Constanolactone D (**30**). A 85:15 mixture of **8** and **26** (11.2 mg, *ca.* 33 μmol) was treated with 103 mg 4-bromobenzoyl chloride (98%, 0.460 mmol) and a catalytic amount of 4-dimethylaminopyridine in dry CH_2Cl_2/triethylamine (5:1, 12 mL). The solution was stirred under N_2 at rt for 22 h. The solvents were evaporated under vacuum and the products partitioned (4x) between Et_2O and dil. $NaHCO_3$ (pH *ca.* 10 by paper). The dried Et_2O extract was triturated with hexanes and purified by preparative TLC (1:1, Et_2O/Bz). The major UV-active band was removed and eluted with EtOAc, the solvent evaporated *in vacuo* and further purified by NP-HPLC (Versapack Si, 2 x 300 mm x 4.1 mm, 30% EtOAc/hexanes, 2.0 mL/min) to yield 8.6 mg of bis-(*p*-bromobenzoyl)-constanolactone B (**31**, 12.3 μmol, 44% yield) and 1.5 mg bis-(*p*-bromobenzoyl)-constanolactone D (**30**, 2.2 μmol, 44% yield). Pure bis-(*p*-bromobenzoyl)-constanolactone B (**31**) was an oil: IR (neat) 2955, 2928, 1720, 1590, 1397, 1267, 1236 cm^{-1}; UV (MeOH) λ_{max} 246 nm (log ε 4.58); CD (MeOH) Δε +6.3 (λ_{max} 250 nm); ^1H NMR: (300 MHz, $CDCl_3$) δ 7.92 (3 broad lines, 4H, -OCOBzBr), 7.59 (4 broad lines, 4H, -OCOBzBr), 5.91 (m, 2H, *J* = 15.7, 6.1, 0.9, H-11), 5.53 (m, 1H, H-12), 5.50 (dt, 1H, H-15), 5.35 (dt, 1H, H-14), 5.07 (dd, 1H, *J* = 8.4, 2.5, H-9), 3.90 (ddd, 1H, H-5), 2.4-2.6 (m, 4H, H-2 and H-13), 2.0 (q, 2H, H-16), 1.6-1.9 (m, 4H, H-3 and H-4), 1.37 (td, 1H, H-8), 1.2-1.3 (m, 7H, H-6 and H-17 to H-19), 0.86 (t, 3H, *J* = 7.0, H-20), 0.78 (dt, 1H, *J* = 8.8, 5.3, H-7b), 0.68 (dt, 1H, *J* = 8.6, 5.4, H-7a).

Bis-(*p*-bromobenzoyl)-Constanolactone D (**30**). Formed as described above during formation of derivative **31**. Pure derivative **30** was an oil: IR (neat) 3450, 2959, 2931, 1719, 1590, 1484, 1398, 1267, 1238, 1102, 1012, 969, 757 cm^{-1}; UV (MeOH) λ_{max} 246 nm (log ε 4.55); CD (MeOH) Δε +6.7 (λ_{max} 272 nm); ^1H NMR (300 MHz, $CDCl_3$) δ 7.92 (3 broad lines, 4H, -OCOBzBr), 7.59 (4 broad lines, 4H, -OCOBzBr), 5.89 (m, 2H, H-10 and H-11), 5.55 (m, 1H, H-12), 5.5 (dt, 1H, H-15), 5.35 (dt, 1H, H-14), 5.30 (m, 1H, H-18), 5.25 (dtt, 1H, *J* = 10.7, 7.0, H-17), 5.07 (bdd, 1H, *J* = 8.4,

2.5, H-9), 3.89 (ddd, 1H, H-5), 2.77 (bt, 2H, J = 6.9, H-16), 2.4-2.6 (m, 4H, H-2 and H-13), 2.02 (m, 2H, H-19), 1.6-1.9 (m, 4H, H-3 and H-4), 1.35 (m, 1H, H-8), 1.23 (m, 1H, H-6), 0.94 (t, 3H, J = 7.5, H-20), 0.79 (dt, 1H, J = 8.7, 5.4, 5.4, H-7b), 0.68 (dt, 1H, J = 8.9, 5.4, 5.3, H-7a); ^{13}C NMR (75 MHz, ^{13}C DEPT 135°, $CDCl_3$) δ 132.18 (CH, C18), 131.69 $(CH)_2$, 131.62 $(CH)_2$, 131.15 $(CH)_2$, 131.09 $(CH)_2$, 130.48 (CH), 129.51 (CH), 126.45 (CH, C17), 123.32 (CH), 122.80 (CH), 81.29 (CH, C5), 76.49 (CH, C9), 73.78 (CH, C12), 32.30 (CH_2, C13), 29.42 (CH_2, C2), 27.83 (CH_2, C4), 25.56 (CH_2, C16), 21.60 (CH, C6), 20.46 (CH_2, C19), 19.72 (CH, C8), 18.25 (CH_2, C3), 14.14 (CH_3, C20), 6.98 (CH, C7); FABMS (3-nitrobenzyl alcohol, negative ion) $[M-H + 3\text{-NBA}]^-$ *m/z* 851/853/855 (1:2:1), 778/780/782 (2:2:1), 744/746/ 748 (0.5:1:0.5), 713/715/717 (0.5:1:0.5), 325.2 (2), 311.1 (1), 198.9/201 (100:93), 79/81 (69:64).

Isolation of MeOH solvolysis products (**32** and **33**). Frozen *C. simplex*, collected May 5, 1992, (250 g dry weight) was repetitively extracted (3X) with warm $CHCl_3$/MeOH (2:1) to yield 2.26 g of dark green oil. The extract was subjected to silica gel vacuum chromatography, using a stepwise gradient from 0 to 100% (v/v) EtOAc in hexanes. Fractions eluting with 20 to 30% (v/v) EtOAc in hexanes were determined by TLC to be of similar composition, and were pooled. This combined fraction was further purified by silica gel flash chromatography, using a stepwise gradient from 1.5 to 50% (v/v) Isopropanol (IPA) in hexanes, MeOH flush. The fractions eluting with IPA concentrations greater than 20% were subjected to preparative NP-HPLC (10-µm Phenomenex Maxsil Si column; 500 x 10 mm; 20% (v/v) IPA in H_2O; Differential refractometer detection; flow rate at 3.0 mL/min) followed by an analytical HPLC separation (dual 10-µm Alltech Versapak Si columns; 300 x 4.1 mm; 15% (v/v) IPA in hexanes; Differential refractometer detection; flow rate 4.0 mL/min) to yield two minor epimeric compounds (**32** 0.5 mg, 0.02% and **33** 1.1 mg, 0.05%).

9-O-Methyl Constanolactone A (**32**). Oil: $[\alpha]_D$ +7.3° (c 0.21, MeOH); IR (neat)

3421, 2955, 2925, 1733, 1724, 1718, 1242, 1080, 1047, 1034, 973 cm^{-1}; ^1H (300 MHz, $CDCl_3$) and ^{13}C NMR (75 MHz, $CDCl_3$) data in Table III.5; GC-EIMS (70 eV) *m/z* [M - MeOH - H_2O]$^+$ 300 (0.7), [M - C_8H_{15}]$^+$ 239 (22), [M - H_2O - C_8H_{15}]$^+$ 221 (4), [M - C_8H_{15} - MeOH]$^+$ 207 (99), [M - C_8H_{15} - MeOH - H_2O]$^+$ 189 (24), 161 (24), 113 (100), 109 (64), 99 (64); FABMS (sulfolane, negative ion), obsd 349.2379 calc for $C_{21}H_{33}O_4$ 349.2379 [M-H]$^-$.

9-O-Methyl Constanolactone B (**33**). Oil: IR (neat) 3421, 2958, 2927, 2857, 1728, 1724, 1287, 1275, 1080, 1074 cm^{-1}; ^1H NMR (300 MHz, $CDCl_3$) data in Table III.5; GC-EIMS (70 eV)[M - AcOH]$^+$ *m/z* 332 (2), [M - MeOH - AcOH]$^+$ 300 (4), [M - C_8H_{15}]$^+$ 281 (5), 249 (4), 239 (24), [M - AcOH - C_8H_{15}]$^+$ 221 (32), [M - C_8H_{15} - MeOH - AcOH]$^+$ 207 (27), 205 (29), [M - C_8H_{15} - MeOH - AcOH]$^+$ 189 (16), 183 (15), 161 (12), 155 (19), 127 (19), 113 (100), 109 (27), 99 (24).

Isolation of Constanolactones E (**34**) and F (**35**). As above, **34** and **35**, were re-isolated as natural products for further investigation. Frozen *C. simplex* (790 g dry weight) was repetitively extracted (3X, as above). The extract was subjected to silica gel vacuum chromatography, using a stepwise gradient from 10 to 100% (v/v) EtOAc in hexanes. The fraction eluting with 50% (v/v) EtOAc in hexanes (60.3 mg) was subjected to NP-HPLC (10-µm Phenomenex Maxsil Si column; 500 x 10 mm; 20% (v/v) isopropanol in hexanes; Differential refractometer detection; flow rate at 6.0 mL/min). A second NP-HPLC (dual 10-µm Alltech Versapak Si columns; 300 x 4.1 mm; 10% (v/v) EtOAc in hexanes; Differential refractometer detection; flow rate 3.0 mL/min) was necessary to separate constanolactone F (**34** 9.0 mg) from G (**35** 3.2 mg).

Constanolactone E (**34**). Oil: $[\alpha]_D$ +33° (c 0.22, MeOH); IR (neat) 3427, 2956, 2927, 1732, 1244, 1048, 1038, 966 cm^{-1}; ^1H (300 MHz, $CDCl_3$) and ^{13}C NMR (75 MHz, $CDCl_3$) data in Table III.6; CIMS (CH_4, positive ion) [M+H]$^+$ *m/z* 337 (14), [M+H - H_2O]$^+$ 319 (100), [M+H - 2(H_2O)]$^+$ 301 (96), 197 (46), 179 (66), 161 (40), 151 (18),

123 (18), 111 (14); HR CIMS (CH_4, positive ion), obs $[M+H]^+$ 337.2377, calc for $C_{20}H_{33}O_4$ 337.2375, obs $[M+H - H_2O]^+$ 319.2273, calc for $C_{20}H_{31}O_3$ 319.2273.

Constanolactone F (**35**). Oil: IR (neat) 3422, 2956, 2925, 1731, 1243, 1080, 1044, 1038, 963 cm^{-1}; ^1H (300 MHz, $CDCl_3$) and ^{13}C NMR (75 MHz, $CDCl_3$) data in Table III.6; CIMS (CH_4, positive ion) $[M+H - H_20]^+$ *m/z* 319 (96), $[M+H - 2(H_20)]^+$ 301 (100), 254 (14), $[M+H - C_8H_{15}]^+$ 225 (7), 197 (26), 179 (78), 161 (40), 147 (31), 129 (27), 123 (62), 111 (20).

Isolation of Constanolactones E-G Per-acetate Derivatives (**37-39**). A silica gel vacuum chromatographic fraction (459 mg, 50% (v/v) EtOAc in hexanes) from the same collection of *C. simplex* which yielded **9** and **10** was subjected to a second silica gel vacuum chromatography, using a stepwise gradient from 0 to 100% (v/v) EtOAc in hexanes. The fraction eluting with 45% (v/v) EtOAc in hexanes (26.9 mg) was dissolved in 0.5 mL pyridine and stirred with 0.5 mL Ac_2O at rt overnight (27.5 h). Three new per-acetate derivatives **37** (6.8 mg, 0.27%), **38** (3.2 mg, 0.13%), and **39** (0.5 mg, 0.02%) were subsequently isolated by NP-HPLC (dual 10-μm Alltech Versapak Si columns; 300 x 4.1 mm; 35% (v/v) EtOAc in hexanes; Differential refractometer detection; flow rate 5.0 mL/min).

Constanolactone E Per-acetate (**37**). Oil: $[\alpha]_D$ -17.4° (c 0.41, MeOH); IR (neat) 3378, 2955, 2928, 2855, 1736, 1370, 1226, 1037, 963 cm^{-1}; ^1H (300 MHz, $CDCl_3$) and ^{13}C NMR (75 MHz, $CDCl_3$) data in Table III.6; ^1H NMR (300 MHz, C_6D_6) δ 5.70 (dd, 1H, *J* = 14.8, 8.3, H-10), 5.62 (dd, 1H, *J* = 8.3, 6.9, H-11), 5.5 (dd, 1H, *J* = 10, 7, H-15), 5.45 (m, 1H, H-12), 5.4 (m, 1H, H-14), 5.29 (dd, 1H, *J* = 14.8, 8.7, H-9), 2.96 (ddd, 1H, *J* = 9.8, 7.1, 2.7, H-5), 2.45 (dt, 1H, *J* = 14.8, 7.8, H-13b), 2.33 (dt, 1H, *J* = 14.8, 5.8, H-13a), 2.02 (m, 2H, H-16), 1.97 (m, 2H, H-2), 1.84 (s, 3H, OAc), 1.72 (s, 3H, OAc), 1.3 (m, 3H, H-8 and H-17), 1.25 (m, 4H, H-18 and H-19), 1.1 (m, 2H, H-3b and H-4b), 0.94 (m, 2H, H-3a and H-4a), 0.88 (t, 3H, *J* = 6.7, H-20), 0.63 (m, 1H, H-

6), 0.32 (m, 2H, H-7); ^{13}C NMR (75 MHz, C_6D_6) δ 169.88, 169.37, 169.24, 139.32, 133.38, 124.11, 122.82, 81.49, 75.23, 73.85, 31.76, 29.56, 29.47, 28.60, 27.72, 27.62, 25.08, 22.94, 20.79, 19.34, 18.40, 10.47; GC-EIMS (70 eV) $[M - AcOH]^+$ *m/z* 360 (1.4), 318 (10), $[M - C_8H_{15}]^+$ 309 (4), $[M - 2(AcOH)]^+$ 300 (18), 281 (14), 267 (15), 207 (33), $[M - 2(AcOH) - C_8H_{13}]^+$ 191 (30), 178 (56), 161 (19), 149 (35), 131 (26), 117 (37), 94 (100).

Constanolactone F Per-acetate (**38**). Oil: $[\alpha]_D$ +55° (c 0.19, MeOH); IR (neat) 3390, 2955, 2930, 2857, 1739, 1372, 1229, 1037, 958 cm^{-1}; ^{1}H (300 MHz, $CDCl_3$) and ^{13}C NMR (75 MHz, $CDCl_3$) data in Table III.6; ^{1}H NMR (300 MHz, C_6D_6) δ 5.62 (dd, 1H, *J* = 7.5, 5.5, H-11), 5.52 (m, 1H, H-15), 5.27 (dd, 1H, *J* = 12.6, 5.5, H-12), 5.49 (m, 2H, H-10 and H-14), 5.34 (dd, 1H, *J* = 15.2, 8.5, H-9), 3.01 (m, 1H, H-5), 2.40 (m, 2H, H-13), 2.00 (m, 2H, H-16), 1.97 (m, 2H, H-2), 1.79 (s, 3H, OAc), 1.70 (s, 3H, OAc), 1.3 (m, 3H, H-8 and H-17), 1.24 (m, 4H, H-18 and H-19), 1.10 (m, 2H, H-3b and H-4b), 0.92 (m, 2H, H-3a and H-4a), 0.87 (t, 3H, *J* = 6.8, H-20), 0.66 (m, 1H, H-6), 0.36 (dt, 1H, *J* = 8.4, 5.2, H-7b), 0.29 (dt, 1H, *J* = 8.8, 5.0, H-7a); ^{13}C NMR (75 MHz, DEPT (135°), C_6D_6) δ 138.18 (CH), 133.27 (CH), 125.39 (CH), 123.39 (CH), 81.02 (CH), 74.06 (CH), 73.68 (CH), 31.51 (CH_2), 29.28 (CH_2), 28.78 (CH_2), 27.39 (CH_2), 27.39 (CH_2), 24.74 (CH), 20.40 (CH_3), 20.40 (CH_3), 18.79 (CH), 18.12 (CH_2), 13.99 (CH_3), 10.16 (CH_2); CIMS (CH_4, positive ion) $[M+H]^+$ *m/z* 421 (13), $[M+H - AcOH]^+$ 361 (38), 329 (13), 319 (15), $[M+H - 2(AcOH)]^+$ 301 (100), 283 (8); HR CIMS (CH_4, positive ion), obs $[M+H]^+$ 421.2590, calc for $C_{24}H_{37}O_6$ 421.2590.

Constanolactone G Per-acetate (**39**). Oil: IR (neat) 3433, 2958, 2918, 2850, 1736, 1712, 1650, 1646, 1366, 1225, 1039 cm^{-1}; ^{1}H NMR (300 MHz, $CDCl_3$) δ 5.45 (m, 1H, H-15), 5.40 (dd, 1H, *J* = 10.9, 7.4, H-18), 5.4 (m, 2H, H-9 and H-14), 5.25-5.45 (m, 2H, H-10 and H-11), 5.3 (m, 1H, H-17), 5.02 (dt, 1H, *J* = 6.7, 5.9, H-12), 3.75 (ddd, 1H, *J* = 10.8, 7.4, 3.1, H-5), 2.75 (bt, 2H, *J* = 7.2, H-16), 2.57 (ddd, 1H, *J* = 17.8, 7.5,

6.5, H-2b), 2.45 (ddd, 1H, J = 17.8, 8.6, 6.9, H-2a), 2.33 (bt, 2H, J = 6.9, H-13), 2.07 (s, 3H, -OAc), 2.06 (m, 2H, H-19), 2.05 (s, 3H, -OAc), 2.0 (m, 1H, H-4b), 1.95 (m, 1H, H-3b), 1.8 (m, 1H, H-3a), 1.7 (m, 1H, H-4a), 1.54 (m, 1H, H-8), 1.13 (m, 1H, H-6), 0.97 (t, 3H, J = 7.6, H-20), 0.76 (dt, 1H, J = 8.6, 5.2, H-7b), 0.69 (dt, 1H, J = 8.7, 5.2, H-7a); (400 MHz, C_6D_6) δ 5.63 (dd, 1H, J = 7.4, 5.8, H-11), 5.5 (m, 3H), 5.4 (m, H), 5.36 (dd, 1H, J = 16.3, 6.9, H-9), 5.28 (dt, 1H, J = 6.9, 5.8, H-12), 3.00 (m, 1H, H-5), 2.80 (m, 2H, J = 6.2, H-16), 2.4 (m, 2H, H-13), 2.0 (m, 6H, H-2, H-19, and H-3), 1.78 (s, 3H, -OAc), 1.69 (s, 3H, -OAc), 1.2-1.37 (m, 1H, H-8), 1.06 (m, 1H, H-4b), 0.91 (t, 3H, J = 7.6, H-20), 0.9 (m, 1H, H4a), 0.66 (m, 1H, H-6), 0.37 (dt, 1H, J = 8.6, 5.2, H-7b), 0.29 (dt, 1H, J = 8.7, 5.2, H-7a); ^{13}C NMR (100 MHz, C_6D_6) δ 169.71, 169.24, 168.64, 138.50, 132.31, 131.71, 124.15, 123.67, 81.20, 74.38, 73.82, 30.14, 29.50, 29.05, 27.60, 25.98, 25.04, 21.50, 20.88, 20.63, 19.04, 18.40, 14.41, 10.43; FABMS (2:1 thioglycerol:glycerol, positive ion) $[M+H]^+$ *m/z* 419.2 (34), $[M+H - AcOH]^+$ 391.3 (22), 359.2 (14), 317.2 (20), $[M+H - 2(AcOH)]^+$ 299.2 (82), 281.1 (14), 215.1 (21), 207.1 (24), 149.1 (20), 121.1 (23), 109.1 (37), 95.1 (48), 81.1 (65), 69.1 (79), 55.1 (100); HR FABMS obs $[M+H - 2(AcOH)]^+$ at 299.2012, calc for $C_{20}H_{27}O_2$ 299.2011.

Formation of the Acetonide of Methyl Constanolactone E (**40**). A catalytic amount of *p*-toluenesulphonic acid was added to 1.1 mg of **34** (3.3 μmol) dissolved in 2, 2-dimethoxypropane (0.5 mL). The solution was stirred at rt for 105 min. Triethylamine (50 μL) was then added to increase the pH prior to evaporation under vacuum. The products were dissolved in hexanes and kept basic with the addition of triethylamine (10 mL) and applied to a small silica flash column. The fraction eluting with 10% (v/v) EtOAc in hexanes was further purified by NP-HPLC (10-μm Alltech Versapak, 2 x 300 mm x 4.1 mm; 25% (v/v) EtOAc in hexanes, 2.0 mL/min) to give *ca.* 1 mg pure methylated acetonide product **40** (2.5 μmol, 75% yield) as an oil: IR (neat) 3485, 2986, 2955, 2931, 2859,

1740, 1457, 1437, 1379, 1368, 1246, 1216, 1166, 1080, 1056, 1012, 967 cm^{-1}; ^1H NMR (400 MHz, $CDCl_3$) δ 5.54 (dd, 1H, *J*= 15.2, 8.2, H-10), 5.49 (m, 1H, H-15), 5.37 (dd, 1H, *J*= 15.2, 8.4, H-9), 5.35 (m, 1H, H-14), 4.48 (dd, 1H, *J*= 8.2, 6.2, H-11), 4.10 (dt, 1H, *J*= 8.0, 6.2, H-12), 3.67 (s, 3H, OCH_3), 3.06 (m, 1H, H-5), 2.35 (t, 2H, *J*= 7.3, H-2), 2.28 (dt, 1H, *J*= 14.6, 8.0, H-13b), 2.15 (dt, 1H, *J*= 14.6, 6.2, H-13a), 2.04 (bq, 2H, *J*= 7.2, H-16), 1.77 (m, 2H, H-3), 1.60 (m, 2H, H-4), 1.48 (s, 3H, acetonide), 1.44 (m, 1H, H-8), 1.35 (m, 2H, H-17), 1.34 (s, 3H, acetonide), 1.3 (m, 4H, H-18 and H-19), 1.00 (7 lines, 1H, H-6), 0.89 (t, 3H, *J*= 6.8, H-20), 0.70 (dt, 1H, H-7b), 0.67 (dt, 1H, H-7a); GC-EIMS (70 eV) $[M - CH_3]^+$ *m/z* 393 (1.0), $[M - H_2O]^+$ 390 (1.5), 361 (2), $[M - CH_3 - (CH_3)_2CO_2]^+$ 334 (1.5), $[M - CH_3 - (CH_3)_2CO_2 - H_2O]^+$ 301 (4), 250 (7), 236 (7), 221 (9), 207 (15), 189 (23), 178 (19), 161 (23), 147 (27), 131 (55), 119 (25), 105 (28), 99 (100).

Formation of Acetonide of Methyl Constanolactone F (**41**). A catalytic amount of *p*-toluenesulphonic acid was added to 4.2 mg of **35** were dissolved in 2, 2-dimethoxypropane (0.5 mL). The solution was stirred at rt (23 °C) for 105 min. Triethylamine (50 μL) was then added to increase the pH prior to evaporation under vacuum. The products were dissolved in hexanes and kept basic with the addition of triethylamine (10 μL) and fractionated over a small silica flash column. A fraction eluting with 10%-100% (v/v) EtOAc in hexanes was further purified by NP-HPLC (10-μm Alltech Versapak, 2 x 300 x 4.1 mm, 25% (v/v) EtOAc in hexanes, 2.0 mL/min) to give 2.0 mg of pure methylated acetonide product **41** (5 μmol, 40% yield) as an oil: IR (neat) 3485, 2985, 2955, 2930, 2859, 1740, 1719, 1457, 1437, 1377, 1370, 1241, 1230, 1222, 1171, 1073, 1054, 1023, 967 cm^{-1}; ^1H NMR (400 MHz, $CDCl_3$) δ 5.55 (m, 1H, H-15), 5.49 (bdd, 1H, *J*= 15.3, 7.8, H-10), 5.4 (m, 1H, H-14), 5.35 (dd, 1H, *J*= 15.3, 8.5, H-9), 3.98 (t, 1H, *J*= 8.1, H-11), 3.70 (dt, 1H, *J*= 8.1, 5.7, H-12), 3.67 (s, 3H, OCH_3), 3.03 (m, 1H, H-5), 2.35 (t, 2H, *J*= 7.3, H-2), 2.32 (m, 2H, H-13), 2.01 (bq, 1H, *J*= 6.9, H-16),

1.77 (m, 2H, H-3), 1.60 (m, 2H, H-4), 1.403 (s, 3H, acetonide-CH_3), 1.396 (s, 3H, acetonide-CH_3), 1.35 (m, 2H, H-17), 1.3 (m, 4H, H-18 and H-19), 1.0 (7 lines, 1H, H-6), 0.89 (t, 3H, J= 6.8, H-20), 0.71 (dt, 1H, J= 8.6, 5.2, H-7b), 0.65 (dt, 1H, J= 8.6, 5.2, H-7a); GC-EIMS (70 eV) $[M]^+$ *m/z* 408 (1), $[M - H_2O]^+$ 390 (1), 361 (1), $[M - CH_3 - (CH_3)_2CO_2]^+$ 334 (2), $[M - CH_3 - (CH_3)_2CO_2]^+$ 319 (2), $[M - CH_3 - (CH_3)_2CO_2 - H_2O]^+$ 301 (4), 250 (9), 236 (8), 221 (10), 207 (15), 189 (27), 178 (38), 161 (26), 147 (29), 131 (58), 119 (30), 109 (46), 105 (29), 99 (100).

Formation of *bis*-(*p*-bromobenzoyl)-Constanolactone E (**42**). Constanolactone E (**34**, 9.9 mg, 29 μmol), 100.7 mg of 4-bromobenzoyl chloride (98%, 0.45 mmol), and a catalytic amount of 4-dimethylaminopyridine were dissolved in dry CH_2Cl_2/triethylamine (5:1, 12.0 mL). The solution was purged with N_2 and stirred at rt (23 °C) for 18 h. The solvents were evaporated under vacuum and the products were dissolved in hexanes and fractionated over a small silica gel flash column. The fractions eluting with Et_2O were further purified by NP-HPLC (10-μm Phenomenex Maxsil Si column, 500 x 10.0 mm, 30% (v/v) EtOAc in hexanes, UV detection at 254 nm, flow rate 8.0 mL/min) to give 10.8 mg of the pure bis-(*p*-bromobenzoate) **42** (15 μmol, 53% yield) as an oil: UV (EtOH) λ_{max} 246 nm (log ε 4.56); CD (EtOH) Δε +9.1 (λ_{max} 252.5 nm); ^{1}H NMR (300 MHz, $CDCl_3$) δ 7.89 (bd, 2H, J= 8.5, 1.7, -$O_2CC_6H_4Br$), 7.82 (bd, 2H, J= 8.5, 1.7, -$O_2CC_6H_4Br$), 7.59 (bd, 2H, J= 8.5, 1.7, -$O_2CC_6H_4Br$), 7.55 (bd, 2H, J= 8.5, 1.7, -$O_2CC_6H_4Br$), 5.71 (dd, 1H, J= 15.0, 8.0, H=10), 5.63 (dd, 1H, J= 8.0, 3.7, H-11), 5.50 (dd, 1H, J = 15.0, 8.4, H-9), 5.40 (m, 2H, H-2 and H-15), 5.35 (m, 1H, H-14), 3.77 (ddd, 1H, J= 10.4, 7.7, 3.0, H-5), 2.56 (dt, 1H, J= 17.6, 6.7, H-2b), 2.5 (m, 2H, H-13), 2.45 (ddd, 1H, J= 17.6, 8.6, 6.8, H-2a), 2.0 (m, 3H, H-4b and H-16), 1.9 (m, 1H, H-3b), 1.8 (m, 1H, H-3a), 1.6 (m, 2H, H-4a and H-8), 1.35 (m, 2H, H-17), 1.3 (m, 4H, H-18 and H-19), 1.09 (7 lines, 1H, H-6), 0.85 (t, 3H, J= 6.7, H-20), 0.79 (dt, 1H, J= 8.6, 5.2, H-7b), 0.71 (dt, 1H, J= 8.6, 5.2, H-7a); ^{1}H NMR (300 MHz, C_6D_6) δ 7.91 (d, 2H, J=

8.4, -$O_2CC_6H_4Br$), 7.83 (d, 2H, J = 8.2, -$O_2CC_6H_4Br$), 7.29 (d, 2H, J = 8.2, -$O_2CC_6H_4Br$), 7.16 (d, 2H, J = 8.4, -$O_2CC_6H_4Br$), 5.97 (dd, 1H, J = 8.0, 4.5, H-11), 5.85 (dd, 1H, J = 15.0, 8.3, H-10), 5.76 (dt, 1H, J = 7.6, 4.5, H-12), 5.53 (m, 2H, H-14 and H-15), 5.45 (dd, 1H, J = 15.0, 8.8, H-9), 3.02 (m, 1H, H-5), 2.65 (dt, 1H, J = 14.0, 7.4, H-13b), 2.53 (m, 1H, H-13a), 2.06 (bq, 2H, J = 6.9, H-16), 2.00 (bq, 2H, J = 6.8, H-2), 1.42 (m, 1H, H-8), 1.32 (m, 2H, H-17), 1.25 (m, 4H, H-18 and H-19), 1.12 (m, 2H, H-3b and H-4b), 0.97 (m, 2H, H-3a and H-4a), 0.91 (t, 3H, J = 6.8, H-20), 0.67 (m, 1H, H-6), 0.39 (m, 2H, H-7); CIMS (CH_4, positive ion) $[M]^+$ *m/z* 700 (3), 623 (2), $[M+H - BrC_6H_4CO_2H]^+$ 501 (15), $[M+H - 2(BrC_6H_4CO_2H)]^+$ 301 (72), $[M+H - 2(BrC_6H_4CO_2H) - H_2O]^+$ 283 (8), 229 (8), $[BrC_6H_4CO_2H+H]^+$ 201 (82), 183 (15), 157 (19), 123 (100).

Formation of *bis*-(*p*-Bromobenzoyl)-Constanolactone F (**43**). Constanolactone F (**35**) (1.4 mg, 0.0042 mmol) , 23.8 mg of 4-bromobenzoyl chloride (98%, 0.106 mmol), and a catalytic amount of 4-dimethylaminopyridine were dissolved in dry CH_2Cl_2/triethylamine (5:1, 6.0 mL). The solution was purged with N_2 and stirred at rt (23 °C) for 17 h. The solvents were evaporated under vacuum and the products were dissolved in hexanes and fractionated over a small silica flash column. The fractions eluting with 36 to 80% Et_2O in hexanes were further purified by NP-HPLC (10-µm Alltech Versapak, 2 x 300 x 4.1 mm, 30% (v/v) EtOAc in hexanes; 254 nm detection, 2.0 mL/min) to give *ca.* 0.5 mg pure bis-(*p*-bromobenzoate) product **43** as an oil: UV (EtOH) λ_{max} 246 nm (log ε 4.29); CD (EtOH) Δε +5.4, -11.8 (λ_{max} 255, 240 nm); ^{1}H NMR (400 MHz, $CDCl_3$) δ 7.81 (bd, 4H, J = 8.4, -$O_2CC_6H_4Br$), 7.51 (bd, 4H, J = 8.4, 1.4, -$O_2CC_6H_4Br$), 5.62 (dd, 1H, J = 15, 7, H-10), 5.56 (bd, 1H, J = 7, H-11), 5.5 (m, 2H, H-12 and H-15), 5.4 (m, 1H, H-9), 5.35 (m, 1H, H-14), 3.73 (m, 1H, H-5), 2.5 (m, 3H, H-2b and H-13), 2.4 (m, 1H, H-2a), 1.99 (m, 1H, H-4b), 1.95 (m, 2H, H-16), 1.8-2.0 (m, 2H, H-3), 1.66 (m, 1H, H-4a), 1.54 (m, 1H, H-8), 1.3 (m, 6H, H-17 to H-19), 1.12 (m, 1H, H-6),

0.81 (t, 3H, *J*=6.8, H-20), 0.76 (m, 1H- H-7b), 0.67 (m, 1H, H-7a); CIMS (CH_4, positive ion) *m/z* $[M]^+$ 700 (0.5), 623 (0.5), $[M+H - BrC_6H_4CO_2H]^+$ 501 (9), $[M+H - 2(BrC_6H_4CO_2H)]^+$ 301 (48), $[M+H - 2(BrC_6H_4CO_2H) - H_2O]^+$ 283 (6), 229 (9), $[BrC_6H_4CO_2H+H]^+$ 201 (92), 183 (16), 157 (22), 123 (100), 105 (19).

General Biosynthetic Methods. *C. simplex* (1 Kg, wet weight) was obtained from exposed low intertidal rocks at Seal Rock, Oregon on 30 August 1989. Voucher specimens of this alga are deposited at the College of Pharmacy, Oregon State University. The alga was frozen on site using dry ice and then stored at -70 °C prior to extraction. Arachidonic acid (AA, 99%) was purchased from Sigma. EtOH from Midwest Grain Products Co. Oxygen-$^{18}O_2$ from Cambridge Isotope Laboratories: MS analysis of this gas mixture showed it to be of random speciation (23.6 % $^{16}O_2$, 48.4 % $^{16}O^{18}O$, 28 % $^{18}O_2$), although originally sold as "Oxygen-$^{18}O_2$;^{18}O, 50%." All other compounds and solvents were of the highest purity commercially available.

Enzyme Extraction and Preparation. *C. simplex* (980 g frozen) was repeatedly extracted with 500 mL fractions of acetone-CO_2 (s) until acetone extract was nearly colorless (slightly yellow). Solvent was removed from tissue by filtration using a 10-20 μm sintered glass funnel. The final residue was then dried under N_2.[143] The dry acetone powder (176 g) was divided into six portions and stored under N_2 at -70 °C. Portions of acetone powder (1.00 g) were then used in all incubations except for the $^{18}O_2$ labeling experiment (see below). Each of these was then dissolved in 125 mL Erlenmeyer flasks with 75 mL of 0.1 M K_2HPO_4 buffer, pH 7.4. Boiling of the enzyme preparation was accomplished by heating with occasional stirring (98-100 °C, 10 min). At the end of this time the enzyme preparation had changed from pink to green. All flasks were allowed to reach the desired temperatures and monitored periodically throughout each incubation.

Acetone Powder Incubations. Arachidonic acid was dissolved in EtOH to a final concentration of 0.1 mg μl^{-1}. Treatments of "AA + AP", "AA + boiled AP", and "AA +

pH 7.4 buffer alone" each received 2.0 mg of AA in 20 µl EtOH at 20 °C. "AA + AP" treatments were then performed in duplicate at 25 °C using 0.0, 1.0, 5.0, and 10.0 mg of AA respectively. "AA + AP" treatments were performed at 9 °C using 0.0 and 5.0 mg of AA. A final "AA + AP" treatment was performed in duplicate at 1 °C using 5.0 mg of AA. All incubations were allowed to run 20 min with continuous agitation.

Enzyme Product Extraction. Following the incubation period, enzyme preparations were adjusted to pH 4 with 10% HCl. Lipids were extracted four times with 60-80 mL portions of $CHCl_3$. The combined extracts were evaporated *in vacuo* and the recovered lipids, stored in Et_2O at -20 °C.

Analysis of Enzyme Products. TLC of the acetone extract and enzyme incubation treatments was performed on silica gel 60 F_{254} using (10% (v/v) MeOH in $CHCl_3$). The TLC was developed then sprayed with a solution of 50% H_2SO_4. Blue char reactions characteristic of oxylipins were produced upon heating. Enzyme products were analyzed by normal phase HPLC (10-µm Alltech Versapak, 300 x 4.1 mm, 85% (v/v) EtOAc in hexanes; 4.0 mL/min) using a Waters M-6000 pump, U6K injector and R 401 differential refractometer. NP-HPLC . Enzyme products were quantified by area under the curve measurements coupled with actual recovered product masses.

Molecular Oxygen Incorporation Study. Incubation was conducted using "Oxygen-$^{18}O_2$; ^{18}O, 50%" in a closed system containing 10 g of *C. simplex* acetone powder stirring in 100 mL of 0.1 M phosphate (K_2HPO_4/HCl) buffer (pH 7.4) at 21.5 °C. The buffer medium and head space (*ca.* 25 mL) were repeatedly gas-stripped with N_2 alternating with water aspirated vacuum. The system was then charged three times with the $^{16}O/^{18}O$ gas mixture and then 10 mg of 90% pure AA dissolved in 100 µl of ethanol was added. After 20 minutes at 21.5 °C the reaction was immediately extracted four times with $CHCl_3$ (125 mL) and evaporated *in vacuo*. TLC analysis (10% (v/v) MeOH in $CHCl_3$) of the oil suggested the presence of several oxidized AA metabolites. The crude extract was

methylated (CH_2N_2/Et_2O) to yield 3.32 mg of a colorless oil. The oil was dissolved in 2 drops dry pyridine to which 2 drops 1,1,1,3,3,3-hexamethyldisilazane and 2 drops trimethylchlorosilane were then added. The mixture was mixed (vortex) and allowed to stand at room temperature for 20 minutes, the reagents evaporated *in vacuo*, and the samples dissolved in hexanes to a concentration of 100-500 ng/μL (dependent upon complexity of mixture). The material was vortex agitated, centrifuged, and the surface hexanes drawn off (decanted) with a pipet to a clean tube prior to GC-MS analysis.

Analysis of ^{18}O-labeled Constanolactones and Derivatives. Following extraction and methylation of the products (as above) the oxylipins were analyzed by GC-EIMS of their corresponding bis-trimethylsilyl (TMSi) ethers (**46** and **47**). Incorporation of labeled O_2 was observed by analysis of isotopic abundance patterns in key MS fragments in labeled and non-labeled products. Significant incorporation of one ^{18}O was achieved as evidenced by an enhancement of the ion at *m/z* 371 $[M - CH_3(CH_2)_4CH{=}CHCH_2 + 2]^+$ (28±1% incorp.), corresponding to α-cleavage to the C-12 TMSi ether (Figure III.36). However, the ^{18}O-label substitution was not clearly identifiable by the fragmentation pattern. Therefore, catalytic hydrogenation (H_2, 5% $PtCl_2$) of ^{18}O-labeled and unlabeled control incubation products afforded constanolactone derivatives which were re-silated (as above) to form a mixture of 10,11,14,15-tetrahydrogenated TMSi ethers (**48** and **49**).

Incorporation of ^{18}O-label into crucial fragments were calculated by first establishing the isotopic contribution of unlabeled product (i.e. $[ion]^+ + 1$, $[ion]^+ + 2$, $[ion]^+ + 3$, etc. as a percentage of the $[ion]^+$), adjusting these figures to a percentage of the $[ion]^+$ abundance in the labeled fragment, and subtracting this contribution from the total abundance of each corresponding ion in the labeled fragment. The remaining ^{18}O-label contribution was then divided by the total ion abundance of the fragment and reported as an average percent incorporation for each pair of constanolactone derivatives.

Methyl-9,12-*Bis*-$(CH_3)_3$Si-Constanolactones (**46** and **47**). GC-EIMS (70 eV),

peak 1: GC-retention 27.9-29.4 min., $[M - C_8H_{15}]^+$ / $[M - C_8H_{15} + 1]^+$ / $[M - C_8H_{15} + 2]^+$ / $[M - C_8H_{15} + 3]^+$ / $[M - C_8H_{15} + 4]^+$ *m/z* 369/370/371/372/373 (59.7/18.8/7.42/1.64/0.31), 279/381 (96.0/7.25), 243/245 (11.2/1.57), 189 (12.2), 129 (17.7), 73 (100), 55 (14.5); peak 2: GC-retention 30.2-31.9 min., $[M - C_8H_{15}]^+$ / $[M - C_8H_{15} + 1]^+$ / $[M - C_8H_{15} + 2]^+$ / $[M - C_8H_{15} + 3]^+$ / $[M - C_8H_{15} + 4]^+$ *m/z* 369/370/371/372/373 (63.4/19.6/7.69/1.72/0.49), 279/381 (77.1/5.58), 243/245 (13.0/1.78), 189 (11.8), 129 (18.1), 73 (100), 55 (15.2).

^{18}O-Labelled Methyl-9,12-*Bis*-$(CH_3)_3$Si-Constanolactones (**46** and **47**). GC-EIMS (70 eV), peak 1: GC-retention 28.2-29.2 min.,$[M - C_8H_{15}]^+$ / $[M - C_8H_{15} + 1]^+$ / $[M - C_8H_{15} + 2]^+$ / $[M - C_8H_{15} + 3]^+$ / $[M - C_8H_{15} + 4]^+$ *m/z* 369/370/371/372/373 (40.9/13.8/20.2/6.39/2.33), 279/381 (69.1/28.7), 243/245 (10.4/4.68), 189 (11.0), 129 (18.3), 73 (100), 55 (16.6); peak 2: GC-retention 29.8-30.6 min., $[M - C_8H_{15}]^+$ / $[M - C_8H_{15} + 1]^+$ / $[M - C_8H_{15} + 2]^+$ / $[M - C_8H_{15} + 3]^+$ / $[M - C_8H_{15} + 4]^+$ *m/z* 369/370/371/372/373 (40.2/13.4/20.3/6.31/1.98), 279/381 (50.0/21.1), 243/245 (12.8/4.7), 189 (9.0), 129 (33.0), 73 (100), 55 (14.8).

Methyl-10,11,14,15-tetrahydro-9,12-*Bis*-$(CH_3)_3$Si-Constanolactones (**48** and **49**). GC-EIMS (70 eV), peak 1: GC-retention 32.3 min., $[M - C_8H_{17}]^+$ / $[M - C_8H_{17} + 1]^+$ / $[M - C_8H_{17} + 2]^+$ / $[M - C_8H_{17} + 3]^+$ *m/z* 371/372/373/374 (10.5/4.05/<1/<1), 342 (3.1), 314/316 (5.07/1.51), 281/283 (28.4/3.64), $[M - C_{14}H_{31}{}^{18}OSi]^+$ / $[M - C_{14}H_{31}{}^{18}OSi + 1]^+$ / $[M - C_{14}H_{31}{}^{18}OSi + 2]^+$ / $[M - C_{14}H_{31}{}^{18}OSi + 3]^+$ 241/242/243/244 (100/16.6/6.66/<1), $[CH_3(CH_2)_7COSi(CH_3)_3]^+$ / $[CH_3(CH_2)_7COSi(CH_3)_3 + 1]^+$ / $[CH_3(CH_2)_7COSi(CH_3)_3 + 2]^+$ / $[CH_3(CH_2)_7COSi(CH_3)_3 + 3]^+$ 215/216/217/218 (15.2/6.66/3.83/<1), 191 (10.3), 185 (20.3), 129/131 (54.7/16.1), 73 (84.6), 55 (23.6); peak 2: GC-retention 33.5 min., $[M - C_8H_{17}]^+$ / $[M - C_8H_{17} + 1]^+$ / $[M - C_8H_{17} + 2]^+$ / $[M - C_8H_{17} + 3]^+$ *m/z* 371/372/373/374 (10.2/3.30/<1/<1), 342 (2.79), 314/316 (13.5/1.43), 281/283 (31.1/4.53), $[M - C_{14}H_{31}{}^{18}OSi]^+$ / $[M - C_{14}H_{31}{}^{18}OSi + 1]^+$ / $[M - C_{14}H_{31}{}^{18}OSi$

+ 2]$^+$ / [M - $C_{14}H_{31}{}^{18}OSi$ + 3]$^+$ 241/242/243/244 (91.6/21.1/7.66/<1), [$CH_3(CH_2)_7COSi(CH_3)_3$]$^+$ / [$CH_3(CH_2)_7COSi(CH_3)_3$ + 1]$^+$ / [$CH_3(CH_2)_7COSi(CH_3)_3$ + 2]$^+$ / [$CH_3(CH_2)_7COSi(CH_3)_3$ + 3]$^+$ 215/216/217/218 (15.5/4.96/2.89/0.97), 191 (15.5), 185 (18.3), 129/131 (61.7/13.1), 73 (100), 55 (20.2).

^{18}O-Labelled Methyl-10,11,14,15-tetrahydro-9,12-Bis-$(CH_3)_3$Si-Constanolactones (**48** and **49**). GC-EIMS (70 eV), peak 1: GC-retention 32.4 min., [M - C_8H_{17}]$^+$ / [M - C_8H_{17} + 1]$^+$ / [M - C_8H_{17} + 2]$^+$ / [M - C_8H_{17} + 3]$^+$ *m/z* 371/372/373/374 (7.66/3.37/3.32/1.79), 281/283 (24.3/8.4), [M - $C_{14}H_{31}{}^{18}OSi$]$^+$ / [M - $C_{14}H_{31}{}^{18}OSi$ + 1]$^+$ / [M - $C_{14}H_{31}{}^{18}OSi$ + 2]$^+$ / [M - $C_{14}H_{31}{}^{18}OSi$ + 3]$^+$ 241/242/243/244 (86.3/18.0/5.46/<1), [$CH_3(CH_2)_7COSi(CH_3)_3$]$^+$ / [$CH_3(CH_2)_7COSi(CH_3)_3$ + 1]$^+$ / [$CH_3(CH_2)_7COSi(CH_3)_3$ + 2]$^+$ / [$CH_3(CH_2)_7COSi(CH_3)_3$ + 3]$^+$ 215/216/217/218 (14.6/7.16/2.35/1.43), 191 (10.1), 185 (21.1), 129/131 (89.5/13.7), 73 (100), 55 (18.5); peak 2: GC-retention 33.5 min., [M - C_8H_{17}]$^+$ / [M - C_8H_{17} + 1]$^+$ / [M - C_8H_{17} + 2]$^+$ / [M - C_8H_{17} + 3]$^+$ *m/z* 371/372/373/374 (4.69/2.31/2.91/2.27), 342 (4.6), 314/316 (14.2/5.37), 281/283 (28.4/11.57), [M - $C_{14}H_{31}{}^{18}OSi$]$^+$ / [M - $C_{14}H_{31}{}^{18}OSi$ + 1]$^+$ / [M - $C_{14}H_{31}{}^{18}OSi$ + 2]$^+$ / [M - $C_{14}H_{31}{}^{18}OSi$ + 3]$^+$ 241/242/243/244 (100/22.4/8.2/2.53), [$CH_3(CH_2)_7COSi(CH_3)_3$]$^+$ / [$CH_3(CH_2)_7COSi(CH_3)_3$ + 1]$^+$ / [$CH_3(CH_2)_7COSi(CH_3)_3$ + 2]$^+$ / [$CH_3(CH_2)_7COSi(CH_3)_3$ + 3]$^+$ 215/216/217/218 (12.5/9.10/8.37/1.03), 191 (18.0), 185 (21.1), 129/131 (51.7/17.5), 73 (94.5), 55 (21.8).

CHAPTER IV.

NAKIENONES A-C AND NAKITRIOL, NEW CYTOTOXIC C_{11} METABOLITES FROM AN OKINAWAN CYANOBACTERIAL (*SYNECHOCYSTIS* SP.) OVERGROWTH OF CORAL

Abstract

Nakienones A-C and nakitriol, a series of reactive cytotoxic metabolites, were isolated from dead and necrotic branches of stony coral (*Acropora* sp.) which were completely covered with a gray-black mat of cyanobacteria (*Synechocystis* sp.). Their structures were determined spectroscopically by interpretation of 2D-NMR experiments, including HMBC and NOESY, and by comparison with model compounds.

Introduction

Marine algal overgrowths have recently been established as contributing factors leading to the destruction of hard-coral communities.[144] Dramatic phase shifts in Caribbean reef species composition have been observed over the past twenty to thirty years. A combination of human and natural disturbances have resulted in severe disruption of the density and diversity of coral reef communities. Overfishing, pollution, disease, and tropical storms have together contributed to destabilize herbivore population density, resulting in large-scale algal blooms and massive destruction of hard-corals. Little is known about how specific chemical-ecological interactions between algae, herbivores, and predatory species may influence the dynamics of disrupted or damaged reef populations.

As part of our ongoing survey of marine algae for biomedical potential, I discovered at a depth of -1 to -2 m several large (diameter 3-4 m), nearly concentric, zones where blackened mats of *Synechocystis* sp. were completely overgrowing and apparently smothering an otherwise heathy-appearing staghorn coral reef (*Acropora* sp.) in the waters off Yonaine at Nakijin Village, Okinawa. While I am unable to prove that this overgrowth caused the death of the subtending coral, I strongly suspect this to be the case due to the observed growth pattern of the cyanobacteria. From this microalgal-coral assemblage, I have isolated four new cytotoxic C_{11} metabolites which may be involved in the chemical ecology of this interaction.

Only cursory data concerning the chemistry of *Synechocystis* spp. is available. However, at least two species of *Synechocystis* contain small molecules (640 to 1250 daltons) which potently act to induce settling of planktonic red abalone larvae (*Haliotis rufescens*).[145] Further, these metabolites were demonstrated to trigger metamorphosis in these larvae, much as gamma-aminobutyric acid (GABA). While these compounds have not been fully characterized, they may be important to the ecology of both organisms.

Results and Discussion

Matted algal material on completely denuded coral (1 L, 1.091 kg dry material) was preserved in 2-propanol and stored at -20 °C until extracted with CH_2Cl_2/MeOH (2:1). The extract was partitioned into two fractions, a non-polar CH_2Cl_2 fraction (2.70 g, dark oil), and a polar aqueous-alcohol (*sec*-butanol) fraction (1.294 g, oil). Two-dimensional TLC analysis of the extracts suggested the presence of several UV-active secondary metabolites in both the lipid and aqueous fractions. Both fractions were subjected to size-exclusion chromatography (Sephadex LH-20, 25 x 340 mm column, 50% (v/v) EtOAc in MeOH and further purified by silica gel flash chromatography with a gradient from hexanes to EtOAc to MeOH). Final purification by repetitive NP-HPLC (50 and 80% EtOAc in hexanes) provided nakienone A (**1**, 21.1 mg, 0.53%), the hydroquinone nakitriol (**2**, 5.9 mg, 0.15%), and a mixture of several other UV active compounds which were subsequently acetylated (Ac_2O/Pyr) and purified by NP-HPLC (25% EtOAc in hexanes) to yield nakienone B (**3**) as the peracetate derivative (**4**, 1.0 mg, 0.012%) (Figure IV.1). Additionally, an unusual rearrangement of triene **1** to a reduced diene hemiacetal **5**, was observed while obtaining initial NMR spectra of **1**.

Analysis of **1** by ^{13}C NMR and HRCIMS (195.1021; -0.01 mmu; CH_4) provided a molecular formula for $[M+H]^+$ of $C_{11}H_{15}O_3$. Examination of the IR (υ = 3650-3100, 1683 cm^{-1}), UV (λ_{max} 234 nm; log ε 4.7; EtOH), and NMR data (Tables IV.1 and IV.2) revealed the presence of two primary hydroxyl groups, a 1,1-disubstituted diene, and an α,β-unsaturated cyclopentenone moiety. With the aid of COSY (Figure IV.2 and Table IV.3) and HETCOR spectra, two distinct spin systems could be assembled (**A** and **B**; Figure IV.3). In fragment **A**, the H8 proton was allylicly coupled to the H11 protons of a primary alcohol methylene, allowing the construction of a conjugated terminal diene.

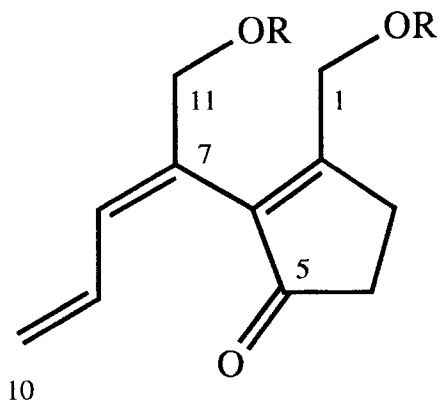

1 R = H
6 R = OAc

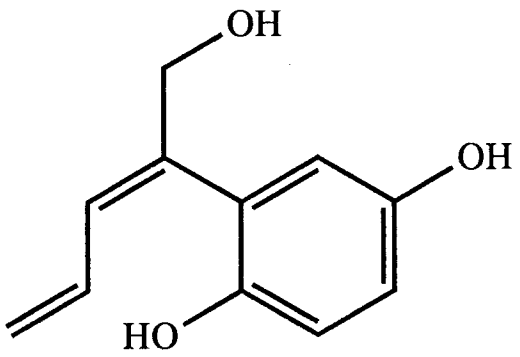

2

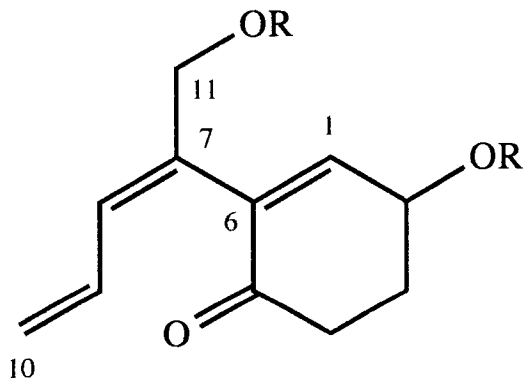

3 R = H
4 R = OAc

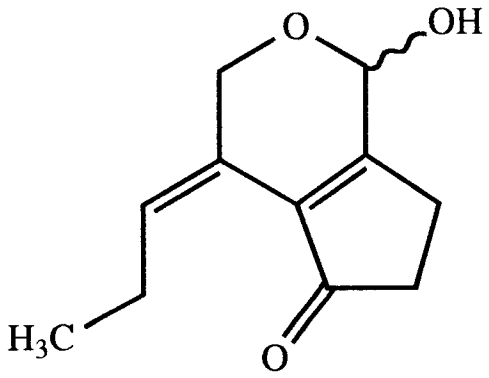

5

Figure IV.1 Structures of Nakienones A-C (**1**,**3**,**5**), Nakitriol (**2**), and Per-acetate Derivatives **4** and **6**.

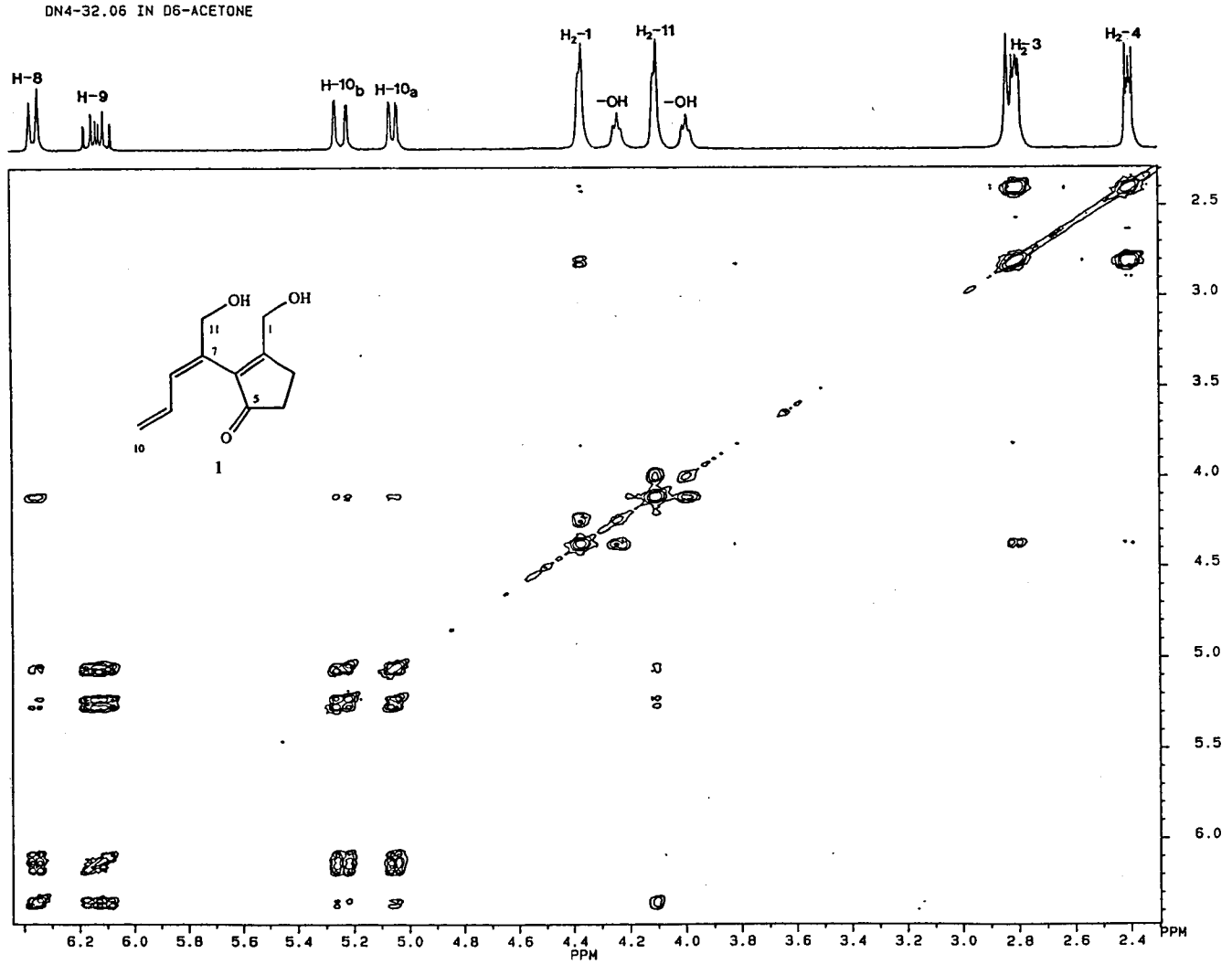

Figure IV.2 COSY Spectrum of Nakienone A (**1**).

Table IV.1 ^{1}H NMR Data for Nakienones.[a]

#C	Nakienone A (**1**)	Nakitriol (**2**)	Nakienone B per-acetate (**4**)	(**5**)
1	4.37 bd 5.0 4.24 bt 5.0 (-OH)	6.49 d 2.9	6.66 dd 2.8, 1.3	5.62 bs 3.11 m (-OH)
2	---	--- 7.71 bm (-OH)	5.64 ddd 8.8, 5.0, 2.8	---
3	2.81 m	6.65 dd 8.5, 2.9	a) 2.14 m b) 2.38 bm	a) 2.60 dt 18.8, 5.0 b) 2.78 dt 18.8, 5.2
4	2.40 m	6.72 d 8.5	a) 2.51 ddd 16.9, 11.8, 4.7 b) 2.70 dt 16.9, 5.2, 5.0	2.52 m
5	---	--- 7.71 bm (-OH)	---	---
6	---	---	---	---
7	---	---	---	---
8	6.35 bd 11.0, 1	6.43 d 11.0	6.34 bd 10.9	5.60 t 7.7
9	6.12 dt 16.9, 10.4	6.27 dt 16.9, 10.2	6.25 bddd 16.3, 10.9, 9.1	a) 2.37 m b) 2.49 m
10	a) 5.04 ddd 10.4, 1.5, 1 b) 5.24 ddd 16.9, 1.5, 1	a) 5.03 dd 10.2, 2.0 b) 5.26 dd 16.9, 2.0	a) 5.20 dd 9.1, 1.5 b) 5.34 dd 16.3, 1.5	1.03 t 7.4
11	4.10 bd 5.0 3.99 bt 5.0 (-OH)	4.31 bs	4.68 m	a) 3.92 bd 11.6 b) 4.32 bd 11.6
			2.12 s ($-OCOCH_3$) 2.04 s ($-OCOCH_3$)	

a) All spectra recorded on Bruker AC-300 or AM-400 spectrophotometers; data presented as δ, multiplicity, J in Hz. Data for **1**, **2**, and **4** were recorded in acetone-d_6 (spectra referenced to the center line of acetone-d_6 methyl pentet at 2.04 ppm). Data for **5** was obtained in $CDCl_3$ (spectra referenced to TMS at 0.0 ppm). Assignments based on ^{1}H-^{1}H COSY and ^{1}H-^{13}C XHCORR spectra.

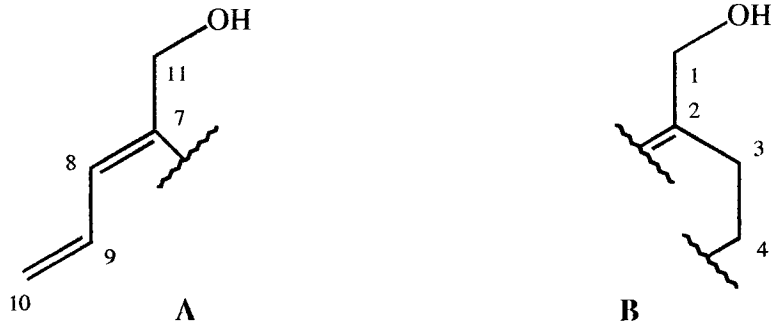

Figure IV.3 Partial Structures for Nakienone A (**1**) from COSY Spectrum.

Fragment **B** also contained a primary alcohol (H1), allylicly coupled to a methylene (H3) through a quaternary carbon. ^{1}H-^{13}C HMBC spectra placed fragment **B** in the α,β-unsaturated pentenone ring and facilitated the attachment of both spin-systems, defining the structure of nakienone A as **1** (Figure IV.1).

Table IV.2 ^{13}C NMR Data for Nakienones.[a]

#C	Nakienone A (1)	Nakitriol (2)	Nakienone B per-acetate (4)	(5)
1	61.10	118.07	146.94	91.00
2	176.94	150.87	67.97	167.30
3	27.81	116.28	28.81	25.90
4	34.92	117.59	35.40	35.29
5	207.85	148.46	196.10	204.75
6	137.46	126.97	132.69	137.49
7	136.95	141.80	137.89	122.28
8	129.46	129.87	133.02	135.85
9	134.63	135.24	132.21	23.58
10	118.15	117.87	120.72	14.24
11	65.03	67.12	67.01	66.04
			(-$OCOCH_3$) 170.24 / 20.98 170.22 / 20.88	

a) All spectra recorded on Bruker AC-300 or AM-400 spectrophotometers; data presented as δ, multiplicity. Data for **1**, **2**, and **4** were recorded in acetone-d_6 (spectra referenced to the center line of acetone-d_6 methyl heptet at 29.8 ppm). Data for **5** was obtained in $CDCl_3$ (spectra referenced to the center line of $CDCl_3$ at 77.0 ppm). Assignments based on ^{1}H-^{1}H COSY and ^{1}H-^{13}C XHCORR spectra.

The C7-C8 olefinic geometry was assigned as *E* by comparison of the C11 primary hydroxy-methylene ^{13}C NMR shift (δ 65.03 ppm, acetone-d_6; 65.82 ppm, $CDCl_3$) with both *E* (range: 65.6-66.3 ppm) and *Z* (range: 59.2-60.3 ppm) 1,1-disubstituted olefinic and dienoic model compounds (Figures IV.4 and IV.5).[146-152] The *E* configuration was confirmed by a NOESY correlation observed between the C1 acetate methyl singlet and H10b in the peracetate (Ac_2O/Pyr) derivative (**6**).

Table IV.3 ^{1}H-^{1}H and Long-Range ^{1}H-^{13}C Correlations for Nakienone A (**1**).

Proton #	^{1}H-^{1}H COSY	^{1}H-^{13}C HMBC (10 Hz)
H-1	(OH-1), H-3	C-2, C-3, C-6 or -7
(OH-1)	H-1	
H-3	H-1, H-4	C-2, C-4, C-6 or -7
H-4	H-3	C-2, C-3, C-5
H-8	H-9, H-10a, H-10b, H-11	C-6 OR -7, C-9, C-10, C-11
H-9	H-8, H-10a, H-10b	C-6 OR -7
H-10 (a)	H-8, H-9, H-10b, H-11	C-8, C-9
(b)	H-8, H-9, H-10a, H-11	C-8, C-9
H-11	(OH-1)	C-6 OR -7, C-8
(OH-11)	H-11	

Table IV.4 ^{1}H-^{1}H and Long-Range ^{1}H-^{13}C Correlations for Nakitriol (**2**).

Proton #	^{1}H-^{1}H COSY	^{1}H-^{13}C HMBC (5 Hz)
H-1	H-3	C-2, C-5, C-7
H-3	H-1, H-4	C-2, C-4, C-6
H-4	H-3	C-2, C-5, C-6, C-7
H-8	H-9, H-11	C-6
H-9	H-8, H-10a, H-10b	C-7, C-8
H-10 (a)	H-9, H-10b, H-11	C-8
(b)	H-9, H-10a, H-11	C-8, C-9
H-11	H-8, H-10a, H-10b	C-6, C-7, C-8

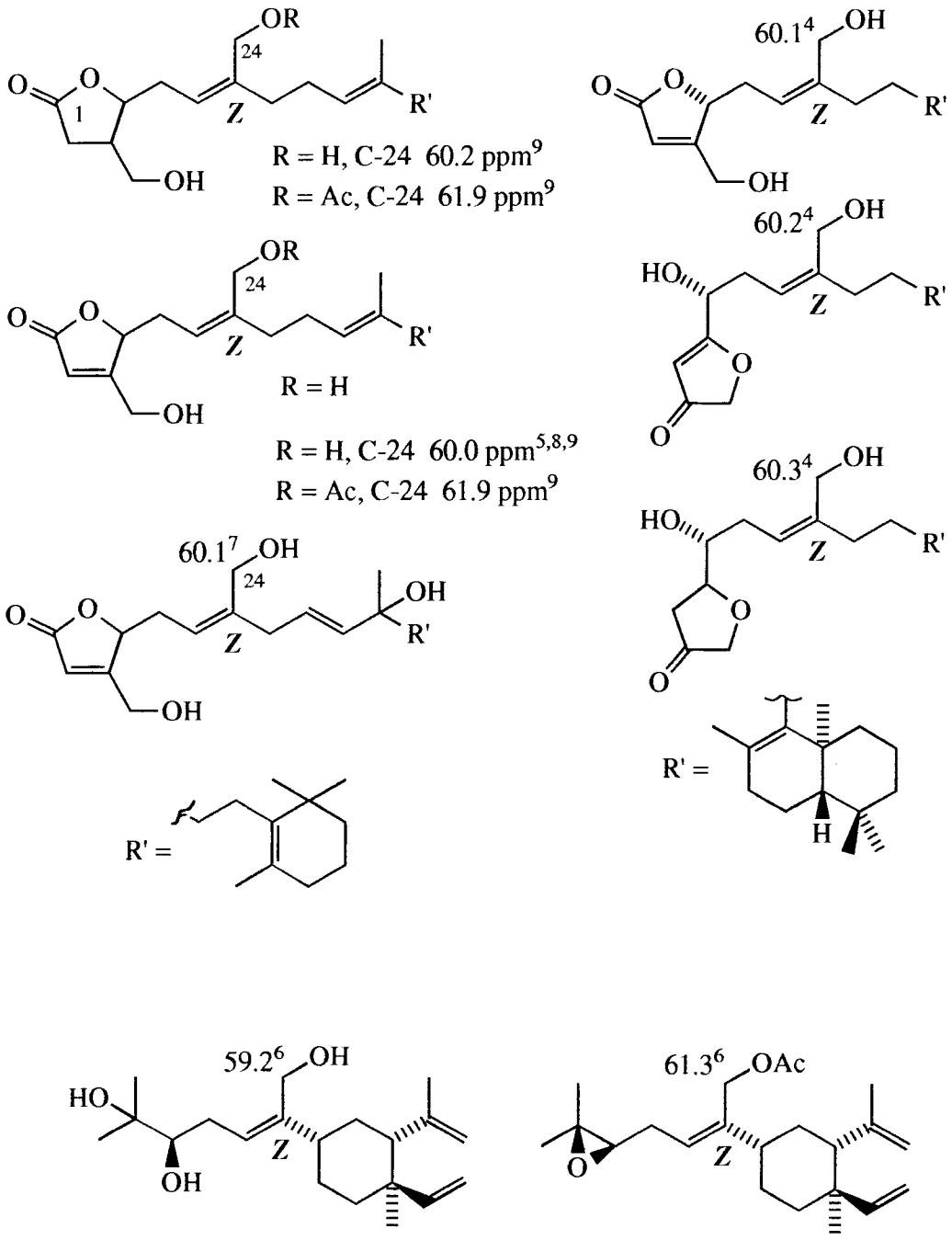

Figure IV.4 *Z*-Geometry Model Compounds Used to Deduce C7-C8 Olefin Geometry in Nakienone Series.

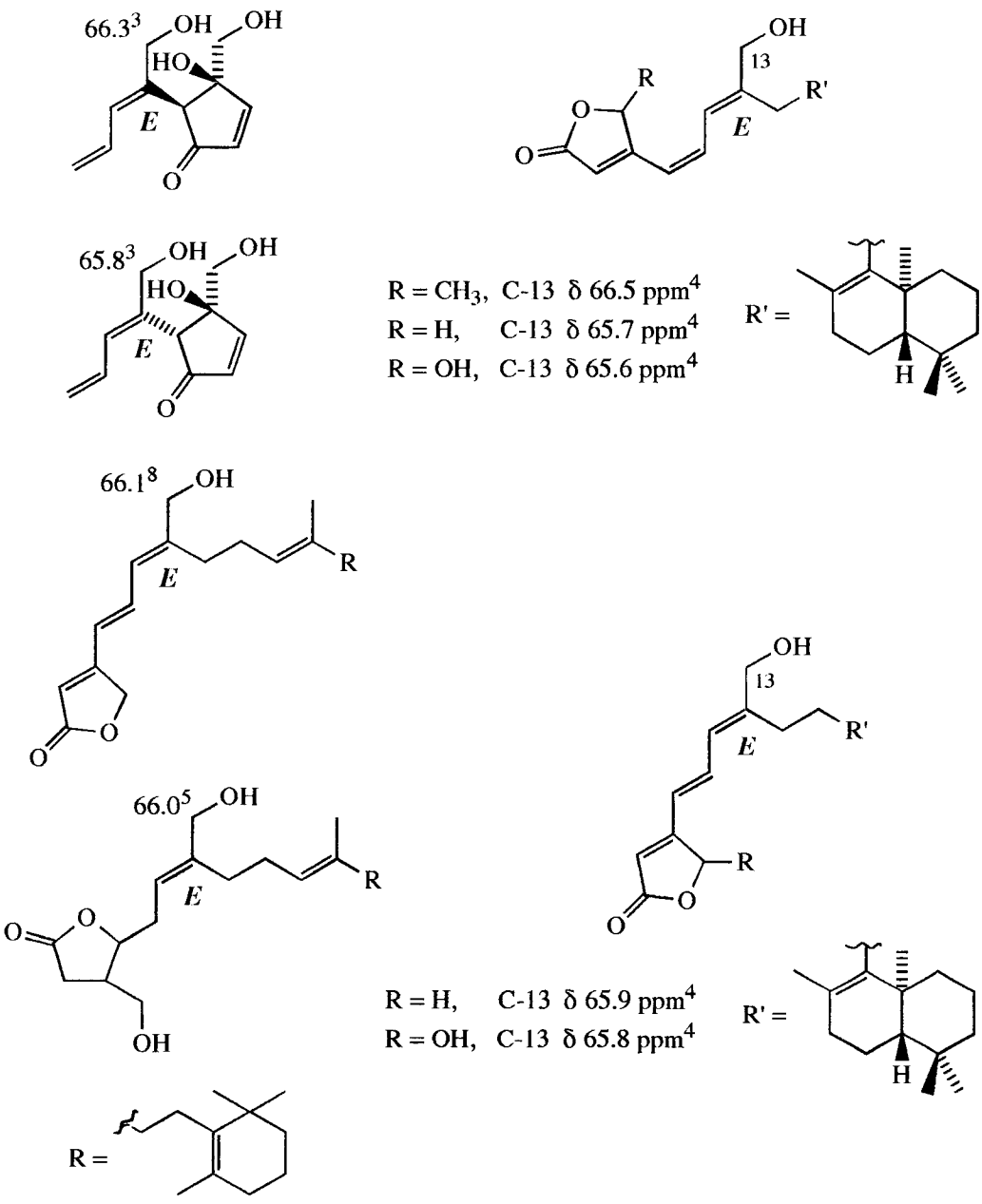

Figure IV.5 *E*- Geometry Model Compounds Used to Deduce C7-C8 Olefin Geometry in Nakienone Series.

Compound **2**, UV (λ_{max} 228, 302 nm; log ε 3.6, 4.3; MeOH), yielded a molecular formula of $C_{11}H_{12}O_3$ by HRCIMS (192.0787; 0.3 mmu; CH_4). While the ^1H and ^{13}C NMR data for **2** were analogous to that of **1** in the 1,1-disubstituted diene spin-system, the IR spectrum for **2**, unlike **1**, did not show a carbonyl stretch. Like **1**, two partial structures were defined for structure **2** by ^1H-^1H correlations from COSY spectra (**A** and **B**; Figure IV.6). An exchangeable ^1H NMR resonance (δ 7.71 bm 2H) and pair of ^{13}C's (δ 150.87 and 148.46) suggested the presence of a hydroquinone moiety. Juxtaposition of the two spin-systems was accomplished by HMBC (Table IV.4). Specifically, correlations from C7 to H1 and from C6 to H8 and H11 defined the structure of metabolite **2**, trivially named nakitriol. Similarly, an *E* configuration was assigned for the C7-C8 olefin from the ^{13}C NMR chemical shift of the C11 methylene (δ 67.12 ppm).

Per-acetate derivative **4**, $[\alpha]_D^{25} = +123^\circ$ (c = 0.11, MeOH), yielded a molecular formula of $C_{15}H_{19}O_5$ for $[M+H]^+$ by HRCIMS (279.1233; +0.1 mmu). Its ^{13}C NMR spectrum differed from that of **1** in the conspicuous absence of the cyclopentenone carbonyl resonance (δ 207. 85 ppm), which was replaced by a cyclohexenone carbonyl

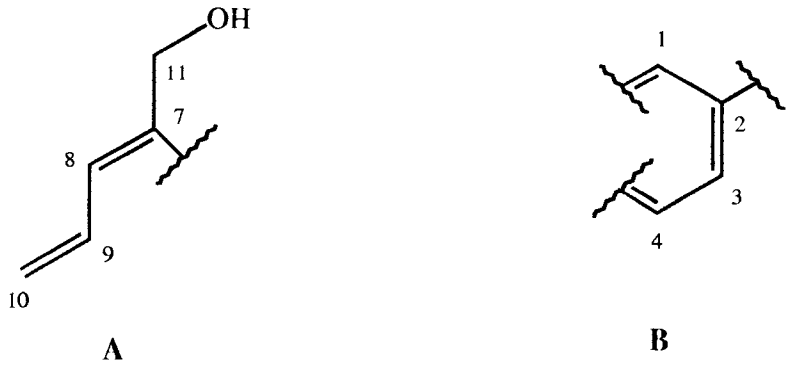

A **B**

Figure IV.6 Partial Structures for Nakitriol (**2**) from COSY Spectrum.

Table IV.5 ^{1}H-^{1}H and Long-Range ^{1}H-^{13}C Correlations for Nakienone B Diacetate (**4**).

Proton #	^{1}H-^{1}H COSY	^{1}H-^{13}C HMBC (7 Hz)
H-1	H-2, H-3b	C-3, C-5, C-6
H-2	H-1, H-3a, H-3b	C-1, (OCOC$\underline{H}_3$) or (OCOC$\underline{H}_3$)′
H-3 (a)	H-2, H-3b, H-4a, H-4b	C-4
(b)	H-2, H-3a, H-4a, H-4b	C-1, C-2, C-4, C-5
H-4 (a)	H-3a, H-3b, H-4b	C-2, C-3, C-5
(b)	H-3a, H-3b, H-4a	C-2, C-3, C-5, C-7
H-8	H-9, H-10b, H-11	C-7, C-10, C-11
H-9	H-8, H-10a, H-10b	
H-10 (a)	H-9, H-10b	
(b)	H-8, H-9, H-10a	C-8
H-11	H-8, H-10a, H-10b	C-6, C-7, (OCOC$\underline{H}_3$) or (OCOC$\underline{H}_3$)′
(OCOC$\underline{H}_3$)		(OCOC$\underline{H}_3$)′
(OCOC$\underline{H}_3$)′		(OCOC$\underline{H}_3$)

resonance at a shift of 196.10 ppm (Table IV.2). HMBC correlations from C6 to H11 and from C7 to H4a and H4b connected the 1,1-disubstituted diene to C6 of a cyclohexenone ring, thus establishing the structure of nakienone B per-acetate as **4** (Figure IV.7 and Table IV.5). An *E* geometry of the C7-C8 olefin was assigned by the C11 ^{13}C chemical shift (δ 67.01 ppm), as previously described for **1** and **2**, using peracetylated model compounds *E* (range: 68.8-69.1 ppm) and *Z* (range: 61.3-61.9 ppm) (Figures IV.5 and IV.6).[152-155] Coincidentally, examination of numerous model compounds uncovered what appears to be a discrepency in the assignment of olefinic geometry of a spatane diterpenoid derivative from the brown alga *Spatoglossum howleii* (see endnote).

Rearrangement of the triene **1** to **5** (also found in the organic extract) was observed while obtaining the initial NMR spectra of **1** in $CDCl_3$. Compound **5** possessed a UV absorbance for a dienone (λ_{max} 262 nm; log ε 4.2; MeOH), was shown

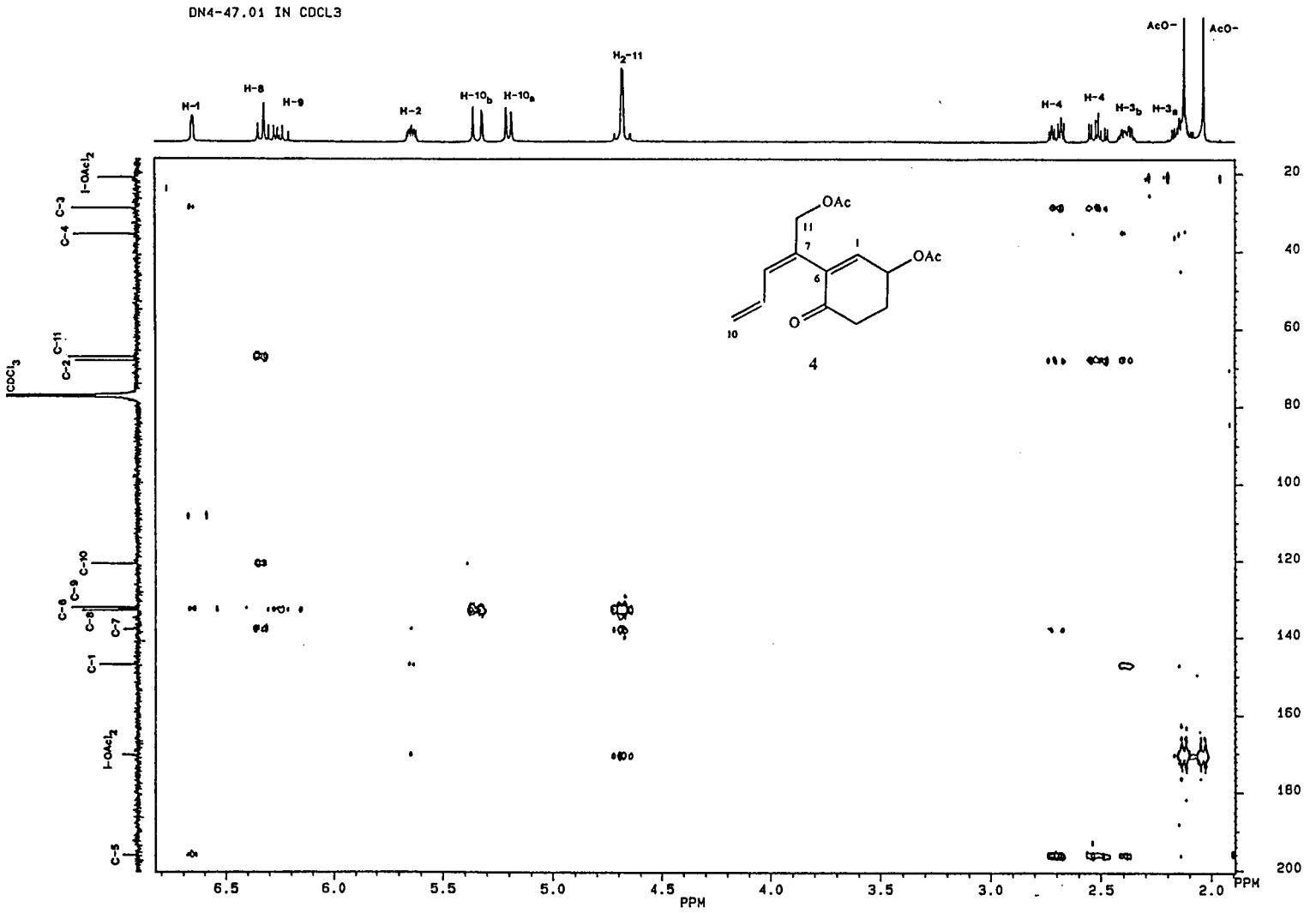

Figure IV.7 HMBC Spectrum of Nakienone B per-acetate (**4**).

to have the same molecular formula as **1** by HRCIMS ($C_{11}H_{15}O_3$; $[M+H]^+$; 95.1022; +0.1 mmu; CH_4). However, the NMR spectra of **5** was notably different from that of **1** (Tables 1 and 2). Specifically, the chemical shift of the C1 carbon now resonated at 91.00 ppm, suggestive of an hemiacetal moiety, and the olefinic methylene signal in **1** (δ 118.15 ppm) was replaced by a methyl signal at δ 14.24 (^{1}H δ 1.03). As with compounds **1**, **2**, and **4**, a 3-bond coupling from C6 to H8 as well as $^3J_{HOC}$ couplings from C1 to H11a and H11b established structure of **5** as a reduced diene hemiacetal (Table IV.6). The rearrangement of reactive **1**, presumably by an acid catalyzed mechanism (Figure IV.8), suggests a potential artifactual origin for **5** as obtained from the crude lipid extract.

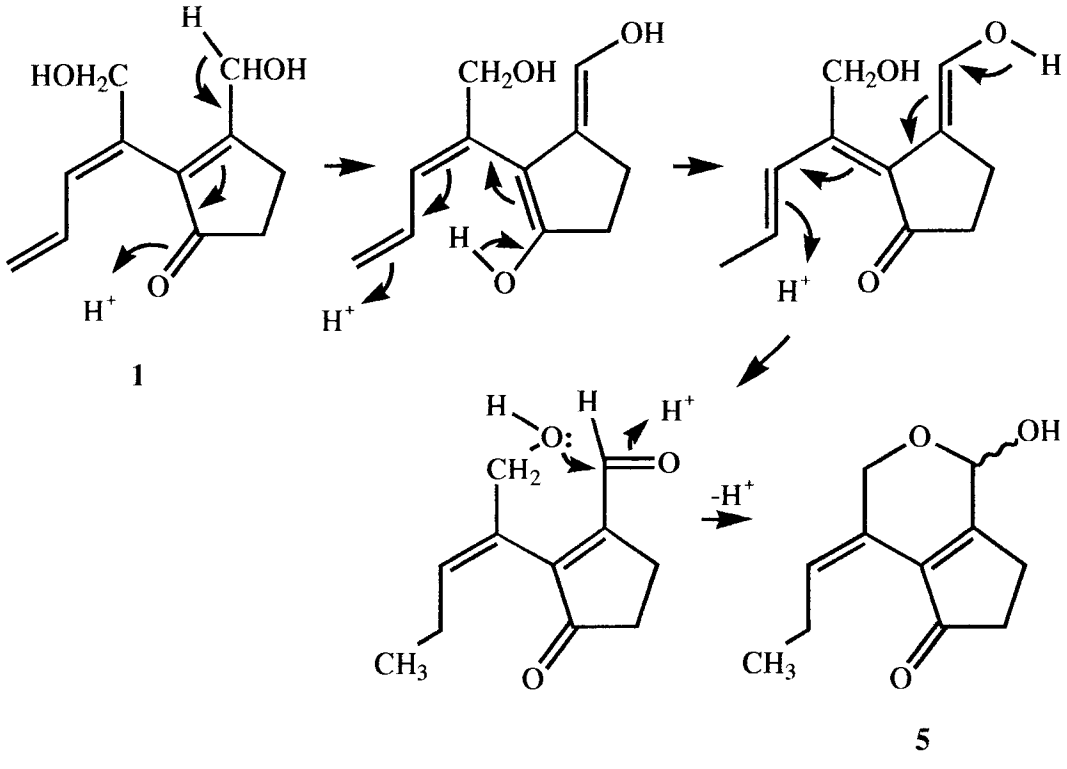

Figure IV.8 Proposed Acid-Catalyzed Rearrangement of Nakienone A (**1**) to Compound **5**.

Table IV.6 ^{1}H-^{1}H and Long-Range ^{1}H-^{13}C Correlations for **5**.

Proton #	^{1}H-^{1}H COSY	^{1}H-^{13}C HMBC (10 Hz)
H-1	(OH-1), H-11a, H-11b	C-6, C-11
(OH-1)	H-1	
H-3 (a)	H-3b, H-4	C-2, C-4, C-5, C-6
(b)	H-3a, H-4	C-2, C-4, C-6
H-4	H-3a, H-3b	C-2, C-3, C-5
H-8	H-9a, H-9b	C-9, C-10
H-9 (a)	H-8, H-9b, H-10	C-7, C-8, C-10
(b)	H-8, H-9a, H-10	C-7, C-8, C-10
H-10	H-9a, H-9b	C-8, C-9
H-11 (a)	H-1, H-11b	C-1, C-7, C-8
(b)	H-1, H-9b, H-11	C-1, C-7, C-8

Both **1** and the rearrangement product **5** are structurally similar to the cytotoxins didemnenones A-D (**7**-**10**, Figure IV.9), isolated from *Didemnum* and *Tridemnum* spp. Both of these ascidians have been reported to harbor unicellular algal symbionts.[146,156] Additionally, the antimicrobial bromophenolic compound aplysinadiene (**11**, Figure IV.9), isolated from the marine sponge *Aplysina aerophoba,* is remarkably similar in structure to nakienone B (**2**) and nakitriol (**3**).[157] The occurrence of these and other related metabolites[158] suggests that symbiotic cyanobacteria may be involved in the production of these compounds in marine invertebrates. To date, three microalgae have been cultured from the original algal infected coral tips.[156]

Nakienone A (**1**) was determined to be cytotoxic to both KB (human epidermoid carcinoma) and HCT 116 (colonic carcinoma) cell lines, with LD_{50}'s of ca. 5 and 20 μg/ml, respectively. Additionally, **2** was shown to be weakly and nonselectively cytotoxic to DNA repair defective cell lines EM9 (topoisomerase I sensitive Chinese

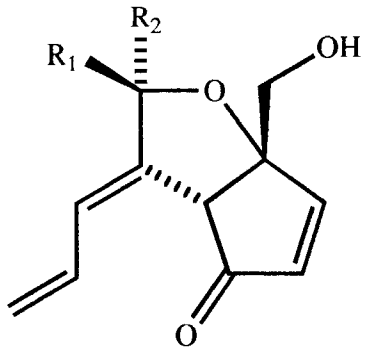

didemnenone A (**7**)
$R_1 = H$, $R_2 = OH$

didemnenone B (**8**)
$R_1 = OH$, $R_1 = H$

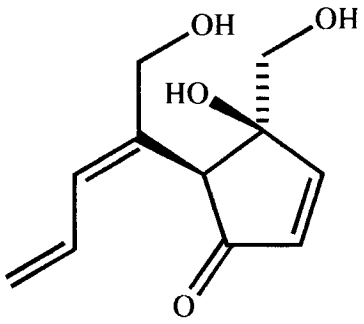

didemnenone C (**9**)

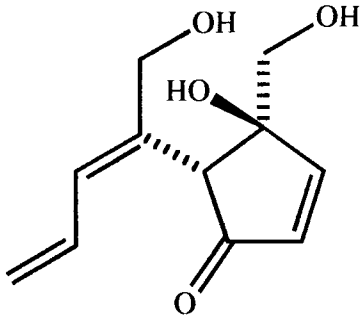

didemnenone D (**10**)

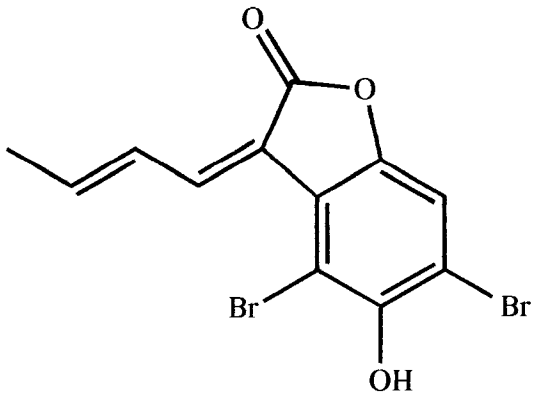

aplysinadiene (**11**)

Figure IV.9 Didemnenones A-D (**7-10**) and Aplysnadiene (**11**).

hamster ovary line), XRS-6 (topoisomerase II sensitive), UV20 (DNA cross-linking agent sensitive), and BR1 (DNA repair competent) cell lines, LD_{50}'s ca. 20 μg/mL. Cytotoxic properties associated with this entire class of chemistry may be due, at least in part, to the presence of activated α,β-unsaturated ketone moieties, acting as Michael acceptors for 1,4- or 1,6-additions.

Experimental

General Methods. UV spectra were recorded on a Hewlett Packard 8452A diode array spectrophotometer and IR spectra were recorded on a Nicolet 510 FT-IR spectrometer. Low resolution mass spectra were obtained on either a Varian MAT CH7 spectrometer or by GC-MS using a Hewlett Packard 5890 Series II gas chromatograph and a 5971 mass selective detector. HRMS were obtained on a Kratos MS 50 TC. HPLC was performed using a M-6000 pump, U6K injector, and either a R401 differential refractometer or a lambda-Max 480 lc spectrophotometer. NMR data were obtained on either Bruker AC 300 or Bruker AM 400 spectrometers. TLC-grade (10-40 μm) silica gel was used for vacuum chromatography and Kieselgel 60 silica (40-63 μm) was used for flash chromatography .

Nakienone A (**1**). FTIR ν_{max}^{film} cm^{-1}: 3367, 2925, 1687, 1683, 1435, 1286, 1154, 1114, 1056, 994, 915; UV λ_{max}^{EtOH} nm: 234 (log ε = 4.7). CIMS (CH_4, positive ion) $[M+H]^+$ *m/z* 195 (30), $[M+H - H_2O]^+$ 177 (100), $[M+H - 2(H_2O)]^+$ 159 (54), 149 (15); HR CIMS (CH_4, positive ion) $[M+H]^+$ at 195.1021 calc for $C_{11}H_{15}O_3$ 195.1021.

Nakienone A Diacetate Derivative (**6**). GC-EIMS (70 eV) $[M - AcOH]^+$ *m/z* 278 (3), 236 (5), 218 (2), 194 (2), 176 (100), 161 (45), 147 (42), 133 (53), 115 (16), 105 (32), 91 (41), 77 (15), 65 (6), 55 (7);

Nakitriol (**2**). FTIR ν_{max}^{film} cm^{-1}: 3309. 1496, 1490, 1447, 1199, 787; UV λ_{max}^{MeOH}nm: 228, 302 (log ε = 4.3, 3.6); CIMS (CH_4, positive ion) $[M+H]^+$ *m/z* 193 (22), $[M+H - H_2O]^+$ 175 (100); HR CIMS (CH_4, positive ion) $[M+H]^+$ at 192.0787 calc for $C_{11}H_{12}O_3$ 192.0786.

Nakienone B Diacetate Derivative **4**. FTIR ν_{max}^{film} cm^{-1}: 1739, 1738, 1684, 1374, 1230, 1045, 1022, 995, 911; $[\alpha]_D^{25}$ +123° (*c* 0.11, MeOH); GC-EIMS (70 eV) $[M - AcOH]^+$ *m/z* 218 (27), 176 (100), 158 (60), 157 (65), 147 (62), 129 (28), 115 (15), 91 (38), 57 (19); CIMS (CH_4, positive ion) $[M+H]^+$ *m/z* 279 (4), $[M+H - AcOH]^+$ 219 (12), $[M+H - (AcOH)_2]^+$ 259 (100); HR CIMS (CH_4, positive ion) $[M+H]^+$ at 279.1233 calc for $C_{15}H_{19}O_5$ 279.1232.

Compound **5**. FTIR ν_{max}^{film} cm^{-1}: 3368, 2967, 2930, 2872, 1702, 1693, 1437, 1401, 1141, 1101, 1080, 1038, 987, 963; UV λ_{max}^{MeOH}nm: 262 (log ε = 4.2); CIMS (CH_4, positive ion) $[M+H]^+$ *m/z* 195 (86), $[M+H - H_2O]^+$ 177 (100), 149 (37); HR CIMS (CH_4, positive ion) $[M+H]^+$ at 195.1022 calc for $C_{11}H_{15}O_3$ 195.1021.

Endnote

The *Z* geometry of the C13-C15 olefin in the spatane tetraol (**1 2**) and its per-acetate derivative (**1 3**) (Figure V.10) were assigned solely upon negative data from nOe experiments.[159] Specifically, the lack of H15 nOe enhancement when the C14 methylene was irradiated was used as the basis for the assignment. The ^{13}C chemical shift of the C14 methylene (δ 68.4 ppm) falls significantly outside the range observed for acetylated primary vinylic alcohols on *Z* olefins (δ 61.3-61.9 ppm).[152-155] However, this chemical shift fits perfectly within the range for *E* geometry models (range: 68.8-69.1 ppm) (Figures IV.5 and IV.6).[152-155] I therefore suggest the true structure of this derivative and the corresponding natural product from which it was prepared to be **1 4** and **1 5**, respectively.

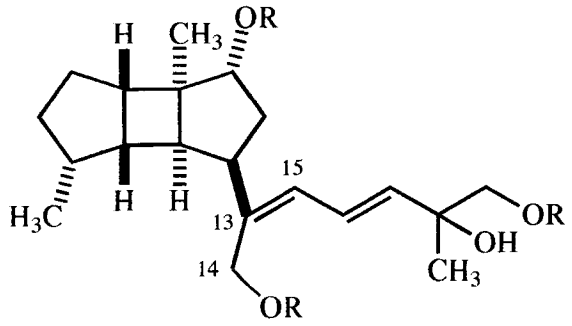

12 R = H
13 R = Ac

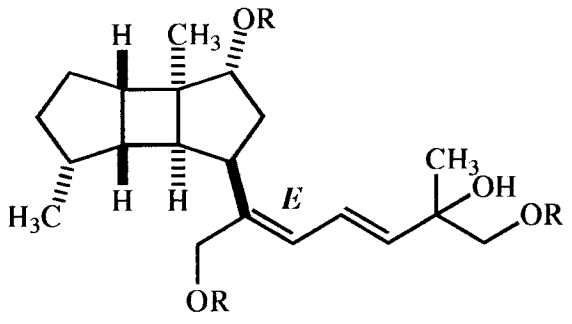

14 R = H
15 R = Ac

Figure IV.10 Original (**12** and **13**) and revised (**14** and **15**) structures of *Spatoglossum howleii* compounds.

CHAPTER V.

BIOLOGICALLY ACTIVE NEW COMPOUNDS FROM *LYNGBYA MAJUSCULA*

Abstract

A survey of marine algae for their biomedical potential has led to the discovery of a chemically rich strain of cyanobacteria with diverse biological properties. Bioassay-guided fractionation of the organic extract of a Curaçao *Lyngbya majuscula* organic extract led to the isolation of an extremely potent brine shrimp toxin with antiproliferative activity. The structure of this new thiazoline ring-containing lipid, curacin A, was deduced from spectroscopic information. NOe data and ^{1}H NMR coupling constants were used to deduce the geometry of three olefins and relative stereochemistry of a cyclopropyl ring. The complete relative and absolute configuration of curacin A was determined by comparison of products obtained from chemical degradation of the natural product with the same substances prepared by synthesis. Curacin A was shown to have a 2*R*, 13*R*, 19*R*, 21*S* absolute configuration. Curacin A is an antimitotic agent (IC_{50} values in 3 cell lines ranging from 7 to 200 nM) that inhibits microtubule assembly and the binding of colchicine to tubulin. A mixed polyketide-amino acid (cysteine) biogenesis, analogous to ceramide biosynthesis, is hypothesized. In addition to curacin A, a potent new ichthyotoxic depsipeptide (antillatoxin), a new malyngamide derivative, and an unusual molluscicidal compound have been isolated from this alga.

Introduction

Cyanobacteria (blue-green algae) are recognized as a rich source of unusual toxins[160] and biologically active lead compounds.[21] Cyanobacterial hepatotoxins represent a worldwide health problem due to algal bloom contamination of water supplies.[161] Microcystins, a large group of cyclic heptapeptides, have been isolated from numerous *Microcystis*, *Anabaena*, *Oscillatoria*, and *Nostoc* species.[160] Nodularins are cyclic pentapeptides which until recently were known only from various *Nodularia* spp.[162,163] The nodularins and microcystins act as potent hepatotoxins by inhibiting protein phosphatases 1 and 2.[164] Microcystin-LR (**1**, Figure V.1), the most common microcystin peptide, displays an LD_{50} of 50 μg/kg in mice.[165] Motuporin (**2**) is a new nodularin derivative which was recently been isolated from the sponge *Theonella swinhoei*.[166] This discovery suggests the possibility that **2** may ultimately be derived from symbiotic cyanobacteria or other microorganisms associated with this marine invertebrate. Recently, *Microcystis aeruginosa* has been shown to simultaneously produce a series of depsipeptides called aeruginopepsins (ie. aeruginopepsin 917S-A, **3**), which appear to enhance the toxic effects of microcystins.[167] Another potent hepatotoxin, cylindrospermopsin (**4**), has been isolated from an Australian *Cylindrospermopsis raciborskii* (Woloszynska) culture which was obtained following an outbreak of hepatoenteritis on Palm Island in northern Queensland.[168] Two small neurotoxic compounds, anatoxin-a (**5**, Figure V.2) and anatoxin-a(s) (**6**) have been characterized from several *Anabaena* spp.[169-171] Numerous animal poisonings have been correlated to *Anabaena* blooms.

Lyngbya mujuscula, a cyanobacterium responsible for an inflammatory condition known as "swimmer's itch," has been demonstrated to produce a diversity of biologically active compounds.[172] Both lyngbyatoxin A (**7**) and debromoaplysiatoxin

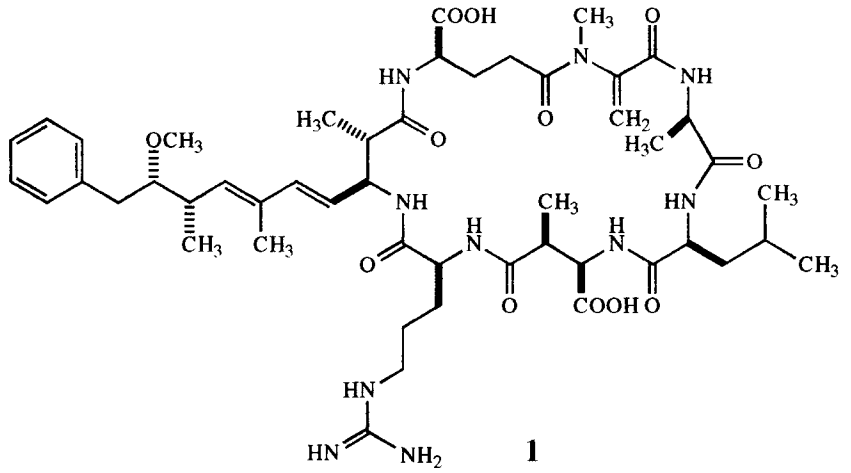

1

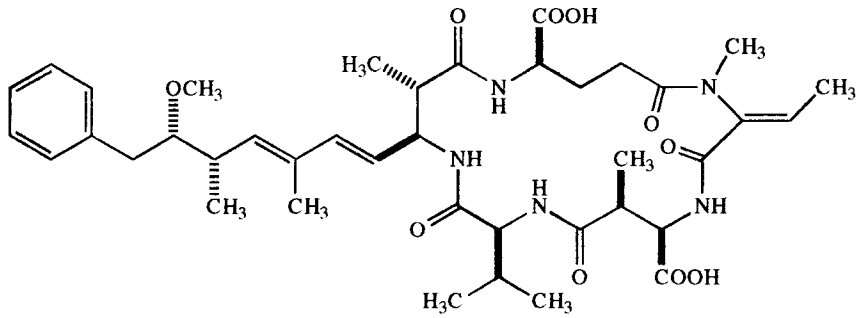

2

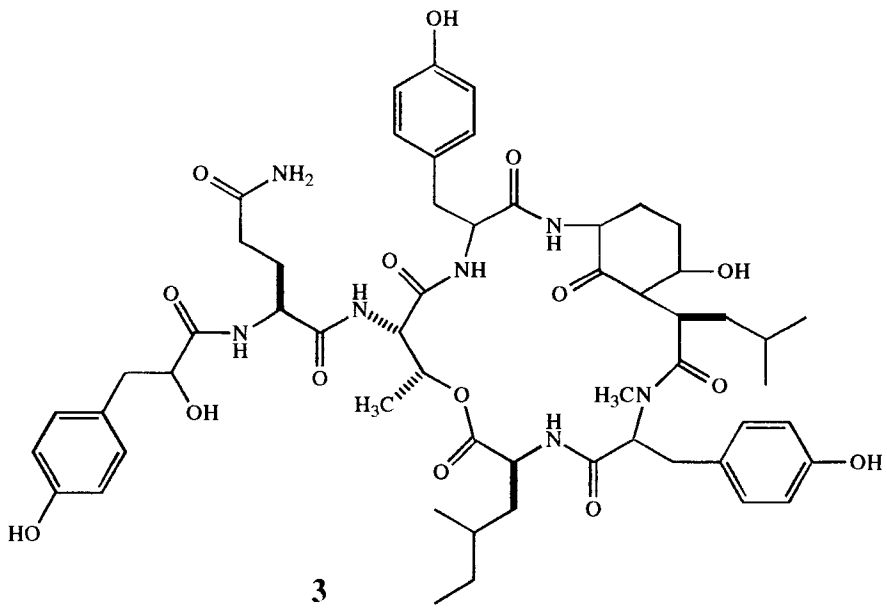

3

Figure V.1 Structures of Microcystin -LR (**1**), Motuporin (**2**), and Aeruginopepsin 917S-A (**3**).

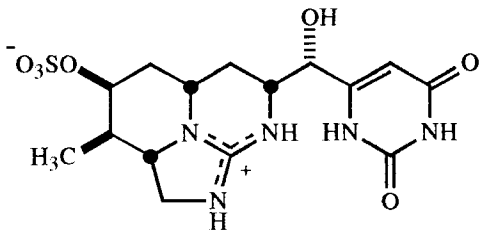

4

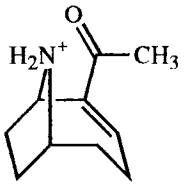

5

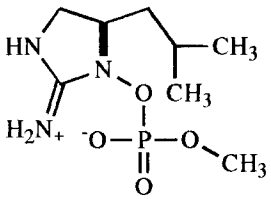

6

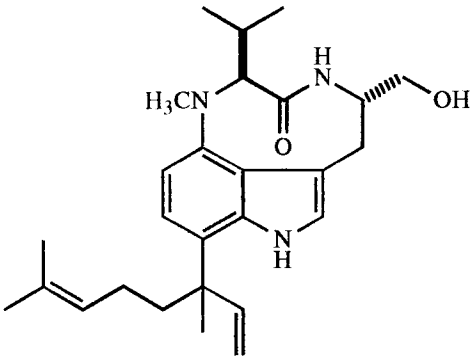

7

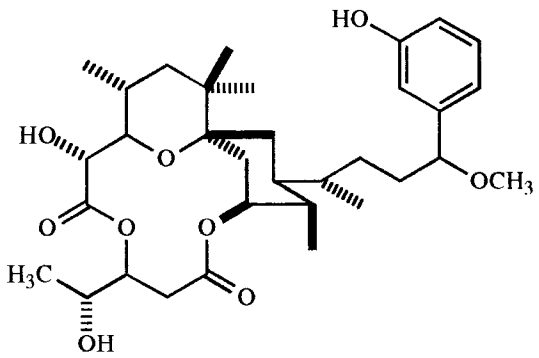

8

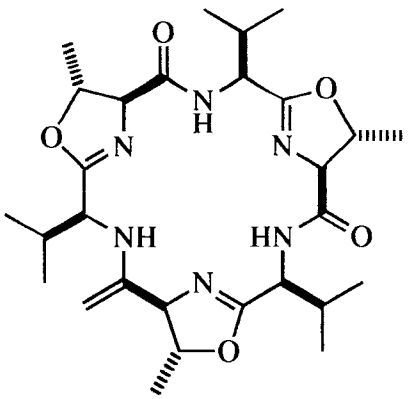

9

Figure V.2 Structures of Neuotoxic and Cytotoxic Compounds From Cyanobacteria.

(**8**) (Figure V.2), pro-inflammatory cytotoxins which are now used as biochemical tools, were first isolated from Hawaiian collections of this organism.[173,174]

Westiellamide (**9**, Figure V.3), a cytotoxic cyclic peptide has recently been isolated from *Westiellopsis prolifica* (Stigonemataceae).[175] The porphyrin-containing *Tolypothrix nodosa* compound tolyporphrin (**10**) potentiates the antimitotic activity of vinca alkaloids.[176] *Tolypothrix*, *Scytonema*, and *Cylindrospermum* species have been shown to contain cytostatic antimitotic metabolites called sytophycins.[177-180] Spurred by selective antitumor activity *in vitro*, one of the scytophycins, tolytoxin (**11**) is currently under investigation as a potential new anticancer agent.[21,181]

Borophycin (**12**), a boron-containing cytotoxin, has recently been isolated from a marine strain of *Nostoc linckia* (Roth).[182] While **12** was potently cytotoxic to two human tumor cell lines in vitro (LoVo: MIC 0.066 μg/mL; KB: MIC 3.3 μg/mL), it showed no tumor selectivity.

Our survey of marine algae for biomedical potential (Chapter 2) has resulted in the identification of several structurally diverse cytotoxic substances from microalgal sources. Hormothamnin A (**13**), isolated from a northern Puerto Rican collection of *Hormothamnion enteromorphoides* Grunow, was found to be potently antimicrobial to *Bacillus subtilus* and cytotoxic to several cancer cell lines (Figure V.4).[183] Caribbean collections of the cryptophyte *Chysophaeum taylori*, which were tentatively misidentified as *H. enteromorphoides*, were found to contain two closely related cytotoxic styrylchromones, hormothamnione A (**14**) and 6-desmethoxyhormothamnione A (**15**).[184,185] Compound **14** was shown to possess pronounced cytotoxic activity toward both lymphocytic and promyelocytic leukemia cell lines. Additionally, **15** has recently been selected for *in vivo* antitumor evaluation at the National Cancer Institute.

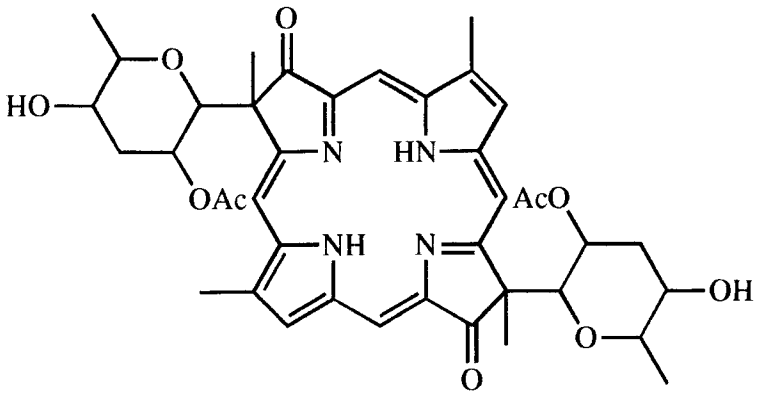

10

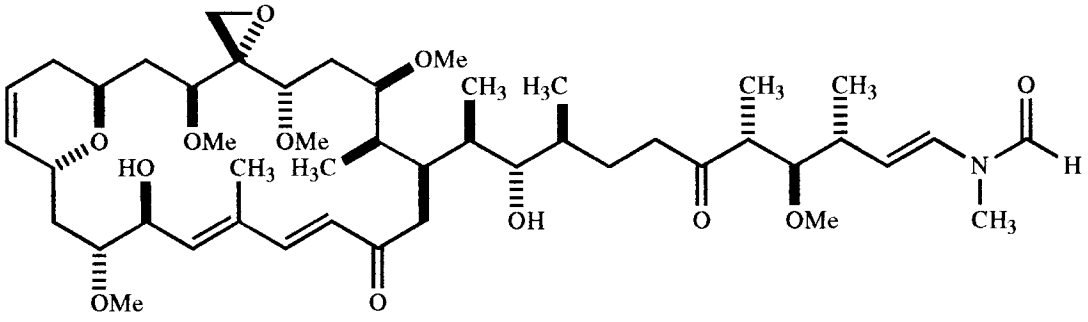

11

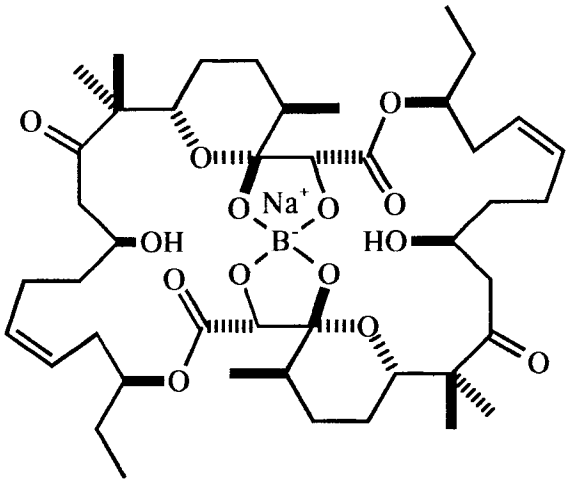

12

Figure V.3 Structures of Westiellamide (**10**), Tolytoxin (**11**), and Borophycin (**12**).

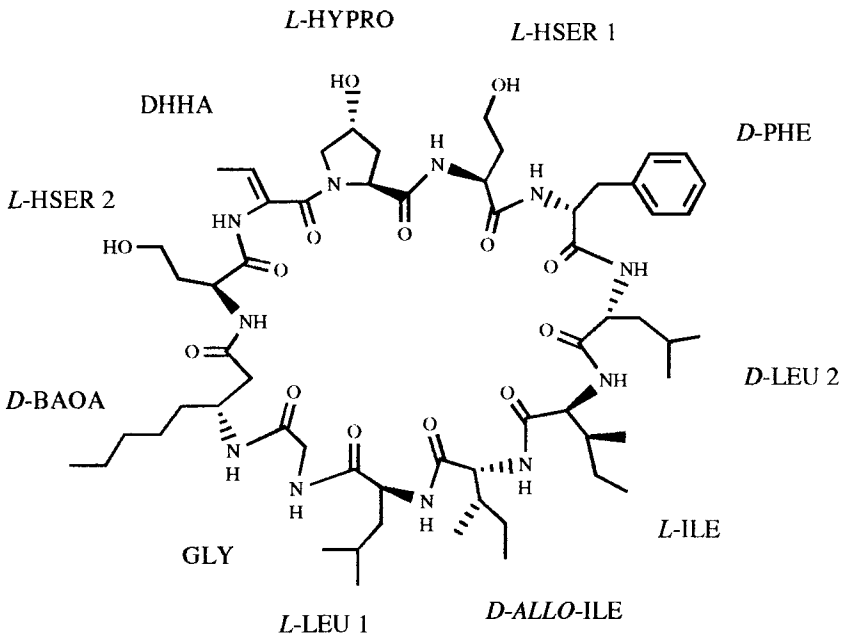

HORMOTHAMNIN A (13)

SW 1271 human lung	IC_{50} = 0.20 µg/ml
A 549 human lung	IC_{50} = 0.16 µg/ml
B16-F10 murine melanoma	IC_{50} = 0.13 µg/ml
HCT-116 human colon	IC_{50} = 0.72 µg/ml

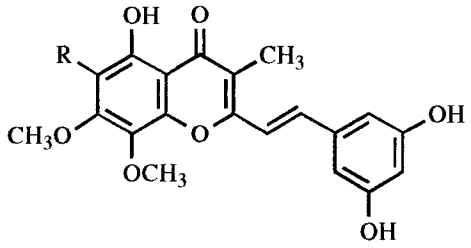

R = OCH_3 HORMOTHAMNIONE A (14)

P-388 lymphocytic leukemia	ID_{50} = 4.6 ng/ml
HL-60 promyelocytic leukemia	ID_{50} = 0.1 ng/ml

R = H DESMETHOXYHORMOTHAMNIONE A (15)

9 KB cells LD_{50} = 1 µg/ml

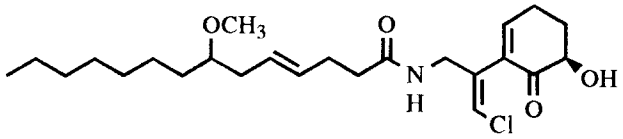

MALYNGAMIDE D (16)

KB cells ID_{50} < 30 µg/ml

Figure V.4 Biologically Active Metabolites From Microalgae Screening Efforts at the OSU College of Pharmacy.

Extracts of *Lyngbya majuscula* collected from shallow mangrove branches in Puerto Rico were found to be antimicrobial toward pathogenic bacteria *in vitro*. The most active antibacterial substance in the extract was found to be elemental sulphur; however, the mildly cytotoxic compound malyngamide D (**16**) was also isolated (Figure V.4).[186]

As with cyanobacteria and the cryptophyte *Chysophaeum taylori* the examination of other microalgae has provided valuable lead compounds for anticancer research. Cultures of the cryptophyte *Poteriochromonas malhamensis* were found to contain compounds which have been shown to inhibit the cancer-linked enzyme protein tyrosine kinase (PTK) *in vitro*. An unusual chlorinated enol sulfate derivative, malhamensilipin A (**17**, Figure V.5), was subsequently isolated and demonstrated to possess PTK activity ($pp60^{v\text{-}src}$ PTK, $IC_{50} = 35\ \mu M$).[187]

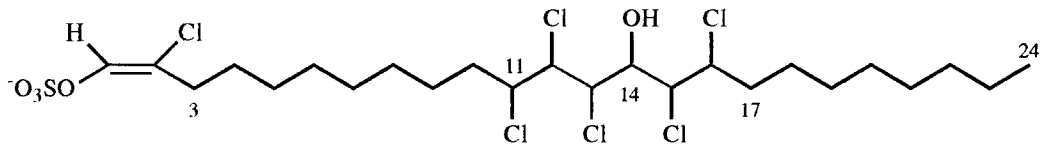

Figure V.5 Structure of Malhamensilipin A (**17**).

Results and Discussion

My anticancer drug discovery efforts have focussed on a Caribbean collection of the cyanobacterium *Lyngbya majuscula* which was strongly cytotoxic against a monkey Vero cell line (ATCC CCL81) (work initiated by Dr. Gerwick). Subsequent evaluation in the National Cancer Institute 60-cell line assay uncovered a potent antiproliferative and cytotoxic activity showing some selectivity for colon, renal and breast cancer-derived cell lines (Figure V.6). The NCI 60-cell line assay was not available for

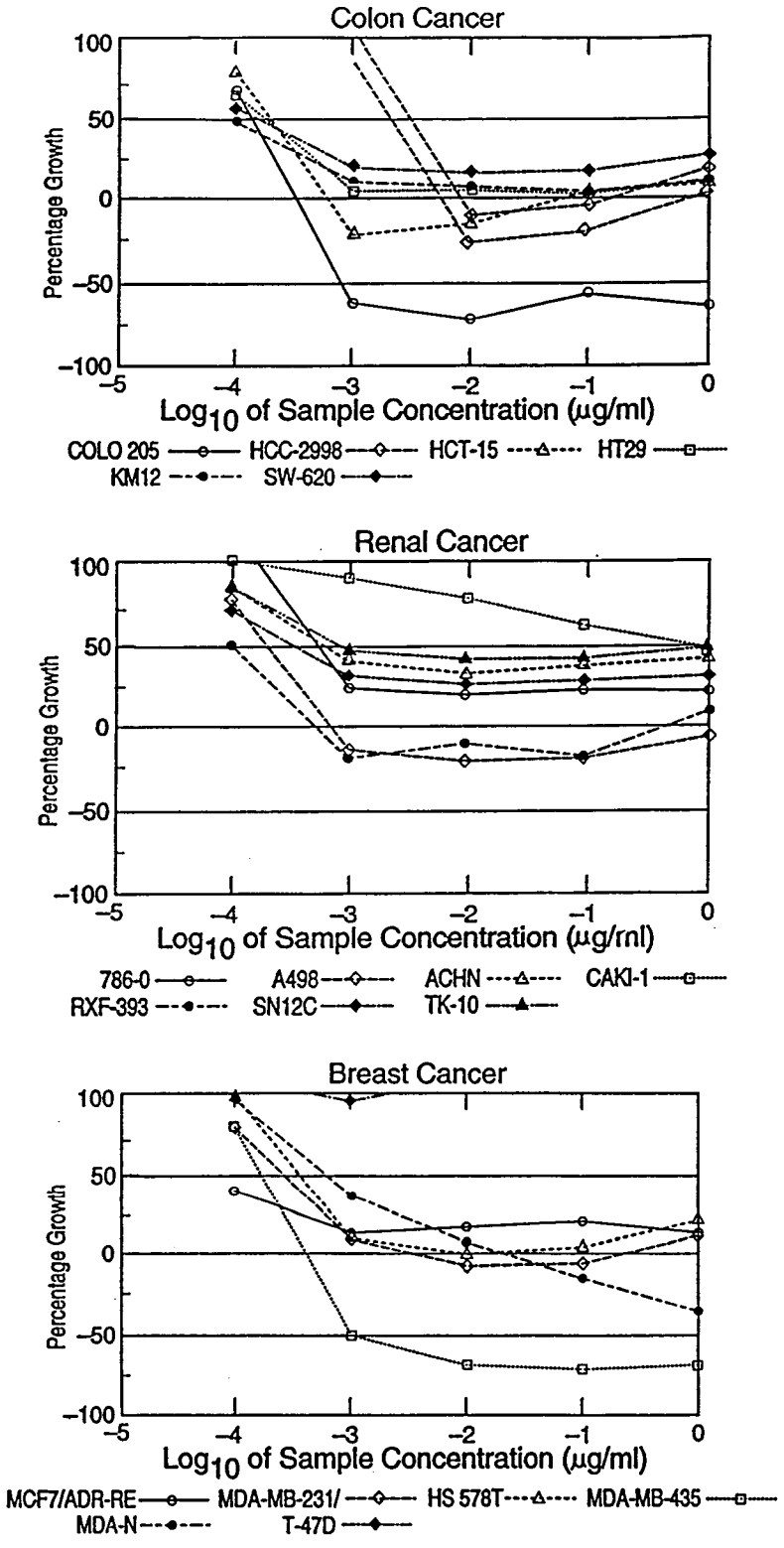

Figure V.6 NCI 60-Cell Line Tumor Growth Inhibition Dose Response Curves for Curacin A (**18**).

evaluating our fractionation, however the extract was also highly toxic to brine shrimp (LC_{50} = 25 ng/mL, Figure V.7a).[98] Using the brine shrimp assay to guide fractionation, a unique metabolite curacin A (**18**, Figures V.7b and V.8), isolated as 8-10% of the crude extract, was found to be responsible for the potent brine shrimp toxicity (LC_{50} = 3 ng/mL, Figure V.7) and mammalian cell antiproliferative activity (IC_{50} = 6.8 ng/mL in the Chinese hamster Aux B1 cell line).[188]

Isopropanol preserved *L. majuscula* was extracted with $CHCl_3$/MeOH (2:1). Gradient vacuum chromatography of the crude extract (543 mg portion) gave **18** contaminated by free fatty acids. After confirming (^{1}H NMR, GC-MS, brine shrimp toxicity) that the bioactive component was unreactive to CH_2N_2, this fraction was methylated and further purified by HPLC to yield 44.2 mg of **18** showing $[\alpha]_D$ = +86° (*c* = 0.64, $CHCl_3$). High resolution FAB MS (positive ion, 3-nitrobenzyl alcohol) gave a major $[M+H]^+$ ion at *m/z* 374.2520 analyzing for $C_{23}H_{36}NOS$ (0.3 mamu dev.). The formula $C_{23}H_{35}NOS$ suggested that curacin A possessed seven degrees of unsaturation, five of which were due to double bonds and two due to rings.

Data from ^{1}H-^{1}H COSY and ^{1}H-^{13}C HETCOR were used to generate three partial structures (**a**-**c**) for **18**. Partial structure **a** contained a monosubstituted terminal olefin adjacent to a methylene group (Figures V.9 and V.10). Neighboring this methylene was a deshielded methine which was shown by HMBC to bear an OMe group (Figure V.11). Sequential ^{1}H-^{1}H correlations placed two consecutive methylene groups contiguous to this deshielded methine, the latter of which was adjacent to a quaternary carbon, concluding partial structure **a**. Partial structure **b** possessed a terminal methylene group bearing a heteroatom which was adjacent to a methine carbon also bearing a heteroatom. This latter resonance coupled to an olefin proton at δ 5.69, which was in turn coupled by 10.7 Hz to its olefinic partner. Two methylene groups

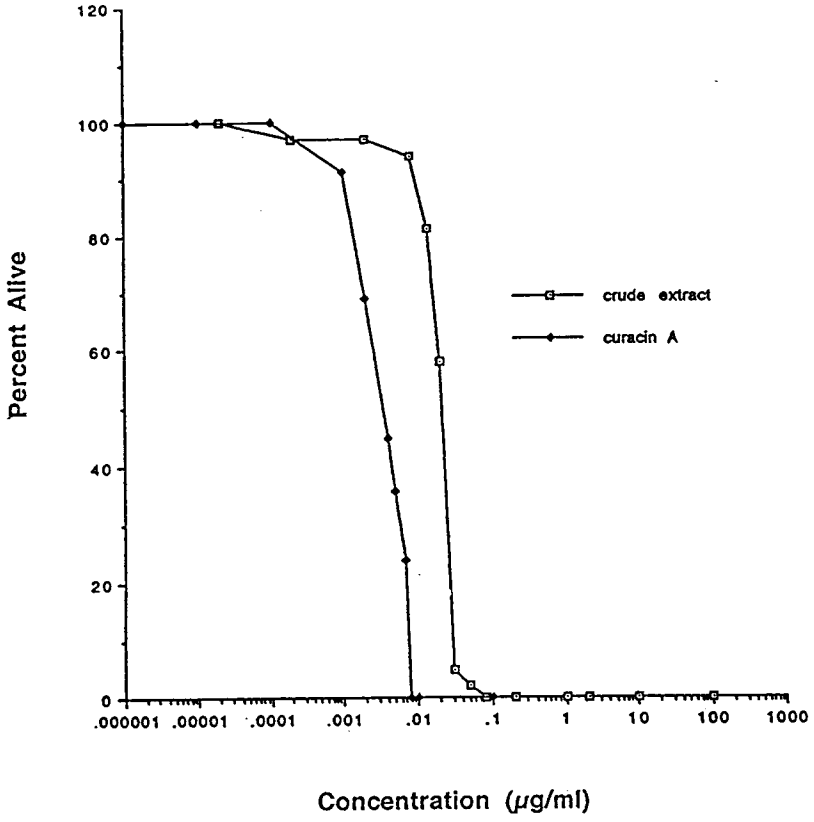

Figure V.7a Dose-Response Curves for *L. Majuscula* Crude Extract and Pure Curacin A in Brine Shrimp Lethality Assay.

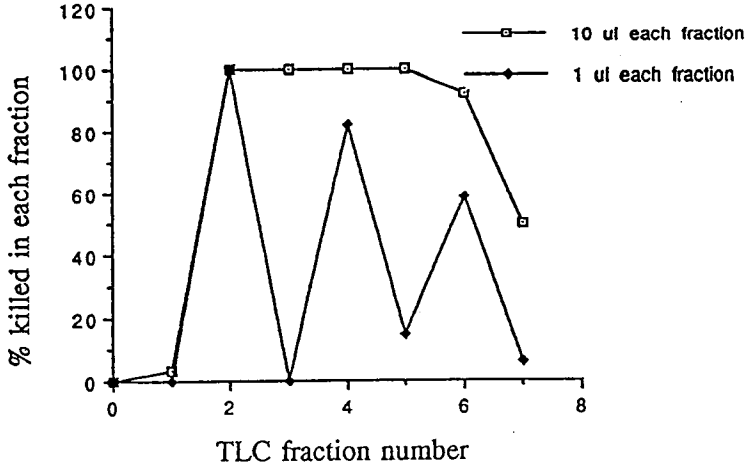

Figure V.7b Evaluation of TLC Fractions for Brine Shrimp Toxicity.

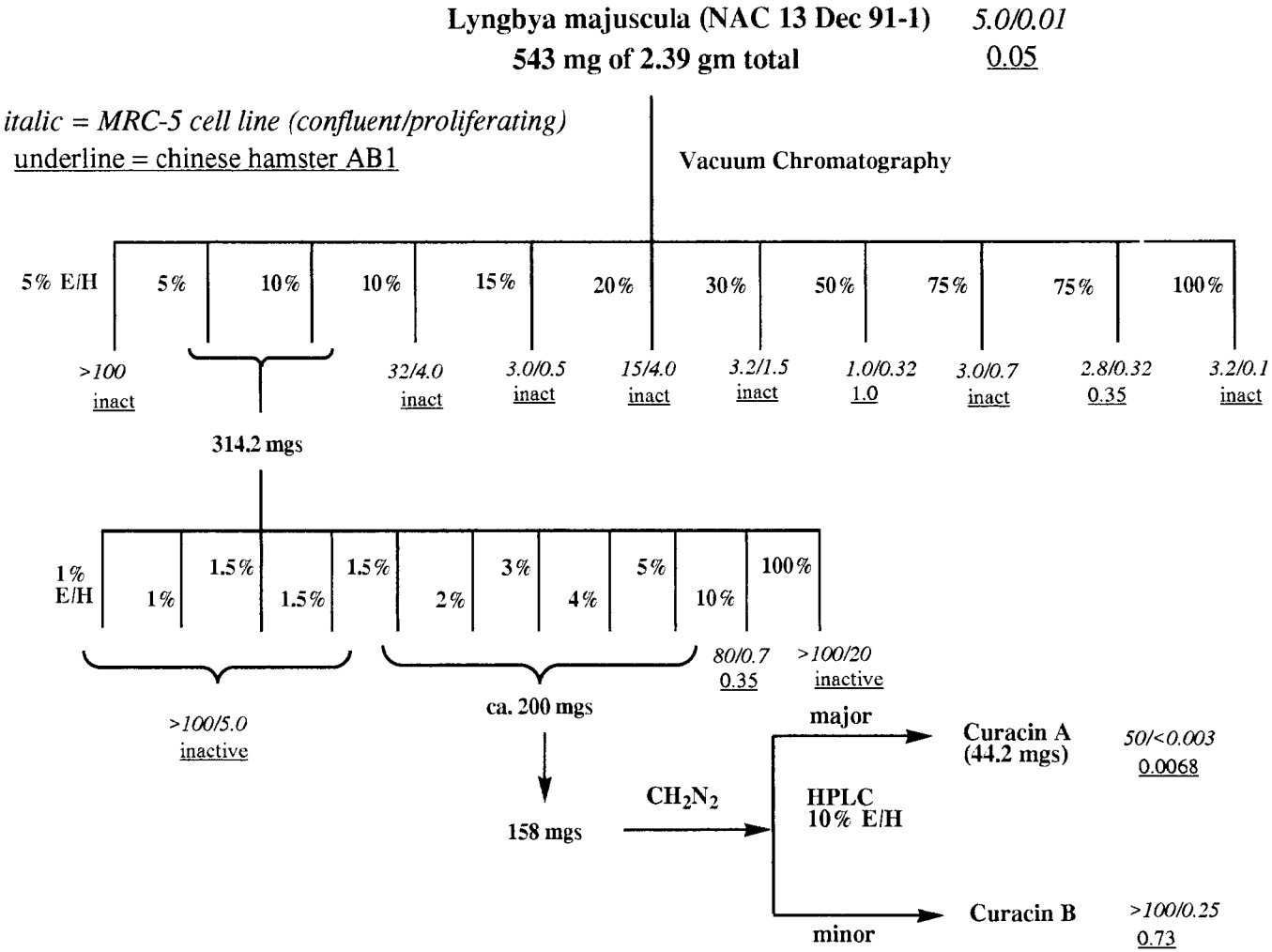

Figure V.8 Antiproliferative and Cytotoxic Activities of Brine Shrimp Toxic *L. majuscula* Fractions.

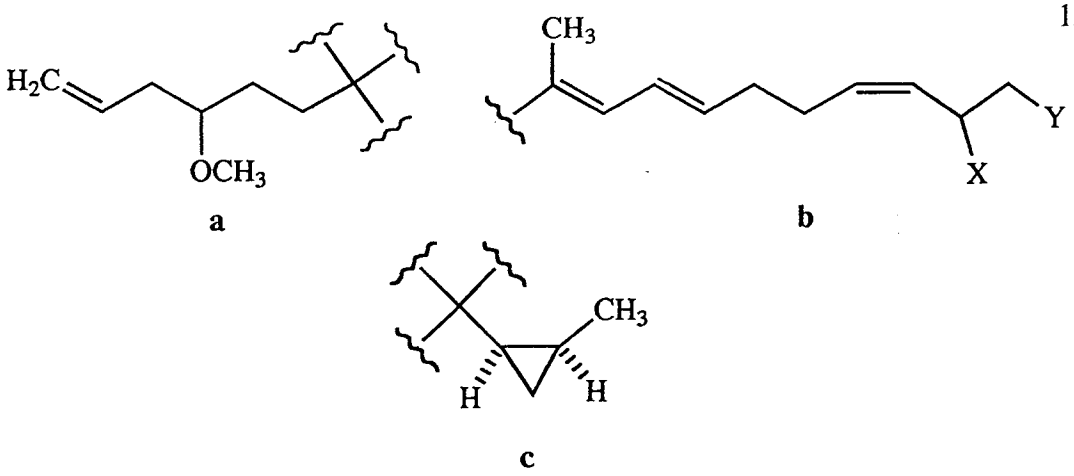

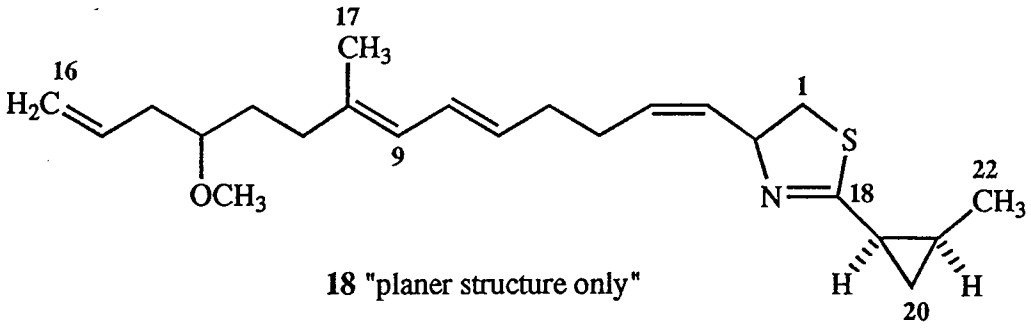

18 "planer structure only"

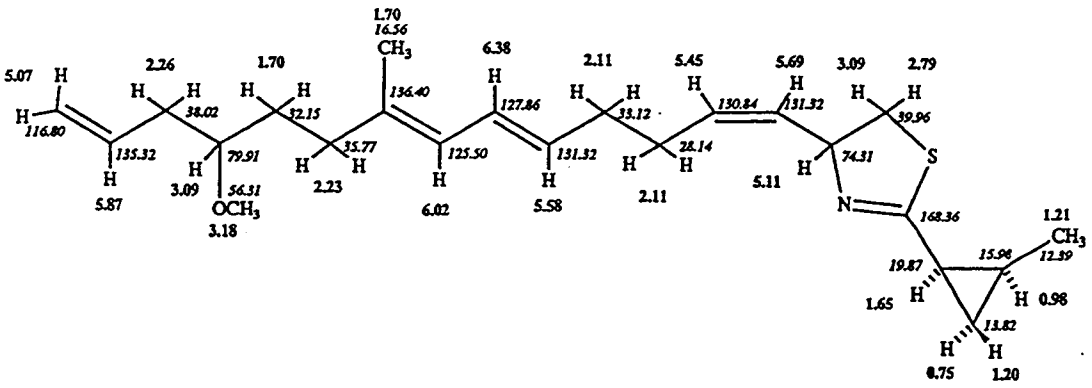

^1H (boldface) and ^{13}C (italics) NMR Data Assignments for Curacin A (**18**). Coupling Constants for **18** (300 MHz, C_6D_6): $J_{1a\text{-}1b}$ = 10.7 Hz, $J_{1a\text{-}2}$ = 10.0 Hz, $J_{2\text{-}3}$ = 8.7 Hz, $J_{2\text{-}4}$ = 1.1 Hz, $J_{3\text{-}4}$ = 10.7 Hz, $J_{4\text{-}5}$ = 7.1 Hz, $J_{6\text{-}7}$ = 7.0 Hz, $J_{7\text{-}8}$ = 15.0 Hz, $J_{8\text{-}9}$ = 10.8 Hz, $J_{9\text{-}17}$ = 1.0 Hz, $J_{19\text{-}20a}$ = 8.2 Hz, $J_{20a\text{-}20b}$ = 4.2 Hz, $J_{20a\text{-}21}$ = 8.2 Hz, $J_{21\text{-}22}$ = 6.2 hz.

Figure V.9 Partial Structures Used to Deduce Structure of Curacin A (**18**).

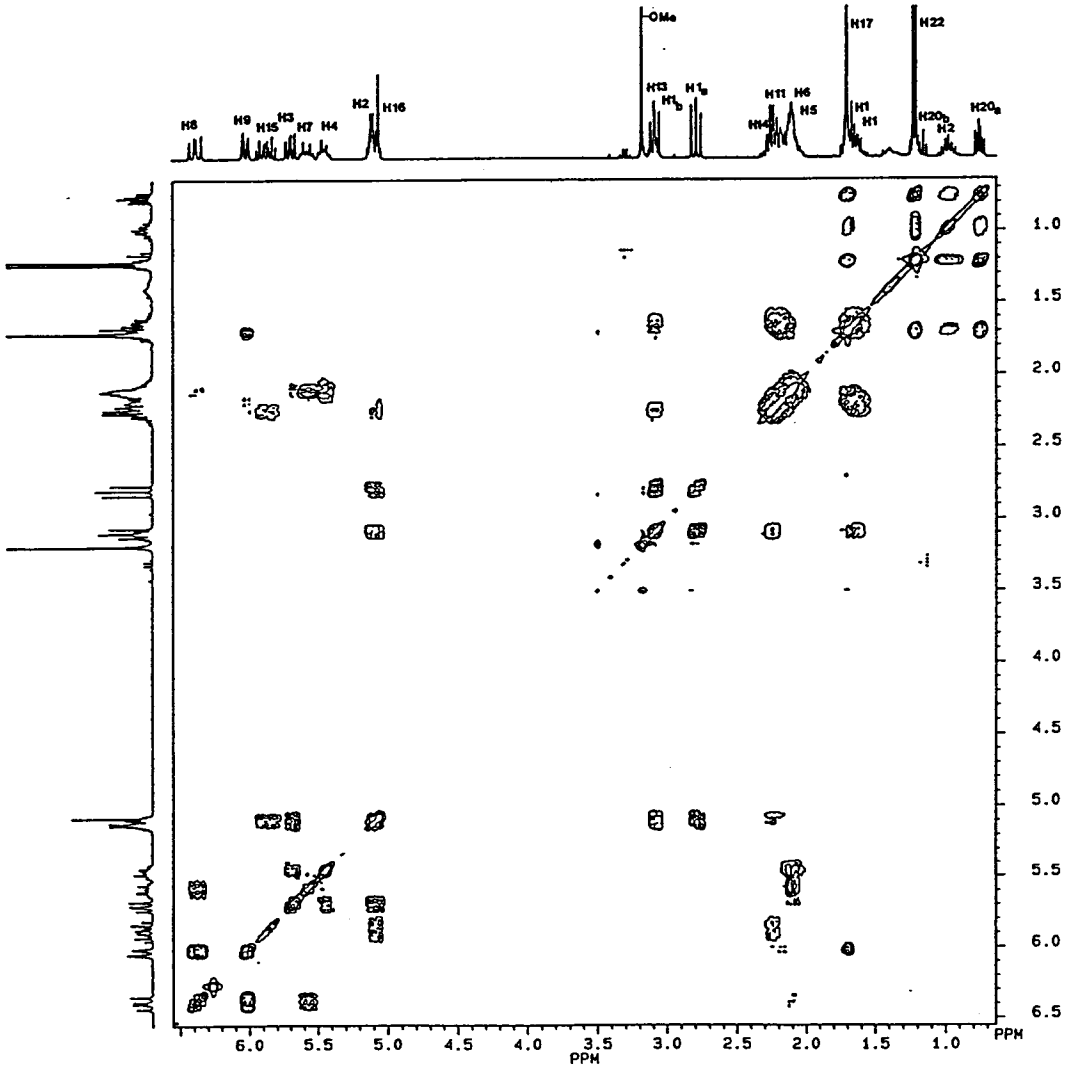

Figure V.10 ^{1}H-^{1}H COSY of Curacin A (**18**) in C_6D_6.

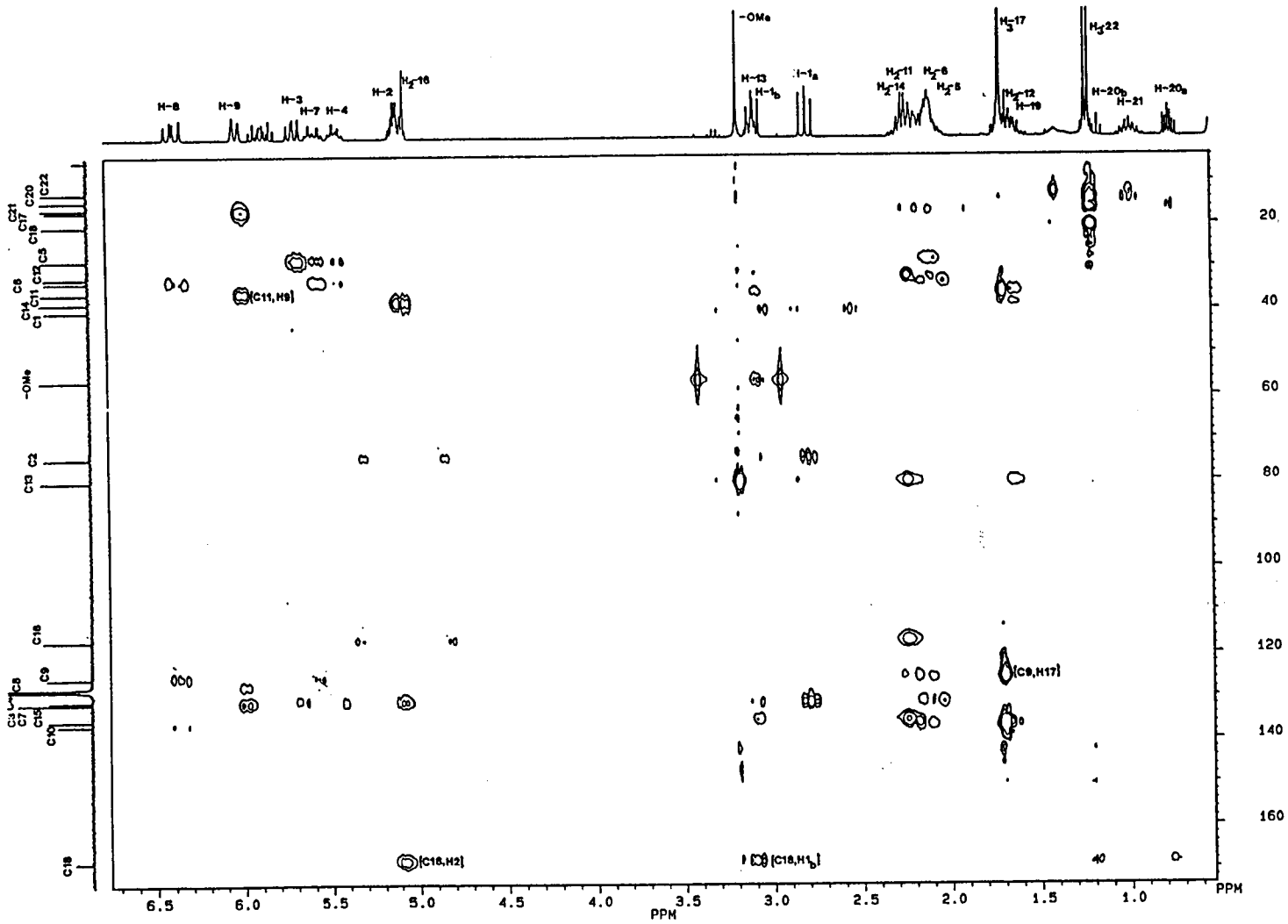

Figure V.11 ^{1}H-^{13}C HMBC Spectrum of Curacin A (**18**) in C_6D_6.

spanned between this olefin and a conjugated diene (λ_{max}^{hex} = 242 nm). The first of these two latter olefins was disubstituted and *trans* while the second was trisubstituted and possessed methyl and alkyl substituents at its distal position. The geometry of this latter olefin was shown to be *E* by virtue of the high field ^{13}C NMR chemical shift of the methyl group (δ 16.56) and observing nOe between the C-17 methyl group (δ 1.74) and H-8 (δ 6.28) in $CDCl_3$. Partial structure **c** was readily formulated by spin coupling information as a *cis*-disubstituted cyclopropyl ring with methyl and quaternary carbon substituents (Figures V.9 and V.10).

HMBC data were used to connect these three partial structures as well as confirm the above structural assignments (Figure V.11). Critically, the protons alpha to the two heteroatoms in partial structure **b** were both correlated to the quaternary carbon of partial structure **c**. Similarly, partial structures **a** and **b** were readily connected by observing long range coupling between the olefinic proton at δ 6.02 (H-9) and methylene carbon at δ 35.77 (C11). Placement of sulfur at C1 and nitrogen at C2 was based on comparisons of ^{13}C NMR chemical shifts with model compounds,[189,190] hence defining a thiazoline ring, and yielding the overall planar structure of curacin A (**18**).

Curacin A was examined in the NCI cell line screen and its differential cytotoxicity pattern was evaluated by the COMPARE algorithm.[191] As this study indicated that **18** was an antitubulin agent,[192] it was subsequently evaluated for its effect on tubulin polymerization. Curacin A was found to inhibit the polymerization of purified tubulin induced either by glutamate or microtubule-associated protein dependent microtubule assembly.[193] Figure V.12 presents a study of the latter reaction condition, comparing curacin A to podophyllotoxin, a well-studied inhibitor of the reaction.[194]

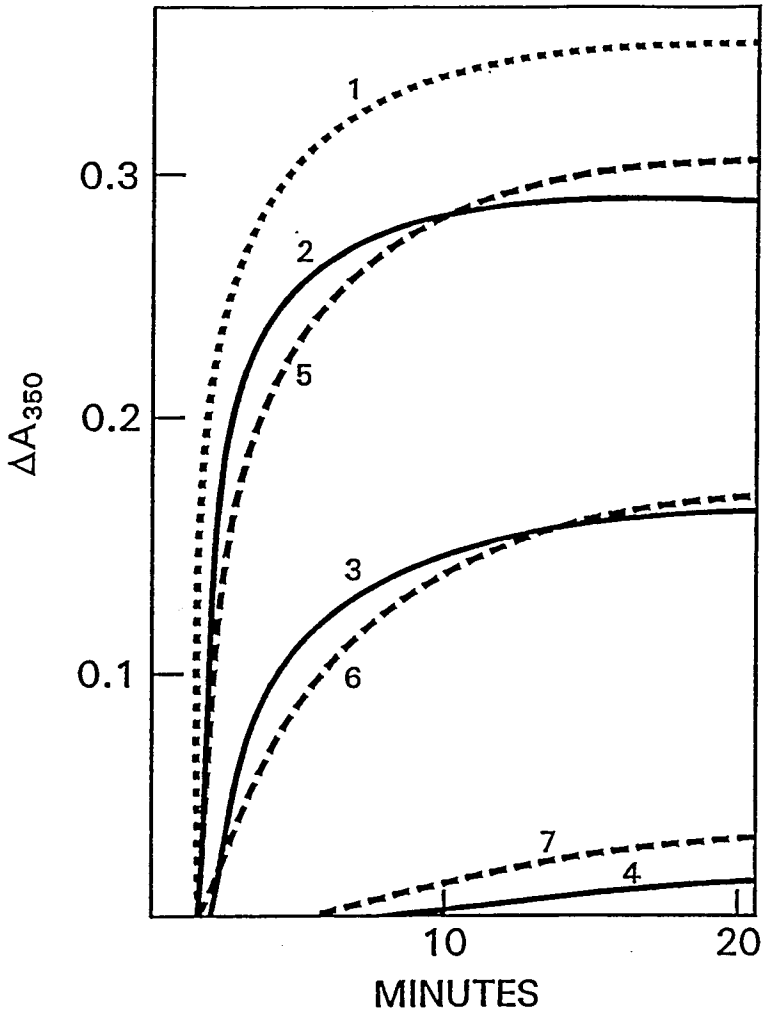

Each 0.25 mL reaction mixture contained 1.5 mg/mL tubulin (15 μM), 0.5 mg/mL heat-treated microtubule-associted proteins (prepared as in ref. 10) 0.2 mM GTP, 0.2 mM $MgCl_2$, 1% (v/v) dimethylsulfoxide (the drug solvent), 0.1 M 4-morpholineethane sulfonate (Mes) (pH 6.9 with NaOH), and drug as follows: curve 1 (dots), none; curves 2-4 (solid), 2 μM, 4 μM, and 6 μM of curacin A, respectively; curves 5-7 (dashes), 2 μM, 4 μM, and 6 μM of podophyllotoxin, respectively. Baselines were established with the cuvette contents held at 0° C; at t_0 the reaction was initiated by a 75 sec temperature jump to 37° C (absorbance measured at 350 nm).

Figure V.12 Inhibition of Microtubule Assembly by Curacin A and Podophyllotoxin.

The two drugs were highly similar in their inhibitory effects, inhibiting the extent of assembly about 50% when present at a concentration of 4 μM and nearly completely at 6 μM.

Cytotoxic agents that inhibit tubulin polymerization routinely cause the accumulation of cells arrested in mitosis at cytotoxic drug concentrations.[194,195] This is also the case with curacin A. We compared it with colchicine in two cell lines (Table V.1). The number of mitotic cells increased with both drugs as the cell number decreased and was maximal at 1 μM, the highest concentration examined. Furthermore, flow cytometric analysis of Chinese hamster cells treated with **1 8** (100 ng/mL) clearly demonstrated that the drug causes cells to accumulate in the G_2/M phase of the cell cycle; G_2/M arrest was also observed with vincristine (300 ng/mL) while hydroxyurea, a ribonucleotide reductase inhibitor (100 ng/ml) produced a distinctly different profile (Figure V.13).

Most inhibitors of tubulin polymerization appear to interact at one of two independent drug binding domains on tubulin and inhibit the binding of either colchicine or vinblastine, but not both. We examined curacin A for such inhibitory activity, comparing it to podophyllotoxin, a known inhibitor of colchicine binding,[194] and to maytansine, a known inhibitor of vinblastine binding[195] (Table V.1). The data demonstrate that **1 8** belongs to the colchicine class of inhibitors, as it inhibits the binding of radiolabeled colchicine, but not radiolabeled vinblastine, to tubulin.

Since the relative stereochemistry of the *cis*-disubstituted cyclopropyl ring was established, eight diastereomeric curacins were possible. It was hoped that constraints on intermolecular distances from nOe difference (NOEDS) and NOESY spectra, together with an estimation of chromophore orientation from circular dichroic (CD) analysis, might provide enough evidence from which to construct an argument for the

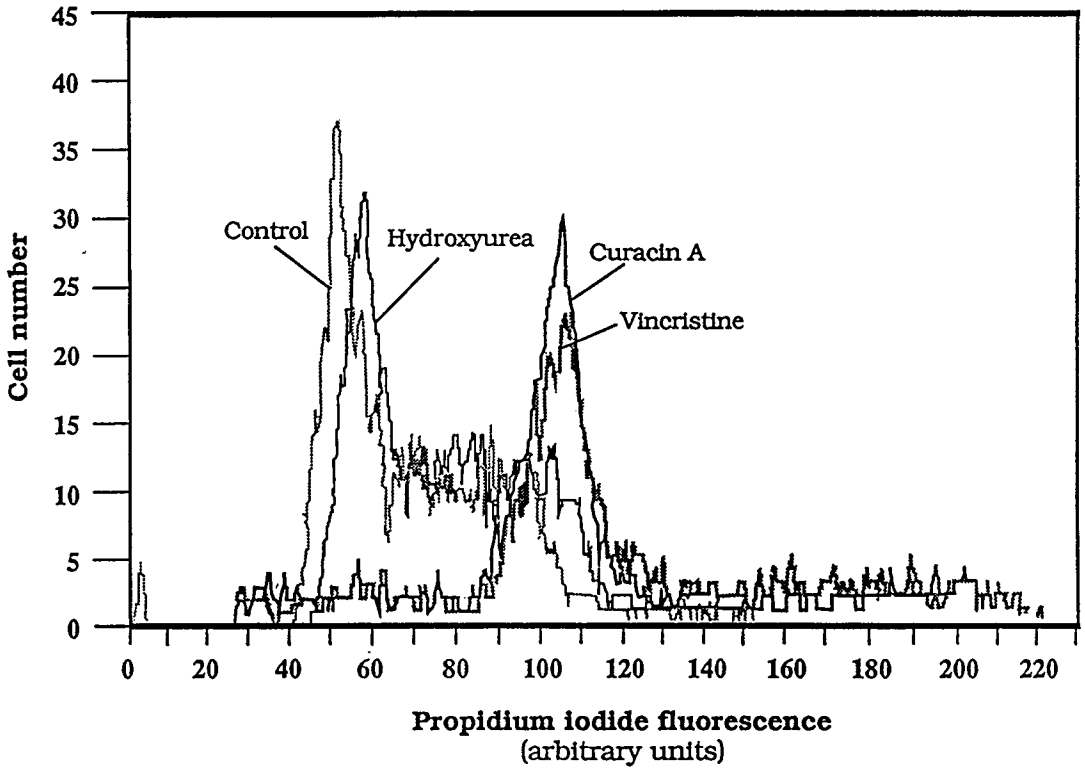

Aux B1 cells were incubated with the indicated drugs for 30 hours in alpha-MEM supplemented with 10% heat-inactivated fetal calf serum. Cells were harvested, washed in phosphate-buffered saline (PBS), fixed in absolute ethanol at -20 °C, and stored overnight at 4 °C. After washing twice in PBS, cells were resuspended in PBS containing 30 KU/mL RNase and 5 µg/mL propidium iodide and incubated at 37 °C for 30 minutes. Samples were then placed on ice. Cell cycle analysis was perfored using a Becton Dickinson FACStar Plus flow cytometer.

Figure V.13 Flow Cytometric Analysis of Chinese Hamster Cells Treated With a) Ethanol Control, b) Curacin A (**18**, 100 ng/mL), c) Vincristine (300 ng/mL), or d) Hydroxyurea (100 ng/mL).

Table V.1 Effects of Curacin A (**18**) on Growth of Leukemia Cells and Ligand Binding to Tubulin.

	L1210 leukemia cells[a]		Burkitt lymphoma cells[a]		ligand binding (% inhibition)	
drug	IC_{50} (M)	Mitotic cells[b] (%)	IC_{50} (M)	Mitotic cells[b] (%)	colchicine[c]	vinblastine[d]
Curacin A (**18**)	9×10^{-9}	46	2×10^{-7}	51	76	4.6
Colchicine (**36**)	4×10^{-9}	41	1×10^{-8}	67		7.5
Podophyllotoxin					94	
Maytansine (**34**)					0	90

a) Cells were grown for 15 hr (L1210 murine leukemia cells) or 24 hr (CA46 human Burkitt lymphoma cells) in RPMI-1640 medium supplemented with 16% fetal bovine serum and 0.03% L-glutamine at 37 °C in 5% CO_2 atmosphere.

b) Mitotic cells are defined as those with condensed chromosomes. Drug concentration was 1.0 μM. L1210 cells were harvested, fixed, and stained with Giemsa. The mitotic index of control cells was 2-3% for both cell lines.

c) The binding of [^{3}H]-colchicine to tubulin was measured by the DEAE-cellulose filter technique. Each 0.1 mL reaction mixture contained 0.1 mg/mL (1.0 μM) tubulin, 2.0 μM [^{3}H]-colchicine (DuPont), potential inhibitor at 10 μM (curacin A, podophyllotoxin) or 50 μM (maytansine), 1.0 M monosodium glutamate (pH 6.6 with HCl), 1 mM $MgCl_2$, 1 mM GTP, 0.1 M glucose 1-phosphate, 0.5 mg/mL bovine serum albumin, and 5% (v/v) DMSO. Incubation was for 30 min at 37 °C. In the control reaction mixture, 0.20 mol of colchicine was bound per mol tubulin.

d) The binding of [^{3}H]-vinblastine to tubulin was measured by centrifugal gel filtration. Each 0.32 mL reaction mixture contained 0.5 mg/mL (5.0 μM) tubulin, 10 μM [^{3}H]-vinblastine (Amersham), potential inhibitor at 100 μM, 0.1 M Mes (pH 6.9 with NaOH), 0.5 mM $MgCl_2$, and 1% (v/v) DMSO. Incubation was for 10 min at 22 °C. Triplicate 100 μL aliquots were placed on syringe-columns containing G-50 (superfine) equilibrated with a solution containing 0.1 M Mes (pH 6.9) and 0.5 mM $MgCl_2$. In the control reaction mixture 0.21 mol of vinblastine was bound per mol of tubulin.

stereochemistry of curacin A. Unfortunately, the CD spectrum of curacin A (**18**) was uninterpretable due to its highly complex nature (Figure V.14a). Hydrogenated derivatives were prepared to simplify the olefinic couplings observed by CD analysis. Small quantities (less than 1 mg) of partially hydrogenated derivatives were produced by catalytic hydrogenation of **18** with trace amounts of Pd (5%) on carbon. Subsequently, the CD spectrum of pure 15, 16-dihydrocuracin A (**19**) was essentially

Table V.2 Activity of Curacin A (**1 8**) and 15,16-Dihydrocuracin A (**1 9**) in Inhibition of Tubulin Polymerization, Inhibition of Colchicine Binding to Tubulin, and the NCI 60-Cell Line Panel.

Compound	Tubulin Inhibition (E. Hamel)	Colchicine Binding (E. Hamel)	MG MID (60-cell line panel, NCI)[c]	Selectivity in TGI[d]
Curacin A (**1 8**)	1.4 ± 0.2 μM	58/95/94[a]	-7.62/-5.17/-4.19	5 colon (10^3) 2 ovarian (10^3) 2 breast (10^3)
15,16-diH_2-Curacin A (**1 9**)	1.3 ± 0.1 μM	68/93/96[b]	-7.79/-5.40/-4.43	2 NSCL (10^3) 4 colon (10^3) 3 CNS (10^3) 1 ovarian (10^3)

a) Three numbers represent % inhibition of colchicine binding at 2 μM, 5 μM, 50 μM of the indicated compound.
b) Three numbers represent % inhibition of colchicine binding at 1 μM, 2.5 μM, 5.0 μM of the indicated compound.
c) The three values given are the "means of all 60-cell lines" for the GI_{50}/TGI/LD_{50} intercepts, respectively. (GI = growth inhibition).
d) The number in parenthesis represents approximate fold greater of the indicated cell lines to the effects of the indicated compound. (TGI = total growth inhibition).

indistinguishable from that of natural **1 8** (Figure V.14b). No direct answers to the question of curacin A stereochemistry were provided by CD spectrum of **1 9**. However, this result suggests that, in regard to chromophoric disposition, both curacin A and dihydrocuracin A adopt similar solution conformations, a critical point in establishing the nature of structure-activity relationships. Further, tubulin inhibition studies, colchicine binding experiments, and NCI 60 cell line antiproliferative data confirmed that this new derivative **1 9** is nearly identical in activity and potency with natural curacin A (Table V.2).

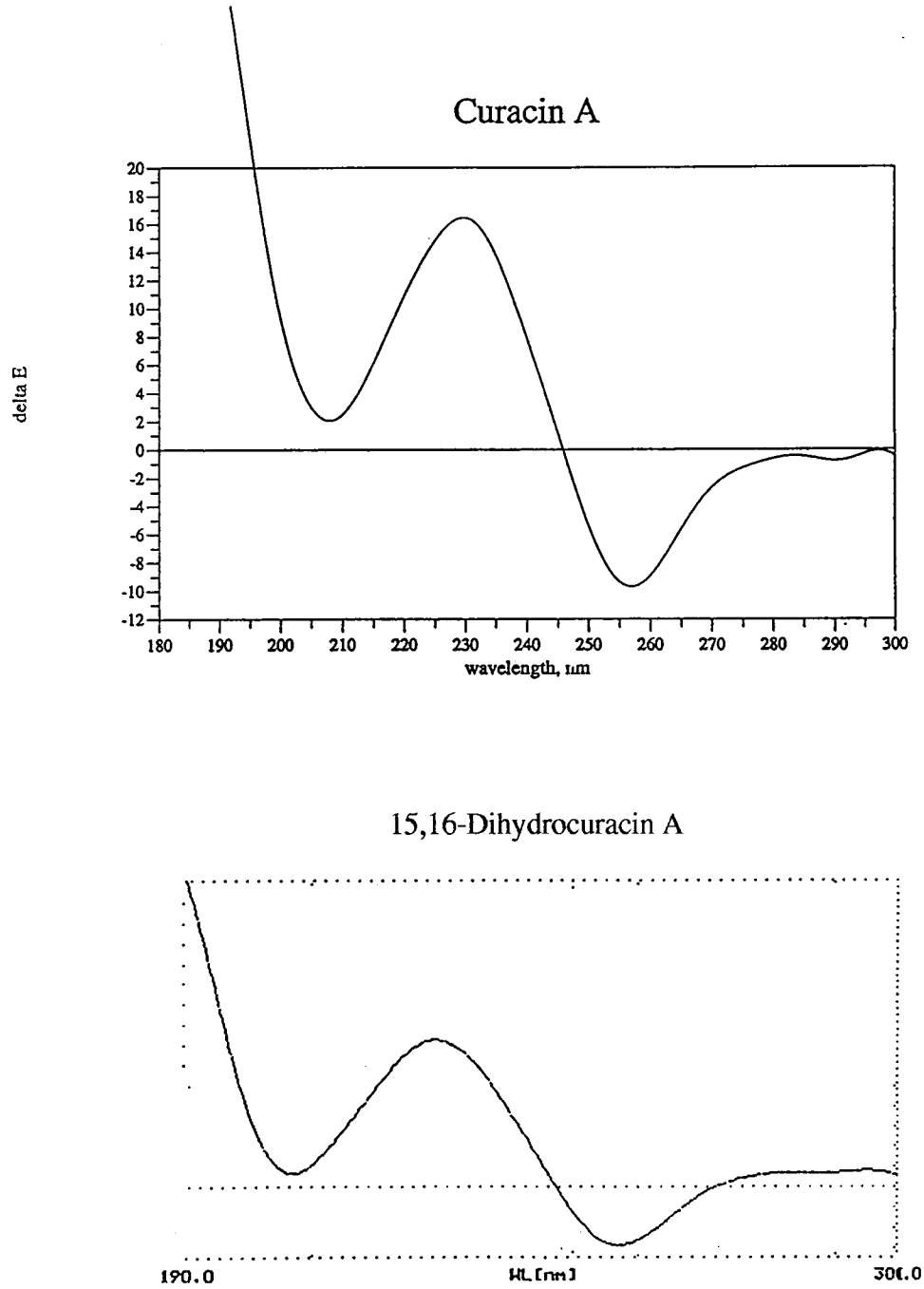

Figure V.14 CD Spectra of Curacin A (**18**, Above) and 15,16-Dihydrocuracin A (**19**, Below).

The absolute configuration of curacin A (**1 8**) remained unassigned. Crucial to developing a more complete appreciation for the nature of the interaction between curacin A and its biomolecular target, and as an essential precondition for efforts aimed at its synthesis, I undertook a degradative approach (collaboration with Dr. James White, OSU Chem. Dept.) to define its relative and absolute stereochemistry.

The strategy for determination of the C13 stereochemistry in **1 8** hinged upon ozonolysis of the C9-C10 olefin to produce a methyl ketone. However, when curacin A was subjected to ozonolysis directly, I was unable to recover a fragment deriving from the C9-C17 region. Suspecting that the C15-C16 olefin was responsible for this undesired reactivity, curacin A was partially hydrogenated with Wilkinson's catalyst to yield a mixture of 15,16-dihydrocuracin A (**1 9**, Figure V.15) and 3,4,15,16-tetrahydrocuracin A (**2 0**) by GC-MS analysis. This mixture was ozonized and the ozonide was reduced with excess dimethyl sulfide to yield, following chromatography, 5-methoxyoctan-2-one (**2 1**). The latter was fully characterized by ^{1}H and ^{13}C NMR and GC-MS, and showed $[\alpha]_D^{23}$ +14.2° (*c* 0.22, $CDCl_3$). Elucidation of the *R* configuration of this fragment was achieved through comparison with (+)-**2 1** obtained by enantiospecific synthesis.

Allylation of 4-pentynal (**2 2**), prepared by Swern oxidation of the corresponding alcohol, with the allylboronate **2 3** derived from (*R*,*R*)-(+)-diisopropyl tartrate[196] gave (5*R*)-1-octyn-7-en-5-ol (**2 4**, Figure V.15). After conversion of **2 4** to its methyl ether **2 5**, the latter was treated with dicyclopentadienylzirconium dichloride in the presence of trimethylaluminum and then with iodine, to yield the *E*-iodooctadiene **2 6**.[197] Selective hydrogenation of the vinylic olefin of **2 6** was accomplished with Wilkinson's catalyst and the resultant alkene was ozonized to afford, after reductive workup, (5*R*)-methoxyoctan-2-one (**2 1**), $[\alpha]_D^{25}$ +10.0° (*c* 0.50, $CDCl_3$). This

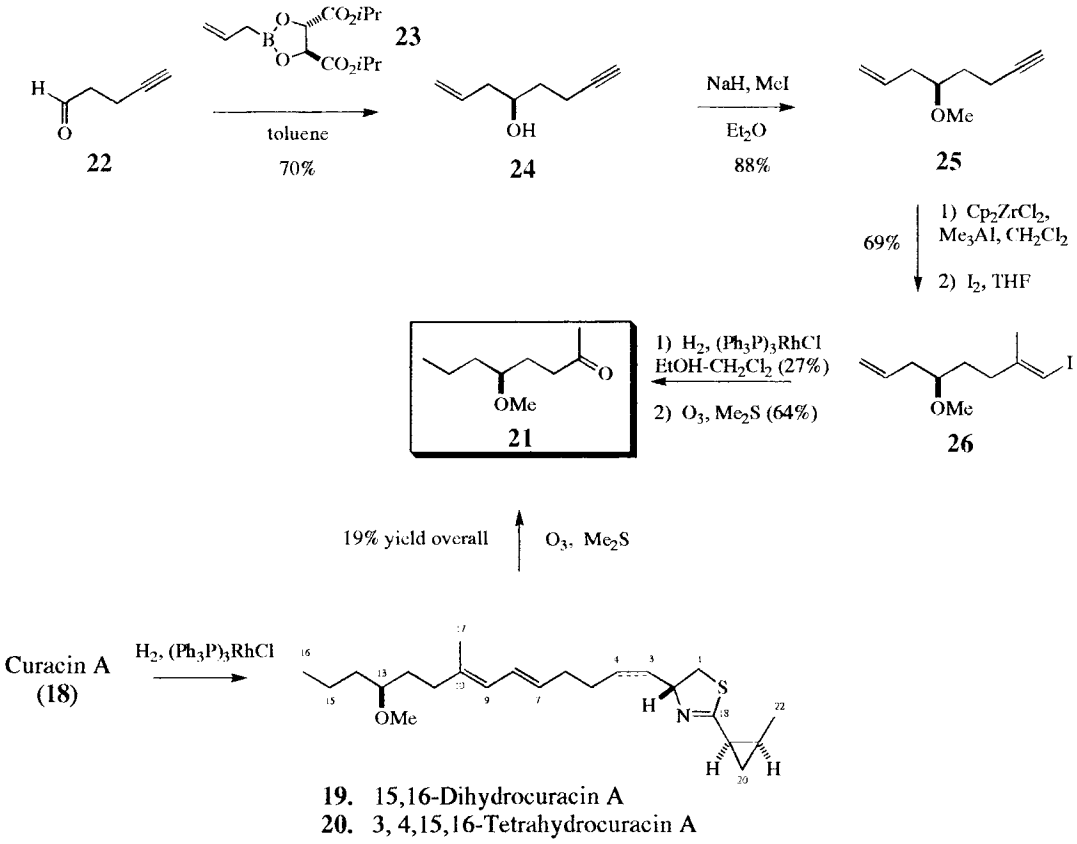

Figure V.15 Convergent Formation of Methylketone **21** From Total Synthesis and From Chemical Degradation of Curacin A (**18**).

substance was identical by comparison of ^{1}H and ^{13}C NMR and GC-MS with the material obtained by degradation of curacin A (Figure V.16).

The strategy for determining the configuration of the C2, C19, and C21 stereocenters in curacin A originally envisioned oxidative cleavage of the C3-C4 olefin and recovery of a methylcyclopropyl- and carboxyl-substituted thiazoline that would be compared with synthetic substances of known chirality. However, ozonolysis of curacin A (-78 °C, $CHCl_3$, 2 min), followed by oxidative workup (H_2O_2, 45 °C, 16 hr) and then reaction with excess CH_2N_2 in Et_2O, gave after flash chromatography and HPLC, methyl sulfonate derivative **27**, $[\alpha]_D^{25}$ -17.1° (*c* 0.12, MeOH) (22% overall

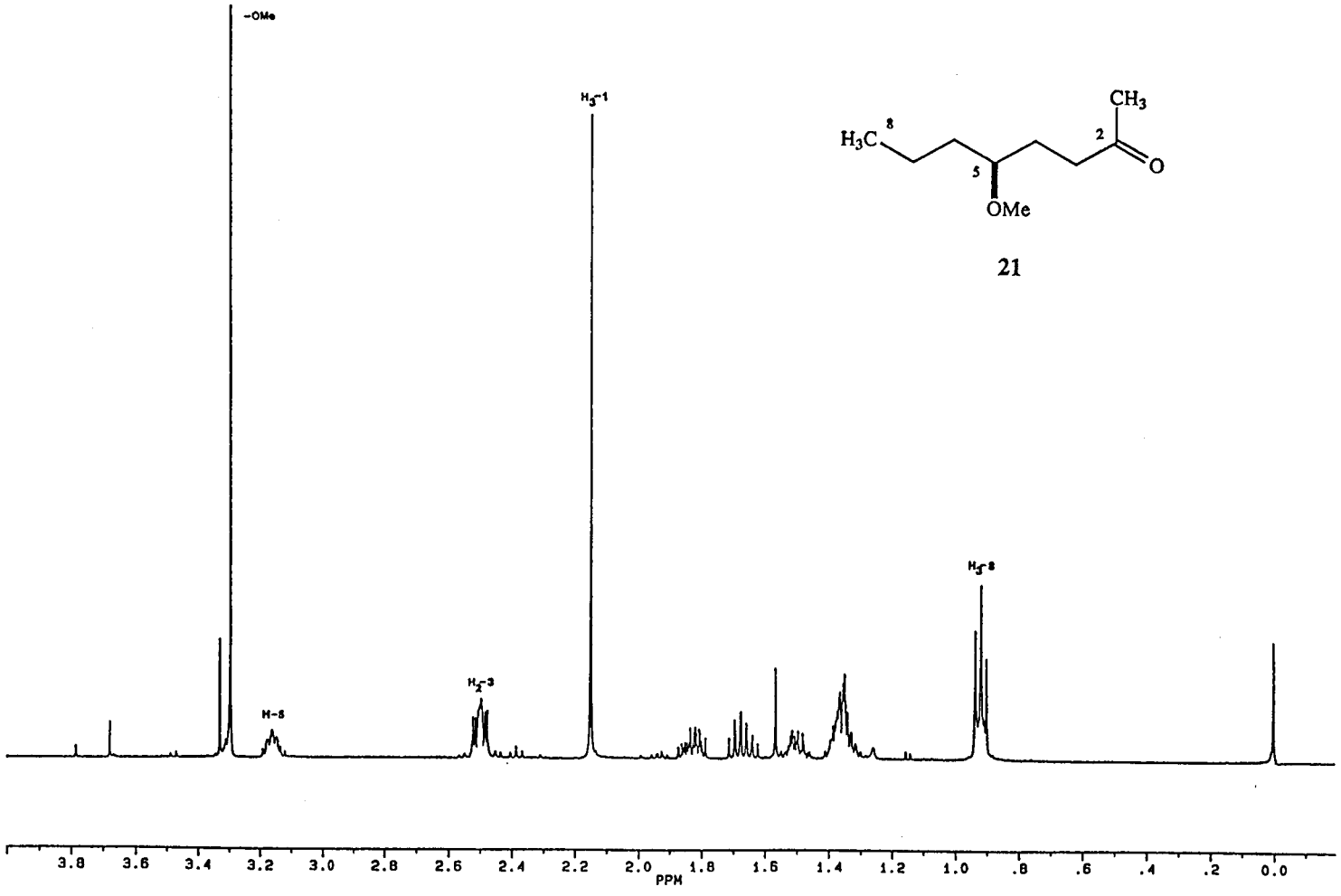

21

Figure V.16 ^1H NMR Spectrum of Methylketone **21** in $CDCl_3$.

yield). The sulfonate **27** (Figure V.17), of molecular constitution $C_{10}H_{17}NO_6S$, displayed IR stretching absorptions for ester (1738 cm^{-1}), amide (1637 cm^{-1}) and sulfonate (1353, 1170 cm^{-1}) functionalities. The methylcyclopropyl and H_2-1 ⇒ H-2 ⇒ NH spin systems were readily evident in the ^1H NMR spectrum of **27**, as were two ester methyl groups at δ 3.88 and δ 3.82. By HMBC, we were able to connect the latter signal to a δ 169.2 carbonyl which in turn showed 3-bond coupling to the C1 methylene protons, thereby providing assignment of the two methyl groups.[196] Combination of these two partial structures through the remaining elements of the molecular formula, "CO", completed the structure determination of this degradation product (**27**).

This assignment was confirmed and the absolute configuration of **27** was established by an asymmetric synthesis from *cis* crotyl alcohol (**28**, Figure V.17). The latter, prepared by hydrogenation of 2-butyn-1-ol over Lindlar's catalyst, was cyclopropanated with diethylzinc and diiodomethane in the presence of the *n*-butylboron complex of (*S*,*S*)-(-)-N,N,N',N'-tetramethyltartaramide (**29**) to give **30** in >95% ee.[198] Oxidation of **30**, first with perruthenate[199] and then with sodium chlorite,[200,201] afforded (1*R*,2*S*)-2-methylcyclopropanecarboxylic acid (**31**) which was coupled with (*R*)-(-)-cystine dimethyl ester dihydrochloride using DCC and HOBT.[202] The resulting disulfide **32** was ozonized and the crude product was treated with diazomethane to furnish **27**, $[\alpha]_D^{25}$ -21.4° (*c* 0.21, MeOH), identical by comparison of ^1H (Figure V.18) and ^{13}C NMR and GC-MS with the corresponding substance obtained by degradation of curacin A. A stereoisomer of **27** derived from (1*S*,2*R*)-2-methylcyclopropane-carboxylic acid, prepared with the tartaramide complex antipodal to **29**, was distinguishable by ^1H NMR , ^{13}C NMR and GC-MS from the sulfonate derived from **18**.

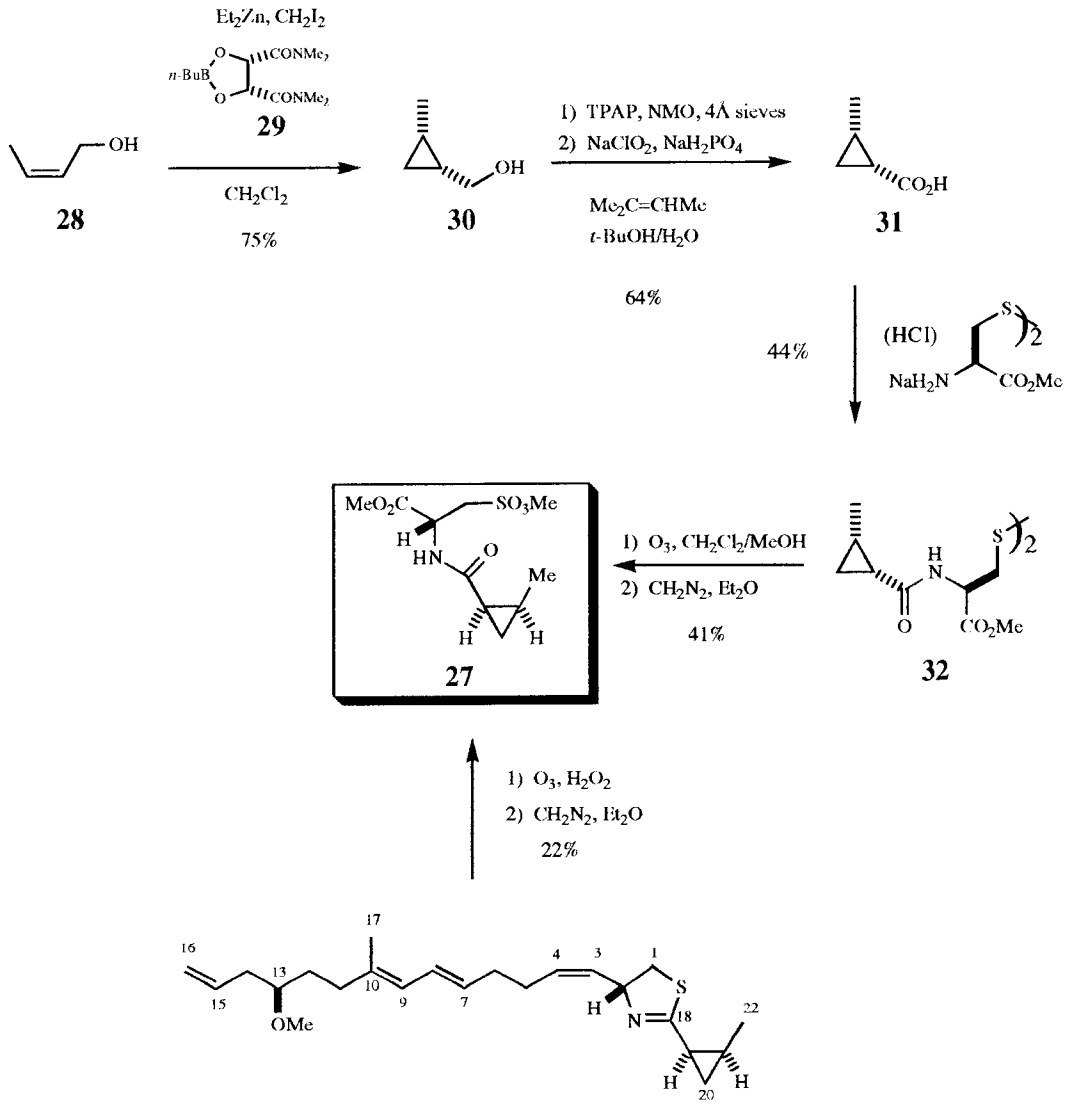

Curacin A
(18)

Figure V.17 Convergent Formation of Sulfonate **27** From Total Synthesis and From Chemical Degradation of Curacin A (**18**).

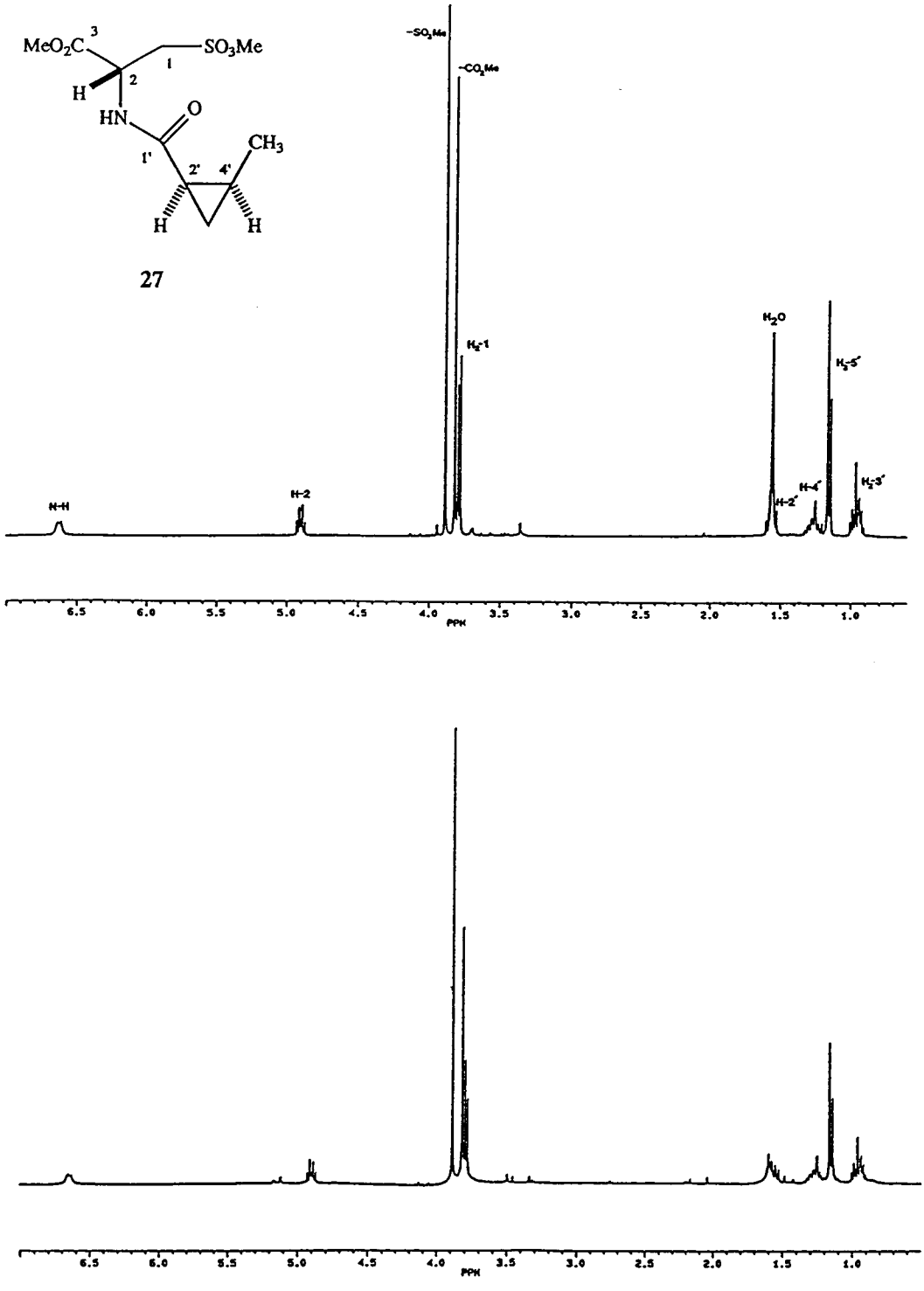

Figure V.18 Comparison of ^{1}H NMR Spectra of Sulfonate **27** Derived From Curacin A (**18**, Above); Enantiospecific Synthesis (Below).

These results fully define the absolute configuration of curacin A (**1 8**). It is noteworthy that **1 8** possesses *R* configuration at the α-amino center (C2), a fact consistent with the thiazoline portion of the molecule being derived from *L*-cysteine.

From chemical and biochemical perspectives, the alkylated thiazoline clearly represents the structurally unique portion of curacin A. In this respect, it bears some relationship to the potent cytotoxins patellazoles A-C (patellazole C (**3 3**), Figure V.19) from the tunicate *Lissoclinum patella.*[203] Similar to curacin A, these latter metabolites possess a four carbon branch, three membered ring, and a long polyketide chain substituents on a thiazole ring. The relationship of heterocyclic ring to diene chromophore in curacin A is similar to that seen in the patellazoles as well as two other antimitotic agents, maytansine (**3 4**) and rhizoxin (**3 5**). However, these latter two metabolites inhibit the binding of vinblastine, but not colchicine (**3 6**), to tubulin.[202] In fact, the interaction of curacin A (**1 8**) with the colchicine binding domain of tubulin is remarkable, considering the lack of apparent structural similarity between the two molecules (Figure V.20).

Biosynthetically, curacin A may derive from two polyketides joined together through a decarboxylated cysteine residue (Figure V.21). The C3-C16 portion of **1 8** may be formed by condensation of a partially reduced and dehydrated polyketide chain with a cysteine derived unit (Figures V.21 and V.22), a sequence analogous to sphingolipid biosynthesis (Figure V.23). Alternatively, carbons 3 through 16 may arise from a cysteine starter unit initiated polyketide chain formation (not shown). The origin of the C1′-C5′ cyclopropane containing unit is less clear. This five carbon unit may derive from mevalonic acid, a polyketide, or an amino acid precursor (Figure V.22).

While curacin A (**1 8**) was the major secondary natural product in this *Lyngbya* sp., other unusual compounds were apparent in the extract by TLC. Subsequently,

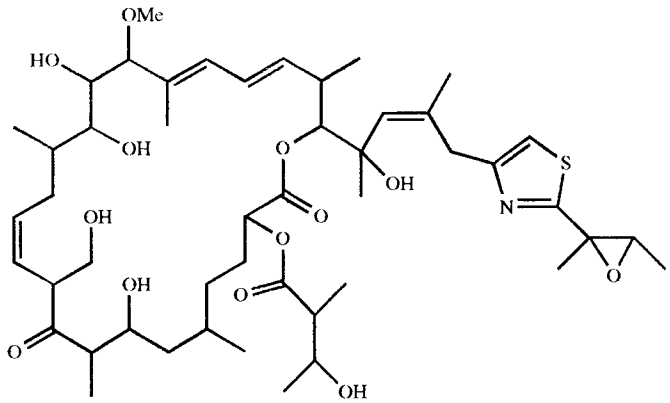

33

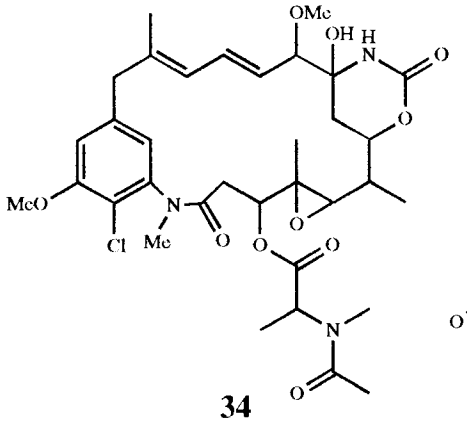

34

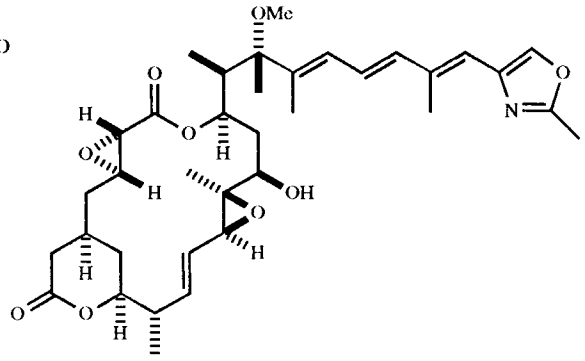

35

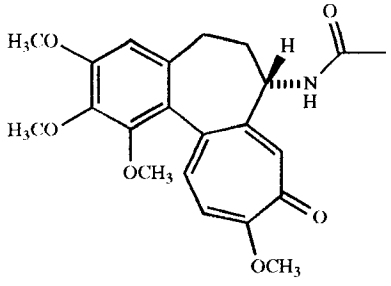

36

Figure V.19 Cytotoxic Agents With Similar Structural Features to Curacin A (**18**).

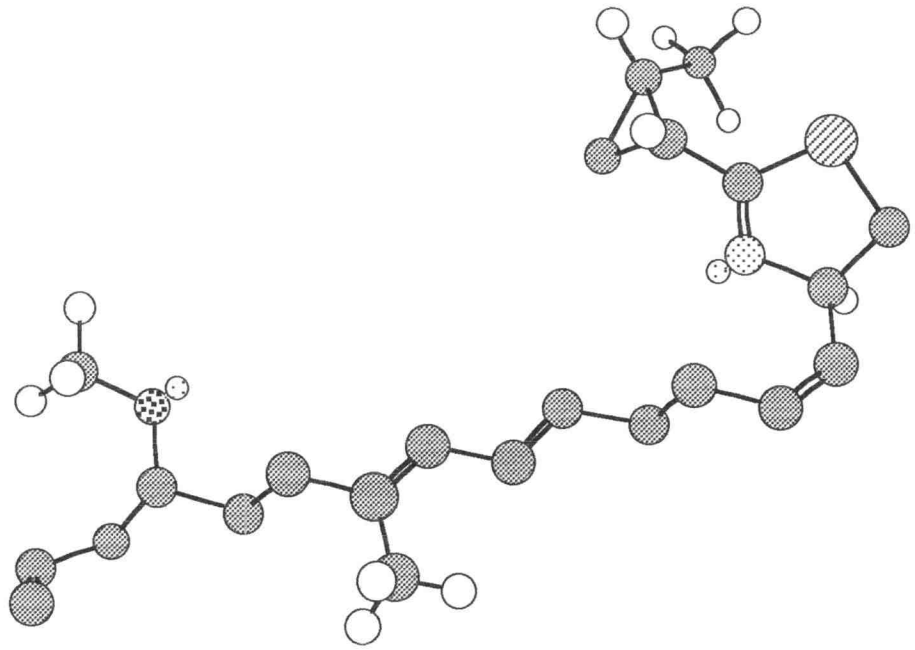

18

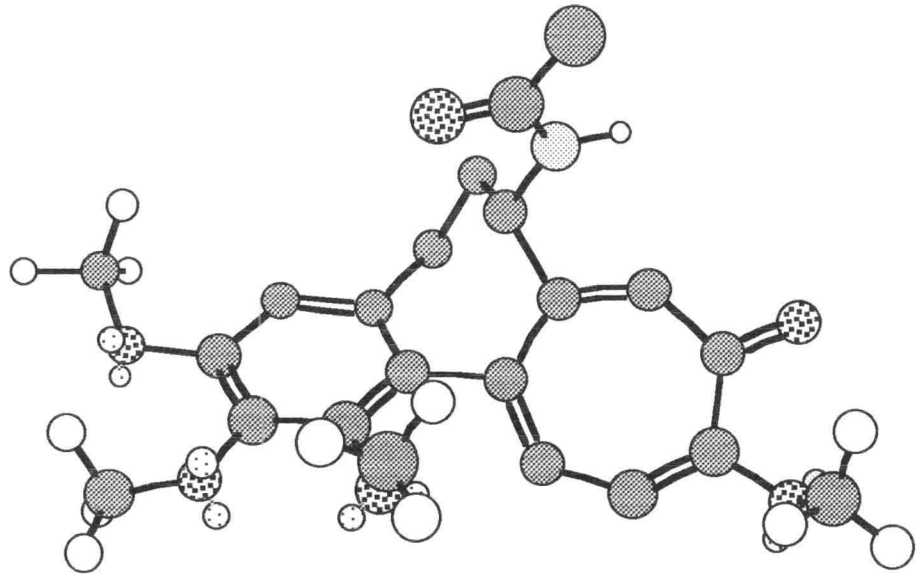

36

Figure V.20 Comparison of 3-Dimensional Energy Minimized (Chem 3D Plus) Structures of Curacin A (**18**) and Colchicine (**36**).

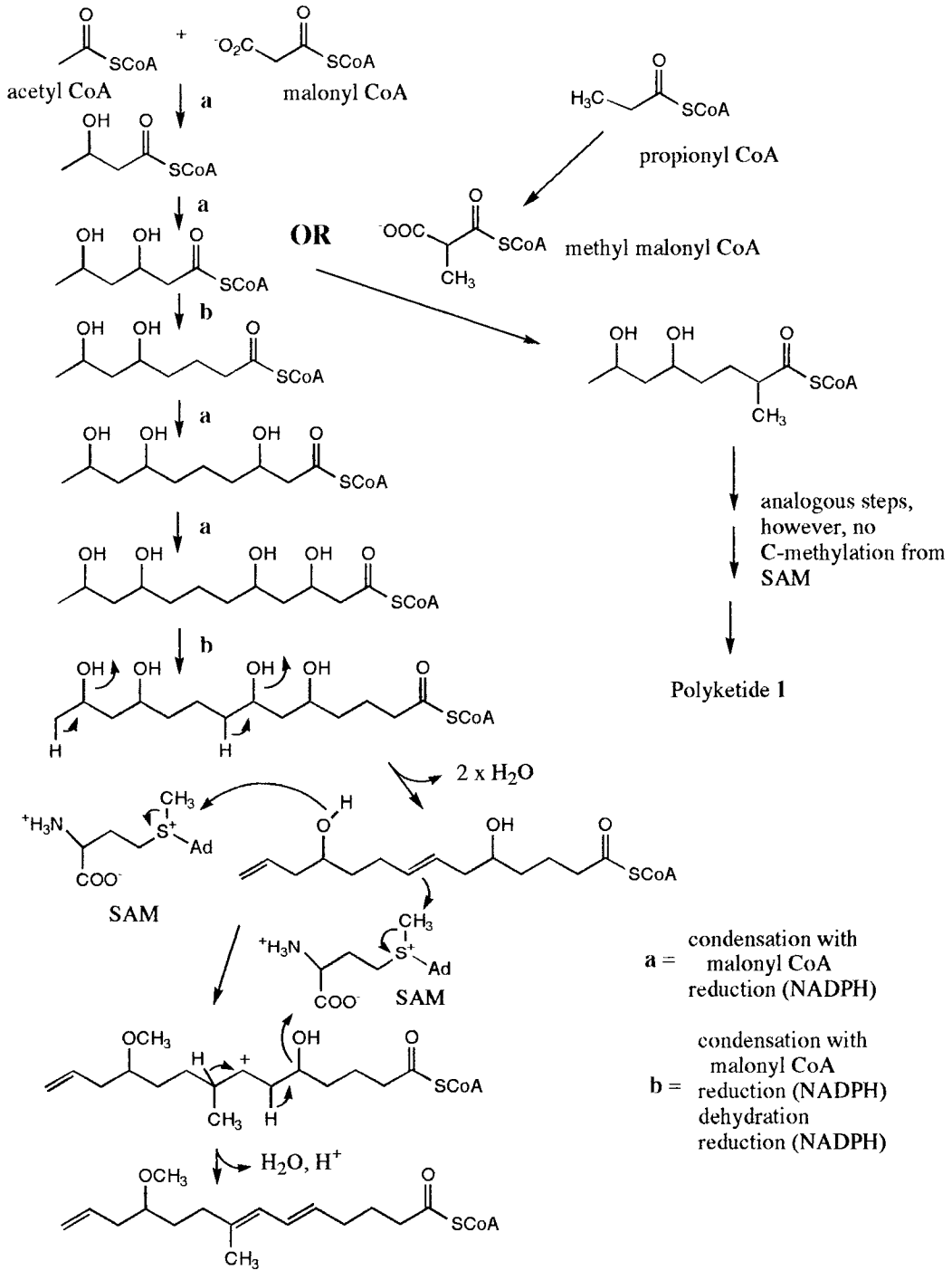

Figure V.21 Proposed Biogenesis of the C3-C16 Polyketide Fragment of Curacin A.

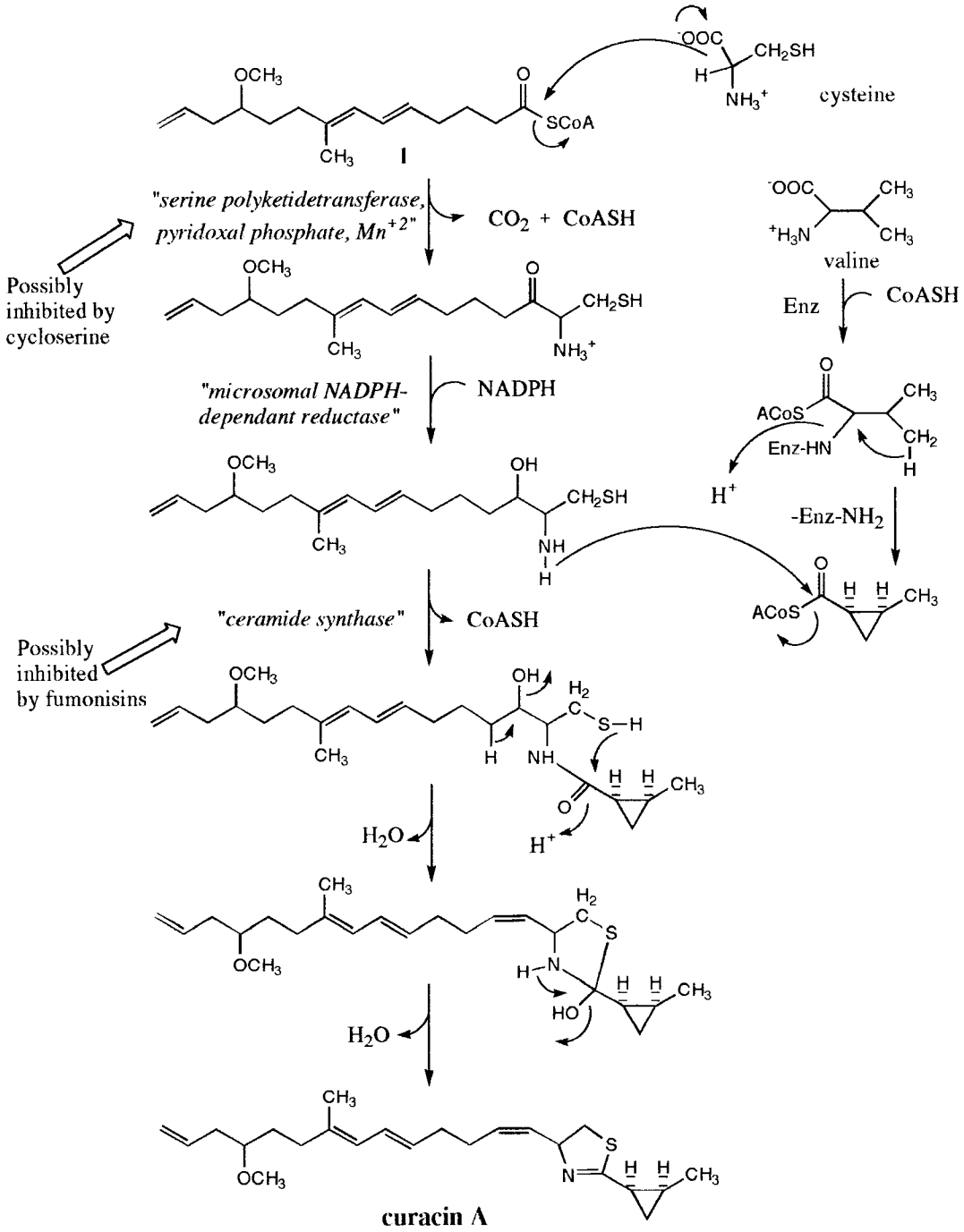

Figure V.22 Proposed Biogenesis of the C1-C5 Fragment and Overall Assembly of Curacin A (**18**).

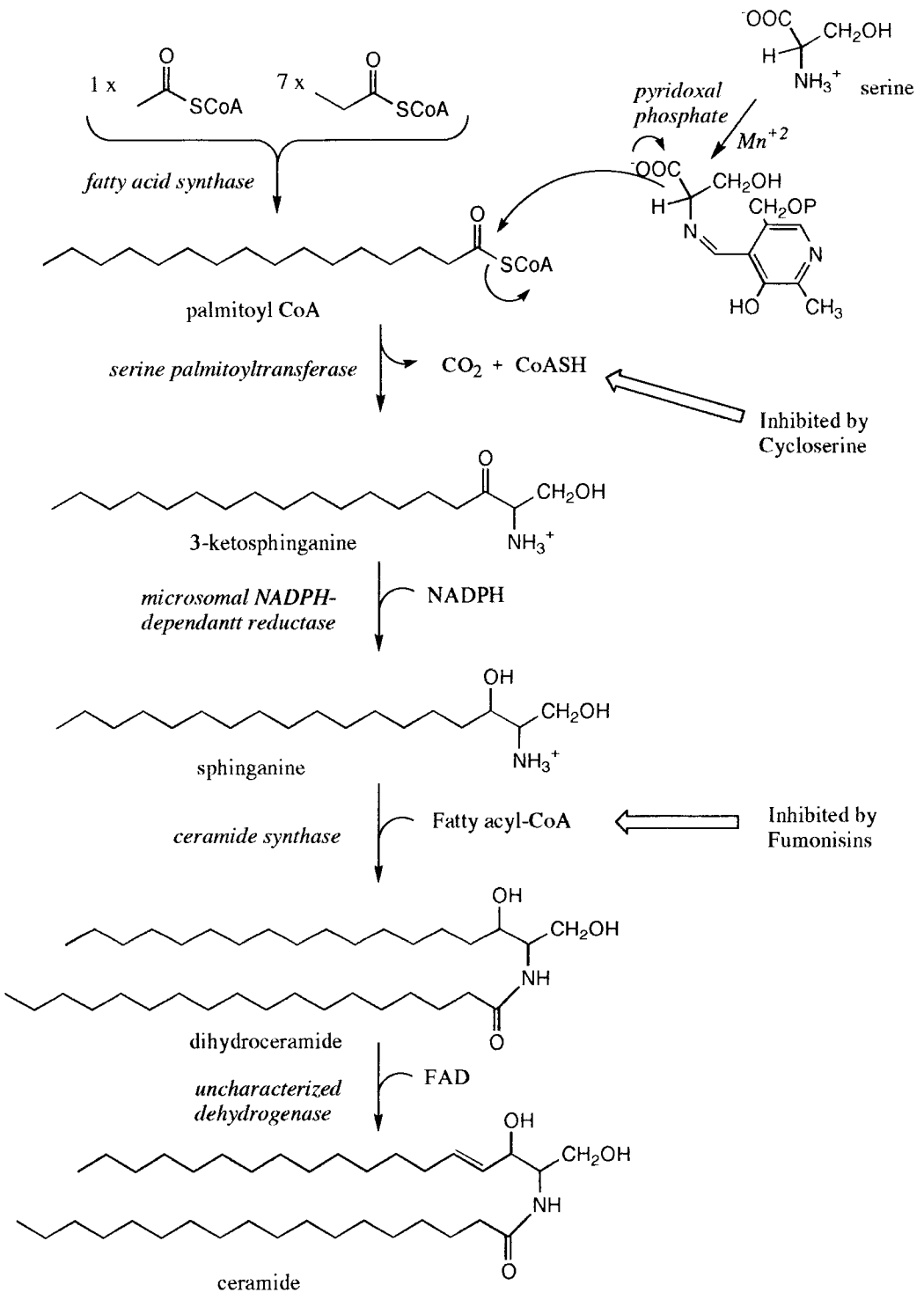

Figure V.23 Biosynthesis of Sphingosine and Ceramide.

I evaluated crude *L. majuscula* extracts and purified ichthyotoxic compounds using a goldfish (*Carassius auratus*) toxicity assay. Both lethality (LD_{50}'s) and sedation as measured by a loss of ability to swim against a manually induced current (EC_{50}'s) were evaluated. The crude *L. majuscula* extract was potently ichthyotoxic (LC_{100} < 25 μg/mL). I was surprised to find that pure **18** showed essentially no fish toxicity. However, on several separate occasions, goldfish tested with **18** showed signs of pathogenic infection and died within a week following exposure.

Bioassay-guided fractionation of the extract (silica gel, Sephadex LH 20, and reversed-phase ODS silica) led to the isolation of a new ichthyotoxic metabolite, **37**, and a previously described compound, 7-methoxytetradec-4(*E*)-enoic acid (**38**, Figure V.24).[204] The structure of **37** was determined by a combination of 1- and 2-D NMR (Dr. Orjala). The absolute stereochemistry of the cyclohexenone moiety was deduced by a combination of NOESY and circular dichroic (CD) spectroscopy. Compound **37** is the newest in a series of related *Lyngbya* metabolites known as malyngamides A-G[186,204-209] and was therefore named malyngamide H. Malyngamide H (**37**) is structurally similar to deacetoxystylocheilamide (**39**), isolated from the sea hare *Stylocheilus longicauda*.[210] However the structure of **37** represents a new carbon skeleton and lacks the characteristic vinylic chloride associated with other malyngamides previously identified from *L. majuscula*. Remarkably, malyngamide H (**37**) is moderately ichthyotoxic (LC_{50} = 5 μg/mL, EC_{50} = 2 μg/mL, Figure V.25), yet is inactive in the brine shrimp assay. Malyngamide A, found in Hawaiian collections of *L. majuscula*, has been reported to act as an antifeedant.[211] This class of chemistry may play an ecological role as herbivore deterrents.

The relatively moderate potency and low yield of **37** (0.32% of crude extract) could not fully explain the ichthyotoxicity of the crude extract. Careful examination of

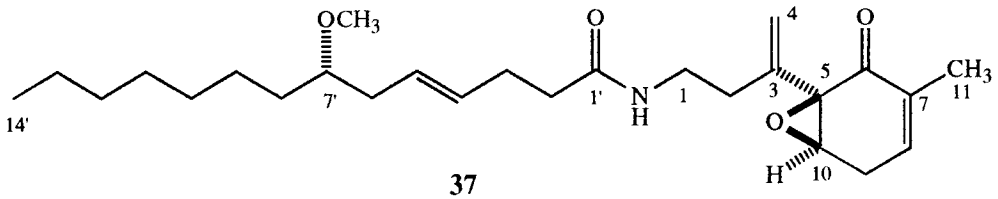

37

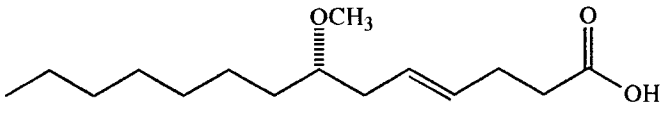

38

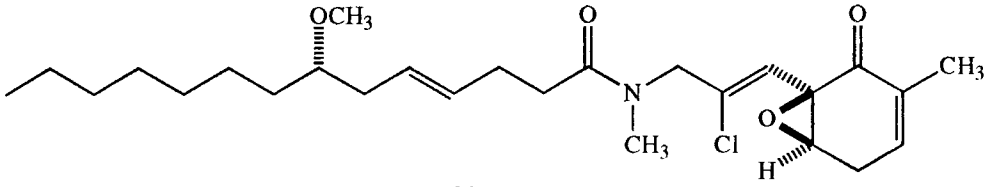

39

Figure V.24 Structures of Malyngamide H (**37**), 7-Methoxytetradec-4(*E*)-enoic Acid (**38**), and Deacetoxystylocheilamide (**39**).

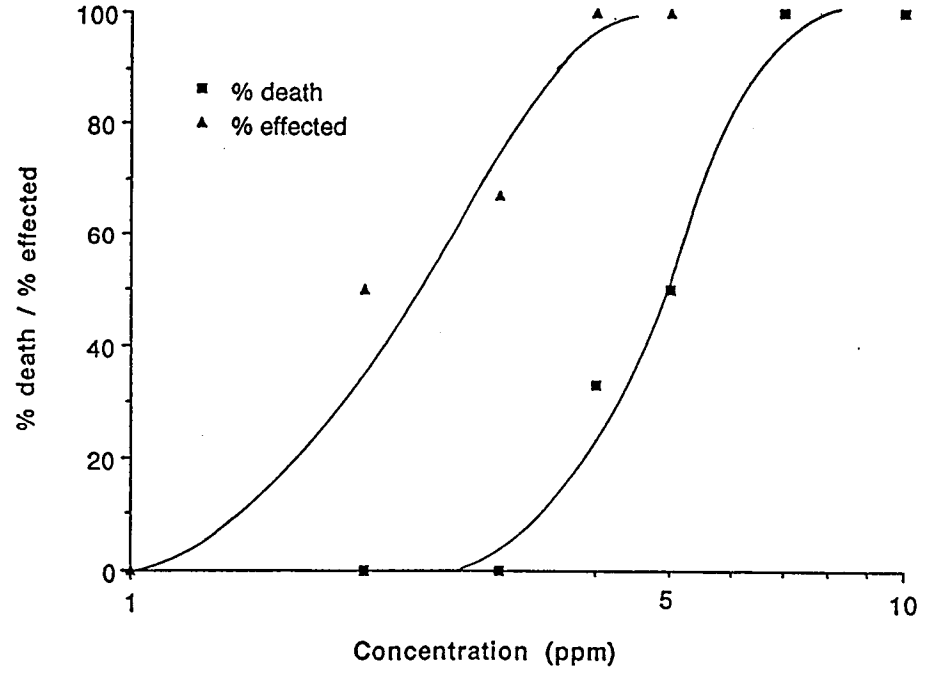

Figure V.25 Ichthyotoxic Effects of Malyngamide H (**37**).

chromatographic fractions prepared during isolation of **37** were consistent with a loss of activity during separation which suggested that a minor component in these fractions was responsible for a considerable portion of this extract's toxicity. Due to the extremely low concentration of this toxic substance it was impossible to follow its isolation with conventional TLC analysis. Therefore, I utilized a bioassay-guided isolation protocol, evaluating the ichthyotoxic potential of all chromatographic fractions. Figure V.26 shows the chromatographic separation used to isolate a fish-toxic minor compound which we have given the name antillatoxin (**40**, Figure V.27). Antillatoxin (**40**) is a rapidly acting and extremely potent ichthyotoxin (Figure V.28). Its toxicity may be vertebrate specific as it does not effect either brine shrimp or the mollusc *Biomphalaria glambrata*.

I evaluated *L. majuscula* fractions for molluscicidal activity and detected the presence of a snail toxic metabolite which we subsequently isolated. The structure of the molluscicidal agent, barbarmide A (**41**, Figure V.27), was deduced spectroscopically (Dr. Orjala). Like **40**, the toxic effects of **41** appear to function rather selectively. Barbarmide (**41**) is not toxic to brine shrimp or fish.

Investigation of the cyanobacterium *L. majuscula* has led to the isolation of a remarkable number of biologically active natural products. These potent toxins may play an important ecological role in the survival of this species. Implementation of multiple screening techniques in the chemical evaluation of this organism was a crucial factor leading to these discoveries. Great potential for the further discovery of unique marine derived lead compounds appears limited only by our understanding of the complex relationships between ecology and biologically active chemistry.

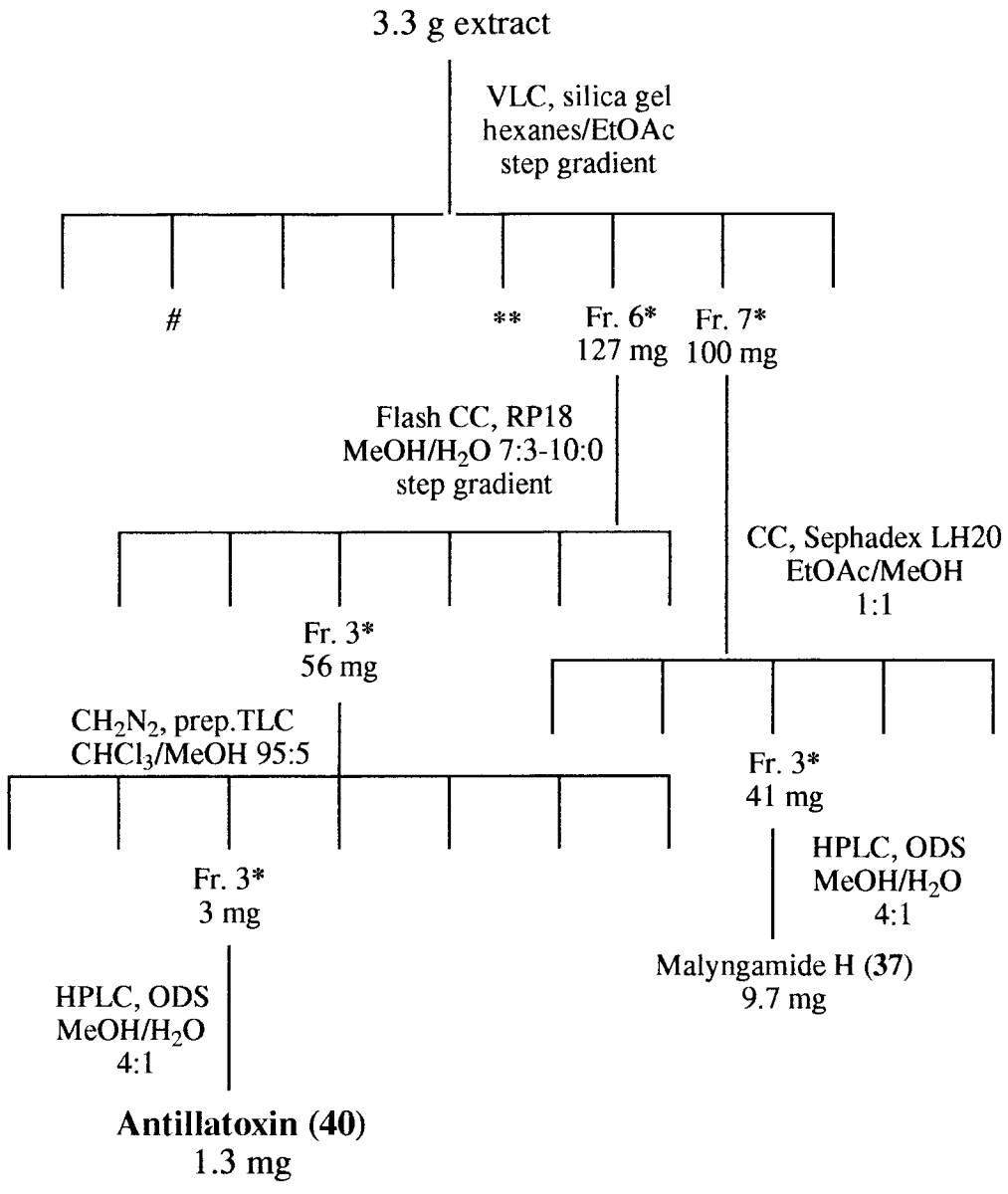

* = Toxic to fish at 10 µg/mL or less
\# = Contains Curacin A (**18**)
** = Molluscicidal at 50 µg/mL

Figure V.26 Bioassay Guided Isolation of Antillatoxin (**40**) From *L. majuscula*.

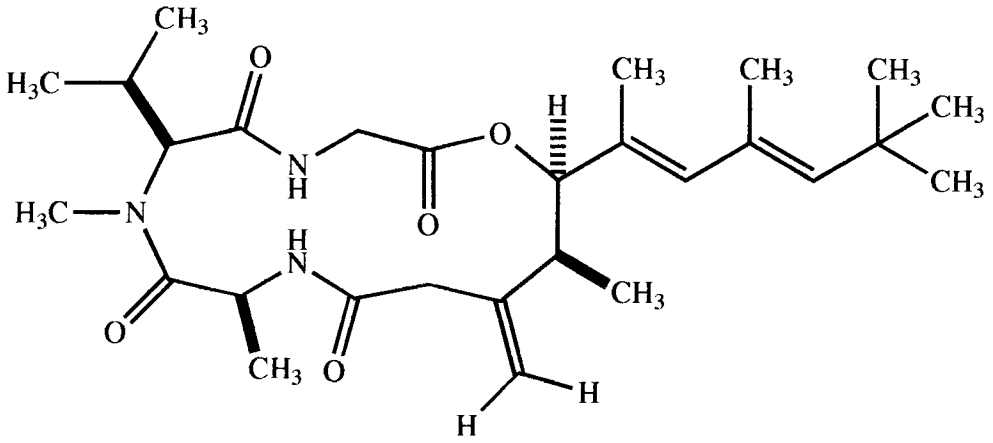

40

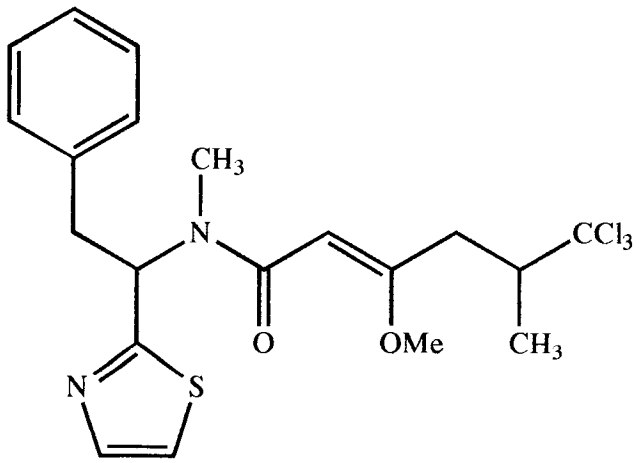

41

Figure V.27 Structures of Antillatoxin (**40**) and Barbarmide A (**41**).

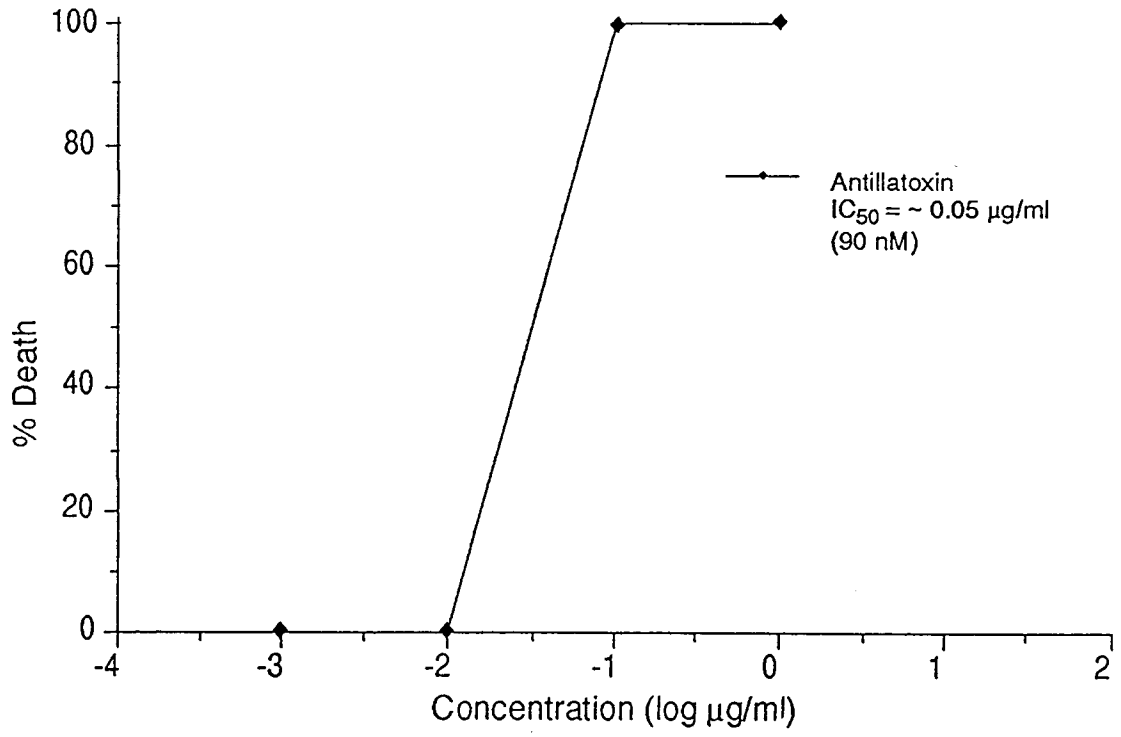

Figure V.28 Ichthyotoxic Effects of Antillatoxin (**40**).

Experimental

General Methods. UV spectra were recorded on a Hewlett Packard 8452A diode array spectrophotometer and IR spectra were recorded on a Nicolet 510 FT-IR spectrometer. CD measurements were obtained on a Jasco 41A spectropolarimeter. Low resolution mass spectra were obtained on either a Varian MAT CH7 spectrometer or by GC-MS using a Hewlett Packard 5890 Series II gas chromatograph and a 5971 mass selective detector. HRMS were obtained on a Kratos MS 50 TC. HPLC was performed using a M-6000 pump, U6K injector, and either a R401 differential refractometer or a lambda-Max 480 lc spectrophotometer. NMR data were obtained on either Bruker AC 300 or Bruker AM 400 spectrometers. ^{1}H NMR spectra were acquired with tetramethylsilane (TMS) as an internal chemical shift reference. ^{13}C spectra referenced to the center line of $CDCl_3$ at 77.0 ppm or C_6D_6 at 128.0 ppm. ^{13}C

assignments are based on ^{1}H-^{13}C HETCOR, DEPT multiplicity data, and comparison with previously identified derivatives. TLC-grade (10-40 μm) silica gel was used for vacuum chromatography and Kieselgel 60 silica (40-63 μm) was used for flash chromatography . Aluminum-backed thin-layer chromatography sheets were used for TLC, and all solvents were distilled prior to use.

Isolation of Curacin A (**18**). One liter of *Lyngbya majuscula* was collected from CARMABI beach, Curaçao, Netherlands Antilles, -0.3 m, 13 December 1991 and preserved in isopropyl alcohol. Compound **18** is named to reflect this site of collection. The collection was repetitively extracted with $CHCl_3$/MeOH (2:1, v/v) and a 543 mg batch of the extract was separated by successive tiers of silica gel vacuum chromatography. Fatty acid contaminants were separated by treatment with N_2CH_2/Et_2O and HPLC (5% EtOAc in hexanes, 2 x 30 cm Versapack Silica 10μ, collected elution volume 57-66 ml) to isolate curacin A (**18**, 44.2 mg, 8.1%).

Curacin A (**18**). FTIR ν_{max}^{film} cm^{-1}: 2928, 1618, 1439,1381, 1097, 1074, 1054, 964; $[\alpha]_D^{30}$ +86° (*c* 0.64, $CHCl_3$); UV $\lambda_{max}^{CH_3CN}$ nm: 242 (log ε = 4.60); CD (CH_3CN): Δε = -9.7, +16.4 (λ_{max} = 257, 229.5 nm); GC EIMS 70 eV *m/z* (rel. int.): 373 $[M]^+$ (3), 358 $[M - CH_3]^+$ (7), 342 $[M - OCH_3]^+$ (8), 332 (12), 300 (7), 288 (5), 274 (11), 180 $[M - C_{13}H_{21}O]^+$ (100) 166 (8), 140 (12), 119 (13), 105 (16), 91 (22), 79 (25); HR FABMS (positive ion, 3-nitrobenzyl alcohol) *m/z* obs. $[M + H]^+$ 374.2520 ($C_{23}H_{36}NOS$, 0.3 mmu dev.).

Partial Hydrogenation of Curacin A (**18**) with Pd on carbon to produce 15, 16-dihydrocuracin A (**19**). Compound **18** (14.39 mg, 38.6 μmol) was dissolved in absolute EtOH (0.50 mL) and 0.2 mg of Pd on activated carbon (5%, 0.094 μmol) was added. A balloon filled with H_2 was attached. After stirring for 3 h, the reaction was passed through a Celite® plug (1 cm) which was subsequently flushed with hexanes.

The solution was reduced *in vacuo*. Final purification by RP-HPLC (5-μ Partisil ODS C_{18} Silica column, 250 x 5.0 mm, 95% (v/v) MeOH in H_2O, UV detection at 254 nm; flow rate at 0.8 mL/min) provided 15, 16-dihydrocuracin A (**19**) as a colorless oil (0.21 mg, 0.56 μmol, 1.5% yield) and unreacted **18**.

15,16-dihydrocuracin A (**19**). FTIR ν_{max}^{film} cm^{-1}: 2929, 1617, 1449, 1439, 1380, 1093, 1074, 1053, 962; $[\alpha]_D^{30}$ +60° (*c* 0.22, $CHCl_3$); UV λ_{max}^{MeOH}nm: 241 (log ε = 4.57); UV $\lambda_{max}^{CH_3CN}$ nm: 242 (log ε = 4.53); CD (CH_3CN): Δε = -7.24, +13.1 (λ_{max} = 257, 229 nm); ^1H NMR (C_6D_6, 400 MHz) δ 6.41 (dd, 1H, *J* = 15.0, 10.8, H-8), 6.05 (bd, 1H, *J* = 10.8, 1-2, H-9), 5.70 (dd, 1H, *J* = 10.7, 9.0, H-3), 5.60 (dt, 1H, *J* = 15.0, 6.2, H-7), 5.46 (dt, 1H, *J* = 11.1, 6.3, H-4), 5.11 (bq, 1H, *J* ≈ 8-9, H-2), 3.22 (s, 3H, -OMe), 3.10 (dd, 1H, *J* = 10.7, 8.4, H-1b), 3.1 (m, 1H, H-13), 2.80 (dd, 1H, *J* = 10.7, 9.8, H-1a), 2.2 (m, 2H, H-11), 2.1 (m, 4H, H-5 and H-6), 1.74 (bs, 3H, H-17), 1.6-1.72 (m, 5H, H-12, H-15, and H-19), 1.41 (m, 2H, H-15), 1.23 (d, 3H, *J* = 6.1, H-22), 1.2 (m, 1H, H-20b), 0.95-1.04 (m, 1H, H-21), 0.76 (td, 1H, *J* = 8.1, 4.3, H-20a); ^{13}C NMR (C_6D_6, 100 MHz) δ 168.61 (C18), 136.62 (C10), 131.31 (2C, C3 and C7), 130.88 (C4), 127.72 (C8), 125.42 (C9), 80.20 (C13), 74.35 (C2), 56.18 (-OMe), 39.95 (C1), 35.98 (C14), 35.80 (C11), 33.13 (C6), 32.21 (C12), 28.15 (C5), 20.12 (C19), 18.79 (C15), 16.64 (C17), 15.97 (C21), 14.49 (C16), 14.23 (C20), 12.32 (C22); GC EIMS 70 eV *m/z* (rel. int.): 375 $[M]^+$ (6), 360 $[M - CH_3]^+$ (8), 344 $[M - OCH_3]^+$ (6), 302 (3), 288 (12), 274 (11), 180 $[M - C_{13}H_{23}O]^+$ (100) 166 (22), 140 (15), 107 (14), 93 (21), 79 (26), 67 $[C_5H_7]^+$ (12), 55 $[C_4H_7]^+$ (13); HR EIMS *m/z* obs. $[M]^+$ 375.2594 ($C_{23}H_{37}NOS$, -0.17 mmu dev.).

Selective Hydrogenation of Curacin A (**18**) with *Tris*-(triphenylphosphine)-rhodium (I) chloride, $[(C_6H_5)_3P]_3RhCl$, "Wilkinson's catalyst" and Ozonolysis to form methyoxy ketone derivative (**21**). Curacin A (**18**, 49.0 mg, 131 μmol) was dissolved

in absolute EtOH (0.50 mL), placed in a 4-dram vial, and a solution consisting of 11.3 mg of $[(C_6H_5)_3P]_3RhCl$, 99.99%, 12.2 μmol) in 0.50 ml dried CH_2Cl_2 was added. The mixture was diluted with an additional 2.5 ml CH_2Cl_2 and a balloon filled with H_2 was attached. After stirring for 7 h, the Wilkinson's catalyst was removed by eluting the reaction mixture through a silica plug (1 cm, TLC-grade) with 20 ml EtOH, then through a second plug with 20 ml Et_2O. GC-MS analysis of the recovered material showed it to consist primarily of 3,4,15,16-tetrahydrocuracin A (**20**). The product (55 mg) was reduced *in vacuo*, redissolved in 25% (v/v) MeOH in CH_2Cl_2 (ca. 4 ml), and cooled to -78 °C (acetone/CO_2 [s]). Ozone was bubbled through the solution (45 min, 0.2 L/min), at which time the solution was allowed to warm to 23 °C. Dimethyl sulfide (130 μL) was added to the ozonide mixture. The vial was stoppered and allowed to stand at RT overnight. After 18 hours, the solvent was carefully evaporated *in vacuo* (volatile product) and redissolved in pentane. The solution was subjected to silica gel flash chromatography using a stepwise gradient from 0 to 100% (v/v) Et_2O in pentane. The fraction eluting with 25% Et_2O in pentane was purified by HPLC (dual 10-μm Alltech Versapak Si columns; 300 x 4.1 mm; 10% (v/v) EtOAc in hexanes; UV detection at 254 nm; flow rate 2.5 mL/min) to give methyoxy ketone derivative (**21**) as a colorless oil (4.0 mg, 25.3 μmol, 19.3 % overall yield).

3,4,15,16-tetrahydrocuracin A (**20**). GC EIMS 70 eV *m/z* (rel. int.): 377 $[M]^+$ (31), 362 $[M - CH_3]^+$ (41), 346 $[M - OCH_3]^+$ (29), 334 $[M - C_3H_7]^+$ (12), 302 (12), 290 $[M - C_5H_{11}O]^+$ (33), 276 $[M - C_6H_{13}O]^+$ (67), 262 $[M - C_7H_{15}O]^+$ (14), 234 (20), 222 (12), 208 (33), 194 (28), 180 $[M - C_{13}H_{23}O]^+$ (40), 176 (50), 166 (35), 154 $[C_8H_{12}SN]^+$ (56), 140 $[C_7H_{10}SN]^+$ (100), 113 (17), 107 (27), 105 (31), 99 $[C_5H_7S]^+$ (21), 93 (45), 91 (40), 87 $[C_5H_{11}O]^+$ (52), 81 (39), 79 (51), 67 $[C_5H_7]^+$ (26), 55 $[C_4H_7]^+$ (36);

5-methoxyoctane-2-one (**21**). FTIR ν_{max}^{film} cm^{-1}: 2958, 2932, 2886, 2874, 1717, 1457, 1361, 1205, 1164, 1129, 1092; $[\alpha]_D^{28}$ +14.2° (*c* 0.22, $CDCl_3$); ^1H NMR ($CDCl_3$, 400 MHz) δ 3.30 (s, 3H, $-OCH_3$), 3.16 (ddd, 1H, *J* = 6, 5, 5, H-5), 2.50 (m, 2H, H-3), 2.15 (s, 3H, H-1), 1.79-1.87 (m, 1H), 1.67 (6-lines, 1H), 1.50 (m, 1H), 1.30-1.41 (m, 3H), 0.92 (t, 3H, *J* = 7.0, H-1); ^{13}C NMR ($CDCl_3$, 100 MHz) δ 208.92 (C-2), 79.75 (C-5), 56.39 (OCH_3), 39.28, 35.59, 29.94, 27.33, 18.52, 14.21 (C-8); GC EIMS 70 eV *m/z* (rel. int.): 143 $[M - CH_3]^+$ (6), 126 (2), 115 (100), 100 (13), 87 (39), 83 (38), 72 (28), 71 (18), 55 (35).

Formation of Dimethyl Sulfonate Derivative **27**. Curacin A (**18**, 13.0 mg, 34.9 μmol) was placed in a 4-dram glass vial, dissolved in 1.5 mL $CHCl_3$, and cooled to -77 °C (acetone/CO_2 [s]). Ozone was bubbled through the solution (2 min), at which time the solution was allowed to warm to 23 °C and reduced *in vacuo*. The ozonide was dissolved in AcOH (1.0 mL, glacial) to which H_2O_2 (0.3 mL, 30%) was added. The vial then was stoppered and placed in a sand bath at 45 °C. After 16 hours, the solvent was evaporated under N_2 at 45 °C, dissolved in MeOH (0.25 mL) and allowed to react with an excess of N_2CH_2/Et_2O (2 min.). The solution was then dried *in vacuo*, subjected to silica gel flash chromatography using a stepwise gradient from 10 to 100% (v/v) EtOAc in hexanes. The fractions eluting with 50 to 80% EtOAc in hexanes were combined and further purified by NP-HPLC (10-μ Phenomenex Maxsil Si column; 500 x 10.0 mm; 40% (v/v) EtOAc in hexanes; differential refractometer detection; flow rate at 6.0 mL/min) to give 2.1 mg pure derivative **27** (7.53 μmol, 21.6% yield). FTIR ν_{max}^{film} cm^{-1}: 3340, 1738, 1637, 1536, 1353, 1275, 1182, 1170, 996, 833; $[\alpha]_D^{25}$ -17.1° (*c* 0.12, MeOH); ^1H NMR ($CDCl_3$, 300 MHz) δ 6.62 (bd, 1H, *J* ≈ 6, N-H), 4.90 (dt, 1H, *J* = 7.3, 4.8, 4.7, H-2), 3.88 (s, 3H, $-SO_3C\underline{H}_3$), 3.82 (s, 3H, $-CO_2C\underline{H}_3$), 3.79 (d, 2H, *J* = 4.8, H-1), 1.55 (m, 1H, H-2′), 1.26 (m, 1H, H-4′), 1.16 (d, 3H, *J* =

6.1, H-5′), 0.95 (m, 2H, H-3′); ^{13}C NMR ($CDCl_3$, 75 MHz) δ 171.80, 169.16, 56.04, 53.23, 50.12 (C-1), 48.81, 20.29 (C-2′), 15.68 (C-4′), 13.00 (C-3′), 11.97 (C-5′); GC EIMS 70 eV *m/z* (rel. int.): 279 $[M]^+$ (7), 264 $[M - CH_3]^+$ (1), 248 $[M - OCH_3]^+$ (1), 220 $[M - CO_2CH_3]^+$ (18), 198 (43), 196 $[M - C_5H_7O]^+$ (9), 184 $[M - SO_3CH_3]^+$ (4), 164 (9), 138 (36), 83 $[C_5H_7O]^+$ (100), 55 (29); HR EIMS *m/z* obs. $[M]^+$ 279.0775 ($C_{10}H_{17}NO_6S$, -0.15 mmu dev.).

BIBLIOGRAPHY

1. Tyler, V.E.; Brady, L.R.; Robbers, J.E. *Pharmacognosy*, 9th ed. Lea and Febiger, Philadelphia, **1988**, p 519.

2. Scheuer, P.J., Ed. *Marine Natural Products: Chemical and Biological Perspectives*; Vols. I-V, Academic, New York, **1978-1983**.

3. Scheuer, P.J., Ed. *Bioorganic Marine Chemistry*; Vols. 1-4, Springer-Verlag, Berlin, **1987-1991**.

4. Scheuer, P.J., Ed. *Topics in Current Chemistry*, Vol. 167, Springer-Verlag, Berlin, **1993**, p 185.

5. Faulkner, D.J. *Tetrahedron.* **1977**, *33*, 1421.

6. Faulkner, D.J. *Nat. Prod. Rep.* **1984**, *1*, 251.

7. Faulkner, D.J. *Nat. Prod. Rep.* **1984**, *1*, 551.

8. Faulkner, D.J. *Nat. Prod. Rep.* **1986**, *3*, 1.

9. Faulkner, D.J. *Nat. Prod. Rep.* **1987**, *4*, 539.

10. Faulkner, D.J. *Nat. Prod. Rep.* **1988**, *5*, 613.

11. Faulkner, D.J. *Nat. Prod. Rep.* **1990**, *7*, 269.

12. Faulkner, D.J. *Nat. Prod. Rep.* **1991**, *8*, 97.

13. Faulkner, D.J. *Nat. Prod. Rep.* **1992**, *9*, 323.

14. Faulkner, D.J. *Nat. Prod. Rep.* **1993**, *10*, 497.

15. Martin, G.E.; Crouch, R.C. *J. Nat. Prod.* **1991**, *54*, 1.

16. Murata, M.; Naoki, H.; Iwashita, T.; Matsunaga, S.; Sakaki, M.; Yokoyama, A.; Yasumoto, T. *J. Am. Chem. Soc.* **1993**, *115*, 2060.

17. Crouch, R.C.; Martin, G.E. *J. Nat. Prod.* **1992**, *55*, 1343.

18. Fenical, W. *Chem. Rev.* **1993**, *93*, 1673.

19. Shimizu, Y. *Chem. Rev.* **1993**, *93*, 1685.

20. Gerwick, W.H.; Roberts, M.A.; Proteau, P.J.; Chen, J.L. *J. Appl. Phycol.* **1994**, *6*, 143.

21. Patterson, G.M.L.; Larsen, L.K.; Moore, R.E. *J. Appl. Phycol.* **1994**, *6*, 151.

22. Arasaki, S.; Arasaki, T. *Low Calorie, High Nutrition VEGATABLES FROM THE SEA to help you look and feel better*, Japan Publications, Inc., Tokyo, **1983**, p 196.

23. Scheuer, P.J. *Med. Res. Rev.* **1989**, *9*, 535, and references therein.

24. McGeer, E.G.; Olney, J.W.; McGeer, P.L., Eds. *Kainic Acid as a Tool in Neurobiology*, Raven Press, New York, **1978**.

25. Daigo, K. *Yakugaku Zasshi* **1959**, *79*, 350.

26. Maeada, M.; Kodama, T.; Tanaka, T.; Yoshizumi, H.; Takemoto, T.; Nomoto, K.; Fujita, T. *Tetrahedron Lett.* **1987**, *28*, 633.

27. Hashimoto, K. *Marine Toxins and Other Bioactive Marine Metabolites*, Japan Scientific Societies Press, Tokyo, **1959**, p 369, and references therein.

28. Girard, J.P.; Marion, C.; Liutkus, M.; Boucard, M.; Rechencq, E.; Vidal, J.P.; Rossi, J.C. *Planta Med.* **1988**, *54*, 193.

29. Hall, S.; Strichartz, G., Eds. *Marine Toxins: Origin, Structure, and Molecular Pharmacology* (ACS Symposium Series 418), American Chemical Society, Washington, DC, **1990**, p 377.

30. Tu, A.T., Ed. *Handbook of Natural Toxins, Vol. 3: Marine Toxins and Venoms*, Marcel, Dekker, Inc., New York, **1988**, p 587.

31. Tsuda, K.; Kawamura, M. *J. Pharm. Soc. Japan* **1952**, *72*, 187, 771.

32. Kao, C.Y.; Levinson, S.R., Eds. *Tetrodotoxin, Saxitoxin, and the Molecular Biology of the Sodium Channel*, The New York Academy of Sciences, New York, **1986**, p 445.

33. Trainer, V.L.; Edwards, R.A.; Szmant, A.M.; Stuart, A.M.; Mende, T.J.; Baden, D.G. *Brevitoxins: Unique Activators of Voltage-Sensitive Sodium Channels.* In *Marine Toxins: Origin, Structure, and Molecular Pharmacology*

(ACS Symposium Series 418), Hall, S. and Strichartz, G., Eds., American Chemical Society, Washington, DC, **1990**, pp 166-75.

34. Withers, N.W. *Ciguatera Fish Toxins and Poisoning.* In *Handbook of Natural Toxins, Vol. 3: Marine Toxins and Venoms*, Tu, A.T., Ed., Marcel, Dekker, Inc., New York, **1988**, pp 31-61.

35. Yasumoto, T.; Murata, M. *Chem. Rev.* **1993**, *93*, 1897.

36. Yotsu-Yamashita, M.; Haddock, R.L.; Yasumoto, T. *J. Am. Chem. Soc.* **1993**, *115*, 1147.

37. Pawlick, J.R. *Chem. Rev.* **1993**, *93*, 1911.

38. Paul, V.J., Ed. *Ecological Roles of Marine Natural Products*, Comstock Publishing Associates, Ithaca, **1992**, p 245.

39. Bergman, W.; Berke, D.C. *J. Org. Chem.* **1955**, *20*, 1501.

40. Pettit, G.R.; Inoue, M.; Kamano, Y.; Herald, D.L.; Arm, C.; Dufresne, C.; Christie, N.D.; Schmidt, J.M.; Doubek, D.L.; Krupa, T.S. *J. Am. Chem. Soc.* **1988**, *110*, 2006.

41. Suffness, M.; Thompson, J.E. *National Cancer Institute's Role in the Discovery of New Antineoplastic Agents.* In *Biomedical Importance of Marine Organisms*, Fautin, D.G., Ed., California Academy of Sciences, San Francisco, **1988**, pp 151-7.

42. Suffness, M.; Newman, D.J.; Snader, K. *Discovery and Development of Antineoplastic Agents from Natural Sources.* In *Bioorganic Marine Chemistry*; Vol. 3, Scheuer, P.J., Ed., Springer-Verlag, Berlin, **1989**, pp 131-68.

43. Fuller, R.W.; Cardellina, J.H. II; Kato, Y.; Brinen, L.S.; Clardy, J.; Snader, K.M.; Boyd, M.R. *J. Med. Chem.* **1992**, *35*, 3007.

44. Gerwick, W.H.; Moghaddam, M.F.; Hamberg, M. *Arch. Biochem. Biophys.* **1991**, *290*, 436.

45. Gerwick, W.H.; Nagle, D.G.; Proteau, P.J. *Oxylipins from Marine Invertebrates.* In *Topics in Current Chemistry*, Vol. 167.; Scheuer, P.J., Ed.; Springer-Verlag: Berlin, **1993**, pp. 117-80.

46. Campbell, W.B. *Lipid-Derived Autocoids: Eicosanoids and Platelet-Activating Factor.* In *The Pharmacological Basis of Therapeutics*, 8th Ed., Gilman, A.G.,

Rall, T.W., Nies, A.S., and Taylor, P., Eds., Pergamon Press, New York, **1990**, pp 600-17.

47. Weinheimer, A.J.; Spraggins, R.L. *Tetrahedron Lett.* **1969**, 5185.

48. Rychnovsky, S.D.; Skalitsky, D.J.; Pathirana, C.; Jensen, P.R.; Fenical, W. *J. Am. Chem. Soc.* **1992**, *114*, 671.

49. Ruggieri, B.; Thoroughgood, C.A. *Mar. Ecol. Prog. Ser.* **1985**, *23*, 310.

50. Brown, J.A.; Gray, C.J.; Hattersley, G.; Robinson, J. *Gen. Comp. Endocrinol.* **1991**, *84*, 328.

51. Gerwick, W.H.; Bernart, M.W.; Moghaddam, M.F.; Jiang, Z.D.; Solem, M.L.; Nagle, D.G. *Hydrobiologia* **1990**, *204/205*, 621.

52. Gerwick, W.H.; Proteau, P.J.; Nagle, D.G.; Wise, M.L.; Jiang, Z.D.; Bernart, M.W.; Hamberg, M. *Hydrobiologia* **1993**, *260/261*, 653.

53. Gerwick, W.H.; Bernart, M.W. *Eicosanoids and Related Compounds from Algae.* In *Marine Biotechnology, Vol. 1: Pharmaceutical and Bioactive Natural Products*, Attaway, D.H. and Zaborsky, O.R., Eds., Plenum Press, New York, **1993**, pp 101-52.

54. Gerwick, W.H. *Chem. Rev.* **1993**, *93*, 1807.

55. Gerwick, W.H. *Biochim. Biophys. Acta* **1994**, *1211*, 243.

56. Munro, M.H.G.; Luibrand, R.T.; Blunt, J.W. *The search for antiviral and anticancer compounds from marine organisms.* In *Bioorganic marine chemistry*, Vol 1, Scheuer, P.J., Ed., Springer-Verlag, New York, **1987**, p 93-176.

57. Corey, E.J. *Pure Appl. Chem.* **1987**, *59*, 269.

58. Wilson, H.V. *J. Exp. Zool.* **1907**, *5*, 245.

59. Wilson, H.V. *J. Exp. Zool.* **1910**, *9*, 537.

60. Wilson, H.V.; Penney, J.T. *J. Exp. Zool.* **1930**, *56*, 73.

61. Galtsoff, P.S. *J. Exp. Zool.* **1925**, *42*, 183.

62. Curtis, A.S.G. *Nature* **1962**, *196*, 245.

63. Spiegel, M. *Ann. NY Acad. Sci.* **1955**, *60*, 1056.

64. Serhan, C.N.; Korchak, H.M.; Weissmann, G. *J. Immunol.* **1980**, *125*, 2020.

65. Dunham, P.; Anderson, C.; Rich, A.M.; Weissmann, G. *Proc. Natl. Acad. Sci. USA* **1983**, *80*, 4756.

66. Serhan, C.N.; Fridovich, J.; Goetzl, E.J.; Dunham, P.B.; Weissmann, G. *J. Biol. Chem.* **1982**, *257*, 4746.

67. Rich, A.M.; Weissmann, G.; Anderson, C.; Vosshall, L.; Haines, K.A.; Humphreys, T.; Dunham, P. *Biochem. Biophys. Res. Commun.* **1884**, *121*, 863.

68. Stanley-Samuelson, D.W. *Am. J. Physiol.* **1991**, *260*, R849.

69. Shimizu, T.; Wolfe, L.S. *J. Neurochem.* **1990**, *55*, 1.

70. Piomelli, D. *Am. J. Physiol.* **1991**, R849.

71. Piomelli, D.; Shapiro, E.; Feinmark, S.T.; Schwartz, J.H. *J. Neurosci.* **1987**, *7*, 3675.

72. Piomelli, D.; Volterra, A.; Dale, N.; Siegelbaum, S.A.; Kandel, E.R.; Schwartz, J.H.; Belardetti, F. *Nature* **1987**, *328*, 38.

73. Sweatt, D.; Volterra, A.; Siegelbaum, S.A.; Kandel, E.R. (1988) *Cold Spring Harbor Symp. Quant. Biol.* **1988**, *53*, 395.

74. Belardetti, F.; Campell, W.B.; Falck, J.R.; Demontis, G.; Rosolowsky, M. *Neuron* **1989**, *3*, 497.

75. Piomelli, D.; Feinmark, S.T.; Shapiro, E.; Schwartz, J.H. *J. Biol. Chem.* **1988**, *263*, 16591.

76. Piomelli, D.; Shapiro, E.; Zipkin, R.; Schwartz, J.H.; Feinmark, S.T. *Proc. Natl. Acad. Sci. USA* **1989**, *86*, 1721.

77. Piomelli, D.; Feinmark, S.T.; Shapiro, E.; Schwartz, J.H. *Ann. NY Acad. Sci.* **1989**, *559*, 208.

78. Feinmark, S.T.; Piomelli, D.; Shapiro, E.; Schwartz, J.H. *Ann. NY Acad. Sci.* **1989**, *559*, 121.

79. Gerhart, D.J. *Mar. Ecol. Prog. Ser.* **1984**, *19*, 181.

80. Cimino, G.; Sodano, G. *Chemica Scripta* **1989**, *29*, 389.

81. Karuso, P. *Chemical ecology of the nudibranchs.* In *Bioorganic marine chemistry*, Vol. 1, Scheuer, P.J., Ed., Springer-Verlag, New York, **1987**, pp 31-60.

82. Faulkner, D.J. *Feeding deterrents in molluscs.* In *Biomedical importance of marine organisms.* Fautin, D.G., Ed., California Academy of Sciences, San Francisco, **1988**, pp 29-36.

83. Faulkner, D.J.; Ghiselin, M.T. *Mar. Ecol. Prog. Ser.* **1983**, *13*, 295.

84. Schulte, G.R.; Scheuer, P.J. *Tetrahedron* **1982**, *38*, 1857.

85. Marin, A.; Di Marzo, V.; Cimino, G. *Mar. Biol.* **1991**, *111*, 353.

86. Clare, A.S.; Walker, G.; Holland, D.L.; Crisp, D.J. *Mar. Biol. Lett.* **1982**, *3*, 113.

87. Holland, D.L.; East, J.; Gibson, K.H.; Clayton, E.; Oldfield, A. *Prostaglandins* **1985**, *29*, 1021.

88. Gardner, H.W. *Biochim. Biophys. Acta* **1991**, *1084*, 221.

89. Beardley, T. *Scientific American* **1994**, *270:1*, 130.

90. Boyd, M.R. *The future of new drug development.* In *Current Therapy in Oncology*, Neiderhuber, J.E., Ed., B.C. Decker, Inc., Philadelphia, **1992**, pp 11-22.

91. Burkholder, P.R.; Ruetzler, K. *Nature*, London. **1969**, *222*, 983.

92. Bergquist, P.R.; Bedford, J.J. *Mar. Biol.* **1978**, *46*, 215.

93. Marston A.; Hostettmann, H. *Assays for Molluscicidal, Cercaricidal, Schistosomicidal and piscicidal Activities.* In *Methods in Plant Biochemistry*, Hostettmann, K. Ed., Academic Press Inc., San Diego, **1991**, pp. 153-78.

94. Backus, G.J.; Green, G. *Science* **1974**, *185*, 951.

95. Marston A.; Hostettmann, H. *Phytochemistry* **1985**, *24*, 639.

96. Benenson, A.S. Ed. *Control of Communicable Diseases in Man.* 14th ed., Americn Public Health Association, Washington, D.C., **1985**, pp. 344-6.

97. WHO *Bull. WHO* **1965**, *33*, 567.

98. Meyer, B.N.; Ferrigni, J.E.; Putnam, J.E.; Jacobson, L.B.; Nichols, D.E.; McLaughlin, J.L. *Planta Med.* **1982**, *45*, 31.

99. McLaughlin, J.L. *Crown Gall Tumors on Potato Discs and Brine Shrimp Lethality: Two Simple Bioassays for Higher Plant Screening and Fractionation.* In *Methods in Plant Biochemistry*, Hostettmann, K. Ed., Academic Press Inc., San Diego, **1991**, pp. 8-32.

100. Lui, M.S.; Faderan, M.A.; Liepniks, J.J.; Natsumeda, Y.; Olah, E.; Jayaram, H.N.; Weber, G. *J. Biol. Chem.* **1984**, *259*, 5078.

101. Morris, R.E.; Wang, J.; Blum, J.R.; Flavin, T.; Murphy, M.P; Almquist, S.J.; Chu, N.; Tam, Y.L.; Kaloostain, M.; Allison, A.C.; Eugui, E.M. *Transplant. Proc.* **1991**, *23*, 19.

102. Ikegami, T.; Natsumeda, Y.; Weber, G. *Anal. Biochem.* **1985**, *150*, 155.

103. Powis, G. *Trends Pharmacol. Sci.* **1991**, *12*, 188.

104. Wong, T.W.; Goldberg, A.R. *J. Biol. Chem.* **1983**, *258*, 1022.

105. Lee, R.H.; Slate, D.L.; Moretti, R.; Alvi, K.A.; Crews, P. *Biochem. Biophys. Res. Commun.* **1992**, *184*, 765.

106. Boyd, M.R. *Status of the NCI Preclinical Antitumor Drug Discovery Screen.* In *Principles and Practice of Oncology Updates*, Vol. 3, No.10, DeVita, V.T., Jr., Hellman, S., Rosenberg, S.A., Eds., Lippincott, Philadelphia, **1989**, pp 1-12.

107. Lopez, A. *The Natural Products Chemistry of the Red Alga Ptilota filicina and Laurencia obtusa.*, M.S. Thesis, Oregon State University, Corvallis, **1987**.

108. Gerwick, W.H.; Proteau, P.J.; Nagle, D.G.; Hamel, E.; Blokhin, A.; Slate, D. *J. Org. Chem.* **1994**, *59*, 1243.

109. Hamel, E.; Blokhin, A.V.; Nagle, D.G.; Yoo, H.-D.; Gerwick, W.H. *Drug Dev. Res.* (in press).

110. Bundy, G.L. *Adv. Prostaglandin Thromboxane Leukotriene Res.* **1985**, *14*, 229.

111. Gerwick, W.H.; Moghaddam, M.F.; Hamberg, M. *Arch. Biochem. Biophys.* **1991**, *290*, 436.

112. Niwa, H.; Wakamatsu, K.; Yamada, K. *Tetrahedron Lett.* **1989**, *30*, 4543.

113. Kigoshi, H.; Niwa, H.; Yamada, K.; Stout, T.J.; Clardy, J. *Tetrahedron Lett.* **1991**, *32*, 2427.

114. Brash, A.R. *J. Am. Chem. Soc.* **1989**, *111*, 1891.

115. Ojika, M.; Yoshida, Y.; Nakayama, Y.; Yamada, K. *Tetrahedron Lett.* **1990**, *31*, 4907.

116. Ojika, M.; Yoshida, Y.; Nakayama, Y.; Yamada, K. *Tennen Yuki Kagobutsu Toronkai Koen Yoshishu* **1989**, *31*, 664.

117. Higgs, M.D.; Mulheirn, L.J. *Tetrahedron* **1981**, *37*, 4259.

118. Fusetani, N.; Hashimoto, K. *Bulletin Jap. Soc. Sci., Fish.* **1984**, *50*, 465.

119. Gregson, R.P.; Marwood, J.F.; Quinn, R.J. *Tetrahedron Lett.* **1979**, *46*, 4505.

120. Thermo Company, Ltd. *Chem. Abs.* **1984**, *101*:14827n.

121. Kurata, K.; Taniguchi, K.; Shiraishi, K; Hayama, N.; Tanaka, I.; Susuki, M. *Chem. Lett.* **1989**, 267.

122. Kurata, K.; Taniguchi, K.; Shiraishi, K; Susuki, M. *Phytochemistry* **1993**, *33*, 267.

123. Todd, J.S.; Proteau, P.J.; Gerwick, W.H. *Tetrahedron Lett.* **1993**, *34*, 7689.

124. Nagle, D.G.; Gerwick, W.H. *Tetrahedron Lett.* **1990**, *31*, 2995.

125. Nagle, D.G.; Gerwick, W.H. *J. Org. Chem.* in press.

126. Nagle, D.G.; Gerwick, W.H. Manuscript in preparation.

127. Powell, J.H. *The Life History of the Red Alga* Constantinea, Ph.D. Thesis, University of Washington, Seattle, **1964**.

128. Powell, J.H. *Amer. Zool. 1986, 26*, 479.

129. Pueschel, C.M.; Cole, K.M. *J. Ultrastruct. Res.* **1980**, *73*, 282.

130. Pueschel, C.M.; Parthasarathy, M.V. *Phycologia* **1984**, *23*, 465.

131. Seckback, J. *J. Ultrastruct. Res.* **1972**, *39*, 65.

132. Ehresmann, D.W.; Deig, E.F.; Hatch, M.T.; DiSalvo, L.H.; Vedros, N.A. *J. Phycol.* **1977**, *13*, 37.

133. Marchant, H.J.; Fowke, L.C. *Can. J. Bot.* **1977**, *55*, 3080.

134. White, J.D.; Jensen, M.S. *J. Am. Chem. Soc.* **1993**, *115*, 2970.

135. Harada, N.; Nakanishi, K. *Circular Dichroic Spectroscopy-Exciton Coupling in Organic Stereochemistry*, University Science Books, Mill Valley, California, **1983**, p 460.

136. Gonnella, N.C.; Nakanishi, K.; Martin, V.S.; Sharpless, K.B. *J. Am. Chem. Soc.* **1982**, *104*, 3775.

137. Gung, B.W.; Karipides, A.; Wolf, M.A. *Tetrahedron Lett.* **1992**, *33*, 713.

138. Chuche, J.; Dana, G.; Monot, M.R. *Bull. Soc. Chim. France* **1967**, *9*, 3300.

139. Proteau, P.J.; Rossi, J.V.; Gerwick, W.H. *J. Nat. Prod.*, in press.

140. Marchant, H.J.; Fowke, L.C. *Can. J. Bot.* **1977**, *55*, 3080.

141. Hamberg, M.; Gerwick, W.H.; Asen, P.A. *Lipids* **1992**, *27*, 487.

142. Oliw, E.H.; Brodowsky, I.D.; Hornsten, L.; Hamberg, M. *Biochem. Biophys.* **1993**, *300*, 434.

143. Moghaddam, M.F.; Gerwick, W.H. *J. Nat. Prod.* **1991**, *54*, 1619.

144. Hughes, T.P. *Science* **1994**, *265*, 1547.

145. Morse, A.N.C.; Froyd, C.A.; Morse, D.E. *Marine Biology* **1984**, *81*, 293.

146. Lindquist, N.; Fenical, W.; Sesin, D.F.; Ireland, C.M.; Van Duyne, G.D.; Forsyth, C.J.; Clardy, J. *J. Am. Chem. Soc.* **1988**, *110*, 1308.

147. Butler, M.S.; Capon, R.J. *Aust. J. Chem.* **1992**, *45*, 1705.

148. De Silva, E.D.; Scheuer, P.J. *Tetrahedron Lett.* **1981**, *22*, 3147.

149. Hamada, T.; Kusumi, T.; Ishitsuka, M.O.; Kakisawa, H. *Chem. Lett.* **1992**, 33.

150. Kobayashi, J.; Zeng, C.; Ishibashi, M.; Sasaki, T. *J. Nat. Prod.* **1993**, *56*, 436.

151. Tsuda, M.; Shigemori, H.; Ishibashi, M.; Sasaki, T.; Kobayashi, J. *J. Org. Chem.* **1992**, *57*, 3503.

152. König, G.M.; Wright, A.; Sticher, O. *J. Nat. Prod.* **1992**, *55*, 174.

153. Paul, V.J.; Littler, M.M.; Littler, D.S.; Fenical, W. *J. Chem. Ecol.*, **1987**, *13*, 1171.

154. Dunlop, R.W.; Wells, R.J. *Aust. J. Chem.* **1979**, *32*, 1345.

155. Needham, J.; Andersen, R.J.; Kelly, M.T. *Tetrahedron Lett.* **1991**, *32*, 315.

156. Preserved voucher specimens were found to consist almost exclusively of a *Synechocystis*-type unicellular cyanobacterium. However, the tunicate symbiont *Prochloron* is a prochlorophyte which is remarkably similar to this species (Lewin, R.A. and Cheng, L., eds. *Prochloron a Microbial Enigma* Chapman and Hall, Inc., New York, **1989**, pp. 129). Several other minor cyanobacteria and diatoms were also found in the algal mat. Attempts to produce nakienones from cultured species have been unsuccessful.

157. Norte, M.; Rodriguez, M.L.; Fernández, J.J.; Egure, L.; Estrada, D.M. *Tetrahedron* **1988**, *44*, 4973.

158. Wratten, S.J.; Faulkner, D.J. *Tetrahedron Lett.* **1978**, 961.

159. Gerwick, W.H.; Fenical, W. *J. Org. Chem.* **1983**, *48*, 3325.

160. Rinehart, K.L.; Namikoshi, M.; Choi, B.W. *J. Appl. Phycol.* **1994**, *6*, 159.

161. Carmichael. W.W.; Jones, C.L.A.; Mahmood, N.A.; Theiss, W.W. "*Algal toxins and water-based diseases.*" In *Critical Reviews in Environmental Control*, 15 (3), C.P. Straub (Ed.), CRC Press, Boca Raton, Florida, **1985**, pp. 275-313.

162. Rinehart, K.L.; Harada, K.; Namikoshi, M.; Chen, C.; Harvis, C.A.; Munro,

M.H.G.; Blunt, J.W.; Mulligan P.E.; Beasly, V.R.; Dahlem, A.M.; Carmichael, W.W. *J. Am. Chem. Soc.* **1988**, 110, 8557.

163. Namikoshi, M.; Choi, B.W.; Sakai, R.; Sun, F.; Rinehart, K.L.; Carmichael, W.W.; Evans, W.R.; Cruz, P.; Munro, M.H.G.; Blunt, J.W. *J. Am. Chem. Soc.* **1994**, 116.

164. MacKintosh, C.; Beattle, K.A.; Klumpp, S.; Cohen, P.; Codd, G.A. *Biochem. Biophys. Res. Commun.* **1990**, *264*, 187.

165. Krishnamurthy, T.; Carmichael, W.W.; Sarver, E.W. *Toxicon* **1986**, *24*, 865.

166. DeSilva, E.D.; Willams, D.E.; Andersen, R.J.; Klix, H.; Holmes, C.F.B.; Allen, T.M. *Tetrahedron Lett.* **1992**, *33*, 1561.

167. Harada, K.; Mayumi, T.; Shimada, T.; Suzuki, M.; Kondo, F.; Park, H.D.; Watanabe, M.F. *Tennen Yuki Kagobutsu Toronkai Koen Yoshishu* **1993**, *35*, 377, and references therein.

168. Ohtani, I.; Moore, R.E.; Runnegar, M.T.C. *J. Am. Chem. Soc.* **1992**, 114, 7941.

169. Huber, C.S. *Acta Crystallographica* **1972**, *B28*, 2582.

170. Devlin, J.P.; Edwards, O.E.; Gorham, P.R.; Hunter, N.R.; Pike, R.K.; Stavric, B. *Can. J. Chem.* **1977**, *55*, 1367.

171. Matsunaga, S.; Moore, R.E.; Niemczura, W.P.; Carmichael, W.W. *J. Am. Chem. Soc.* **1989**, *111*, 8021.

172. Moore, R.E. *Pure Appl. Chem.* **1982**, *54*, 1919.

173. Cardellina II, J.H.; Marner, F.-J.; Moore, R.E. *Science* **1979**, *204*, 193.

174. Mynderse, J.S.; Moore, R.E.; Kashiwagi, M.; Norton, T.R. *Science* **1977**, *196*, 538.

175. Prinsep, M.R.; Moore, R.E.; Levine, I.A.; Patterson, G.M.L. *J. Nat. Prod.* **1992**, *55*, 140.

176. Prinsep, M.R.; Caplan, F.R.; Moore, R.E.; Patterson, G.M.L.; Smith, C.D. *J. Am. Chem. Soc.* **1992**, *114*, 385.

177. Ishibashi, M.; Moore, R.E.; Patterson, G.M.L.; Xu, C.; Clardy, J. *J. Org. Chem.* **1986**, *51*, 5300.

178. Carmeli, S.; Moore, R.E.; Patterson, G.M.L. *J. Nat. Prod.* **1990**, *53*, 1533.

179. Patterson, G.M.L.; Carmeli, S. *Arch. Microbiol.* **1992**, *157*, 406.

180. Jung, J.H.; Moore, R.E.; Patterson, G.M.L. *Phytochemistry* **1991**, *30*, 3615.

181. Patterson, G.M.L.; Smith, C.D.; Kimura, L.H.; Britton, B.A.; Carmeli, S. *Cell Motil.Cytoskeleton* **1993**, *24*, 39.

182. Hemscheidt, T.; Puglosi, M.P.; Larsen, L.K.; Patterson, G.M.L.; Moore, R.E.; Rios, J.L.; Clardy, J. *J. Org. Chem.* **1994**, *59*, 3467.

183. Gerwick, W. H.; Jiang, Z.D.; Agarwal, S.K.; Farmer, B.T. *Tetrahedron* **1992**, *48*, 2313.

184. Gerwick, W.H.; Lopez, A.; Van Duyne, G.D.; Clardy, J.; Ortiz, W.; Baez, A. *Tetrahedron Lett.* **1986**, *27*, 1979.

185. Gerwick, W.H. *J. Nat. Prod.* **1989**, *52*, 252.

186. Gerwick, W.H.; Reyes, S.; Alvarado, B. *Phytochemistry* **1987**, *26*, 1701.

187. Chen, J.L.; Proteau, P.J.; Roberts, M.A.; Gerwick, W.H.; Slate, D.L.; Lee, Rita, H. *J. Nat. Prod.* **1994**, *57*, 524.

188. Bruno, N.A.; Slate, D.L.; *J. Natl. Cancer Inst.* **1990**, *82*, 419.

189. Hawkins, C.J.; Levin, M.F.; Marshall, K.A.; van den Brenk, A.L.; Watters, D.J. *J. Med. Chem.* **1990**, *33*, 1634.

190. Jalal, M.A.F.; Hossain, M.B.; van der Helm, D.; Sanders-Loehr, J.; Actis, L.A.; Crosa, J.H. *J. Am. Chem. Soc.* **1989**, *111*, 292.

191. Paull, K.D.; Shoemaker, R.H.; Hodes, L.; Monks, A.; Scudiero, D.A.; Rubenstein, L.; Plowman, J.; Boyd, M.R. *J. Natl. Cancer Inst.* **1989**, *81*, 1088.

192. Paull, K.D.; Lin, C.M.; Malspeis, L.; Hamel, E. *Cancer Res.* **1992**, *52*, 3892.

193. Hamel, E.; Lin, C.M. *Biochemistry* **1984**, *23*, 4173.

194. Sackett, D.L. *Pharmacol. Ther.*, in press.

195. Hamel, E. *Pharmacol. Ther.* **1992**, *55*, 31.

196. Roush, W.R.; Walts, A.E.; Hoong, L.K. *J. Am. Chem. Soc.* **1985**, *107*, 8186.

197. Negishi, E.-i.; Van Horn, D.E.; King, A.O.; Okukado, N. *Synthesis* **1979**, 501.

198. Charette, A.B.; Juteau, H. *J. Am. Chem. Soc.* **1994**, *116*, 2651.

199. Griffith, W. P.; Ley, S.V.; Whitcombe, G.P.; White, A.D. *J. Chem. Soc., Chem. Commun.* **1987**, 1625.

200. Lindgren, B.O.; Nilsson, T. *Acta Chem. Scand.* **1973**, *27*, 888.

201 Kraus, G.A.; Taschner, H.J. *J. Org. Chem.* **1980**, *45*, 1175.

202. Windridge, G.C.; Jorgensen, E.C. *J. Am. Chem. Soc.* **1971**, *93*, 6318.

203. Zabriskie, T.M.; Mayne, C.L.; Ireland, C.M. *J. Am. Chem. Soc.* **1988**, *110*, 7919.

204. Moore, R.E. *Constituents of Blue-Green algae.* In *Marine Natural Products: Chemical and Biological Perspectives*, Vol. IV, Scheuer, P.J., Ed., Academic Press, New York, **1981**, pp 1-54.

205. Cardellina II, J.H.; Dalietos, D.; Marner, F.J.; Mynderse, J.S.; Moore, R.E. *Phytochemistry* **1978**, *17*, 2091.

206. Cardellina II, J.H.; Marner, F.J.; Moore, R.E. *J. Am. Chem. Soc.* **1979**, *101*, 240.

207. Ainsle, R.D.; Barchi Jr., J.J.; Kuniyoshi, M.; Moore, R.E.; Mynderse, J.S. *J. Org. Chem.* **1985**, *50*, 2859.

208. Mynderse, J.S.; Moore, R.E. *J. Org. Chem.* **1978**, *43*, 4359.

209. Praud, A.; Valls, R.; Piovetti, L.; Banaigs, B. *Tetrahedron Lett.* **1993**, *34*, 5437.

210. Rose, A.F.; Scheuer, P.J.; Springer, J.P.; Clardy, J. *J. Am. Chem. Soc.* **1978**, *100*, 7665.

211. Wylie, C.R.; Paul, V.J. *Ecol. Prog. Ser.* **1988**, *45*, 23.

APPENDIX

APPENDIX

NEW SPHINGOLIPIDS FROM THE OREGON MARINE SPONGE *HALICHONDRIA PANICEA*

Abstract

A novel sphingolipid containing an *iso*-fatty acid, (4*E*, 8*E*)-N-13′-methyl-tetradecanoyl-1-O-β-D-galactopyranosyl-4-sphingadiene, was isolated from the Oregon marine sponge *Halichondria panicea* and its structure determined using a combination of spectroscopic and chemical degradation techniques. A second galactosyl-ceramide which contained an unusually long chain fatty acid amide component was also isolated from *H. panicea*.

Introduction

Sponges have long been recognized to be a rich source of structurally novel lipids including unique sterols, fatty acids, phospholipids, and triglycerides.[1-3] The major point of structural novelty in sponge sterols is the incorporation of additional carbon atoms as branches on the side chain. Further, the unique fatty acids, either in free form or as present in phospholipids and triglycerides, not only incorporate additional branch carbons, but many are of unusual length with unique patterns of unsaturation. These findings suggest that fundamental differences may exist between sponge membranes and those of all other animals. While the presence of sphingolipids in sponges was first suggested from TLC evidence over twenty years ago,[4,5] structural proof for the existence of cerebrosides in sponges was not provided until the mid-seventies.[6] Recently, *Halichondria japonica* has been shown to contain galactosylceramides with branches in the sphingosine base portion.[7]

Results and Discussion

As part of our continuing evaluation of the chemistry of Pacific Northwest marine organisms,[8] the lipid extract of the marine sponge *Halichondria panicea* Pallas (Homorrhaphidae, Demospongiae) was found to possess several interesting acid-charring compounds by TLC and appeared to warrant further investigation. Herein we report our isolation and structure elucidation of a novel galactopyranosyl-(β1-1′)-ceramide from this temperate water sponge which contains an *iso*-fatty acyl group.

The $CHCl_3$-MeOH (2:1) extract of *H. panicea* was largely a complex mixture of homologous glycolipids (21%). These were separated following acetylation of the crude mixture (Ac_2O-pyridine) by repeated Si gel vacuum chromatographic separation and rp-hplc. High field ^{1}H-NMR analysis of the glycolipid mixture before acetylation showed there to be no acetate groups of natural origin. In this fashion, the polar acid-charring

compound (**1**) was first isolated as the optically active per-acetate derivative (**2**, Figure A.1), and its molecular formula determined as $C_{49}H_{83}O_{13}N_1$ by negative ion hr-FABMS.

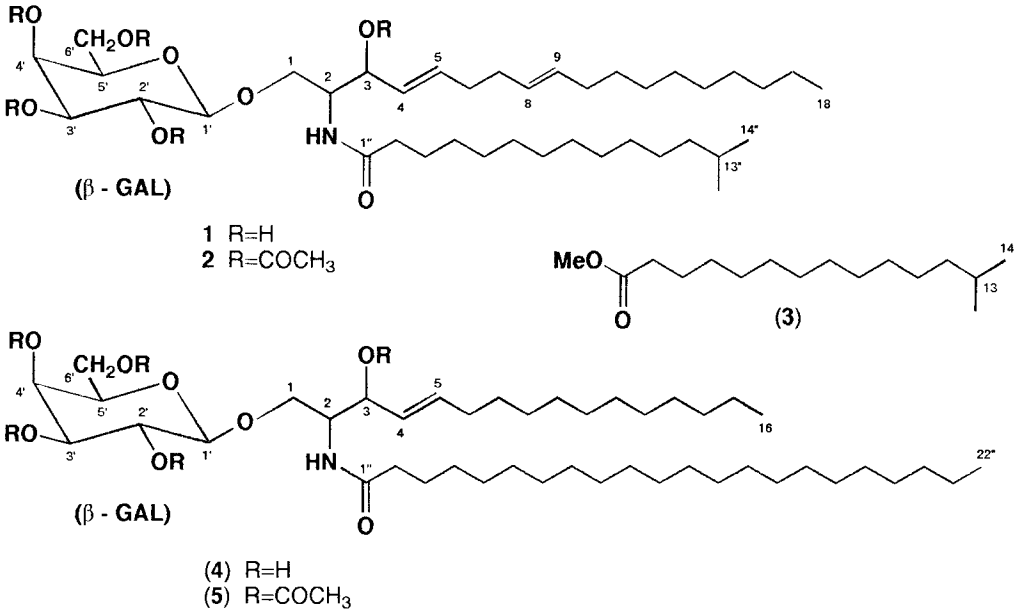

Figure A.1 Structures of *Halichondria panicea* Sphingolipids.

Four spin systems were determined in **2** from analysis of the ^1H-^1H COSY (Table A.1). The first ^1H-^1H spin system was that of a sugar moiety, assigned as the tetra-acetate ester of a β-galactopyranosyl residue from $^3J_{HH}$ values and a comparison to models.[9,10] From observation of a correlation between the signals at δ 4.34 (m, H-2) and δ 5.72 (d, J = 4.2, N-H) a second spin system was established as the C-3 acetate ester of a mono-unsaturated sphingosine base unit.

A third spin system was assigned as a saturated ceramide acyl group. A 6H signal in the methyl region, δ 0.86 (d, J = 6.6), was correlated to a methine resonance at δ 1.51 (m) and suggested that either the sphingosine base or the acyl chain contained a terminal gem-dimethyl group. Overlap in the methylene region made placement of the gem-dimethyl group and chain length determination impossible from ^1H-NMR alone.

Table A.1 ^{1}H and ^{13}C NMR Data for Derivative 2[a].

C#	^{1}H NMR	^{13}C NMR
	Sphingosine Base	
1(A)	3.58 dd (10.4, 4.5)	67.14
(B)	3.94 dd (10.4, 4.2)	
2	4.34 m	50.52
3	5.26 t (6.8)	73.76
4	5.4 m	124.92
5	5.80 dt (15.3, 6.2)	136.25
6	2.1 m	32.44[b]
7	2.05 m	32.03[b]
8	5.39 m	128.98
9	5.41 m	131.28
10	1.96 q (6.6)	32.63
11	1.3 m	29.2-.9[c]
12	1.26 m	29.2-.9[c]
13	1.26 m	29.2-.9[c]
14	1.26 m	29.2-.9[c]
15	1.26 m	29.2-.9[c]
16	1.26 m	29.2-.9[c]
17	1.25 m	29.2-.9[c]
18	0.88 t (6.5)	14.12
	Sugar	
1′	4.44 d (7.8)	101.03
2′	5.15 dd (10.4, 7.8)	68.88
3′	5.00 dd (10.4, 3.2)	70.76
4′	5.4 m	66.95
5′	3.90 t (6.6)	70.76
6′	4.13 dd (6.6)	61.24
	Fatty Acid	
N-H	5.72 d (4.2)	-----
1″	-----	172.68
2″	2.14 m	36.89
3″	1.62 m	25.72
4″	1.3 m	29.2-.9[c]
5″	1.26 m	29.2-.9[c]
6″	1.26 m	29.2-.9[c]
7″	1.26 m	29.2-.9[c]
8″	1.26 m	29.2-.9[c]
9″	1.26 m	29.2-.9[c]
10″	1.26 m	29.2-.9[c]
11″	1.26 m	29.2-.9[c]
12″	1.14 q (6.8)	39.09
13″	1.51 m	27.99
14″,15″	0.86 d (6.6) 6H	22.66 (2C)
	Acetate Esters	
	2.17 s	21.12[d] 170
	2.06 s	20.83[d] 170
	2.05 s	20.67[d] 170
	2.05 s	20.67[d] 170
	1.99 s	20.65[d] 170

a) All ^{1}H NMR spectra recorded at 400 MHz and ^{13}C NMR spectra at 100 MHz in $CDCl_3$ with 0.05% TMS as internal chemical shift reference.

b-d) Values with the same superscript may be interchanged.

However, the positional attachments of the sugar, sphingolipid base, and fatty acid amide moieties were established from spectroscopic comparison with well characterized galactopyranosyl-(β1-1′)-ceramide analogues.[6,10,11]

The length and branching pattern of the fatty acyl chain was determined by base hydrolysis of derivative **2** (10% KOH in EtOH-H_2O), methylation (CH_2N_2 in Et_2O), and lr-GCMS. Although, the lr-MS fragmentation pattern for this fatty acid methyl ester (**3**) gave a 93% match with that of a standard sample of methyl *n*-pentadecanoic acid, the presence of a gem-dimethyl group in **3** was confirmed by ^{1}H-NMR analysis which established its structure as the methyl ester of 13-methyl-tetradecanoic acid (*iso*-pentadecanoic acid).

The trans (*E*) configuration of the C-4 and C-8 double bonds in derivative **2** was assigned by a combination of ^{1}H coupling constants, ^{13}C chemical shifts, and comparison with known C-4, C-8 diene sphingolipids.[10-12] The length of the sphingosine backbone was deduced from consideration of the molecular composition of derivative **2** and **3**, and the partial structures described above, thus defining the structure of **1** as (4*E*, 8*E*)-N-13′-methyl-tetradecanoyl-1-O-β-D-galactopyranosyl-4-sphingadiene.

Further study of *H. panicea's* polar lipids resulted in the partial isolation of a number of sphingolipid constituents including compound **4** (Figure A.1). These isolation efforts were complicated by the occurrence of a number of structural homologs within each structure class of sphingolipid. Comparison of ^{1}H-NMR, ^{13}C-NMR, ^{1}H-^{1}H COSY,^{1}H-^{13}C HETCOR, as well as lr-FABMS established compound **4**, isolated as its per-acetate derivative **5**, as a structural analogue of derivative **2** differing in the absence of a gem-dimethyl grouping, C-8 olefin, and the length of the fatty acid amide and sphingolipid base chains (Table A.1). The principal methyl ester (82%) of the fatty acyl chain obtained from **5** upon base hydrolysis and methylation was shown to be methyl-docosanoate by lr-GCMS (m/z 354 $[M]^+$). Correspondingly, the sphingolipid backbone chain length was deduced

from hr-MS, yielding the structure of **4** as (4*E*)-N-docosanoyl-1-O-β-D-galactopyranosyl-4-hexadecasphinganine. The fatty acid amide chain lengths of several structurally related minor impurities in this preparation of derivative **5** were determined from lr-GCMS of their corresponding methyl ester derivatives (**5b**, eicosanoate, 10%; **5c**, tetracosenoate, 6%; **5d**, tricosanoate, 1.7%; see experimental).

Djerassi and coworkers have suggested that the unusual branched and elongated fatty acyl chains found in sponge phospholipids may be the result of necessary adaptations to impart fluidity deep within the membrane bilayer, and may have evolved in conjunction with the "fluidizing" methylated sterols found in these marine animals.[13] If these unusual sterol and phospholipid structural modifications are important to functional characteristics of sponge membranes, it is conceivable that other membrane components, including the sphingolipids, may have evolved similar methylation and chain elongation patterns. This study of the novel sphingolipid chemistry of *H. panicea,* which contains these unusual methylation and chain length modifications, supports this hypothesis. Compound **1** is, to our knowledge, the first reported ceramide to contain an *iso*-fatty acid at C-2.

Experimental

Spectroscopic Data. Ir spectra were recorded on a Beckman Acculab 7 spectrophotometer. Optical rotation(s) was measured on a Perkin Elmer Model 141 polarimeter using a 10-cm microcell. NMR spectra were obtained at 400 MHz for ^{1}H and 100 MHz for ^{13}C on a Brucker AM 400-NMR spectrometer, and all shifts are reported relative to an internal TMS standard. Low resolution gas chromatography-electron impact mass spectra (lr GC-EIMS) of methylated fatty acid fragments were obtained on a Finnigan 4023 spectrometer, and low and high resolution mass measurements (hr-MS) of acetylated glycosphingolipids were obtained on a Kratos MS 50 TC. Hplc employed a Waters M-

6000 pump, U6K injector, R 401 differential refractometer, and TLC used Merck aluminum-backed TLC sheets (Si gel 60 F_{254}) with 50% H_2SO_4 as a spray indicator. All solvents were distilled from glass prior to use.

Sponge Material. *Halichondria panicea* (collection SH 15VII87-1: voucher available from WHG) was collected from exposed low intertidal rock surfaces (-1.0 to -0.5 m) at Strawberry Hill on the Oregon coast in July 1987. The sponge material was immediately frozen at the site in CO_2 (s) and stored at -20°.

Extraction and Isolation of Glycosphingolipids. The sponge (1 gallon) was broken into small pieces and extracted with 2 L of $CHCl_3$-MeOH (2:1) to produce 10.9 g of a dark green-brown oil. Vacuum chromatography of this extract over normal phase Si gel and eluting with mixtures of EtOAc in isooctane gave 10 fractions. TLC showed that fractions 5 and 6 contained a nearly equal distribution of extremely polar non-uv active acid-charring substances. These fractions were combined (2.3 g) and acetylated over an 18-h period at room temperature in 6 ml of Ac_2O-pyridine (1:1). The reaction was terminated with the addition of ice and then H_2O and extracted (4X) with Et_2O. The combined Et_2O layers were sequentially washed with 5% HCl (3X), saturated $NaHCO_3$ (3X), distilled H_2O (2X), and then dried over $MgSO_4$. Following filtration the solvents were removed in vacuo to yield 2.0 g of oil. The oil was then subjected to additional vacuum chromatography over Si gel and eluted with mixtures of EtOAc in isooctane to give 9 fractions (1′-9′). Fractions 3′ and 4′ were shown by TLC to contain nearly all of the acetylated material. RP-hplc (10 mm X 25 cm LiChrosorb® 7 μ C-18 column, 5% H_2O in MeOH) of fraction 3′ (0.652 g) resulted in the separation of 15 structurally related per-acetate derivatives including derivative **2** (44.8 mg). RP-hplc (conditions as above) of fraction 4′ (0.652 g) resulted in the isolation of a similar, if not identical, set of related derivatives including derivative **5** (23.8 mg).

Preparation of Fatty Acid Derivatives. The fatty acyl components of the glycosphingolipids were obtained by reaction of the per-acetylated glycosphingolipid derivatives with 10% KOH in EtOH-H_2O (4:1), reflux for 20-h. The hydrolysate was adjusted to pH 4 with 5% HCl and partitioned between $CHCl_3$ and H_2O (3X) after removal of the EtOH *in vacuo*. The organic extract was then washed repeatedly with distilled H_2O to remove any salts. The fatty acids were methylated (1-2 ml CH_2N_2 in Et_2O, 1-h) and purified by hplc (4.1 mm X 30 cm Versapack® Si 10 μ column, 2% EtOAc in isooctane) or analyzed directly by lr-GCMS.

Derivative 2. Oil, ir (CCl_4) 3100, 3004, 2390, 1720, 1661, 1346, 1225, 1070 cm^{-1}; $[\alpha]_D$ -11.7° (c=1.56, $CHCl_3$); lr-FABMS (3-nitrobenzyl alcohol, neg. ion) *m/z* [M + 3-NBA]$^-$ 1046.6 (52), 939.6 (38), [M-H]$^-$ 892.6 (11), 850.6 (47), 808.6 (12.5), 746.5 (5), 500.4 (11), 472.4 (5), 240.2 (2.5), 153.1 (100); hr-FABMS *m/z* (neg. ion) [M + 3-NBA + H]$^-$ 1047.6352 ($C_{56}H_{91}O_{16}N_2$) 1.6 mmu dev.; deduced molecular formula of derivative **2**: $C_{49}H_{83}O_{13}N_1$; ^1H and ^{13}C-NMR see Table 1.

Derivative 3: (Fatty Acid Methyl Ester of Derivative 2). Oil, lr GC-EIMS *m/z* $[M]^+$ 256 (55) , $[M-CH_3]^+$ 241 (2), 225 (13), $[M-CH(CH_3)_2]^+$ 213 (39), 199 (16), 185 (11), 171 (11), 157 (17), 143 (44), 129 (21), 97 (30), 87 (62), 83 (33), 74 (100), 69 (40); ^1H-NMR (400 MHz, $CDCl_3$) δ 3.68 (3H, s, $-OCH_3$), 2.31 (2H, t, *J* =7.5, C-2´´), 1.65 (2H, m, C-3´´), 1.55 (1H, m, C-13´´), 1.26 (16H, s, H-4´´ to H-11´´), 1.18 (2H, m, C-12´´), 0.86 (6H, d, *J* = 6.6, C-14´´ and C-15´´).

Derivative 5. Oil, ir (CCl_4) 3100, 2960, 2930, 1750, 1680, 1225, 1070 cm^{-1}; lr-FABMS (3-NBA, neg. ion) *m/z* [M + 3-NBA]$^-$ 1119 (69), 1012 (62), [M-H]$^-$ 965 (22), 923 (86), 53 (38), 380 (100); ^1H-NMR (400 MHz, $CDCl_3$) δ 5.75 (1H, dt, *J* =15.6, 6.6, H-5), 5.7 (1H, d, *J*=10, N-H), 5.4 (1H, m, H-4´), 5.4 (1H, m, H-4), 5.28 (1H, t, *J* =7.0, H-3), 5.15 (1H, dd, *J*=10.6, 8.0, H-2´), 5.00 (1H, dd, *J*=10.6, 3.2, H-3´), 4.44 (1H, d, *J*=7.9, H-1´), 4.35 (1H, m, H-2), 4.14 (1H, d, *J*=6.6, H-6´), 3.93 (1H, dd, *J*

=10.0, 3.7, H-1a), 3.92 (1H, t, *J*=6.6, H-5′), 3.58 (1H, dd, *J*=10.0, 4.2, H-1b), 2.17 (3H, s, -OAc), 2.15 (2H, m, H-2′′), 2.06 (3H, s, OAc), 2.05 (3H, s, -OAc), 2.04 (3H, s, -OAc), 2.04 (2H, m, H-6), 1.99 (3H, s, -OAc), 1.6 (2H, m, H-3′′), 1.35 (2H, m, H-7), 1.3 (2H, m, H-4′′), 1.26 (32H, m, H-5′′ to H-21′′), 1.26 (18H, m, H-8 to H-16), 0.88 (6H, t, *J*=6.6, H-16 and H-22′′); ^{13}C-NMR (100 MHz, $CDCl_3$) δ 172.70 (C-1′′), 170.32 (-O<u>C</u>OCH_3), 170.19 (-O<u>C</u>OCH_3), 169.92 (-O<u>C</u>OCH_3), 170.0 (-O<u>C</u>OCH_3), 169.59 (-O<u>C</u>OCH_3), 137.07 (C-5), 124.67 (C-4), 100.95 (C-1′), 73.75 (C-3), 70.80 (C-5′), 70.72 (C-3′), 68.85 (C-2′), 67.07 (C-1), 66.91 (C-4′), 61.18 (C-6′), 50.50 (C-2), 39.05, 36.80 (C-2′′), 36.60, 34.39, 31.90, 30.02, 29.93, 29.69, 29.54, 29.49, 29.40, 29.32, 28.97, 27.95, 27.40, 27.10, 25.09, 22.66, 21.08 (-OCO<u>C</u>H_3), 20.80 (-OCO<u>C</u>H_3), 20.61 (2C, -OCO<u>C</u>H_3), 19.20 (-OCO<u>C</u>H_3), 14.14 (C-16), 14.12 (C-22′′).

<u>Derivative **5a**: (Major Fatty Acid Methyl Ester of Derivative **5**).</u> (82%), oil, lr GC-EIMS *m/z* 354 (87) [M]+ for $CH_3(CH_2)_{20}CO_2CH_3$, 323 (9), 311 (19), 297 (3), 283 (1), 269 (4), 255 (10), 241 (3), 227 (1.5), 213 (3), 199 (12), 185 (6), 171 (2), 157 (4), 143 (37), 129 (12), 115 (3), 101 (7), 97 (11), 87 (75), 74 (100), 55 (21), 43 (31);

<u>Derivatives **5b-d**: (Minor Fatty Acid Methyl Esters of Derivative **5**) **b.**</u> (10%) lr GC-EIMS *m/z* 340 (93) $[M]^+$ for $CH_3(CH_2)_{19}CO_2CH_3$, 309 (10), 297 (21), 283 (2), 255 (5), 241 (9), 199 (9), 185 (6), 157 (3), 143 (34), 129 (11), 111 (5), 97 (12), 87 (76), 74 (100), 69 (16), 55 (21), 43 (29); <u>**c.** methyl tetracosenoate</u> (6%) lr GC-EIMS *m/z* 380 (9) $[M]^+$ for $CH_3(CH_2)_nCH{=}CH(CH_2)_{20-n}CO_2CH_3$ (n<20), 348 (100), 306 (12), 264 (14), 250 (8), 236 (6), 222 (5), 208 (5), 194 (4), 180 (4), 166 (5), 152 (9), 138 (8), 125 (13), 111 (22), 97 (42), 87 (29), 83 (43), 74 (39), 69 (47), 55 (53), 43 (27); <u>**d.**</u> (1.7%) lr GC-EIMS *m/z* 368 (100) $[M]^+$ for $CH_3(CH_2)_{21}CO_2CH_3$, 337 (3), 325 (19), 311 (2), 283 (3), 269 (7), 255 (2), 241 (2), 227 (2), 213 (2), 199 (9), 185 (6), 157 (3), 143 (37), 129 (12), 111 (6), 97 (13), 87 (78), 74 (98), 69 (18), 55 (22), 43 (36).

Acknowledgements

We would like to thank Rodger Kohnert for assistance in obtaining NMR data [OSU Department of Chemistry's Bruker AM 400 (NSF CHE-8216190 and M.J. Murdock Charitable Trust), Brian Arbogast and Don Griffin for hr-MS and lr-GCMS (OSU Department of Agricultural Chemistry, NIH DRR 1S10RR01409). We gratefully acknowledge the American Society of Pharmacognosy for an Undergraduate Research Award to conduct this research. This work was supported by the Oregon Sea Grant Program (R/SH-1).

References

1. W. Bergman; A.N. Swift, *J. Org. Chem.*, **16**, 1206 (1951).
2. R.W. Morales; C. Litchfield, *Lipids*, **12**, 570 (1977).
3. E. Ayanoglu; K. Kurtz; J.M. Kornprobst; C. Djerassi, *Lipids*, **20**, 141 (1985).
4. N.K. Kochetkov; V.E. Vaskovsky; I.G. Zhukova; G.P. Smirnova; E.Y. Kostetsky, *Dokl. Akad. Nauk SSSR*, **173**, 1448 (1967).
5. V.E. Vaskovsky; E.Y. Kostetsky; V.I. Svetashev; I.G. Zhukova; G.P. Smirnova, *Comp. Biochem. Physiol.*, **34**, 163 (1970).
6. F.J. Schmitz; F.J. McDonald, *J. Lipid Res.*, **15**, 158 (1974).
7. A. Hayashi; Y. Nishimura; T. Matsubara, *Biochim. Biophys. Acta*, **1083**, 179 (1991).
8. W.H. Gerwick; M.W. Bernart; M.F. Moghaddam; Z.D. Jiang; M.L. Solem; D.G. Nagle, *Hydrobiologia*, **204/205**, 621 (1990).
9. K. Falk; K. Karlsson; B. Samuelsson, *Arch. Biochem. Biophys.*, **192**, 164 (1979).
10. Y. Kawano; R. Higuchi; R. Isobe; T. Komori, *Liebigs Ann. Chem.*, 19 (1988).

11. R.D. Sitrin; G.C. Chan; J. Dingerdissen; C. DeBrosse; R. Mehta; G. Roberts; S. Rottschaefer; D. Staiger; J. Valenta; K. Snader; R.J. Stedman; J.R.E. Hoover *J. Antibiotics*, **41**, 469 (1988).

12. K. Chebaane; M. Guyot, *Tetrahedron Lett.*, **27**, 1495 (1986).

13. R.D. Walkup; G.C. Jamieson; M.R. Ratcliff; C. Djerassi, *Lipids*, **16**, 631 (1981).